SYNTHESIS AND EVALUATION OF ALPHA-FLUORO ANALOGUES OF CAPSAICIN AND 2-(AMINOMETHYL)PIPERIDINE DERIVATIVES

Thomas Moraux

A Thesis Submitted for the Degree of PhD
at the
University of St. Andrews

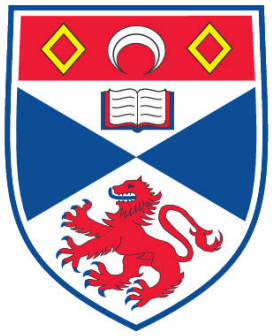

2011

Synthesis and evaluation of α-fluoro analogues of capsaicin and 2-(aminomethyl)piperidine derivatives

A thesis presented for the degree of Doctor of Philosophy

to the School of Chemistry - University of St-Andrews

Thomas Moraux

April 2011

SUBMISSION OF PHD AND MPHIL THESES
REQUIRED DECLARATIONS

1. Candidate's declarations:

I, Thomas Moraux, hereby certify that this thesis, which is approximately 35.000 words in length, has been written by me, that it is the record of work carried out by me and that it has not been submitted in any previous application for a higher degree.

I was admitted as a research student in October 2005 and as a candidate for the degree of Doctor of Philosophy in August 2006; the higher study for which this is a record was carried out in the University of St Andrews between 2005 and 2010.

Date …….. signature of candidate ……...

2. Supervisor's declaration:

I hereby certify that the candidate has fulfilled the conditions of the Resolution and Regulations appropriate for the degree of Doctor of Philosophy in the University of St Andrews and that the candidate is qualified to submit this thesis in application for that degree.

Date ……. signature of supervisor ……...

3. Permission for electronic publication:

In submitting this thesis to the University of St Andrews I understand that I am giving permission for it to be made available for use in accordance with the regulations of the University Library for the time being in force, subject to any copyright vested in the work not being affected thereby. I also understand that the title and the abstract will be published, and that a copy of the work may be made and supplied to any bona fide library or research worker, that my thesis will be electronically accessible for personal or research use unless exempt by award of an embargo as requested below, and that the library has the right to migrate my thesis into new electronic forms as required to ensure continued access to the thesis. I have obtained any third-party copyright permissions that may be required in order to allow such access and migration, or have requested the appropriate embargo below. The following is an agreed request by candidate and supervisor regarding the electronic publication of this thesis:

Access to printed copy and electronic publication of thesis through the University of St Andrews.

Date …… signature of candidate …… signature of supervisor ……..……

Acknowledgements

I would like to express my gratitude to my supervisor Professor David O'Hagan, for having given me the opportunity to work in his group and for the numerous valuable discussions during my PhD.

I would like to join to this acknowledgement all the technical staff at the School of Chemistry and the BMS for providing such outstanding working conditions. I thank Professor Alexandra M.Z. Slawin, Dr Tomas Lebl, Melanja Smith, Caroline Horsburgh and Peter Pogorzelec for their respective help in crystal structure, NMR analyses and mass spectroscopic analyses.

This PhD also gave me the opportunity to meet numerous people, and I would like to thanks in particular the members of the DOH group, past and present. The *three musketeers* who read this work were Dr Nawaf Al-Maharzik, Dr Neil Keddie, Dr Michael Corr, and Dr Yi Wang. My thoughts are also going to the *old-timers*: Matthieu, Guillaume, Vincent, Nelly, Paul, Pitak, Romain, Dr Daniel Farran, Dr Margit Winkler… *et al.*! Finally, Stefan *Lazy German*, Maciek *Cookie Monster*, and particularly Danny *Cheeky Chicken* have made this lab the most enjoyable place to work in!

Abbreviations

ACN	acetonitrile
Bn	benzyl
br	broad
BuLi	buthyl lithium
CM	cross-metathesis
d	doublet
DAST	diethylaminosulfur trifluoride
DCM	dichloromethane
de	diastereomeric excess
DIEA	diisopropylethyl amine
DMAP	4-(*N*,*N*-dimethylamino)pyridine
DMF	*N*,*N*-dimethylformamide
dr	diastereomeric ratio
ee	enantiomeric excess
eq	equivalent
Hz	Hertz
HRMS	high resolution mass spectroscopy
IR	infrared spectroscopy
J	coupling constant
LDA	Litium diisopropyl amide
m	multiplet
μmol	micromol (10^{-6} mol)

Mp	melting point
NFSI	*N*-fluorobenzene sulfonimide
NFOBS	*N*-fluoro-*O*-benzenedisulfonimide
NMR	nuclear magnetic resonance
ppm	parts per million
PTFE	polytetrafluoroethylene
RNA	ribonucleic acid
RTX	resiniferatoxin
rt	room temperature
s	singlet
t	triplet
TBAF	*N*-tetrabutylammonium fluoride
TfO	trifluoromethanesulfonate (triflate)
THF	tetrahydrofurane
TLC	thin layer chromatography
TMS	trimethylsilyl
TRPV1	transient receptor potential vanilloid subtype 1
TsO	*p*-methyl benzene sulfonate (tosyl)
^{19}F NMR	fluorine nuclear magnetic resonance
^{19}F $\{^{1}$H$\}$ NMR	proton decoupled fluorine nuclear magnetic resonance

Table of contents

Chapter 1- Fluorine in bioactive molecules

Chapter 2: α-Fluorinated capsaicins to alter the biological response of TRPV1 pain receptor

Chapter 3: Synthesis and organocatalysis from 2-(aminomethyl)piperidine

Chapter 4: Experimental

Abstract

Chapter 1 gives an overview of the fluorine chemistry field, from its early developments to recent applications in medicinal chemistry. The development of asymmetric electrophilic or nucleophilic installation of fluorine in organic molecules is highlighten.

Chapter 2 of this thesis discusses the enantioselective synthesis of α-fluoroamides. The study is applied to the synthesis of fluoroenantiomers of the bioactive molecule capsaicin and short-chain analogues. The biological activity of these compounds is assayed with the TRPV1 receptor. Results show that enantioselective α-fluoroamides (*R*)-**97**, (*R*)-**99** and (*S*)-**99** can generate differentiated biological responses, from TRPV1 agonists to TRPV1 antagonists.

Chapter 3 focuses on the optimisation and development of 2-(aminomethyl)piperidine (*R*)-**251** dihydrochloride. The development of 2-(aminomethyl)piperidine (*R*)-**251** as its ditetrafluoroborate salt proved to offer excellent reactivity and solubility for the preparation of derivatives. This tetrafluoroborate salt was used to improve the syntheses of organocatalysts 2,2,2-trifluoro-*N*-(piperidin-2-ylmethyl)acetamide **363** and 4-methyl-*N*-(piperidin-2-ylmethyl)benzenesulfonamide **364**.The catalytic properties of these latter two molecules for asymmetric Mannich reaction is demonstrated. Both (*R*)-**363** and (*R*)-**364** show up to 86% ee, in a typical 20 mol% loading, but loading of (*R*)-**363** as low as 5 mol% still induces the catalysis.

1 - Fluorine in bioactive molecules

1.1- Discovery and development of fluorine chemistry

The history of fluorine chemistry can be traced to the 16th century when the German scholar Agricola was the first to describe the use of fluoride in a mineral form (**Figure 1.1**).

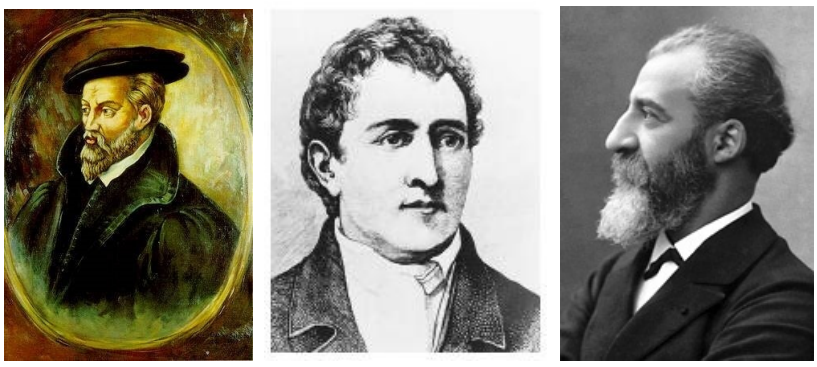

Figure 1.1: Portraits of Agricola, Scheele and Moissan.

The mineral was fluorspar, composed of calcium fluoride (CaF_2) and was used in metallurgy to assist in fusion. In this respect, the etymology of fluorine derives from the latin *fluere* ("to flow").

Studies on fluorspar were continued by Carl Wilhelm Scheele in the 17th century. He noticed that the mineral would etch glass after acid treatment, and hence he can be attributed with the discovery of hydrofluoric acid (HF).

Due to its very high reactivity and toxicity, elemental fluorine was only isolated in 1886. This was achieved by Henry Moissan (Nobel Prize in 1906). The Moissan process starts with the production of hydrofluoric acid by heating fluorspar (CaF_2) at 250 °C in the presence of sulfuric acid (H_2SO_4). Addition of potassium fluoride (KF) as an electrolyte forms potassium bifluoride KHF_2, which emits hydrogen gas at the cathode when electrolysed, and fluorine gas is formed at the anode (**Scheme 1.1**).

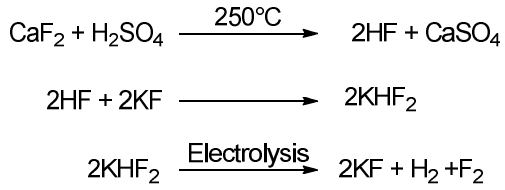

Scheme 1.1: Moissan process for elemental fluorine production by electrolysis.

The method of production of fluorine (HF and F_2) developed by Moissan has since been extensively applied on the industrial scale and has allowed the development of fluorine chemistry in both research and industry.

An important example of an industrial process resulting from fluorine reactivity is the enrichment of fissionable U^{235} from natural uranium.[1] This specialised application was initiated during World War II, where it was used for the development of the nuclear bomb (Manhattan Project). Elemental fluorine is used to generate volatile uranium hexafluoride (UF_6). In the reaction, uranium ore yellow cake (U_3O_8) is converted into uranium dioxide

(UO_2), which then reacts with F_2 in a two step process to provide uranium hexafluoride (UF_6) *via* uranyl fluoride (UO_2F_2) (**Scheme 1.2**).

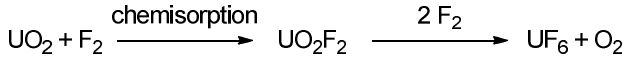

Scheme 1.2: Uranium hexafluoride (UF_6) synthesis.

Uranium hexafluoride is heated to a gaseous state allowing the separation of isotopomers U^{235} and U^{238} through diffusion membranes or by centrifugation to provide the fissionable uranium (U^{235}) used in nuclear power stations.

The chemistry of fluorinated alkanes was first explored by Frédéric Swarts who developed a fluorine exchange catalyst, enabling the conversion of chlorocarbons to mixed chlorofluorocarbons (**Scheme 1.3**).

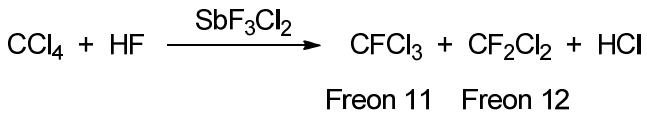

Scheme 1.3: Freon gas production.

This process was applied by General Motors during the 1930s for the industrial-scale synthesis of Freon gases. This family of inert gases was extensively used as non-flammable refrigerants until the end of the 1990s, when it was banned for ecological environmental reasons.

Research on chlorofluorocarbons (CFCs) then led to a second major commercial product. In 1938, Roy Plunckett of the DuPont company discovered the perfluorinated polymer poly-

tetrafluoroethylene (PTFE), now marketed as Teflon® or Gore-Tex®. The synthesis of PTFE is initiated with the thermal fragmentation of $CHClF_2$ into difluorocarbene, which then homocouples to give tetrafluoroethylene (TFE). This monomer is subjected to radical polymerisation to generate PTFE (**Scheme 1.4**).

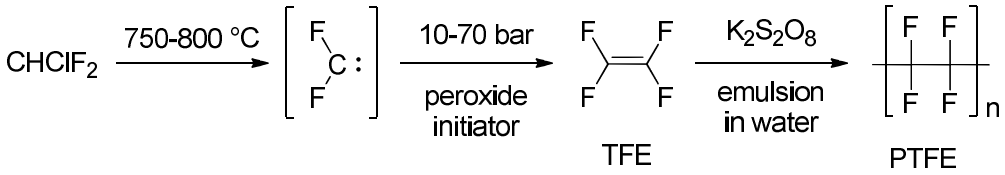

Scheme 1.4: DuPont synthesis of perfluoroethylene (PTFE).

Fluorine also brought specific properties to compounds of biological and medicinal interest. A major medical application appeared in the mid 1950s within the field of anaesthesiology. The "*fluorine revolution*" led to the replacement of diethyl ether by fluorinated general anaesthetics.[2] The first of these products used on patients was Fluoroxene® **1** in 1953 (**Figure 1.2**). Halothane® **2** became the main anaesthetic in clinical use until the 1980s, and was used in about 80% of all operations. The clear advantage of the fluorinated anaesthetics was the reduction in flammability and therefore their ease of use. Currently Sevoflurane® **3** and Desflurane® **4** are the main anaesthetics used in surgery. Delivery is improved thanks to their lower blood-gas partition coefficient. As a consequence, side-effects are reduced and recovery times are shortened because of lower levels of metabolism.

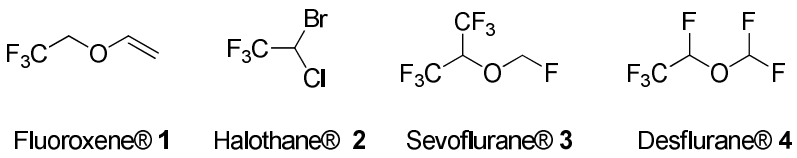

Figure 1.2: Fluorinated anaesthetics.

Fluorine has also contributed to the development of numerous agrochemicals: herbicides, fungicides and insecticides. Fluorine incorporation has improved their efficiency in terms of solubility and toxicology.[3]

The influence of fluorine attached to chiral centres on the biological properties of a bioactive molecule was exemplified in 1954 by Joseph Fried and Emily F. Sabo with their synthesis of corticosteroid 9α-fluorocortisone acetate **5** (**Figure 1.3**).[4] In previous studies they described the replacement of the 9α-hydrogen atom by halogens.[5] The 9-halocorticoids showed an enhanced glucocorticoid activity, which in the case of the chloro-derivatives exceeded that of the parent hormones by a factor of four. They concluded the activity was inversely proportional to the size of the halogen.

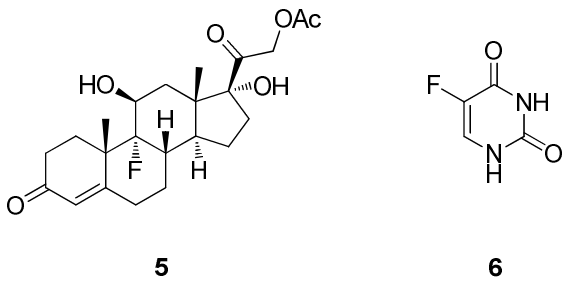

5 **6**

Figure 1.3: Examples of important fluorinated bioactives.

Three years later, 5-fluorouracil (5-FU) **6** was synthesised as a novel anti-tumour drug by Charles Heidelberger, Robert Duschinsky and Robert Schnitzer at Hoffman-La Roche.[6] 5-FU affects cellular reproduction, and it is especially active on fast growing cancer cells. This molecule is indeed an analogue, but also an antimetabolite, of the pyrimidine nucleosides. When incorporated into RNA, 5-FU inhibits RNA replication enzymes, thereby arresting RNA synthesis and the subsequent growth of cancer cells.

1.2- Controversial effects of fluorine on health

The synthesis of fluorinated organic and bioorganic compounds is a relatively new field that emerged significantly in the 1970s, with an approximate rate of three drug candidates per year (**Figure 1.4**).[7, 8] There was a clear rise in fluorinated drugs around 1982, following early developments on selective fluorination methods using new reagents such as (diethylamino)sulfur trifluoride (DAST).[9, 10] The percentage of fluorinated drugs (green bars) has remained relatively constant at between 5-15% of all drugs launched annually over the last thirty years. Since 2002 there has been an apparent increase (15-40%) in fluorinated drugs by comparison with the total number of approved pharmaceuticals. However, the total number of drugs introduced onto the market is now very low at less than twenty per year, by comparison with the 50-60 per year in the 1980s.

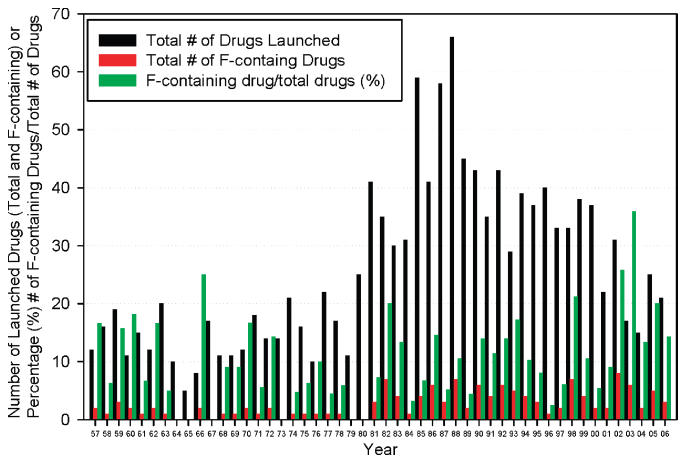

Figure 1.4: Number of launched drugs and the percentage containing fluorine (green) between the 1957-2006 period.[7]

Significant methodology improvements in fluorination chemistry in recent years (discussed in **section 1.6)**, have resulted in an increasing number of fluorinated products of greater variety

and structural complexity. Unfortunately the persistence and bio-accumulation of fluorine in any form is an ongoing issue. For instance, fluoride ion enriched products such as toothpastes or NaF enriched kitchen salts were introduced onto the market in the 1970s. Fluoride helps the prevention of dental cavities by remineralisation of tooth enamel and renders it resistant to acid damage,[11, 12] but the addition of fluoride to food and to the water supply remains controversial.

In the early 1930s, toxicity associated with high intakes of fluoride ion as well as indirect contamination *via* ingestion of fluoride from food or fluoridated water was already noted.[13]

A more recent concern in the bio-accumulation of fluorinated products was formalised in 2003 by the United States Environmental Protection Agency (EPA) relating to population exposure to perfluorooctanoic acid (PFOA) **7**.

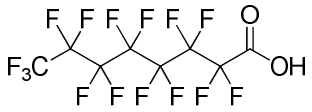

7

Figure 1.5: Perfluorinated acid PFOA.

According to the EPA, residual PFOA in Teflon® coatings or PFOA resulting from degradation of PTFE at high temperature is potentially carcinogenic, by extrapolation on human beings of tumours developed by rats and mice exposed to this chemical.[14] At the beginning of 2009, a study showed that blood serum levels of PFOA are potentially linked to infertility for both women and men.[15] If installation of fluorine on molecules is designed to improve their efficiency, bio-accumulation of fluorinated compounds is clearly an issue that will continue to be newsworthy.

1.3- Significance of fluorine in natural products

The importance of fluorine in pharmaceuticals can be contrasted with the virtual absence of natural fluorinated compounds. Much of the halogen contained in the earth's crust (270-740 ppm, compared to that of chlorine at 10-180 ppm) remains insoluble and therefore is not bioavailable. Also, fluoride ion has a high solvation energy (439 $kJ.mol^{-1}$)[16] and is not free as a nucleophile, thus few enzymes have evolved that can utilise it. To date, only five fluorinated natural compounds have been ultimately identified either in plants or microorganisms and there is no direct evidence of *de novo* biosynthesis of organofluoro-metabolites in animals (**Figure 1.6**).[17] In addition, eight metabolites of **10** have been found in the seed lipids of *Dichapetalum toxicarium*, from Sierra Leone.[18]

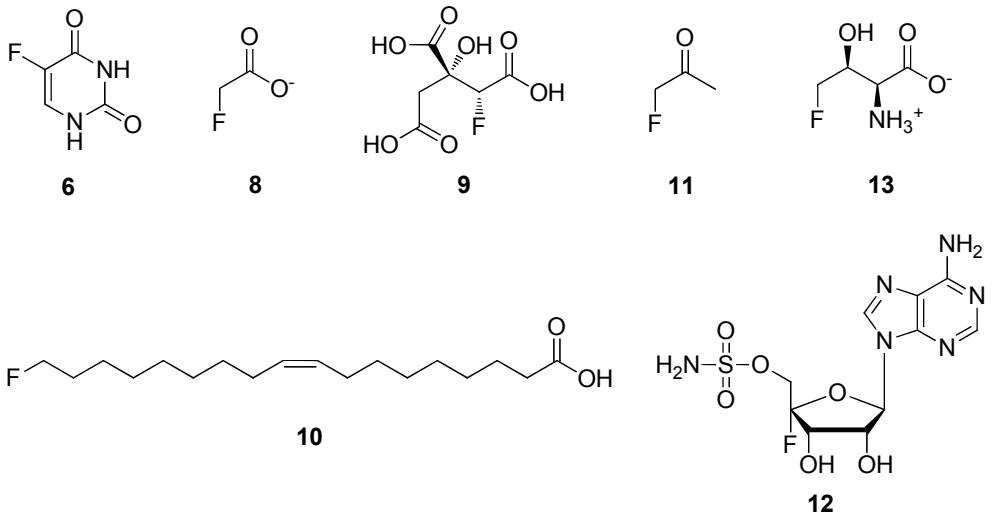

Figure 1.6: Examples of claimed fluorinated natural products.

Fluoroacetate **8** was discovered in 1943 by Marais from plant *Dichapetalum cymosum*,[19] and 4-fluorothreonine **13** was isolated from the bacterium *Streptomyces cattleya* in 1986.[20]

Recently, 5-fluorouracil **6** and derivatives were isolated from the marine sponge *Phakellia fusca* collected in the South China Sea, although this is more likely the bioaccumulation of 5-FU in industrial effluent.[21] The bacterium *Streptomyces calvus* was found to produce nucleocidin **12**. The details of the full biosynthetic pathways to the metabolites have not been elucidated, except in the case of *Streptomyces cattleya,* which produces fluoroacetate **8** and 4-fluorothreonine **13**.[22-25]

1.3.1- Metabolites from plants

The fluoroacetate metabolite **8** seems to be ubiquitously synthesized by plants in tropical and subtropical regions but some have evolved a particular capacity for defense purposes.[19]

A co-evolution phenomenon has made endogenous animals resistant to fluoroacetate-producing plants with the most dramatic effect in herbivores, which are more exposed to the toxin.[26] ω-Fluorofatty acids are almost certainly biosynthesised from fluoroacetate **8** *via* fluoroacetyl CoA and fatty acid synthase.[27]

1.3.2- Metabolites from micro-organisms

Nucleocidin **12** was isolated in 1957, from the bacterium *Streptomyces calvus* even though fluorine in its structure was only elucidated in 1969.[28] It is an adenine-containing antibiotic of broad spectrum activity that was revealed to be too toxic for clinical use. Novel attempts to re-isolate this product, and therefore, determine the nature of the biological fluorination

process have failed.[29] It is possible that one essential plasmid encoding the gene for nucleocidin biosynthesis has been lost during the freeze-drying process of the bacterium.

Streptomyces cattleya has proved to be of great interest as studies on this bacterium demonstrated that it is able to produce fluoroacetate **8**, and the amino acid 4-fluorothreonine **13** and a summary of the pathway is shown in **Scheme 1.5**.[25, 30]

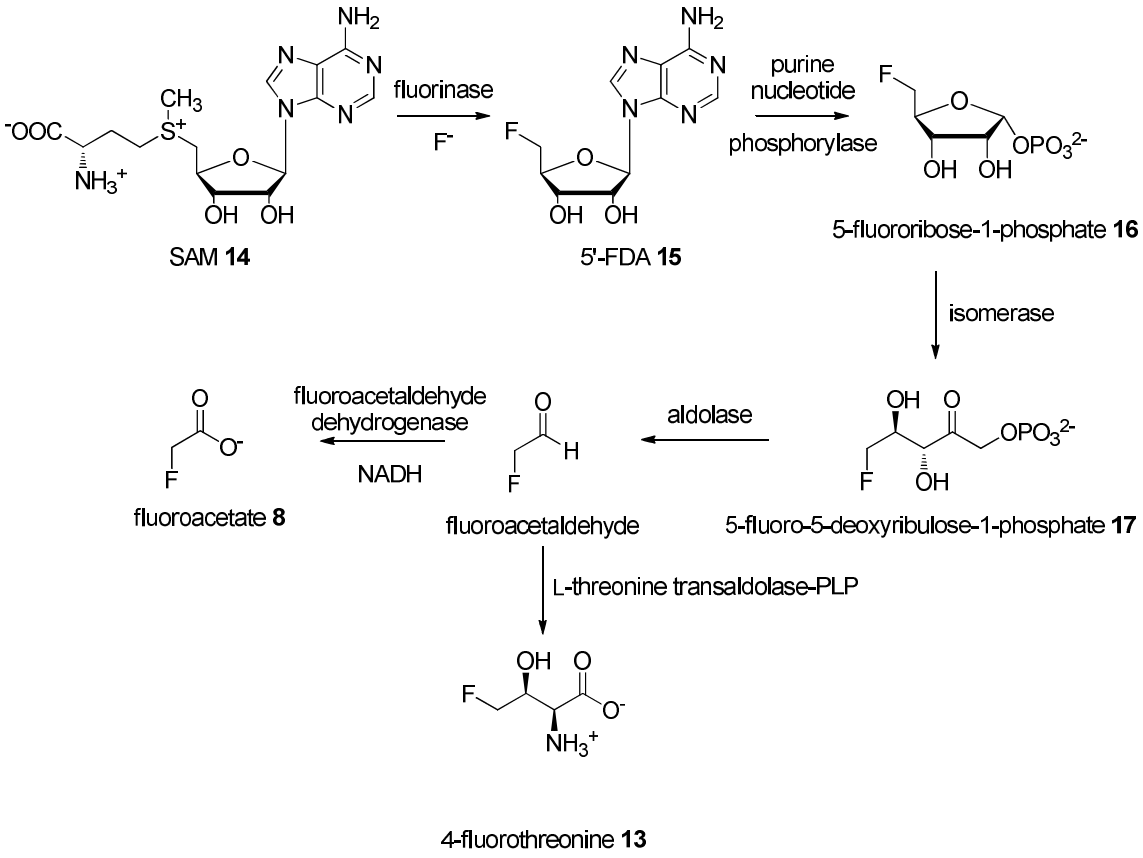

Scheme 1.5: Biosynthetic pathway in *Streptomyces cattleya.*

4-Fluorothreonine **13** exhibits antimicrobial activity against a range of bacteria. The enzyme that forms the C–F bond has been isolated and identified as 5'-fluoro-5'-deoxyadenosine synthase, which is more commonly termed the "*fluorinase*".[31] The enzyme catalyses the reaction of fluoride ion with *S*-adenosyl-L-methionine (SAM) **14** and generates 5'-fluoro-5'-deoxyadenosine (5'FDA) **15** and L-methionine as products.

1.4- Properties of fluorine

1.4.1- The fluorine atom

Fluorine has nine electrons distributed in two valence shells with the electronic configuration $1s^2\ 2s^2\ 2p^5$. The Van der Waals radius is 1.47 Å, which makes it the second smallest atom of the periodic table after hydrogen (1.20 Å) able to make covalent bonds with carbon. Due to its small size, electrons are strongly attracted to the nucleus and fluorine has been assigned the most electronegative value in the periodic table (3.98 on Pauling scale, **Table 1.1**). The high ionisation energy suggests removing an electron is unlikely. Indeed the only ionic form of fluorine is the fluoride anion.

Atom	**Van der Waals radius (Å)**	**Pauling electronegativity**	**Polarisability ($Å^3$)**	**Ionisation energy ($kcal.mol^{-1}$)**
H	1.20	2.20	0.667	313.6
F	1.47	3.98	0.557	401.8
O	1.52	3.44	0.82	314.0
N	1.55	3.04	1.10	335.1
C	1.70	2.55	1.76	240.5
Cl	1.75	3.16	2.18	299.0
Br	1.85	2.96	3.05	272.4
I	1.98	2.66	4.7	241.2

Table 1.1: Atomic parameters of fluorine relative to other common atoms.

The case of fluoride is interesting as it generates ordered clusters with water, although the solvation structure is not clear. It seems likely that F^- shows a tetrahedral coordinated solvation shell,[32] although there are some indications that the coordination number is solute-concentration-dependent.[33] The nature of the cation can also significantly affect the hydration state.[34, 35] This propensity to solvation renders fluoride unreactive as a nucleophile.[36] Elemental fluorine (F_2) has a much lower bond energy (157 $kJ.mol^{-1}$) relative to hydrogen (H_2) (434 $kJ.mol^{-1}$) or chlorine (Cl_2) (242 $kJ.mol^{-1}$). Thus the reactivity of elemental fluorine is very high.

1.4.2- Physical properties of the C–F bond

Incorporation of fluorine in place of hydrogen into organic molecules often leads to decreased boiling points in the case of high levels of fluorination or perfluorination. Polyfluorination also enhances density, viscosity or compressibility, making perfluorocarbons relatively fluidic (see **Table 1.2**).

	C_6H_{14}	$CF_3(CF_2)_2(CH_2)_3H$	C_6F_{14}
Boiling point (°C)	69	64	57
Density d^{25} ($g.m^{-3}$)	0.655	1.265	1.672
Viscosity η^{25} (cP)	0.29	0.48	0.66
Compressibility β (10^{-6} atm^{-1})	150	198	254

Table 1.2: Some physical properties of non-, partially- and per-fluorinated compounds.

Polarity is decreased according to the degree of fluorination, having impacts on the solubility. In the extreme, perfluorocarbons are not miscible in organic solvents or water, rather forming a third phase known as the "fluorous phase". Effects on lipophilicity will be explored further in **section 1.5.1.2**. This parameter is crucial in medicinal chemistry as it dictates the passage of drug candidates through biological barriers.

1.4.3- Stereoelectronic properties of the C–F bond

1.4.3.1- Polarity

The high electronegativity of fluorine and its inductive electron withdrawing character renders the C–F bond rather electrostatic than covalent in character. The C–F bond is polarised from the carbon (δ^+) to the fluorine (δ^-), forming a large dipole which can interact with other dipoles. This high electronegativity is also responsible for holding tightly the three lone pairs and reduces their ability to become involved in resonance. When fluorine is bound to sp^2 carbon, an electron donating mesomeric effect can occur, but this is much weaker than for oxygen or nitrogen (**Figure 1.7**).

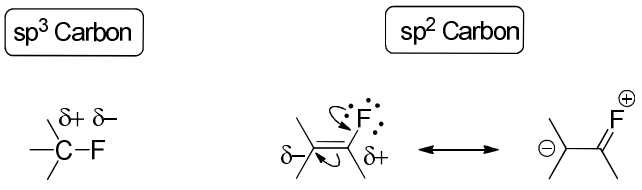

Figure 1.7: Electronic effects of fluorine.

1.4.3.2- Bond strength

Table 1.3 illustrates that fluorine forms a stronger bond to carbon than all of the other halogens (entry 1-3). Indeed, fluorine forms the strongest bond to carbon. Fluorine also has effects on proximate bonds, the strengthening effect being increased with the number of fluorine substituents (entry 3 to 5). The reinforced strength of C–H and C–C bonds in polyfluorinated compounds generates high thermal and oxidative stability of such compounds.

Entry	**Molecule**	**Bond dissociation energy (kcal.mol^{-1})**
1	H_3C-F	108.3
2	H_3C-Cl	82.9
3	H_3C-CH_3	88.8
4	H_3C-CF_3	101.2
5	F_3C-F	130.5

Table1.3: C–X bond dissociation energy of halogenated compounds.

1.5- Fluorine in medicinal chemistry

1.5.1- Effects of fluorine on the properties of organic molecules

1.5.1.1- Perturbation of pK_a

Fluorine is strongly electron withdrawing when it is incorporated into organic molecules, *vide infra*. This property affects the acidity of adjacent functional groups. For instance fluorine substitution of amines renders them less basic.[37] **Table 1.4** illustrates that for each fluorine added, the pK_a is lowered by a similar magnitude.[8] In addition, fluorine substitution also makes alcohol and carboxylic acid functionality more acidic.

Amines	**pK_a**
$CH_3CH_2NH_3^+$	10.7
$CH_2FCH_2NH_3^+$	9.0
$CHF_2CH_2NH_3^+$	7.3
$CF_3CH_2NH_3^+$	5.7
$CH_3CH_3CH_2NH_3^+$	10.7
$CH_2FCH_2CH_2NH_3^+$	9.9
$CF_3CH_2NH_3^+$	8.7

Carboxylic acids and alcohols	**pK_a**
CH_3COOH	4.76
CH_2FCOOH	2.66
CHF_2COOH	1.24
CF_3COOH	0.23
CH_3CH_2OH	16.0
CF_3CH_2OH	12.37

Table 1.4: The effect of fluorine substitution on pK_a values of organic amines, carboxylic acids and alcohols.[8]

Drugs p*K*a are evaluated early during the clinical development of a lead molecule, as it can have strong effects on the drug metabolism. For example, novel indole derivatives **18-20** developed to treat migraine were studied for their bioavailability (**Figure 1.8**).[38]

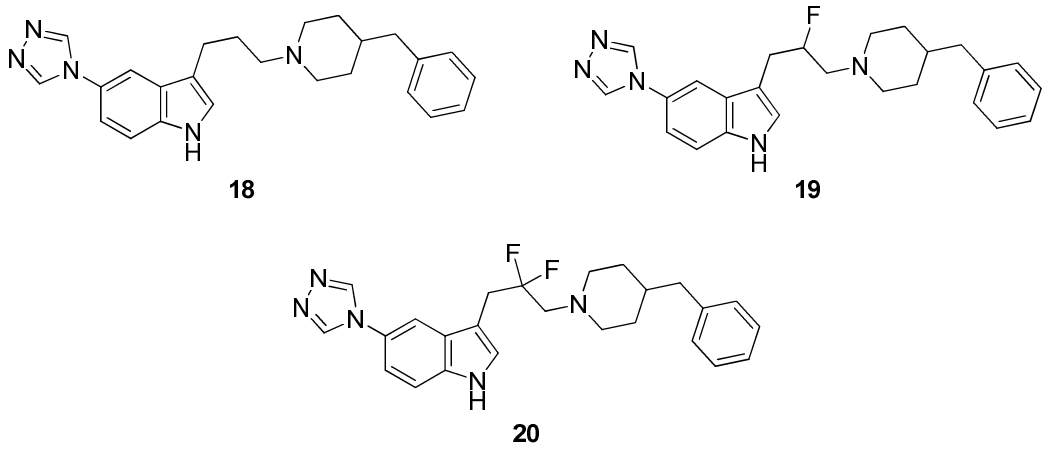

Figure 1.8: Indole derivatives studied for their bioavailability.

Introduction of one or two fluorine atoms significantly reduces the basicity of the amine, showing an improvement in the bioavailability of the lead compound **18**, although this compromised receptor affinity. The difluoro compound **20** was no longer basic enough to achieve high binding affinity for the 5-HT_{1D} migraine receptor (**Table 1.5**).

Structures	**pK_a**	**IC_{50} 5-HT_{1D}**	**Bioavailablility**
18	9.7	0.3	Poor
19	8.7	0.9	Good
20	6.7	78	NA

Table 1.5: Correlation between pKa of non-, mono- and difluorinated compounds and their IC_{50}.[38]

1.5.1.2- Modulation of lipophilicity

The balance between lipophilicity and overall molecular polarity is an important factor in drug design. Drugs require a reasonable lipophilicity to pass through cell membranes and provide good binding to the target protein. The distribution coefficient (log *D*) measures the lipophilicity of the molecule, also expressed as the partition coefficient log *P*, at a given pH (usually 7.4). The "Lipinski's rule of five", used to predict good drug candidates, has empirically set up that log *P* should be less than 5 to lead to better solubility and complete absorption of the drug. In general, fluorine substitution increases lipophilicity; however this is not always the case. A study by Roche on 293 compounds from their in-house database correlated the effect of the substitution of hydrogen by fluorine on lipophilicity.[7] The histogram of changes in log *D* in **Figure 1.9** reveals a Gaussian distribution. The maximum at 0.25 log *D* units shows the average increase in lipophilicity. However, this data shows a significant tail under zero, for compounds with decreased lipophilicity.

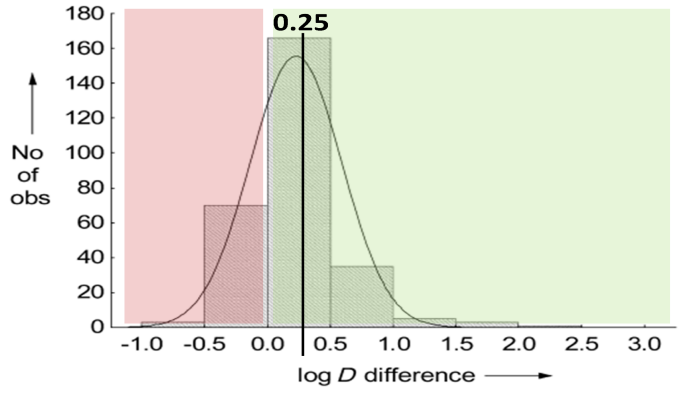

Figure 1.9: Effect of monofluorination on lipophilicity of drugs.[7]

1.5.1.3- Steric and conformational changes

The steric change carried by the substitution of hydrogen or a hydroxyl group is minor, in regards of the similar van der Waals radius (r_v) of fluorine (1.47 Å) with that of oxygen (1.57 Å) and hydrogen (1.20 Å). The electronic properties are altered by the replacement of hydrogen by fluorine, but the replacement of oxygen is a most neutral change.

The methyl group is often isosterically replaced by the trifluoromethyl group to improve lipophilicity, although it has about twice the volume.[39]

The combination of the steric influence of fluorinated groups and the electronegativity of fluorine often generates a conformational change. A clear example is provided with substituted benzene rings. A methoxyl substituent prefers to lie planar to the aromatic ring whereas a O–CF_3 group lies perpendicular. Therefore O–CF_3 cannot be considered simply as an isosteric analogue for O–CH_3. This difference was applied in the design of more potent inhibitors of the cholesteryl ester transfer protein (**Figure 1.10**).[40]

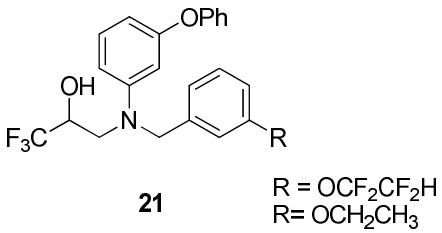

Figure 1.10: Structure of inhibitors of the cholesteryl ester transfer protein.

This protein functions to transfer the cholesteryl ester from high-density lipoprotein to low-density lipoprotein, a process which alleviates coronary heart disease. Switching the R group from OCH_2CH_3 to OCF_2CF_2H on **21** led to an 8-fold increase in potency. As confirmed by DFT calculations, the pentafluoroethyl substituent is orientated out of the plane compared to

the phenyl group, dramatically improving the binding efficiency to the target protein. In addition, it is also suggested that the steric and electronic properties of Ph–OCF_2CF_2H are similar to 2-phenylfuran, another non-planar substituent. This offers a new tool to medicinal chemists as furans are metabolically unstable and therefore it can be of advantage to replace them by OCF_2CF_2H.

1.5.2- Metabolic stability

Once a drug is administered, it is generally metabolised prior to distribution to the target site. This metabolism is the physiological response of detoxification that occurs mainly in the liver. Cytochrome P450 monooxygenases are primarily responsible for the oxidation of xenobiotic compounds, decreasing their lipophilicity to enhance water solubility and hence excretion.[41]

1.5.2.1- Oxidative mechanism

Oxidation of drugs by cytochrome P450 enzymes is often combated by selective fluorination. This is exemplified by the lead optimisation of the cholesterol inhibitor Ezetimibe (Schering-Plough) **23**.[41, 42]

Part of the oxidative metabolism was blocked after incorporation of fluorine (**Figure 1.11**) into the *para* positions of the phenyl groups. Such substitutions prevent oxidation of the phenyl ring to phenol and dealkylation of the methoxyl group, because of the strong electronic withdrawing effect of the fluorine deactivating the phenyl ring.

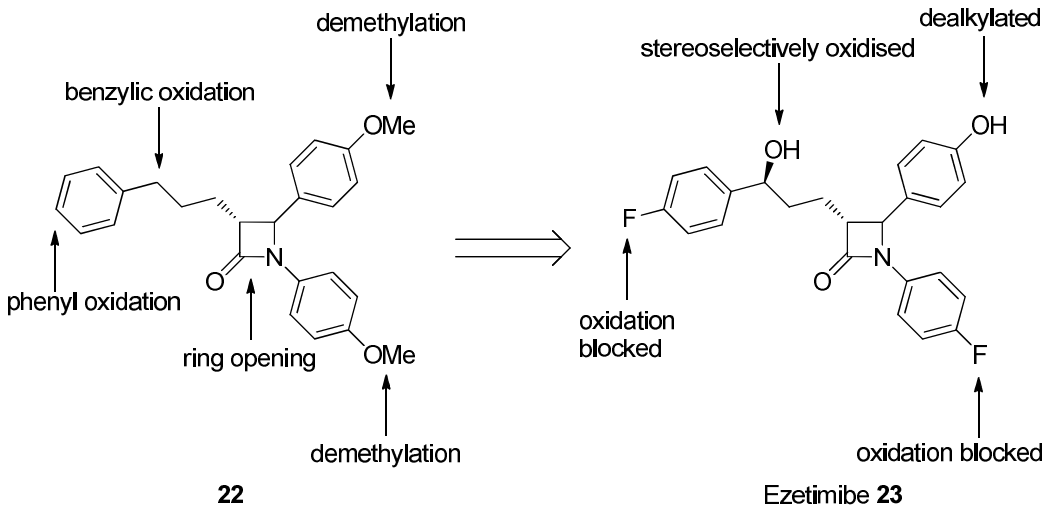

Figure 1.11: Strategies to block aryl oxidative metabolism of Ezetimibe.[42]

In an extreme case, the incorporation of fluorine may bring excessive stability that prevents the drug being metabolised. This has been exemplified by the cyclo-oxygenase 2 (COX 2) inhibitor Celecoxib **25** which presented a very long biological half-life.[43] Stability has been altered by substituting the fluorine on lead compound **24** with a methyl group, which is more inclined to be metabolised and excreted from the patient (**Figure 1.12**).

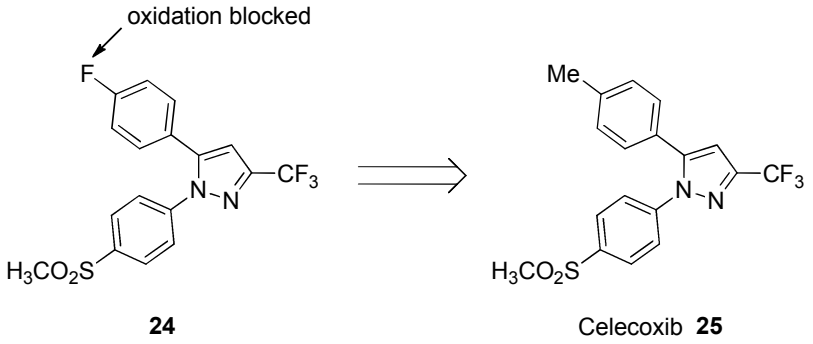

Figure 1.12: An example of retro-drug design with Celecoxib to decrease its metabolic half-life.[43]

1.5.2.2- Hydrolytic metabolism

In vivo hydrolysis of some drugs can occur at acidic or neutral pH. For example, prostacyclin (PGI_2) **26** is a vasodilator, and used for vascular disease treatment. The labile enol ether moiety of this compound is hydrolysed *in vivo*, with a half-life of 10 minutes, to give the inactive compound 6-oxo-$PGF_{1\alpha}$.**29** (**Scheme 1.6**).[44]

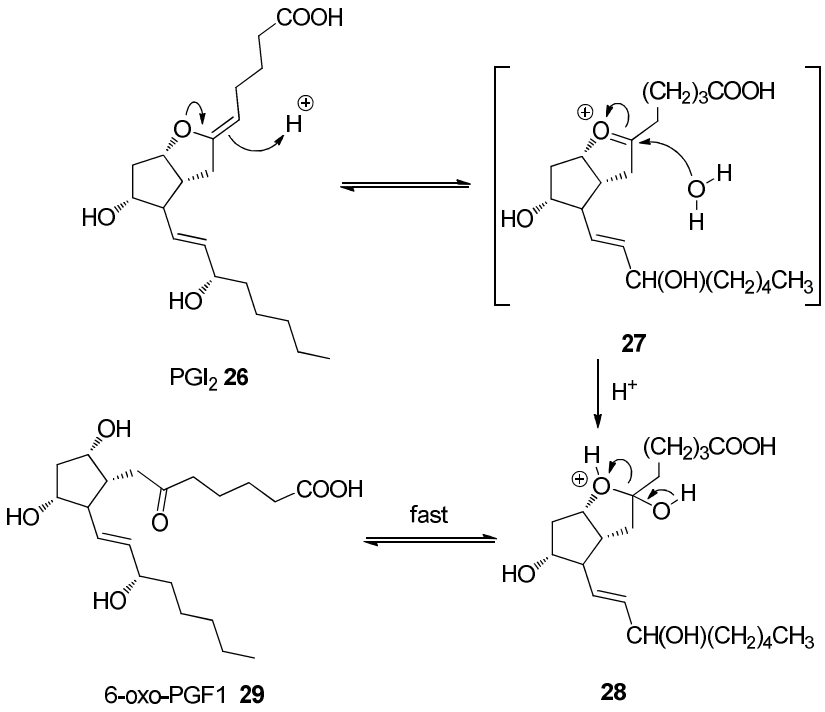

Scheme 1.6: Mechanism of the hydrolytic metabolism of prostacycline **26**.[44]

Introducing fluorine into this molecule decreased the hydrolysis rate as a result of reducing the electron density of the enol ether. The mono-fluorinated derivative 7-F-PGI_2 **30** has a half-life of 30 days[45] whereas the difluoro derivative AFP-07 **31** has a half-life of 90 days,[46] significantly extended from the initial time of 10 minute for **26** (**Figure 1.13**).[45]

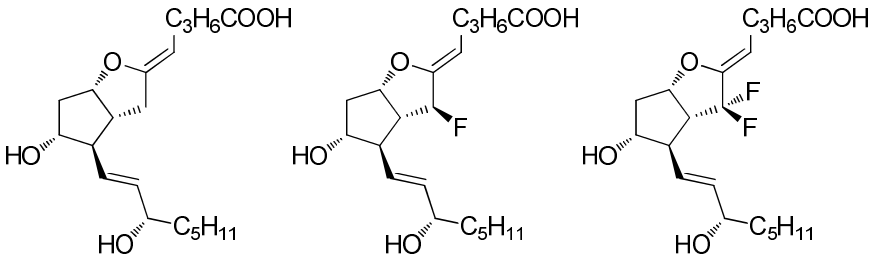

PGI$_2$ **26** 7-F-PGI$_2$ **30** AFP-07 **31**

Figure 1.13: Blockage of hydrolytic metabolism with fluorine in prostacycline analogues.

1.5.2.3- In vivo racemisation

Racemisation of drugs can also occur under physiological conditions, as exemplified by thalidomide **32** (**Scheme 1.7**). Thalidomide is a sedative hypnotic prescribed to mothers during their pregnancy. It emerged that the (*R*)-enantiomer gives the sedative hypnotic properties, whereas the (*S*)-enantiomer is responsible of the dramatic teratogenic side-effects. It appears the acidic hydrogen situated on the stereogenic centre is able to epimerise rapidly under physiological conditions, a process that can be prevented by substitution of the hydrogen by fluorine such as in **32c**.[41]

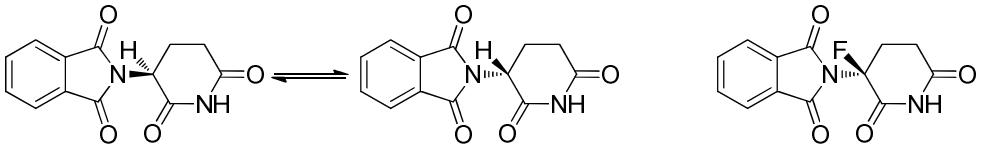

(3S)-thalidomide **32a** *(3R)*-thalidomide **32b** *(3R)*-fluorothalidomide **32c**

Scheme 1.7: Epimerisation of thalidomide **32**.

1.5.3- Protein–Ligand interactions

The presence of fluorine on a ligand will affect its binding to a target protein. The fluorination can have a direct effect where it makes interactions with the protein. But indirect effects can also result from the fluorine modulating the polarity of proximate functional groups of the ligand, which then directly interact with the protein. As discussed in **Section 1.5.1.2**, introduction of fluorine generally increases lipophilicity, which results in a global and non-specific enhancement of the binding affinities of drugs. For example, the case of $5HT_{1D}$ agonists quoted in **Section 1.5.1.1** illustrates how the change of acidity can indirectly affect the binding.

1.5.3.1- Electrostatic interactions

Diederich and Müller introduced the concept of fluorophilicity/fluorophobicity of a protein active site. They suggested that fluorine has specific properties which cannot easily be classified as hydrophobic or lipophilic.[47] They reported the systematic fluorine substitution of a thrombin inhibitor in order to explore the fluorophilicity of the thrombin active site, concluding that the C–F···C=O protein-ligand interactions increase binding affinities. Indeed, the fluorinated thrombin inhibitor analogue **33** displayed a five-fold higher activity than the corresponding non-fluorinated compound. The X-ray crystal structure of the protein-ligand complex showed that the amide carbonyl groups on the protein backbone provided a fluorophilic environment (**Figure 1.14**).

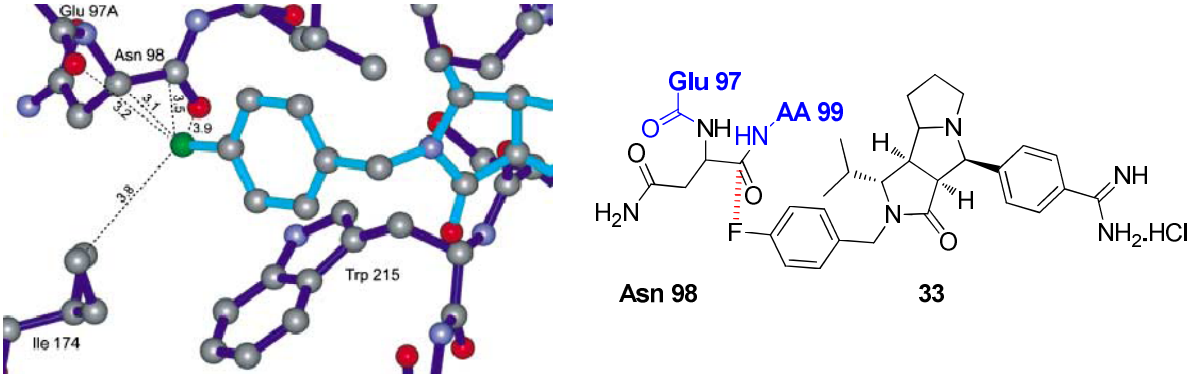

Figure 1.14: Direct polar interaction between fluorine and an amide carbonyl group.[47]

As illustrated in **Figure 1.14**, the fluorine atom of the inhibitor **33** is making a direct polar interaction with the carbonyl moiety of Asn 98 of thrombin and is positioned close to the trigonal axis of the carbonyl. This result is interesting as amide carbonyl groups are numerous and an integral part of protein active sites. Therefore, such a strategy offers a solution for using fluorine to enhance ligand affinity in structure-based drug design.

1.5.3.2- Hydrogen bonding

Pauling stated that the strength of the hydrogen bond increases with the electronegativity of the donor atom. Therefore, it is expected that for chlorine, nitrogen, oxygen and fluorine, their hydrogen bonds strength should increase in this order. This hypothesis was corrected by Pauling himself: "It is interesting that in general fluorine atoms attached to carbon do not have significant power to act as proton acceptors in the formation of hydrogen bonds in the way that would be anticipated from the large difference in electronegativity of fluorine and carbon."[48]

Dunitz *et al.*[49] and O'Hagan *et al.*[50] evaluated, in parallel studies, the propensity of fluorine to act as a hydrogen bonding acceptor. These studies reviewed short F···H contacts from X-ray structures deposited in the Cambridge Crystallographic Data Center (CCDC) (**Table 1.6**).

	Number of structures	**Short C–F···H–X contact (length)**
Dunitz	5947	37 (≤ 2.3 Å)
O'Hagan	548	166 (≤ 2.35 Å) 1 (≤ 2.0 Å)

Table 1.6: Studies of short C–F···H–X contact.[50]

Amongst the 37 compounds found by Dunitz *et al.* containing C–F···H–X distances less than 2.3 Å, only two could be considered as hydrogen bonds and the others as weak interactions. They offered two reasons to explain this paradox. In the formation of a hydrogen bond, donors and acceptors must present a similar proton affinity. Thus the energies of the two orbitals competing for the proton must be close, which is not the case with fluorine as its 2p orbital binding energy is 3 eV higher than that of oxygen (2p) and 6 eV higher than that of nitrogen (2p).[51]

Other parameters highlighted the role played by electron delocalisation within molecules and cooperativity in extended systems. Contrary to oxygen (carbonyl) and nitrogen (imine), which both attract electrons through their π-systems, fluorine can only engage in single bonds. Covalently bonded fluorine shows a partial negative charge, but this is counter-balanced with its low proton affinity (low basicity, low-lying lone pair orbitals, and tightness of the electron shell). Therefore, covalently bonded fluorine can only engage in weak polar interactions rather than hydrogen bonds.

1.5.4- Fluorine in nuclear medicine

Radioisotopes are used in nuclear medicine for both diagnosis and treatment of disease. Positron emission tomography (PET) is a non-invasive medical imaging technique that allows the *in vivo* assessment, at a high-resolution level, of metabolic processes. The applications are very varied, because diverse physiological parameters can be analysed, *i.e.* blood flow, drug distribution metabolism.[52] The most common isotopes (^{18}F, ^{11}C, ^{13}N, ^{15}O) are also the most common elements in organic chemistry and, therefore, the constituents of all biological molecules. The process of producing a radiolabeled PET tracer is a complex task, but has to be carried out in the restricted time frame of the radioisotope short-life. Because fluorine-18 has a longer half-life (110 min), it is the most suitable for clinical research and investigations (**Table 1.7**).

Radionuclide	^{11}C	^{13}N	^{15}O	^{18}F
$t_{1/2}$ (min)	20	10	2	110

Table 1.7: Common positron emitting radionuclides and their half-lives.

The ^{18}F isotope is generated by a cyclotron, in which ^{18}O enriched water is bombarded by accelerated protons (H^+). The resultant ^{18}F fluoride ion is then introduced chemically into a radiotracer *via* a potassium salt complex (**Scheme 1.8**).

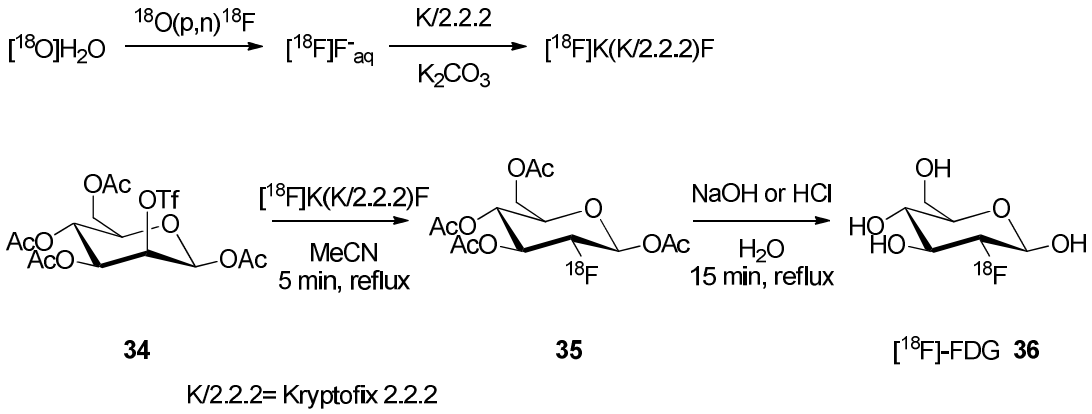

Scheme 1.8: Radiosynthesis of [^{18}F]-FDG.

Currently, the number of radiotracers in clinical use is increasing, but the most commonly used is 2-deoxy-2-[^{18}F]-fluoro-D-glucose ([^{18}F]-FDG) **36**. As a glucose analogue, this compound is adapted to the detection of glucose metabolic pathways, including brain, kidney or cancer cells detection.[41] After its absorption, [^{18}F]-FDG is phosphorylated at C-6, which prevents its release from the cell. The absence of a hydroxyl group at the C-2 position blocks **36** entering the glycolysis pathway. Consequently, [^{18}F]-FDG-6-phosphate remains within the cell until the ^{18}F decays and its accumulation is measured by a positron emission camera.[53]

The radiosynthesis of [^{18}F]-FDG has been optimised and takes only 20 min in a two step protocol. Fluorination occurs by nucleophilic substitution of [^{18}F] fluoride to triflate as illustrated in **Scheme 1.8**. The rapid hydrolysis of the acetylated sugar provides [^{18}F]-FDG.

Beyond uses in oncology, a new field for radiotracers is now emerging to help in the drug development process, as for *in vivo* visualisation of the drug biodistribution. With this technique, Merck studied the NK_1 receptor occupancy by the drug candidate Apprepitant **37**, a drug used to reduce nausea in patients undergoing chemotherapie (**Figure 1.15**).

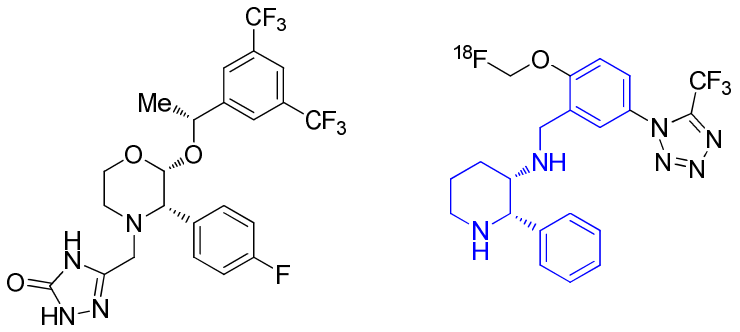

Aprepitant **37** [^{18}F]SPA-RQC **38**

Figure 1.15: The drug Aprepitant and its tracer in PET imaging.[54]

The calculation of NK_1 receptors prevalence is based on a comparison of brain PET images before and after the drug trial. A selective radiotracer for NK_1 receptors, [^{18}F]SPA-RQC **38**, mimicking the core of Aprepitant **37** (highlighted in blue in **Figure 1.15**), was injected to healthy volunteers.[54] The purpose of this PET study is to evaluate drugs in early clinical development with small amounts of product. Combination of this technique with structure-activity relationships refines the approach towards drug development even though it requires specifically designed radiotracers.

1.6- Methods of fluorination

Approaches to chemical fluorination can be classified under three categories. The fluorine atom can be installed *via* an electrophilic fluorinating reagent, a nucleophilic attack by fluoride ion, or with the use of a fluorinated building-block. Recent developments have generated the necessity to introduce fluorine in a stereoselective manner, notably in medicinal chemistry. The following section will describe the most commonly used fluorinating reagents and review the latest methods of asymmetric fluorination.

1.6.1- Nucleophilic reagents for fluorination

Fluoride ions are sensitive to solvation thus rendering them less nucleophilic. Conversely, aprotic solvents such as DMF or acetonitrile strengthen the nucleophilicity, but also the basicity of fluoride. The first sources of fluoride involved metallic fluorides with metals such as potassium (KF), sodium (NaF), cesium (CsF) and silver (AgF). Ammonium fluorides such as tetrabutylammonium fluoride (TBAF) **39** effectively improved the nucleophilicity of fluoride. The large sterically hindered cation tetrabutylammonium can delocalize the positive charge and thus reduces the ion pairing (**Figure 1.16**).

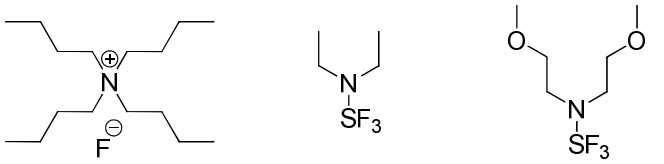

TBAF **39** DAST **40** Deoxo-Fluor **41**

Figure 1.16: Common nucleophilic reagents for fluorination.

Nucleophilic fluorination can be carried out with solutions of hydrofluoric acid (HF) complexed to amines. Neat HF is not anymore considered in the laboratory day-to-day use because of its high toxicity and corrosive properties. Olah's reagent is a complex of HF and pyridine (70:30). This reagent is still very corrosive and is often replaced by triethylamine in Et_3N-3HF.

The sulfur fluorides (S–F) reagents form another class of nucleophilic reagents where fluoride is combined with a soft Lewis base. The first reagent was sulfur tetrafluoride SF_4. This toxic gas was not easy to handle and stability was improved by replacing one of the fluorines by a dialkylamine. The dialkylamino group reduces the reactivity of the reagent due to its inductive effect and steric hindrance. Amongst such regents are diethylaminosulfur trifluoride (DAST) **40** and Deoxo-fluor® **41** (**Figure 1.16)**. DAST[55] still has the disadvantage that it can decompose spontaneously, particularly on heating. The second generation reagent Deoxo-fluor® emerged with improved stability over DAST and can be used at temperatures above 90°C without degradation or danger of explosion. Deoxofluor is also cost-efficient and can be used as an alternative for large scale syntheses.[56]

Other reagents such as Ishikawa's reagent ($F_3CCHFCF_2NEt_2$) and Yakorenko's reagent ($ClCHFCF_2NEt_2$) for fluorodeoxygenation reactions have been reported but their use and availability remains limited. Tetrafluorodiethylamine (TFEDMA) **42** developed by DuPont® is the adduct of tetrafluoroethylene and dimethylamine. 4-*tert*-Butyl-2,6-dimethylphenyl-sulfur trifluoride marketed as FLUOLEAD® **43** is the latest fluorination reagent, introduced onto the market in 2009, and therefore its scope is not yet well-defined (**Figure 1.17**).

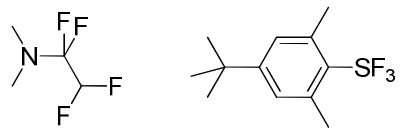

TFEDMA **42** FLUOLEAD **43**

Figure 1.17: Recently commercialised nucleophilic reagents.

DAST is often used to mediate the fluorodeoxygenation of alcohols. The mechanism involves nucleophilic attack by the hydroxyl group of the substrate to generate a reactive intermediate **45**. The configuration at carbon is inverted after nucleophilic attack of the intermediate by fluoride (**Scheme 1.9**).

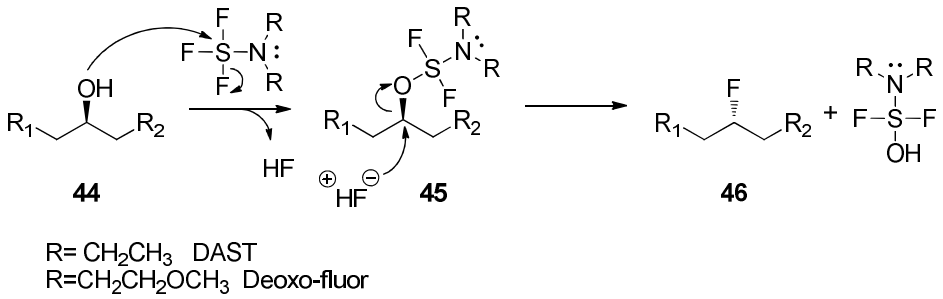

Scheme 1.9: Mechanism of fluorodeoxygenation by DAST or Deoxo-fluor.

However DAST can also promote elimination reactions due to the strong basicity of fluorides as illustrated in **Scheme 1.10** where cyclooctanol **47** when treated with DAST, lead to the formation of (*Z*)-cyclooctene **49** along the desired fluorocyclooctane **48**.[10]

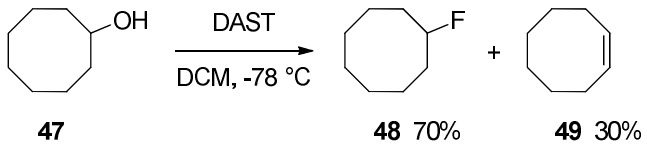

Scheme 1.10: DAST-mediated fluorodeoxygenation can induce elimination.[10]

Schlosser developed a strategy for opening epoxides to convert them in a stereoselective manner to vicinal difluorides.[57] The epoxide (*R,S*)-**50** is first opened using HF/Et_3N, with an inversion of configuration at carbon. The second fluorine is introduced by nucleophilic attack

of the hydroxyl group of (*R,R*)-**51** by fluoride to give the *anti* vicinal difluoro product **52** (**Scheme 1.11**).

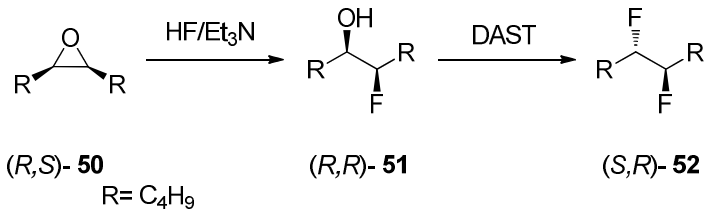

Scheme 1.11: Fluorodeoxygenation of alcohols.[57]

Recent work in the group at St-Andrews has consisted of controlling the installation of several vicinal fluorines. The new compounds have a degree of fluorination intermediate between alkanes and perfluoroalkanes. The research group has prepared single isomers of compounds with four **53**, five **54** and six **55** vicinal fluorine to study their conformations.[58, 59]

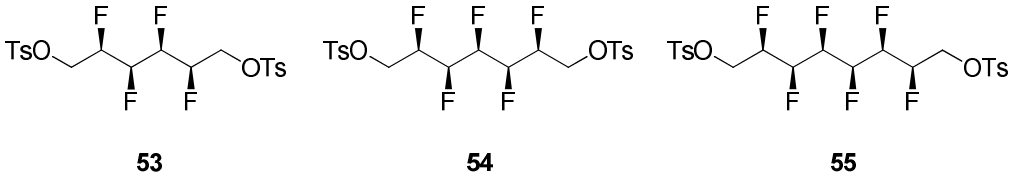

Figure 1.18: Example of four, five and six vicinal fluorine compounds.

The synthesis of the tetrafluoroisomer **53** started with 3 HF/Et_3N mediated regioselective ring-opening of the enantiopure (*R*)- butadiene oxide **56** as illustrated in **Scheme 1.12**. A loss of enantiopurity was observed in the reaction, due to its partial S_N1 character. However, a very high enantiopurity was recovered during the homo cross-metathesis reaction of the allyl fluoride **58**. Separation of *(S,S)* and *(S,R)* isomers of **59** on silica gel chromatography allowed

the major (*S,S*) product to be obtained in 98% ee. Dihydroxylation of the latter with potassium permanganate generated the difluoro diol **60** in a 4:1 dr. After removal of the minor isomer, the subsequent cyclic sulfate **61** was opened stereoselectively by nucleophilic attack of fluoride ion using TBAF. The fourth fluorine atom was installed with Deoxo-fluor after swapping the terminal protective groups from benzyl ethers to tosyl esters. In this study, the absolute configuration of each stereocenter was confirmed by X-ray crystal structure analysis. Interestingly, these all *syn* compound have a helical nature.

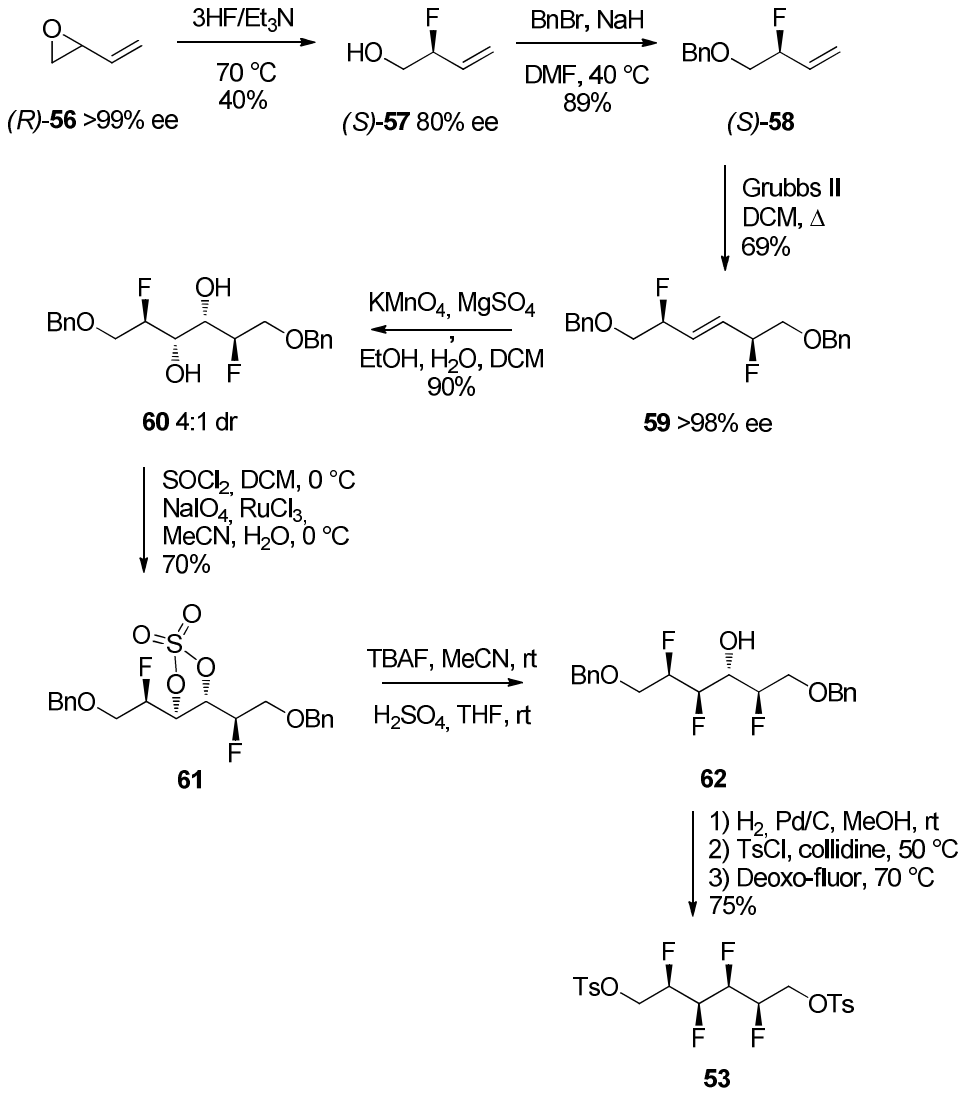

Scheme 1.12: Synthesis of a tetra- vicinal fluorinated compound.[58]

1.6.2- Electrophilic reagents for fluorination

The first electrophilic fluorination reagent to be developed was elemental fluorine F_2. This reagent is highly reactive and has the disadvantage of being explosive and promoting exothermic reactions. Despite its toxicity and lack of selectivity, it was used since the 1950s on a routine basis in industry and on a large scale. Elemental fluorine F_2 is generally diluted in an inert gas such as nitrogen or argon.

A good example is the synthesis of the anti-cancer agent 5-fluorouracil (5-FU) **6** in acetic acid as solvent (**Scheme 1.13**).[60] Elemental fluorine requires specific equipment to handle which limits its use in academic laboratories.

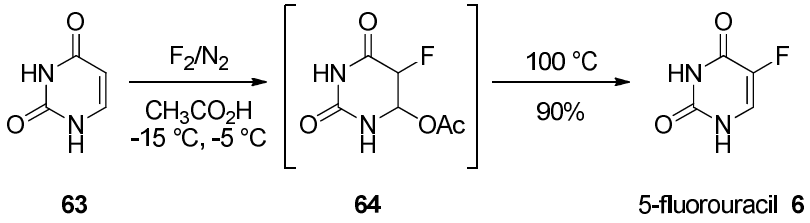

Scheme 1.13: Synthesis of 5-fluorouracil with elemental fluorine.[60]

A second generation of F^+ reagents involved a fluorine atom directly bonded to oxygen or nitrogen atoms. Hypofluorites reagents activate fluorine by oxygen. This class of reagents (for instance CH_3COOF, CF_3OF) has been abandoned due to their lack of selectivity and strong oxidative properties. Nitrogen offers a lower electronegativity relative to oxygen and as a consequence, the *N*–F bond is stronger. This increased strength renders the reagents more stable and easier for laboratory handling. *N*–F reagents have proved to be important in the field of electrophilic fluorination reagents (**Figure 1.19**). Selectfluor (F-TEDA-BF_4) **65** [61] and *N*-fluoropyridinium triflate **66** [62] show greatly improved selectivity compared to F_2. Another

class of commonly used *N*–F reagents are the sulfonyl derivatives *N*-fluoro-*O*-benzene-disulfonimide (NFOBS) **67**,[63] and *N*-fluorobenzenesulfonimide (NFSI) **68**.[64]

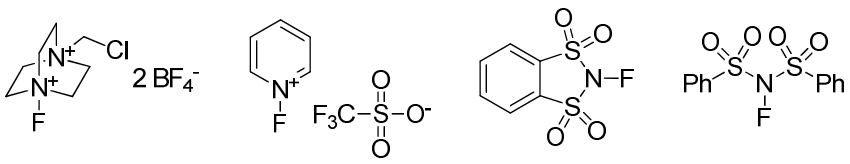

Selectfluor **65** | *N*-Fluoropyridinium triflate **66** | NFOBS **67** | NFSI **68**

Figure 1.19: Electrophilic reagents for fluorination.

1.6.3- Enantioselective monofluorination

Asymmetric fluorination has evolved rapidly over the last decade and many efficient methods have been developed. Such fluorinations can be controlled in a regio- and stereo- selective manner with the use of approaches driven by the substrate itself, the reagent, or the catalyst. Such approaches are outlined in this section, including different methods to achieve the stereoselective fluorination for molecules of wide general interest.

1.6.3.1- Substrate control

An important approach to stereoselective fluorination is to install the fluorine atom after coupling of the target molecule to a chiral auxiliary. The chiral auxiliary requires removal after the fluorination, which lengthens the synthetic pathway. However, many successful examples of the use of an oxazolidinone as a chiral auxiliary have been provided by Evans or

Davis (**Scheme 1.14**).[65, 66] The diastereoselectivity of these reactions is controlled by the oxazolidone enolate. Fluorination is then achieved by reactions with electrophilic fluorinating reagents such as NFOBS or NFSI.

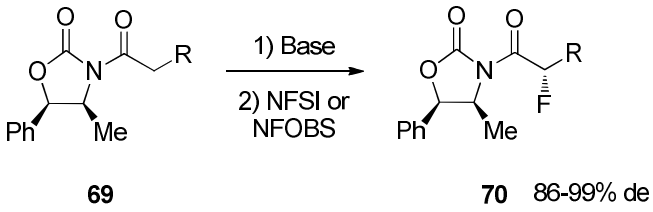

Scheme 1.14: Asymmetric fluorination using chiral oxazolidinone methodology.

1.6.3.2- Reagent control

Cinchona alkaloids offer non-expensive biomolecules for asymmetric organocatalysis. They also have the potential for structural modification. The combination of cinchona alkaloids with Selectfluor was developed independently by Cahard in France[67] and Shibata in Japan (**Scheme 1.15**).[68]

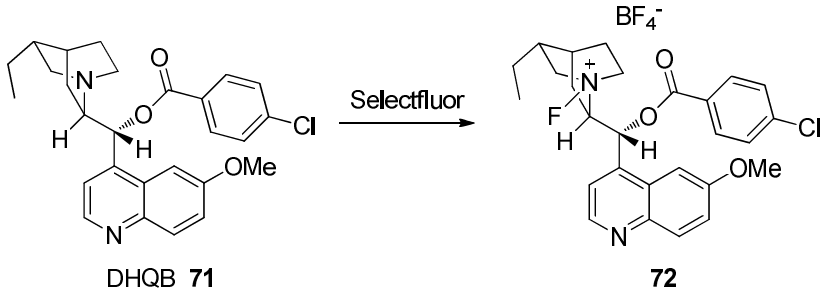

Scheme 1.15: Preparation of dihydroquinine electrophilic fluorinating reagent.

In the following example, dihydroquinine **71** promoted the catalytic electrophilic fluorodesilylation of **73** (**Scheme 1.16**).[68]

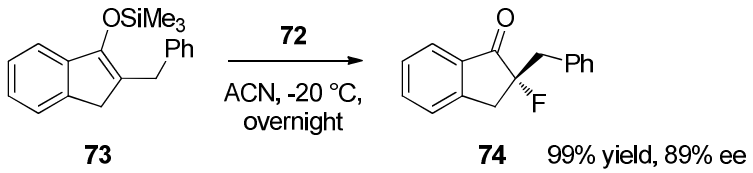

Scheme 1.16: Example of cinchona alkaloids mediated enantioselective fluorination.[68]

The *N*-fluoroalkaloid is generated *in situ* prior to electrophilic addition of the substrate. The reaction involves a fluorine transfer from the reagent to the alkaloid to make a tertiary fluoroammonium salt **72**. This method requires stoichiometric amounts of cinchona alkaloids, thus selectivity issues occur in the case of sub-stoichiometric conditions. The efficiency of the method, however, is in the faster rate of transfer of fluorine onto the cinchona alkaloid rather than the direct reaction of Selectfluor with the enolate.

1.6.3.3- Catalyst control

Catalyst control covers a large field of methods, from metal complexes to organocatalysts. The TADDOL auxiliary chelates to various metals e.g. Mg, Pd, or Ti. TADDOL derivatives can promote enantioselective synthesis as a stoichiometric chiral reagent, but they are also widely used for catalytic hydrogenation or even metathesis polymerisation.

Togni constructed a titanium-based TADDOL complex **75** to catalyse the first Lewis acid-catalysed enantioselective α-fluorination of branched β-keto-esters **76** (**Scheme 1.17**).[69]

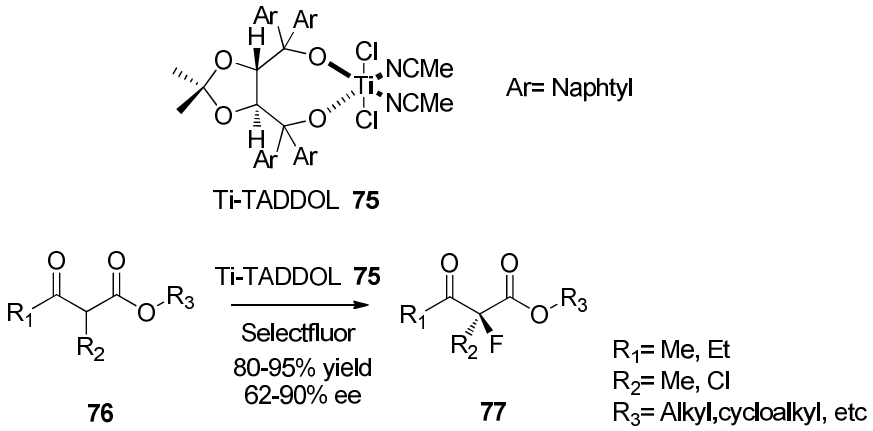

Scheme 1.17: TADDOL–modified titanium complex.[69]

The suggested mechanism of fluorination of the β-keto-esters **76** is illustrated below (**Scheme 1.18**), where titanium promotes the formation of the enolate complex. Consequently, the TADDOL derivative blocks one face of the enolate complex and thus favors a *Si*-face attack.

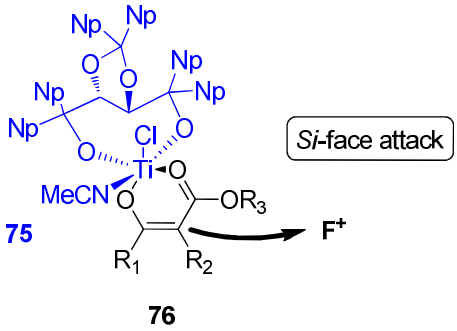

Scheme 1.18: Ti-TADDOL orientates a *Si*-facial attack.

Cahard and Shibata have also reported catalytic asymmetric fluorination of β-keto esters using PheBOX catalysts.[70, 71] PheBOX is a C*2*-symmetric bis (oxazoline) metal complex, used in association with NFSI as the source of F^+. Their studies have also shown the importance of the metal in the enantioselective process. The relative coordination symmetry of the metal is found to control the enantioselectivity of the reaction. For instance, Cu and Ni complexed to *(S)*-PheBOX **78**, provide the opposite stereoinduction (**Scheme 1.19**).

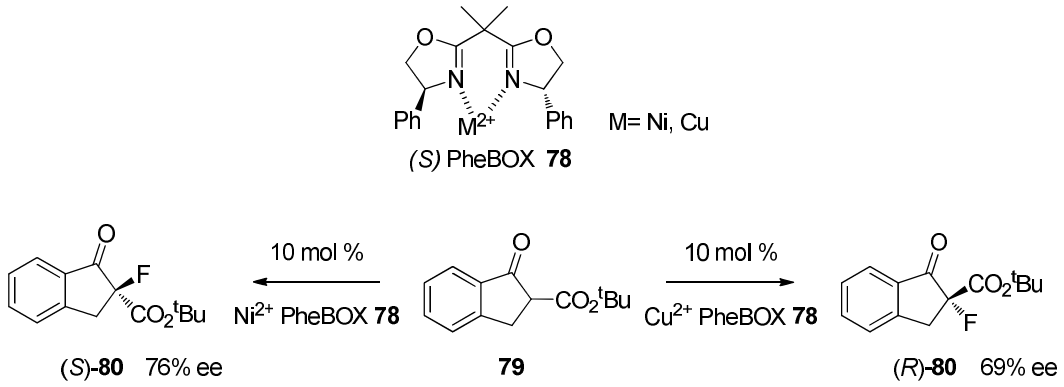

Scheme 1.19: Reversible enantioselection induced by PheBOX-metal complexes.

Organocatalysts have been a growth area in recent years in organic chemistry. An early example was described in 1971, with the enantioselective intramolecular aldol reaction catalysed by (*S*)-proline. Fluorination of carbonyl compounds has taken advantage of chiral amines as catalysts, with electrophilic fluorine reacting on enamine or iminium intermediates. In 2005, the first asymmetric fluorination controlled by an organocatalyst was carried out on aldehydes and ketones by Enders and Hüttl.[72] Their best result was obtained on cyclohexanone **82** with the silylated L-hydroxyproline **81**, but the reaction proved to be slow and with a poor enantioselectivity (34% ee) (**Scheme 1.20**).

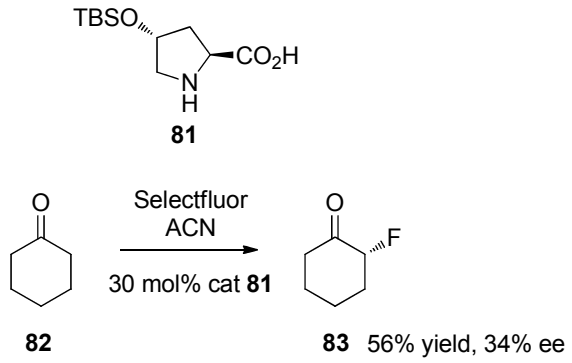

Scheme 1.20: Direct organocatalytic α-fluorination of cyclohexanone.[72]

There was a subsequent focus on this asymmetric fluorination, and in the same year, Jørgensen, Barbas, and MacMillan all independently offered new solutions to decrease the enolisation of the product by improving the design of the organocatalyst. For instance, Jørgensen reported the enantioselective α-fluorination of an aldehyde **85** with NFSI and at only 1% loading of catalyst (**Scheme 1.21**).[73] The bulky silylated prolinol **84** proved to be more reactive than the original L-proline. The high enantioselectivity (up to 97%) is explained by blockage of the *Re*-face of the enamine intermediate by the bulky substituents of the proline derivative.

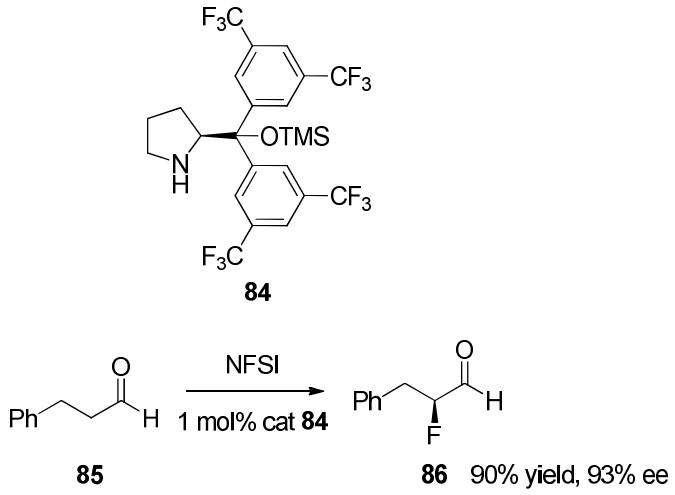

Scheme 1.21: Jorgensen organocatalytic α-fluorination.[73]

Barbas[74] and MacMillan[75] developed imidazolidones **87** and **88** for the α-fluorination of aldehydes (**Figure 1.20**).

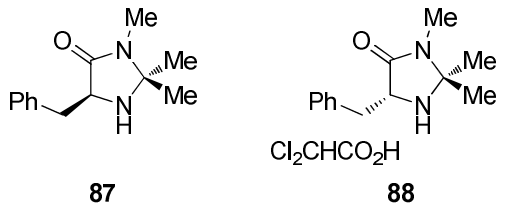

87 **88**

Figure 1.20: Imidazolidinones for α-fluorination of aldehydes.

They used higher loadings of their catalysts (20-30 mol%) and as in Jørgensen's work, NFSI proved the best source of F^+ (**Scheme 1.22**).

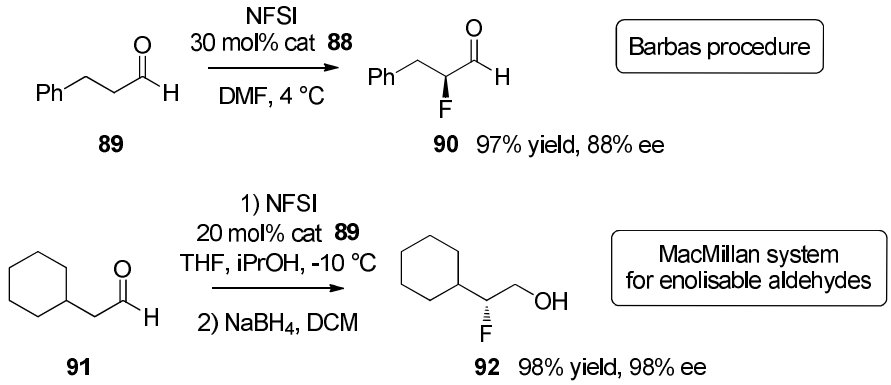

Scheme 1.22: Enantioselective α-fluorination of aldehydes by imidazolidone organocatalysts.[74, 75]

Although the yields and enantioselectivities were excellent, for analyses and purification purposes, the unstable *α*-fluorinated aldehydes had to be derivatized *in situ* either by reduction to their corresponding alcohols or reaction to hydrazones.

1.7-Conclusion

This chapter has highlighted the singular properties of fluorine and how it can be used to influence the behaviour and metabolism of biologically active molecules. The introduction of fluorine onto a lead molecule often increases its pharmacokinetic properties. Fluorine can form weak interactions with proteins and provide a more active molecule. The recent developments in asymmetric synthesis accompanied by the introduction to the market of new fluorinating reagents have generated a variety of new methods for creating C–F bonds in organic chemistry and in an enantioselective manner, either by electrophilic or nucleophilic fluorination processes.

1. W. Krasny-Ergen, *Nature*, 1940, **145**, 742-743.
2. W. R. Dolbier, *J. Fluorine Chem.*, 2005, **126**, 157-163.
3. P. Jeschke, *ChemBioChem*, 2004, **5**, 570-589.
4. J. Fried and E. F. Sabo, *J. Am. Chem. Soc.*, 1954, **76**, 1455-1456.
5. J. Fried and E. F. Sabo, *J. Am. Chem. Soc.*, 1953, **75**, 2273-2274.
6. C. Heidelberger, N. K. Chaudhuri, P. Danneberg, D. Mooren, L. Griesbach, R. Duschinsky, R. J. Schnitzer, E. Pleven and J. Scheiner, *Nature*, 1957, **179**, 663-666.
7. D. B. H.-J. Böhm, S. Bendels, M. Kansy, B. Kuhn, K. Müller, U. Obst-Sander, and M. Stahl, *ChemBioChem*, 2004, **5**, 637-643.
8. W. K. Hagmann, *J. Med. Chem.*, 2008, **51**, 4359-4369.
9. L. N. Markovskii, V. E. Pashinnik and A. V. Kirsanov, *Synthesis*, 1973, 787-789.
10. W. J. Middleton, *J. Org. Chem.*, 1975, **40**, 574-578.
11. Z. M. Stadt, *N. C. Med. J.*, 1948, **9**, 23-30.
12. J. W. Nicholson and B. Czarnecka, *Fluorine Health*, 2008, 333-378.
13. P. H. Phillips, J. G. Halpin and E. B. Hart, *J. Nutr.*, 1935, **10**, 93-98.
14. G. L. Kennedy, J. L. Butenhoff, G. W. Olsen, J. C. O'Connor, A. M. Seacat, R. G. Perkins, L. B. Biegel, S. R. Murphy and D. G. Farrar, *Crit. Rev. Toxicol.*, 2004, **34**, 351 - 384.
15. C. Fei, J. K. McLaughlin, L. Lipworth and J. Olsen, *Hum. Reprod.*, 2009, **24**, 1200-1205.
16. C.-G. Zhan and D. A. Dixon, *J. Phys. Chem. A*, 2004, **108**, 2020-2029.
17. D. B. Harper and D. O'Hagan, *Nat. Prod. Rep.*, 1994, **11**, 123-133.
18. D. O'Hagan and D. B. Harper, *J. Fluorine Chem.*, 1999, **100**, 127-133.
19. J. S. C. Marais, *Onderstepoort J. Vet. Res.*, 1943, **18**, 203-206.
20. M. Sanada, T. Miyano, S. Iwadare, J. M. Williamson, B. H. Arison, J. L. Smith, A. W. Douglas, J. M. Liesch and E. Inamine, *J. Antibiot.*, 1986, **39**, 259-265.
21. X.-H. Xu, G.-M. Yao, Y.-M. Li, J.-H. Lu, C.-J. Lin, X. Wang and C.-H. Kong, *J. Nat. Prod.*, 2003, **66**, 285-288.
22. K. A. Reid, J. T. Hamilton, R. D. Bowden, D. O'Hagan, L. Dasaradhi, M. R. Amin and D. B. Harper, *Microbiology*, 1995, **141**, 1385-1393.
23. J. T. G. Hamilton, C. D. Murphy, M. R. Amin, D. O'Hagan and D. B. Harper, *J. Chem. Soc., Perkin Trans. 1*, 1998, 759-768.
24. D. O'Hagan, *J. Fluorine Chem.*, 2006, **127**, 1479-1483.

25. H. Deng, S. M. Cross, R. P. McGlinchey, J. T. G. Hamilton and D. O'Hagan, *Chem. Biol.*, 2008, **15**, 1268-1276.
26. L. E. Twigg and D. R. King, *Oikos*, 1991, **61**, 412-430.
27. J. T. G. Hamilton and D. B. Harper, *Phytochemistry*, 1997, **44**, 1129-1132.
28. S. O. Thomas, V. L. Singleton, J. A. Lowery, R. W. Sharpe, L. M. Pruess, J. N. Porter, J. H. Mowat and N. Bohonos, *Antibiot. Annu.*, 1957, 716-721.
29. A. R. Maguire, W. D. Meng, S. M. Roberts and A. J. Willetts, *J. Chem. Soc., Perkin Trans. 1*, 1993, 1795-1808.
30. C. D. Murphy, C. Schaffrath and D. O'Hagan, *Chemosphere*, 2003, **52**, 455-461.
31. D. O'Hagan, C. Schaffrath, S. L. Cobb, J. T. G. Hamilton and C. D. Murphy, *Nature*, 2002, **416**, 279.
32. M.-H. Ho, M. L. Klein and I. F. W. Kuo, *J. Phys. Chem. A*, 2009, **113**, 2070-2074.
33. A. K. Soper, *Phys. Rev. B Condens. Matter Mater. Phys.*, 2005, **72**, 104201-104212.
34. G. Beurskens and G. A. Jeffrey, *J. Chem. Phys.*, 1964, **41**, 917-923.
35. R. K. McMullan, M. Bonamico and G. A. Jeffrey, *J. Chem. Phys.*, 1963, **39**, 3295-3310.
36. M. A. Vincent and I. H. Hillier, *Chem. Commun.*, 2005, 5902-5903.
37. M. Morgenthaler, E. Schweizer, A. Hoffmann-Roder, F. Benini, E. Martin Rainer, G. Jaeschke, B. Wagner, H. Fischer, S. Bendels, D. Zimmerli, J. Schneider, F. Diederich, M. Kansy and K. Muller, *ChemMedChem*, 2007, **2**, 1100-1115.
38. M. B. van Niel, I. Collins, M. S. Beer, H. B. Broughton, S. K. F. Cheng, S. C. Goodacre, A. Heald, K. L. Locker, A. M. MacLeod, D. Morrison, C. R. Moyes, D. O'Connor, A. Pike, M. Rowley, M. G. N. Russell, B. Sohal, J. A. Stanton, S. Thomas, H. Verrier, A. P. Watt and J. L. Castro, *J. Med. Chem.*, 1999, **42**, 2087-2104.
39. K. Muller, C. Faeh and F. Diederich, *Science*, 2007, **317**, 1881-1886.
40. M. A. Massa, D. P. Spangler, R. C. Durley, B. S. Hickory, D. T. Connolly, B. J. Witherbee, M. E. Smith and J. A. Sikorski, *Bioorg. Med. Chem. Lett.*, 2001, **11**, 1625-1628.
41. S. Purser, P. R. Moore, S. Swallow and V. Gouverneur, *Chem. Soc. Rev.*, 2008, **37**, 320-330.
42. S. B. Rosenblum, T. Huynh, A. Afonso, H. R. Davis, N. Yumibe, J. W. Clader and D. A. Burnett, *J. Med. Chem.*, 1998, **41**, 973-980.
43. T. D. Penning, J. J. Talley, S. R. Bertenshaw, J. S. Carter, P. W. Collins, S. Docter, M. J. Graneto, L. F. Lee, J. W. Malecha, J. M. Miyashiro, R. S. Rogers, D. J. Rogier,

S. S. Yu, G. D. Anderson, E. G. Burton, J. N. Cogburn, S. A. Gregory, C. M. Koboldt, W. E. Perkins, K. Seibert, A. W. Veenhuizen, Y. Y. Zhang and P. C. Isakson, *J. Med. Chem.*, 1997, **40**, 1347-1365.

44. M. J. Cho and M. A. Allen, *Prostaglandins*, 1978, **15**, 943-954.
45. K. Bannai, T. Toru, T. Oba, T. Tanaka, N. Okamura, K. Watanabe, A. Hazato and S. Kurozumi, *Tetrahedron*, 1983, **39**, 3807-3819.
46. C.-S. Chang, M. Negishi, T. Nakano, Y. Morizawa, Y. Matsumura§ and A. Ichikawa, *Prostaglandins*, 1997, **53**, 83-90.
47. J. A. Olsen, D. W. Banner, P. Seiler, U. Obst Sander, A. D'Arcy, M. Stihle, K. Müller and F. Diederich, *Angew. Chem. Int. Ed.*, 2003, **42**, 2507-2511.
48. L. C. Pauling, *The Nature of the Chemical Bond and the Structure of Molecules and Crystals. An Introduction to Modern Structural Chemistry. 3rd ed*, 1960.
49. J. D. Dunitz and R. Taylor, *Chem. Eur. J.*, 1997, **3**, 89-98.
50. J. A. K. Howard, V. J. Hoy, D. O'Hagan and G. T. Smith, *Tetrahedron*, 1996, **52**, 12613-12622.
51. H. O. Pritchard and H. A. Skinner, *Chem. Rev.*, 1955, **55**, 745-786.
52. R. Hustinx and A. Alavi, *Handb. Radiopharm.*, 2003, 629-642.
53. S. Ben-Haim and P. Ell, *J. Nucl. Med.*, 2009, **50**, 88-99.
54. M. Bergström, R. J. Hargreaves, H. D. Burns, M. R. Goldberg, D. Sciberras, S. A. Reines, K. J. Petty, M. Ögren, G. Antoni, B. Långström, O. Eskola, M. Scheinin, O. Solin, A. K. Majumdar, M. L. Constanzer, W. P. Battisti, T. E. Bradstreet, C. Gargano and J. Hietala, *Biological Psychiatry*, 2004, **55**, 1007-1012.
55. W. J. Middleton, *J. Org. Chem.*, 2002, **40**, 574-578.
56. G. S. Lal, G. P. Pez, R. J. Pesaresi, F. M. Prozonic and H. Cheng, *J. Org. Chem.,* 1999, **64**, 7048-7054.
57. T. Hamatani, S. Matsubara, H. Matsuda and M. Schlosser, *Tetrahedron*, 1988, **44**, 2875-2881.
58. L. Hunter, D. O'Hagan and A. M. Z. Slawin, *J. Am. Chem. Soc.*, 2006, **128**, 16422-16423.
59. D. Farran, A. M. Z. Slawin, P. Kirsch and D. O'Hagan, *J. Org. Chem.*, 2009, **74**, 7168-7171.
60. R. Filler, *Organofluorine chemicals and their industrial applications*, edited by R. E. Banks & E. Horwood, 1979, 123-153.
61. R. E. Banks, *J. Fluorine Chem.*, 1998, **87**, 1-17.

62. T. Umemoto, K. Kawada and K. Tomita, *Tetrahedron Lett.*, 1986, **27**, 4465-4468.
63. F. A. Davis and W. Han, *Tetrahedron Lett.*, 1991, **32**, 1631-1634.
64. E. Differding and H. Ofner, *Synlett*, 1991, 187-189.
65. F. A. Davis and W. Han, *Tetrahedron Lett.*, 1992, **33**, 1153-1156.
66. F. A. Davis and P. V. N. Kasu, *Tetrahedron Lett.*, 1998, **39**, 6135-6138.
67. D. Cahard, C. Audouard, J.-C. Plaquevent and N. Roques, *Org. Lett.*, 2000, **2**, 3699-3701.
68. N. Shibata, E. Suzuki and Y. Takeuchi, *J. Am. Chem. Soc.*, 2000, **122**, 10728-10729.
69. L. Hintermann and A. Togni, *Angew. Chem.*, 2000, **39**, 4359-4362.
70. J.-A. Ma and D. Cahard, *Tetrahedron: Asymmetry*, 2004, **15**, 1007-1011.
71. N. Shibata, T. Ishimaru, T. Nagai, J. Kohno and T. Toru, *Synlett*, 2004, 1703-1706.
72. D. Enders and M. R. M. Huettl, *Synlett*, 2005, 991-993.
73. M. Marigo, D. Fielenbach, A. Braunton, A. Kjærsgaard and K. A. Jørgensen, *Angew. Chem. Int. Ed.*, 2005, **44**, 3703-3706.
74. D. D. Steiner, N. Mase and C. F. B. III, *Angew. Chem. Int. Ed.*, 2005, **44**, 3706-3710.
75. T. D. Beeson and D. W. C. MacMillan, *J. Am. Chem. Soc.*, 2005, **127**, 8826-8828.

2- α-Fluorinated capsaicins to alter the biological response of TRPV1 pain receptor

2.1- Introduction

Over the last decade TRPV1 (transient receptor potential vanilloid subtype 1) has become the model receptor for pain signal integration. This receptor constitutes an alternative for pain treatment to the commonly targeted COX pathway. Management of pain is essential for patients and the discovery of a new drug target constitutes a prime economical interest for pharmaceutical companies.

Pain is integrated as an electric signal on nerves by receptors sensitive to a broad array of stimuli. Such polymodal nociceptors can detect variations in temperature (heat/cold), mechanical changes (pressure, cuts) and chemical stimuli.[1] Activation of these receptors induces a gradual depolarisation of the membrane that can initiate action potentials when the membrane potential (typically at -70 mV during resting) reaches a threshold of intensity (-55 mV). Action potentials are conducted by the axon along the pain pathway to the central nervous system (CNS).

A strong noxious stimulus will spontaneously generate a physiological nociceptive pain, which proves to be useful to the body in playing a role in the protection of healthy tissues. Pain can also be induced by inflamed tissues. An inflammation is produced by the release of inflammatory mediators present in the nociceptor, and would typically be associated with symptomatic signs such as redness, heat, swelling and pain. The nociceptors have a unique expression profile of receptors, and then show a wide range of reactivity in the transduction of the stimuli into action potentials. The mechanism of transduction implies the opening of cation channels that leads to the depolarisation of the neuron endings. Another consequence of inflammation is the activation of additional ion channels and thus the intensity of sensory potentials is increased. One of these ion channels is TRPV1 (VR1 on **Figure 2.1**), a receptor with a preponderant action in the induction of thermal hyperalgesia.[2]

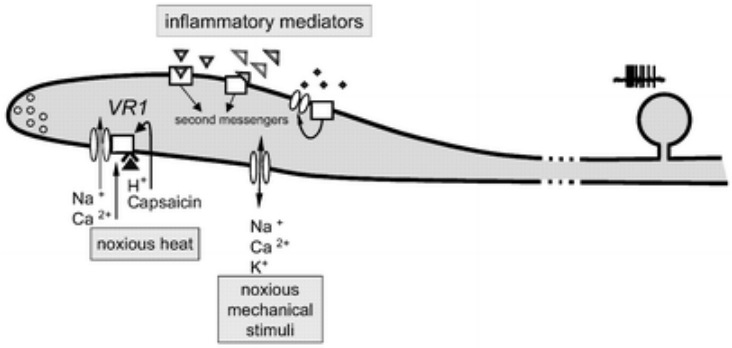

Figure 2.1: Sensitisation of neurons endings during inflammation.[3]

The TRPV1 receptor is also chemically activated by the plant natural product capsaicin **93**.[4] This receptor is of interest as a new drug target, as antagonists would expand the variety of molecules used to manage pain. Indeed, current drugs on the market such as aspirin **94**, ibuprofen **95** and celecoxib **96** (non-steroidal anti-inflammatory drugs NSAIDs, **Figure 2.2)** act on the cyclooxygenase (COX) pain pathway. They inhibit the synthesis of prostaglandins,

which are responsible for stimulating the common inflammatory mediators with the TRPV1 pathway, histamine and bradykinine.[5]

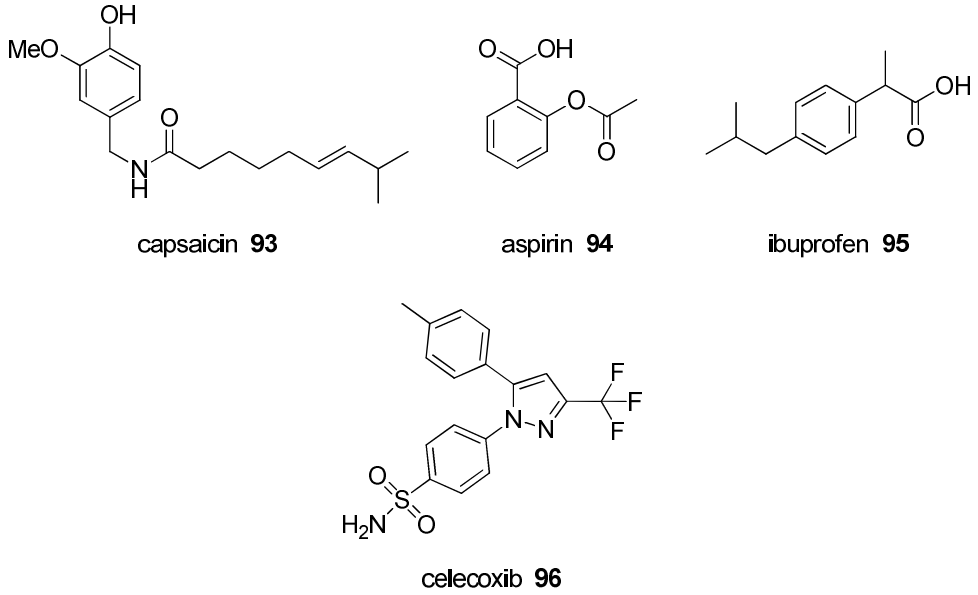

Figure 2.2: Structures of capsaicin and common NSAIDs.

Recent advances show interest in molecules that simultaneously act on the COX and the TRPV1 pathways.[6] Therefore, drug candidates which target the TRPV1 receptor certainly have potential as anti-inflammatory drug or for analgesic uses.

This study was aimed at testing the TRPV1 receptor response through various fluorinated analogues of its chemical mediator capsaicin **93**. It is proposed to investigate the synthesis of enantiomers of selectively fluorinated capsaicins **97a/ 97b** to establish whether fluorine could be used as a tool to evaluate the binding conformation of capsaicin on the receptor. Additionally, it was envisaged that fluorinated derivatives of capsaicin such as fluorodihydrocapsaicin **98a**/ **98b** and shorter analogues **99a** and **99b** could be prepared and explored as minimal capsaicin analogues (**Figure 2.3**).

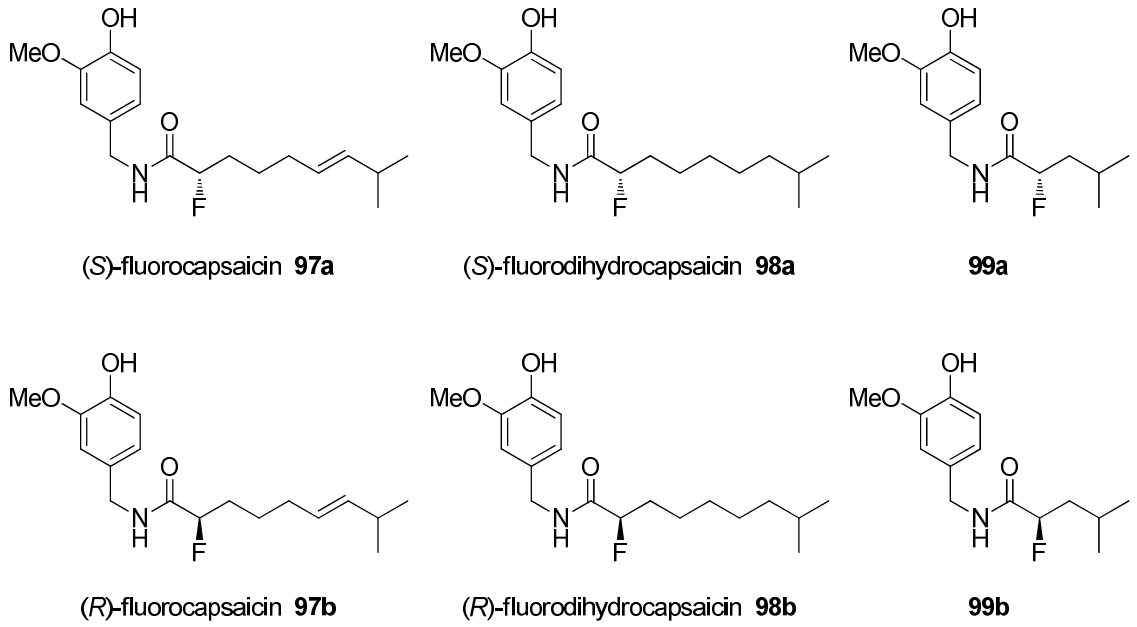

Figure 2.3: Target enantiomers fluoro-analogues of capsaicin.

The benefits brought to a molecule by the introduction of a single fluorine atom have been discussed in **Chapter 1.5**, in particular the modulation of its lipophilicity and pK_a. Nowadays, this approach is established in pharmaceuticals during the drug development process.

However, this study investigates a new approach to the use of fluorine in medicinal chemistry, in which the protein-ligand interactions are modified by a conformational change induced by installing a fluorine atom α- to the amide carbonyl. Indeed when a C–F bond is placed on an open chain structure adjacent to a carbonyl group such as in α-fluoroamides **100**, stereoelectronic effects dictate that the C–F bond is preferentially aligned antiparallel to the amide carbonyl and *syn* to the N–H (**Figure 2.4**).

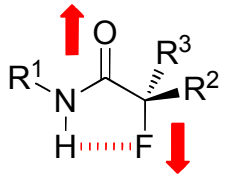

100

Figure 2.4: The conformational preference of α-fluoroamides **100**.

This effect was previously described by O'Hagan *et al.* in a study evaluating the rotational energy profile of *N*-methyl-2-fluoropropionamide **101**, illustrated in **Figure 2.5** (left).[7] There is a single minimum at 180° on the rotational energy profile of **101** calculated by *ab initio* computation, which corresponds to the anti-parallel *trans*-conformer resulting from C–F/C=O dipole-dipole relaxation. This *trans*-conformer is favoured over the *syn* by ~8 kcal.mol^{-1}.

X-Ray structure analysis of *N*-phenyl-2-fluoropropionamide **102** also showed the *trans*-conformation in the solid state (highlighted in red in **Figure 2.5**, right).

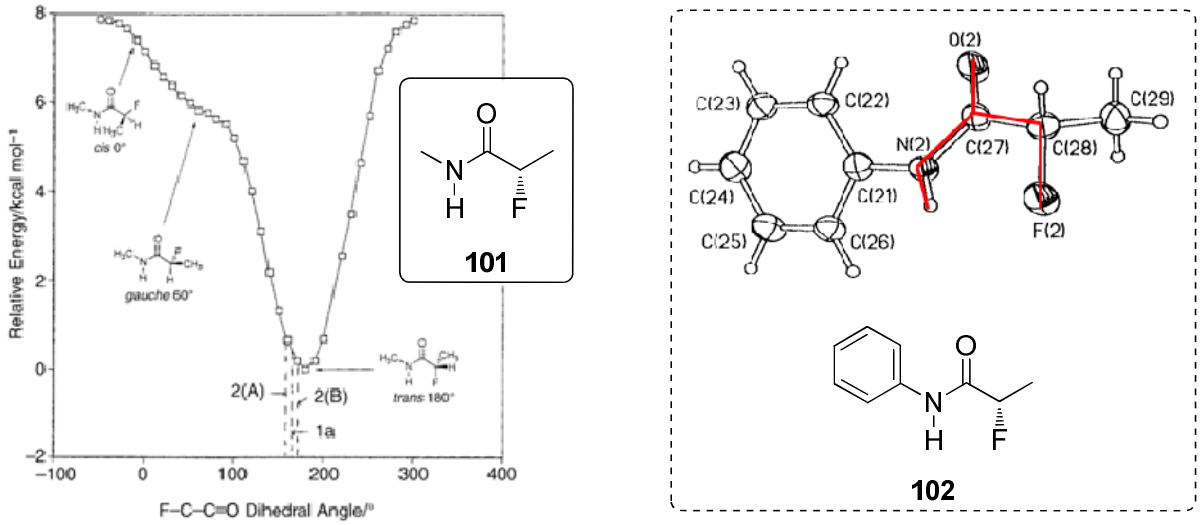

Figure 2.5: Rotational energy profile (**101**) and X-Ray structure (**102**) showing the preferred *anti* geometry of NH–CO–CF.[7]

Analysis of X-ray structures of α-fluoroamides confirms the planar preference, as in 2-fluoro-*N*-(2-fluoroethyl)-propionamide **103** (2°) and *N*-methyl-2-fluoropropionamide **101** (9.9°).[7, 8] A broader search in the Cambridge Structural Database (CSD) highlighted the preference for the antiperiplanar conformation of non-cyclic structures with F–C–C=O dihedral angles distributed between 150° and 200° (**Figure 2.6**).[9]

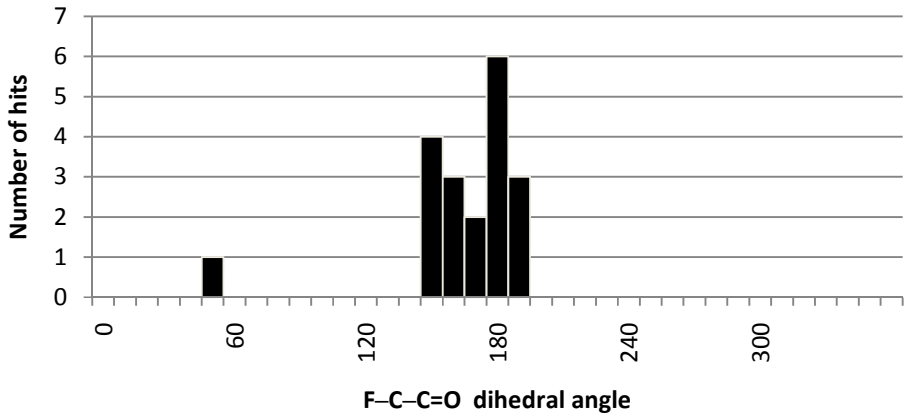

Figure 2.6: F–C–C=O dihedral angle in X-ray structures of α-fluoroamides in the CSD.[9]

As a consequence of this preference, the R^2 and R^3 groups connected to the fluorinated carbon are orientated in the predicted manner (**Figure 2.4**), with fluorine showing limited steric impact over hydrogen. Therefore, it is suggested that a C–F bond installed adjacent to an amide group could be used as a design tool to influence the conformation of bioactive amides. Extending this analysis to the case of capsaicin **93**, for the enantiomers of α-fluorocapsaicin **97**, the alkenyl side-chain will be enantiomerically orientated in different directions for each fluoro-enantiomer. Therefore the relative efficacies of these fluoro-enantiomers (*S*)-**97a** and (*R*)-**97b** might report an enantiomeric preference for side-chain binding to the TRPV1 receptor. As a consequence, it informs on the local chiral environment of the receptor, offering details on the spatial aspects of agonists or antagonist binding.

2.2- TRPV1 receptor

The vanilloid receptor (VR1) was cloned in 1997. It is an ion channel able to bind capsaicin and structurally related molecules.[10-12] Subsequently, this receptor was classified as one of the six members of the superfamily of Transient Receptors Potential (TRP) cation channels, and has been termed TRPV1. Initially discovered in the central nervous system, TRPV1 has been found to be widely distributed in the body, even in non-neuronal tissues and TRPV1 has become the model receptor for the TRPV family. The steadily growing interest in this receptor can be expressed by the number of publications: from 21 articles in 1998 to an average of 500 each year since 2006. Although the structure of TRPV1 was recently determined, its functions are complex due to its multiple levels of regulation as highlighted in **Figure 2.7**, and a detailed understanding of the control mechanisms of TRPV1 are still subjected to research.

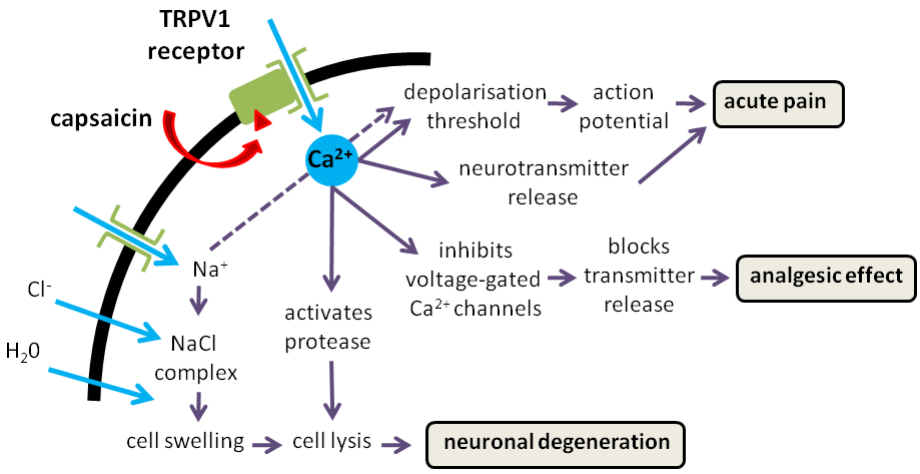

Figure 2.7: Mechanisms induced by TRPV1.

2.2.1- Structure of TRPV1

TRPV1 is a non-selective calcium (Ca^{2+}) channel. Its structure features six transmembrane (TM) domains, with its N- and C- termini in the cytosol, and has a relatively conserved hydrophobic pore domain between the fifth and the sixth TM domains (see **Figure 2.8**). This topology is characteristic of ion channels and has already been reported in voltage-gated K^+ channels.[13]

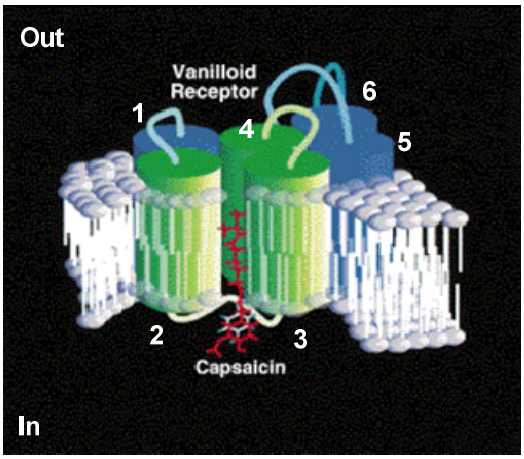

Figure 2.8: Model of the structure of transmembrane TRPV1.[14]

Regarding its primary structure, TRPV1 shares sequence homology with other receptors of the TRPV family. The C- terminus contains the TRP domain, a 25 amino acid segment highly conserved in the TRP superfamily. At the other extremity, the long amino terminus contains three ankyrin-fold domains, which are motifs composed of 33 residues forming two helices separated by a loop region (**Figure 2.9**). The ankyrin-repeat domain is a very common structural motif that accommodates protein-protein interactions. In membrane proteins, this

motif binds to cytosolic proteins.[15] TRPV1 ankyrin-repeats has been found to bind to calmodulin (CaM), the calcium-binding protein.[16]

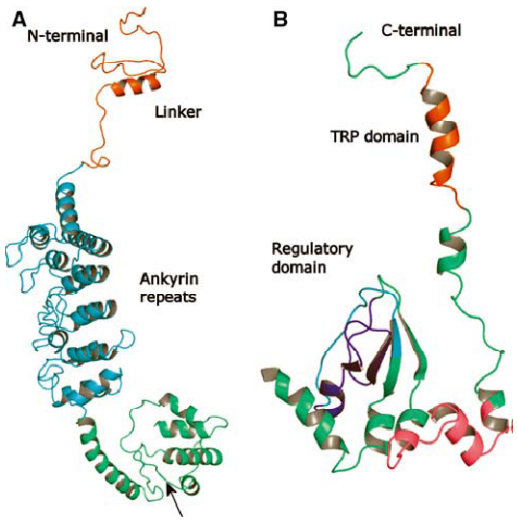

Figure 2.9: Models of TRPV1 N-terminal and C-terminal domains.[17]

By itself, TRPV1 is a tetramer that forms a large signalling complex when associated with the G protein-coupled receptor, phospholipase C, and protein kinase C.[11] Interestingly, the TRPV3 gene is adjacent to TRPV1 on the genome and it is co-expressed in neurones of dorsal root ganglia (DRG), which allows the formation of heteromers with TRPV3 subunits. These heteromers are thought to increase their functional diversity and, in the case of TRPV3, they may reduce the response to capsaicin.[18, 19]

2.2.2- Activation of the TRPV1 receptor

The TRPV1 receptor is activated by capsaicin **93** and its analogues, such as the naturally occurring resiniferatoxin (RTX) **104** from the Moroccan plant *Euphorbia resinifera*.[4, 12] These

molecules are lipophilic and the gap time between the injection of capsaicin and the resulting pungent sensation suggests that the molecules are passing through the cell membrane to bind to cytoplasmic sites of TRPV1.[20] A few other molecules are structurally related to capsaicin **93**, such as the endovanilloid neurotransmitter anandamide **105,**[21] which shows agonistic properties and the synthetic capsazepine **106** that acts as a competitive antagonist.[22]

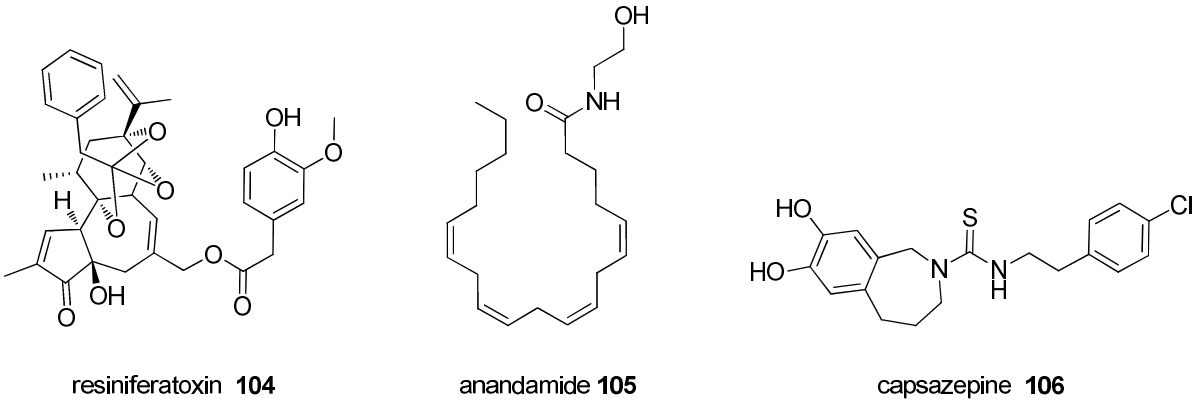

resiniferatoxin **104** anandamide **105** capsazepine **106**

Figure 2.10: Examples of TRPV1 agonists.

2.2.2.1- The critical residues for binding to TRPV1

The primary sequence of TRPV1 has been studied by mutational analysis to discern the critical amino acids for activation, and this approach revealed the importance of Tyr 511 (Y511) and Ser 512 (S512) for forming interactions with the vanilloid ligand. These amino acids are located in the cytosol, on a loop region between the second and third TM domains (**Figure 2.11**).[23] The study has been extended to capsaicin analogues and Leu 547 (L547) proved to have an influence on the agonist potency of RTX and the antagonist potency of capsazepine.[24, 25] It was finally found that Tyr 550 (Y550) contributes to vanilloid binding, and Arg 114 (R114) and Glu 761 (E761) help the recognition of agonists.[26, 27] These critical

residues, though widely distributed in the primary sequence are indeed close to each other in the functional receptor. A third locus, able to control ligand binding, has been found after mutations in the lipophilic pore between the fifth and sixth TM domain.

The position of Tyr 511 on a cytoplasmic loop directed toward the lipid layer would suggest that the vanilloid moiety of capsaicin **93** interacts with Tyr 511 and the surrounding amino acids in the cytoplasm when the lipophilic moiety binds to the lipid interface of the second and third TM domains.

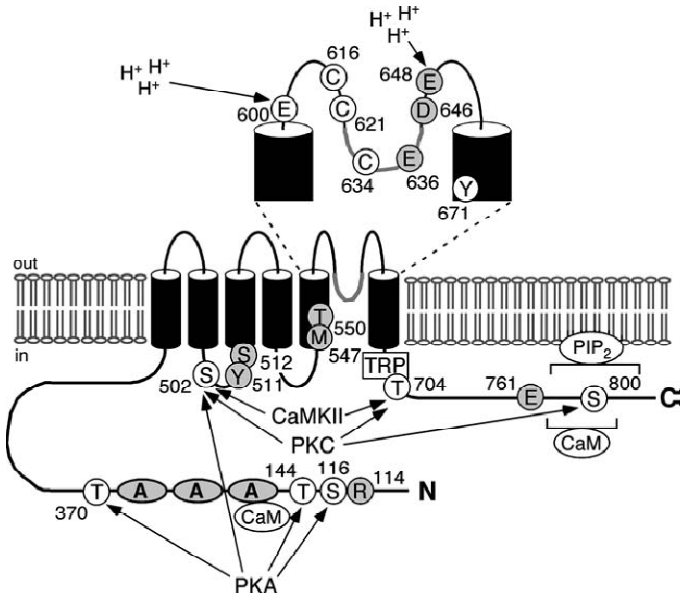

Figure 2.11: Developing structural model: Domains and amino acids involved in TRPV1 function.[11]

The key residues responsible for sensitivity to the multiple stimuli can set off a response cascade when activated. The conformational change induced in the TRPV1 receptor then generates the calcium influx and favours interactions with other potential activating molecules such as anandamide **105**.[28]

2.2.2.2- The activation stimuli

TRPV1 is also activated by stimuli such as acidic pH and high physiological temperature. It is known that protons influence the receptor at two different levels. Firstly, protons from the extracellular region potentiate the response to capsaicin and lower the minimum threshold of temperature. Second, a further acidification (pH <5.3) causes the opening of the channel at physiological temperature.[29] Thus, protons do not interact directly with the vanilloid binding site but increase the probability of channel opening.

The TRPV1 mechanisms of temperature sensitivity remain unclear. Analysis of the receptors from the TRP family indicates that some are thermosensitive, in particular, TRPV1-TRPV4 with the presence of a heat-sensor domain confirmed in TRPV1.[30] The major role played by heat on TRPV1 activation is suggested by the existence of a phosphorylation mechanism (phosphorylases) decreasing the temperature threshold.[23, 29, 31]

In the case of a selective activation of TRPV1 by capsaicin, the biological response is various, generating either the expected pain signal, or paradoxically analgesia (**Figure 2.8**).[11] This desensitisation occurs after a prolonged exposure to capsaicin, and allows patients suffering from diabetic neuropathies or rheumathoid arthritis to be treated with capsaicin.[32] Long exposure to capsaicin leads to the dephosphorylation of TRPV1, but this is inhibited by phosphorylation of Ser 116 by PKA (protein kinase A). Calmodulin is also involved in the desensitisation process. The protein binds to the first ankyrin domain and to the C- terminus of TRPV1, on the 767-801 segment. Regulation of TRPV1 is also mediated by lipids, such as anandamide **105**, oleoylethanolamide **107** (OEA) and phosphatidylinositol 4,5-bisphosphate (PIP_2) **108** (**Figure 2.12**).[21]

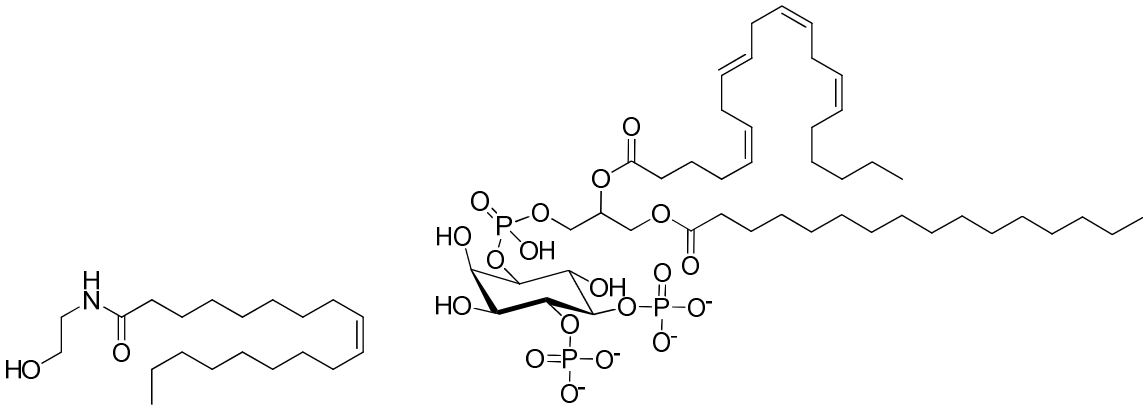

Figure 2.12: Example of lipids that regulates TRPV1.

2.2.3- Recent structural insights

Recently, the structure of TRPV1 was further resolved by electron cryomicroscopy. The recombinant receptor gene (rat) was expressed in the yeast, *Saccharomyces cerevisiae*. Cryomicroscopy is the technique of choice to study biological macromolecular assemblies in their native environment. The resultant three-dimensional structure of the 500 KDa protein is represented in **Figure 2.13** as an isosurface.

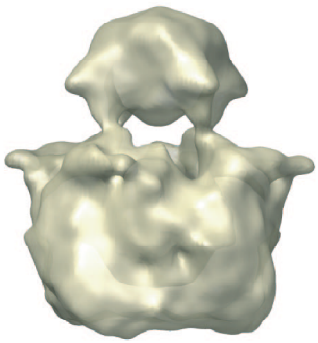

Figure 2.13: 3-D representation of rat TRPV1 as deduced by cryomicrospcopy.[33]

The structure is composed of two distinct parts and exhibits a clear four-fold symmetry. A small compact region is believed to be the transmembrane region consistent with a channel function. The larger region comprises 70% of the total volume and is proposed to be orientated toward the cytoplasm and locates the N- and C-termini. The two regions have been assigned by fitting crystal structures of homologous channel and isolated TRPV1 ankyrin domains.[33]

Molecular modelling based on gene homology has also guided the developing structural hypothesis. The full TRPV1 receptor has been constructed by assembling the different regions following all available physical, biochemical and functional information (**Figure 2.14**).[17]

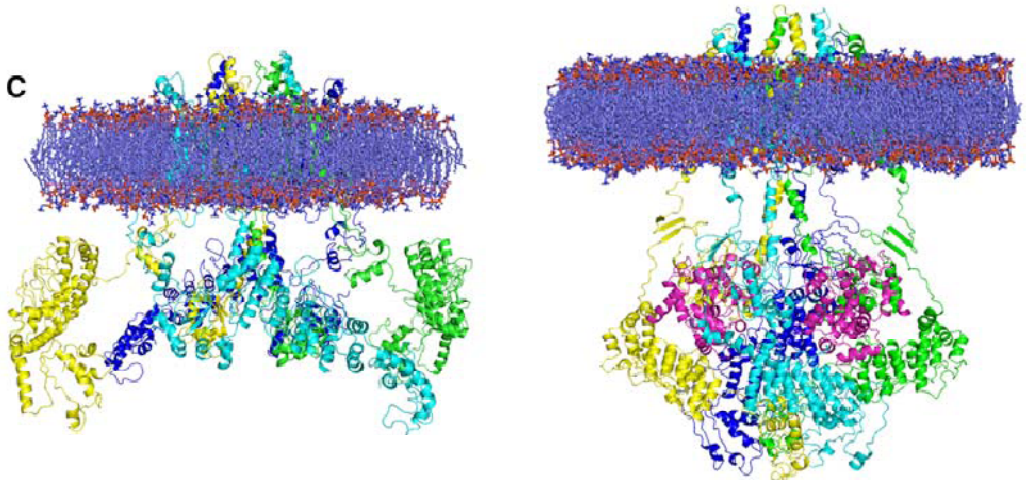

Figure 2.14: Global view of TRPV1 model inserted into the lipid bilayer (left: closed state, right: desensitised state of TRPV1).[17]

2.3- Capsaicinoids

2.3.1- Structural elucidation of the capsaicinoids

Capsaicinoids are a large family of natural products related to the parent capsaicin (8-methyl-*N*-vanillyl-6-nonenamide) **93**, discovered in 1961 by Japanese chemists.[34] However, capsaicin **93** was already known to be the molecule giving chilli peppers (*Capsicum*) their spiciness. Indeed, in 1919, Nelson showed the pungency of chillis resulted from vanillyl amides[35] and contributed to solving the structure of capsaicin in 1923.[36] All capsaicinoids have a common vanillylamine moiety, linked to a variable acyl group where variation affects the degree of the pungency.[37]

The pungency is measured by the Scoville organoleptic test, a test of dilution of a pepper extract in sugar syrup. The Scoville scale ranks 0 Scoville Heat Units (SHU) for Bell pepper, 30.000 SHU for cayenne pepper and reaches 1 million SHU for Naga Jolokia (Ghost pepper). In comparison, pure capsaicin is evaluated at 16 million SHU and law enforcement grade pepper sprays are formulated at 5 million SHU (see **Table 2.1**).

Because of their spiciness, capsaicinoids are used as repellents against mammals. For example, veterinary surgery applies them to protect sutures. They can be added to coatings for protection of seeds or cables, or additives in toxic products such as paints or liquid soaps to prevent accidental ingestion.

Beyond their spiciness, capsaicinoids have been used through the ages in empirical medicine to cure, for example, arthritic pain. It has also been shown in recent studies that capsaicin has anti-inflammatory, anti-cancer and anti-obesity properties.

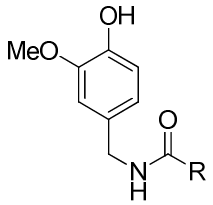

vanillylamide of R acid

Structure of R	Capsaicinoid	Pungency*
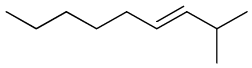	Capsaicin **93**	16
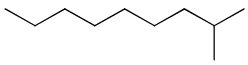	Dihydrocapsaicin **109**	15
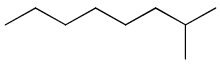	Nordihydrocapsaicin **110**	9
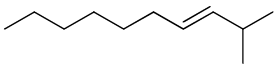	Homocapsaicin **111**	8.6
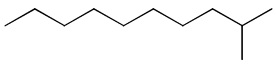	Homodihydrocapsaicin **112**	8.6
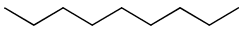	Pseudocapsaicin **113**	NA

*Scoville Heat Units $x10^6$

Table 2.1: Structure and pungency of some capsaicinoids.

2.3.2- Biosynthesis of capsaicin

The capsaicinoids natural products are exclusive to the peppers (genre *Capsicum*). The biosynthesis of capsaicin **93** by the key enzyme capsaicin synthase occurs in the epidermal cells of the fruit placenta, easily recognised as it makes the white flesh surrounding the seeds. The enzyme couples vanillylamine **118** and 8-methylnonenoate **120** to generate an amide bond (**Scheme 2.1**). It is thought the steps leading from feruloyl-CoA **114** to vanillylamine **118** involving hydroxycinnamoylcoA hydratase/lyase and potentially an aminotransferase, are

specific to peppers. The spiciness of the peppers is correlated to the amount of capsaicinoid and depends on the gene expression of the enzymes driving the capsaicin biosynthetic pathway.

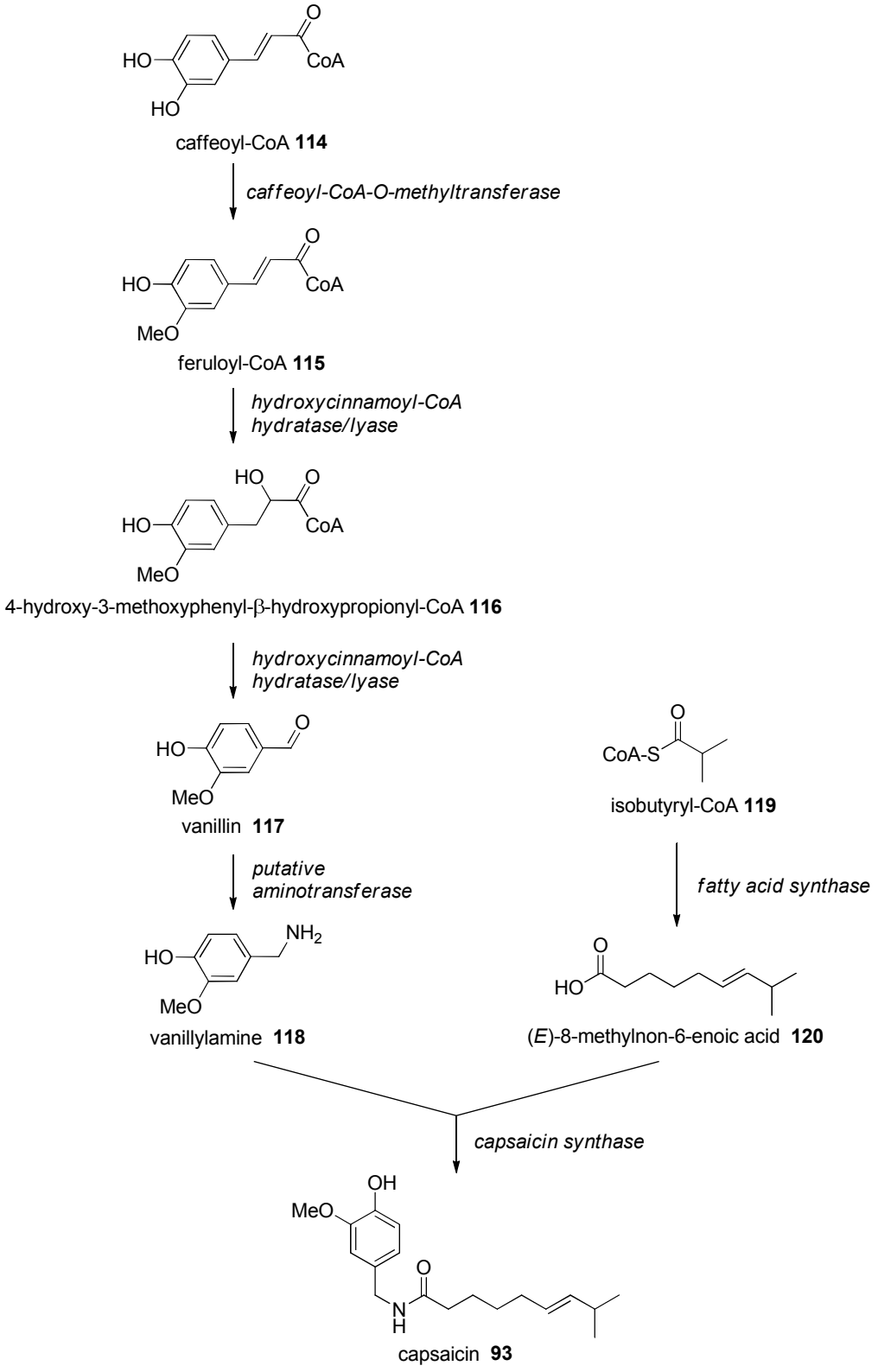

Scheme 2.1: Biosynthesis of capsaicin **93**.[38]

2.4- Previous syntheses of capsaicin

The structure of the capsaicinoids is conveniently divided into two distinct parts, each being responsible for an effect on TRPV1. The benzylamine moiety is retained through the family. It is known to be responsible for binding to the TRPV1 receptor, and this essential role restricts structural variation. Varying the length of the chain, the presence of functionalities or the degree of saturation (**Figure 2.15**) tunes potency. The mid-region can also be modified where the original amide bond is inverted or replaced by an ester, to generate derivatives such as homovanillic acid amides and capsiates.

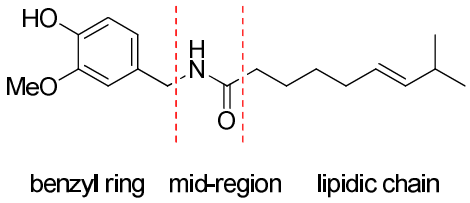

Figure 2.15: Structure of capsaicin.

Interest in capsaicinoids started at the beginning of the 20th century. After the synthesis of vanillylacyl-amides reported by Nelson in 1919,[35] Späth and Darling described the first synthesis of capsaicin in 1930.[39] The retro-synthesis of these compounds disconnects capsaicin **93** at the amide bond. The benzylamine moiety derives from vanillin **117** and the resultant lipidic precursor is therefore *(E)*-8-methylnon-6-enoic acid **120** (**Scheme 2.2**). Full syntheses of capsaicin has been completed at various periods but any synthetic approach to capsaicin or its derivatives requires high stereochemical control of the *(E)*-double bond.

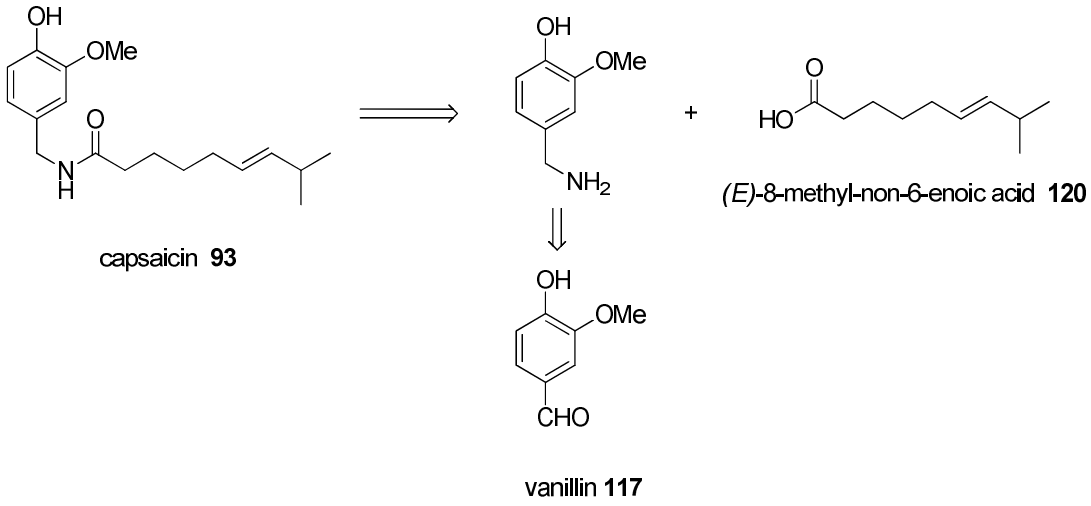

Scheme 2.2: Retrosynthesis of capsaicin.

2.4.1- Synthesis of vanillylamine

Nelson prepared vanillyl oxime **121** by heating vanillin **117** with hydroxylamine. The resultant oxime was then reduced with sodium amalgam to generate the amine, and isolated as the hydrochloride salt.[40] Ganett assayed palladium and platinum to catalyse this reduction.[41] PtO_2 led to partial over-reduction and a method was developed using palladium on carbon to provide the vanillylamine hydrochloride **118** (**Scheme 2.3**).

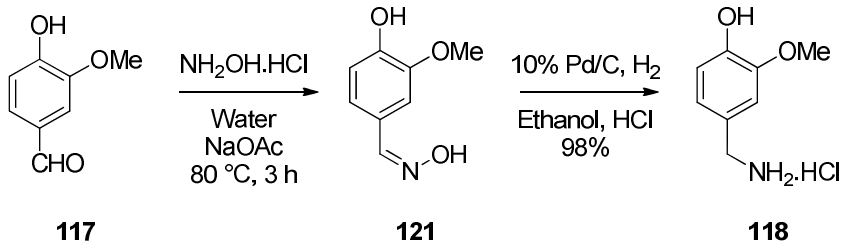

Scheme 2.3: Synthesis of vanillylamine hydrochloride.

2.4.2- Syntheses of 8-methylnon-6-enoic acid

Späth and Darling were the first to prepare 8-methylnon-6-enoic acid **120** as shown in **Scheme 2.4**. This involved an organozinc addition to acyl chloride **122**. Reduction and bromination then gave the acid **125**. However the elimination of HBr gave rise to a mixture of both *E* and *Z* isomers, and these geometric isomers could not be separated by chromatography, distillation or crystallisation, so this synthesis was rather unsatisfactory.[39]

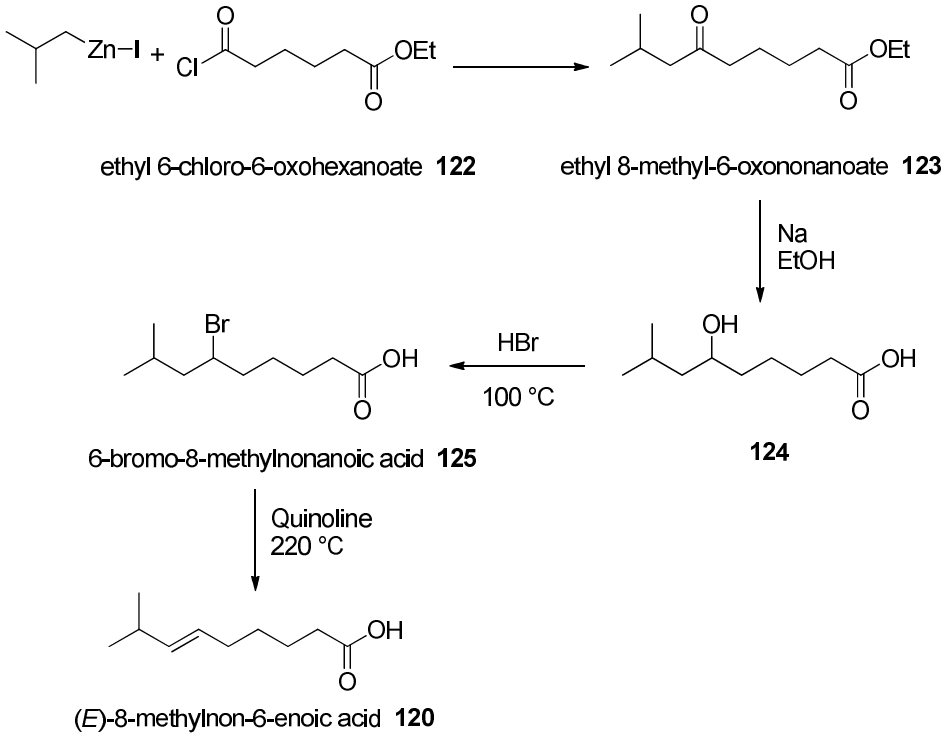

Scheme 2.4: Early approach to acyl moiety **120**.[39]

In order to improve both the regio- and stereo- selectivity, Crombie and co-workers emerged with an impressive solution.[42] They treated 3-chloro-pyran **127** with sodium metal to generate only the (*E*)- isomer of alcohol **128** by elimination. This stereospecificity arises as a consequence of elimination from the 6-membered ring. This reaction proved to be

regiospecific as only isobutyraldehyde was obtained after ozonolysis. Bromination of the alcohol **128** into **129** followed by a malonate condensation/decarboxylation sequence completed this elegant synthesis to 8-methylnon-6-enoic acid **120** (**Scheme 2.5**).

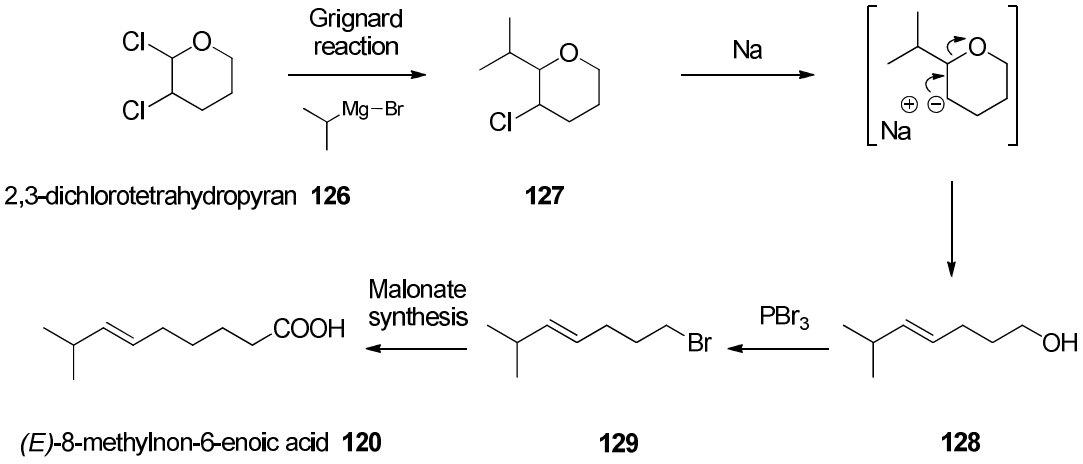

Scheme 2.5: Crombie's controlled elimination route to 8-methylnon-6-enoic acid **120**.[42]

2.4.3- The Wittig approach

The synthetic method developed by Crombie and described above (**Scheme 2.5**) was successfully used for the synthesis of capsaicin **93**. However, it suffered from a lack of generality in its ability to provide a variety of capsaicinoids. Therefore, Gannet applied a Wittig approach to construct the double-bond.[41] This approach also offered more structural variety.

The condensation of ω-oxo-esters **130** with an *iso*propylphosphonium salt **131** lead to the predominant (*Z*)-alkene **132b** with an *E/Z* ratio between 1:4 and 1:10, depending on the conditions of the reaction, with the best results obtained with potassium *tert*-butoxide in

DMF. The ylide produced during the reaction is not stabilised and consequently the (*Z*)-isomer predominates (**Scheme 2.6**).

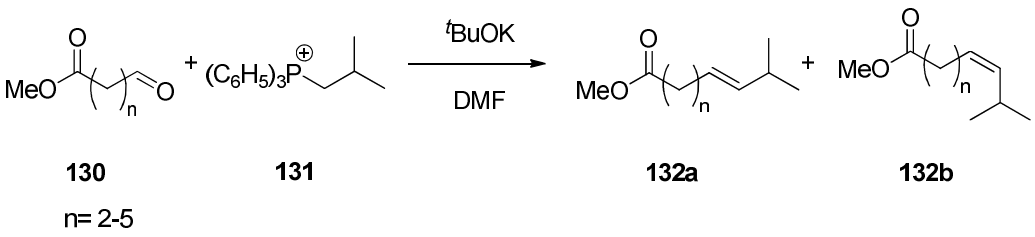

Scheme 2.6: Wittig approach to capsaicinoid synthesis.[41]

An alternative approach to obtain the (*E*)-series applied the Kocienski-Lythgoe-Julia procedure, which allowed reductive elimination of a benzoyloxy-sulfone to obtain a 9:1 *E/Z* mixture in good yields (70%).[43] The method requires that ω-oxo-esters **130** are condensed with *iso*butylphenyl sulfone **133** and benzoyl chloride, to generate the benzoyloxy-sulfone **134** as a 3:1 mixture of diastereoisomers. Subsequent treatment with sodium amalgam lead to a non-stereospecific elimination, but giving the thermodynamically favoured (*E*)-alkene **132a** (**Scheme 2.7**).

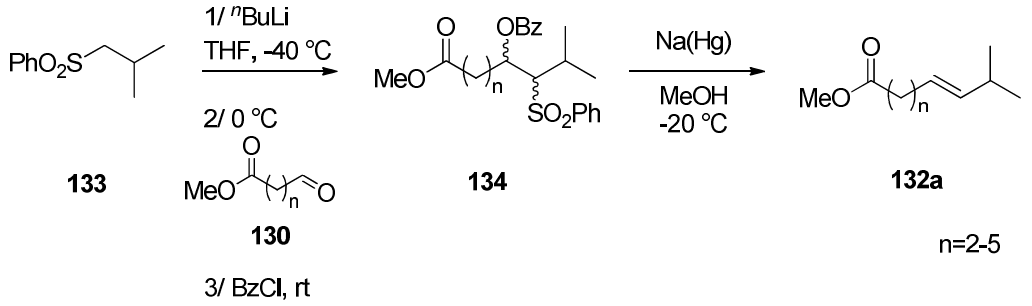

Scheme 2.7: The Kocienski-Julia-Lythgoe procedure.[43]

Introducing the (*E*)-double-bond can also be achieved by isomerisation of (*Z*)-products, prepared by the Wittig chemistry. Gannett has reported a photochemical isomerization (*hv*, hexane, I_2 as catalyst) of the (*Z*)-side chain leading to an *E/Z* ratio of 7:3 from an initial ratio of 1:10.[41] Kaga and co-workers used a nitrous acid-induced isomerization of *Z* to *E* olefins for a synthesis of capsaicin,[44] a method previously reported by Sonnet for the synthesis of insect sex pheromones and *E*-fatty acids such as for **135**.[45] This method allowed a maximum *E/Z* ratio of 8:1 from a starting mixture of 1:11 (**Scheme 2.8**).

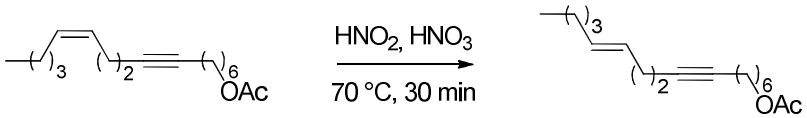

135b **135a**

Scheme 2.8: Isomerisation of the double-bond.[45]

2.4.4- The Ortho-ester Claisen rearrangement

The *(E)*-olefination procedures reported above are based on regioselective elimination mechanisms and show only moderate to good stereoselectivities. However, these methods did generate reasonable amounts of capsaicinoids for biological investigations, particularly as natural capsaicinoid extracts are contaminated with structurally related amides. In order to eliminate any (*Z*)-capsaicinoids in these synthetic routes, Kaga developed a method based on the use of the Claisen orthoester rearrangement (**Scheme 2.9**).[46]

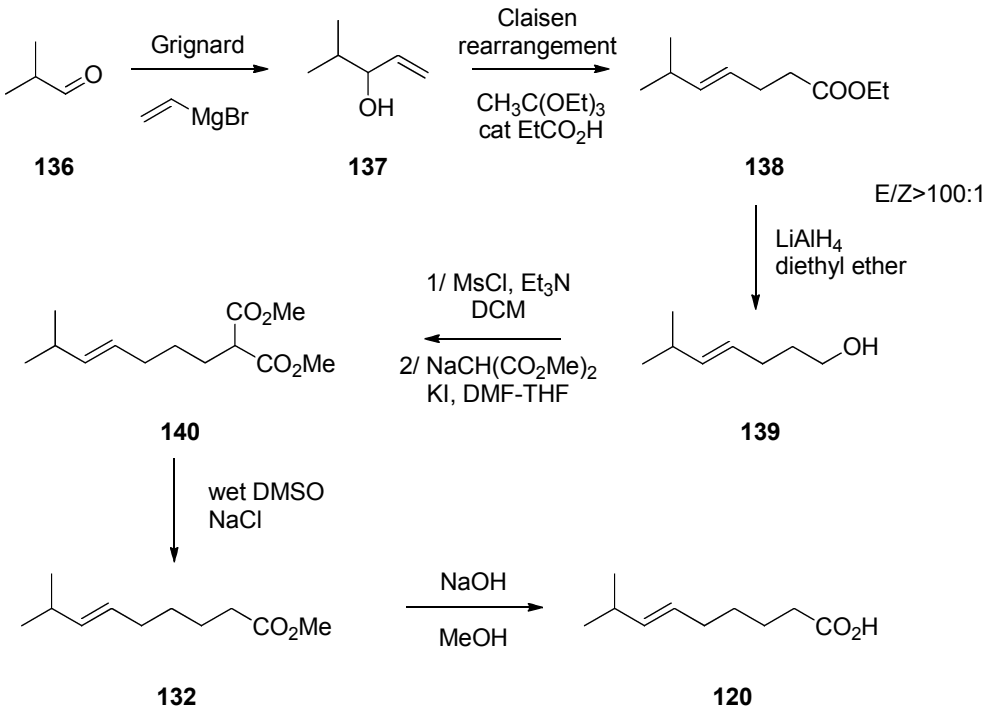

Scheme 2.9: Claisen rearrangement and malonic ester synthesis.[46]

The method requires that an allylic alcohol **137** is prepared by a Grignard reaction of the corresponding aldehyde **136** with vinyl magnesium bromide. The product is then subjected to a Claisen ortho-ester rearrangement by heating with triethyl orthoacetate in the presence of a catalytic amount of propionic acid. The intermediate (*E*)-6-methyl-4-heptenoate **138** is obtained with a very high *E/Z* ratio of >100:1. This route also presented the potential for an iterative synthesis since all of the homologues were prepared *via* carbon chain elongation either by cyanation or by malonic acid ester synthesis.

2.5- Aims and objectives

As discussed previously, the fluoro-amide motif NH–CO–CF displays a strongly preferred C–F/C=O *trans* planar conformation. It was envisaged that both enantiomers (*S*)-**97a** and (*R*)-**97b** (see **p. 50**, **Figure 2.3**) would be prepared for comparative biological assay with the TRPV1 receptor. It was also envisaged that enantiomers of shorter chain analogues of α-fluorocapsaicin would be prepared for further comparison with the TRPV1 receptor.

In the case of fluorocapsaicin **97**, the double-bond could be accessed by a "classical" Wittig route or a cross-metathesis method, never previously been attempted for the synthesis of capsaicinoids. Installation of fluorine would be explored using asymmetric oxazolidinone methodology. A cross-metathesis strategy requires ethyl 6-heptenoate **175** coupled to the chiral oxazolidinone. Three general strategies emerge (**Scheme 2.10**) with the cross-metathesis being attempted on ester **144**, the *N*-acyloxazolidinone **170** or the fluorinated *N*-acyl oxazolidinone **172a**.

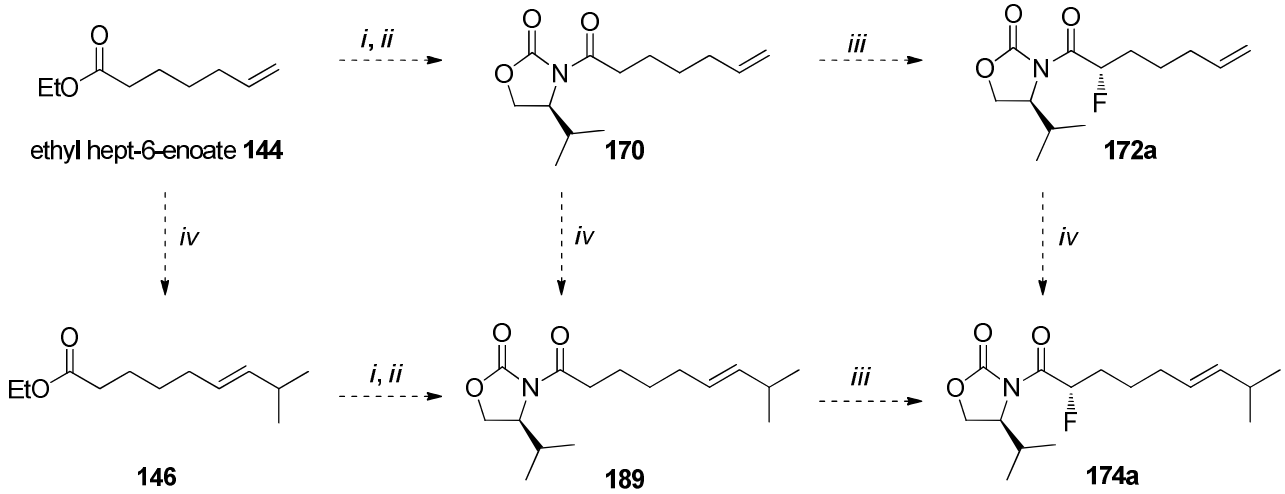

Scheme 2.10: Three general approaches to 2-fluorocapsaicin analogues.

The Wittig route could start from ethyl 6-hydroxyhexanoate **179**, which requires to be oxidised to the corresponding aldehyde **180** for reaction to generate *(E)*-ethyl 8-methyl-non-6-enoate **181**. Hydrolysis followed by coupling to a chiral oxazolidinone would then provide a strategy for asymmetric fluorination as illustrated in **Scheme 2.11**.

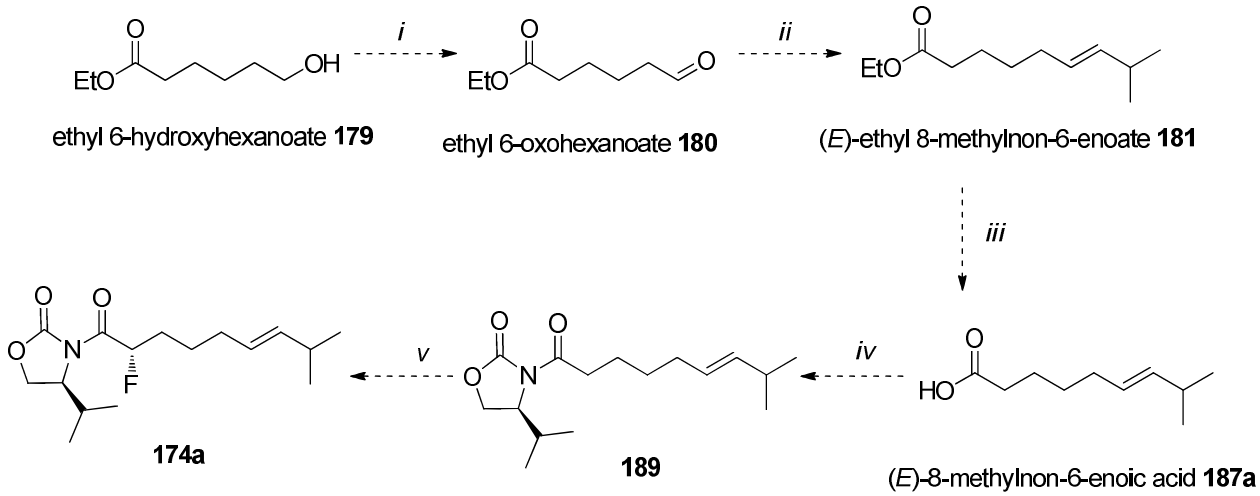

Scheme 2.11: Wittig approach to 2-fluoro enantiomers of capsaicin.

Removal of the chiral oxazolidinone by standard methods would allow coupling to vanillylamine **118** to complete the synthesis.

The synthesis of (*R*) or (*S*)- 2-fluoro dehydrocapsaicins **98a/b** is also envisaged by a hydrogenation reaction of the corresponding fluorinated capsaicin **97** or one of the synthetic precursors **187** or **174** (**Scheme 2.12**).

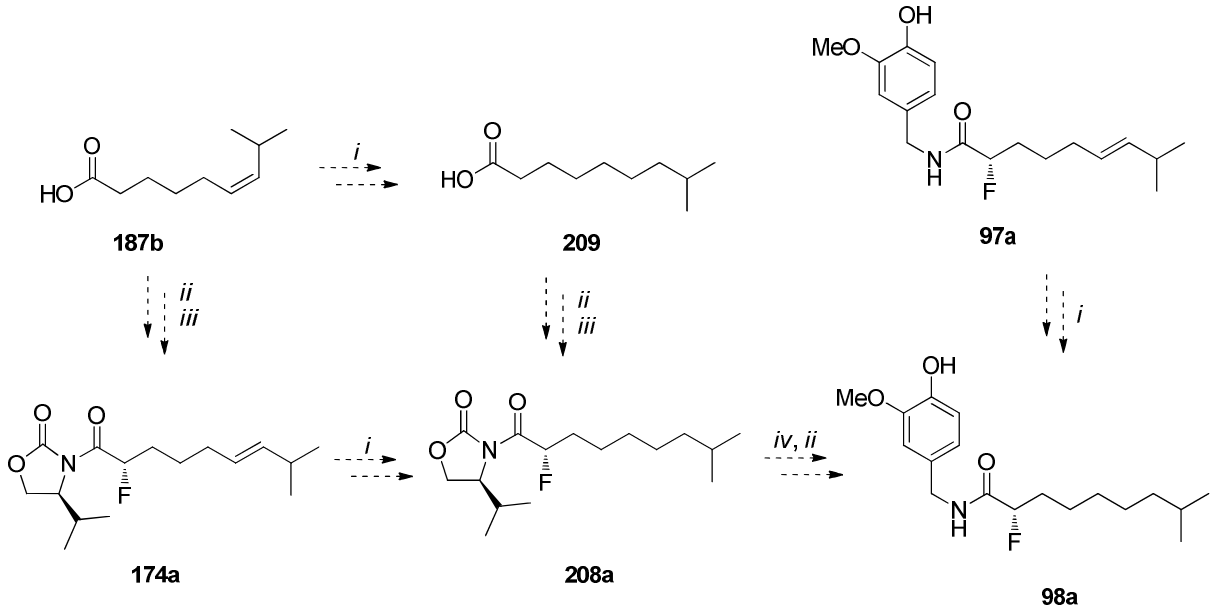

Scheme 2.12: Route to (*S*)-2-fluorodehydrocapsaicin **98a**.

Scheme 2.13 shows the envisaged synthesis of short chain analogues of capsaicin by deaminative fluorination of the amino acid leucine **224** to generate the corresponding 2-fluorocarboxylic acid **227**.

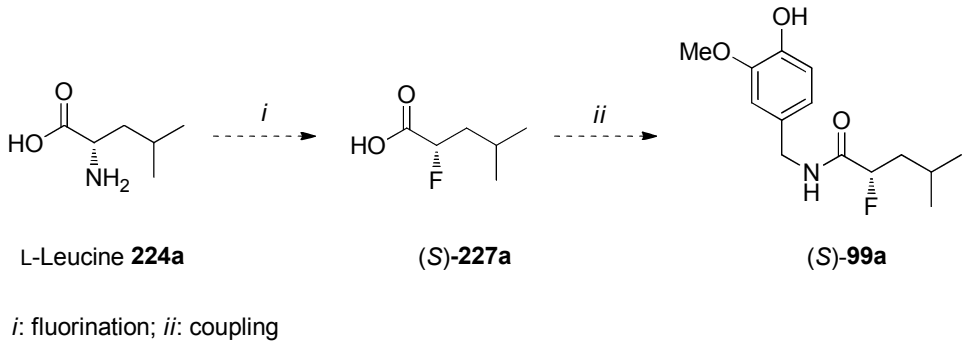

L-Leucine **224a** (*S*)-**227a** (*S*)-**99a**

i: fluorination; *ii*: coupling

Scheme 2.13: Deaminative fluorination to generate **99**.

Alternatively, the synthesis of 2-fluoroacid **227** could be approached using the MacMillan asymmetric fluorination to compare the enantioselectivity as illustrated in **Scheme 2.14**.

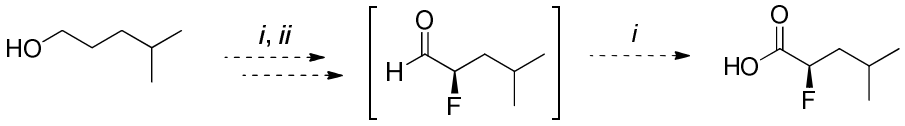

233 (*R*)-**235b** (*R*)-**227b**

i: oxidation; *ii*: fluorination

Scheme 2.14: Envisaged synthesis of **181** with Macmillan asymmetric fluorination strategy.

2.6- Results and discussion

2.6.1- Synthesis of (*S*)-fluorocapsaicin 97a with Evans'oxazolidinone chiral auxiliary

2.6.1.1- Cross-metathesis (CM) strategy

Cross-metathesis (CM) was addressed as a method of olefin introduction. Catalysts **142** and **143**, are coordinating ruthenium to an *N*-heterocycle carbene ligand (**Figure 2.16)**. They tolerate a wide range of functional groups in the structure of the alkene.

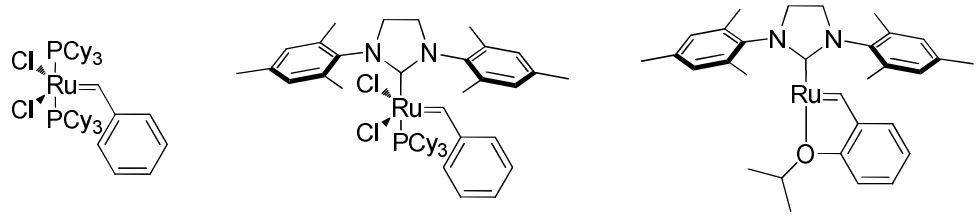

Grubbs catalyst 1st generation **141**

Grubbs catalyst 2nd generation **142**

Grubbs-Hoveyda catalyst **143**

Figure 2.16: Examples of CM catalysts.

Preliminary experiments were explored to evaluate the best conditions for the cross-metathesis of olefins **144** and **145** to generate **146**. Ethyl 6-heptenoate **144** was treated with 3-methyl-1-butene **145** (5-20 eq) using the Grubbs II catalyst **142** (5-30 mol%), for reactions up to 2 days (**Scheme 2.15**).[47]

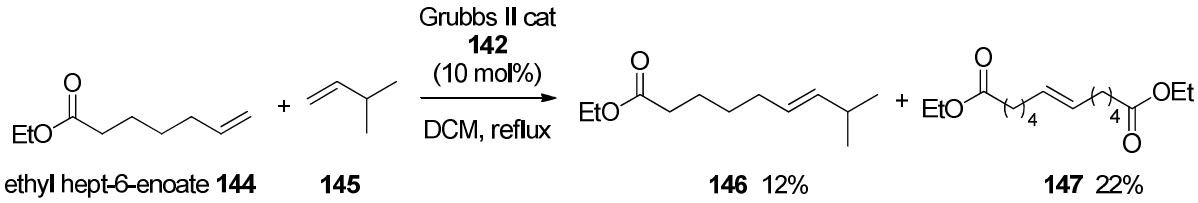

Scheme 2.15: Assay of CM with ethyl 6-heptanoate **144**.

Two products were isolated when 10 mol% catalyst was used, the desired product **146** and a homodimer **147**. Dimer **147** resulted from self cross-metathesis of **144**. After purification, **146** was recovered but in a poor yield (12%). It was found that, after extended reaction times and at any concentration of catalyst **142**, the product **146** started to degrade, even though the reaction had not gone to completion. It appeared that the volatility of 3-methyl-1-butene prevented its entering the catalytic cycle despite a large excess (20 eq), and thus self-metathesis of the alkene **144** (R^1=) emerged as the major product (**Scheme 2.16**).[48]

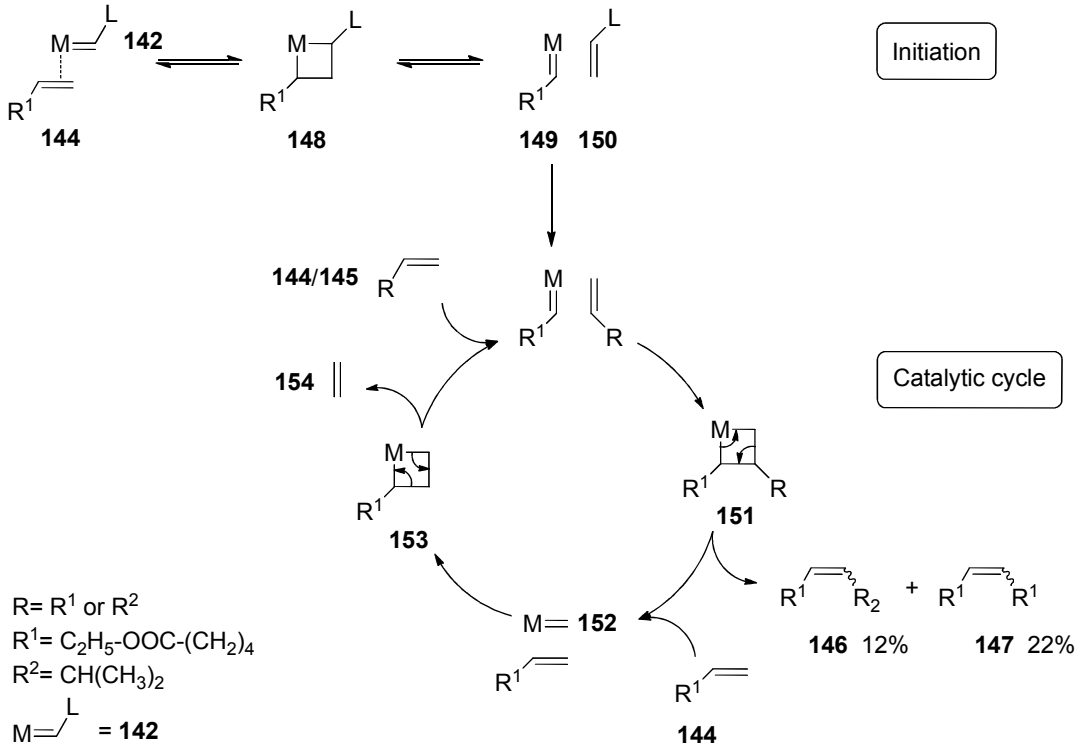

Scheme 2.16: The mechanism for cross-metathesis reaction.

This initial study revealed that the self condensation side-reaction was significant. Nevertheless, it was decided to prepare the enantiopure *N*-acylated oxazolidinones **170**/**171** for asymmetric fluorination studies (**Figure 2.17**). Successful fluorination would then provide a suitable substrate for further CM exploration.

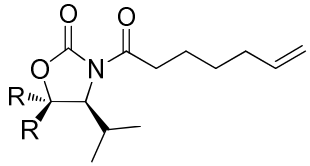

170: R= H
171: R= Ph

Figure 2.17: *N*-Acylated oxazolidinones substrates for CM and asymmetric fluorination.

A general method for the preparation of chiral *N*-acylated oxazolidinones **157** involved condensation of the carbamate with an acyl chloride (**Scheme 2.17**). A wide range of electrophiles including *N*-bromosuccinimide,[49] di-*tert*-butylazodicarboxylate,[50] tosyl azide,[51] alkyl halide[52] or electrophilic fluorinating reagents[53] can then react with the enolate **158** to insert specific functional groups α to the carbonyl, in an asymmetric manner. These reactions are often highly stereoselective and have led to products **159**-**162** with diastereoisomeric excesses (d.e.) higher than 90%.

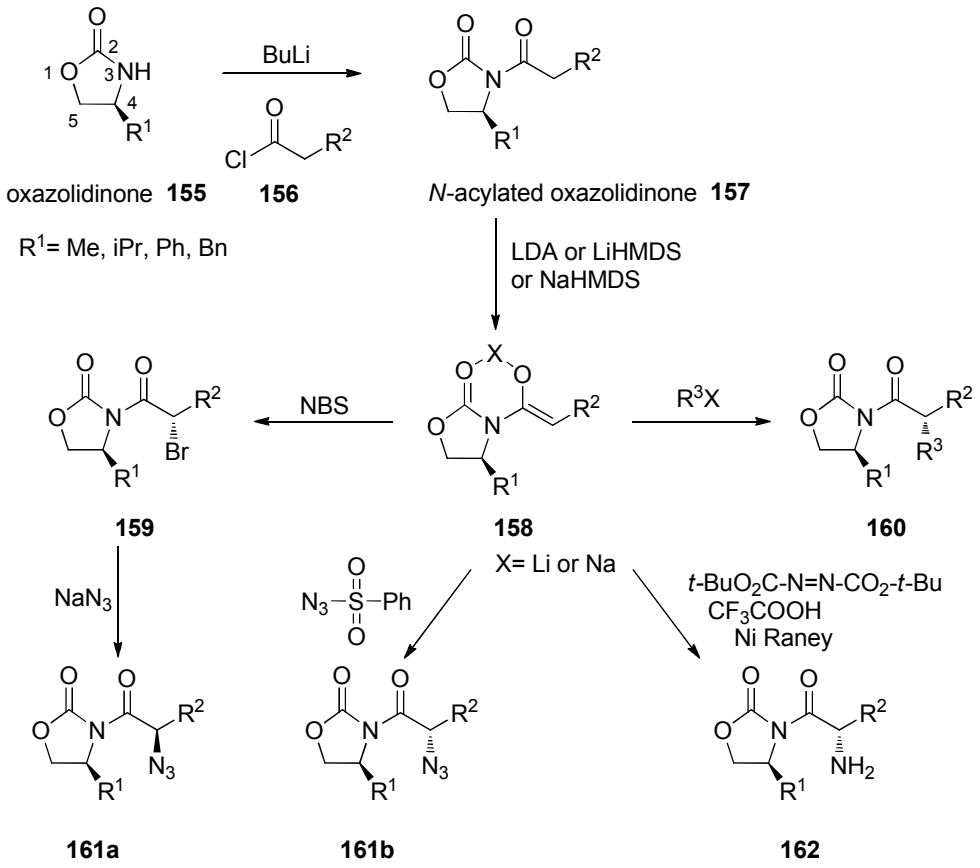

Scheme 2.17: Example of electrophilic insertion into enolates of oxazolidinone auxiliaries.[49-54]

Disubstitution at 5-position of the oxazolidinone ring is believed to prevent nucleophilic attack to the carbamate carbonyl.[55, 56] The heterocyclic core of the oxazolidinone is quite flat. Substitution at C-4 is designed to hinder one face of the enolate and promote electrophilic attack to the opposite face.[57]

The use of such chiral oxazolidinones constituted our method of choice as they have already proven to be efficient for asymmetric electrophilic fluorination. In particular, Davis has developed diastereoselective electrophilic fluorinations, using Evans' oxazolidinones applied to the synthesis of α-fluoroacids,[53] α-fluoroketones[58] and fluorinated carbohydrates.[59] Marquez used the method for the synthesis of a fluorinated intermediate of an anti-HIV

drug.[60] Staunton, has also described the use of a chiral auxiliary for asymmetric fluorination of analogues of the antibiotic tetronasin.[61]

The fluorination requires electrophilic fluorinating reagents to react with the enolate. The strategy was first developed with NFOBS, but more recent studies have shown that NFSI achieves the best stereoselectivity (**Scheme 2.18**).

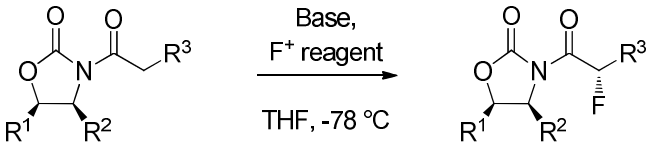

163 **164** > 95% de

Scheme 2.18: Electrophilic fluorination using oxazolidinone auxiliaries.

A summary of the conditions for these studies are reported in **Table 2.2** and shows that fluorinated products could be formed in good yields (up to 86%) and high diastereoselectivity (de > 95%).[62]

Entry	R^1	R^2	R^3	F^+ reagent	Base	Yield	d.e.
1	H	^{i}Pr	^{n}Bu	NFOBS	LDA	85%	96%
2	H	^{i}Pr	*tert*-Bu	NFOBS	LDA	80%	97%
3	Ph	Me	Ph	NFOBS	LDA	86%	86%
4	Ph	Me	Ph	NFSI	NaHMDS	85%	97%
5	H	Bn	C_5H_9	NFSI	LiHMDS	78%	98%

Table 2.2: Selective electrophilic α-fluorination using oxazolidinone auxiliaries.[62]

Accordingly, in our case, the synthesis of *N*-acylated oxazolidinones **170** and **171** started with the alkaline hydrolysis of ethyl 6-heptenoate **144**, followed by acidic work-up to give carboxylic acid **165**, which was purified by distillation (**Scheme 2.19**).

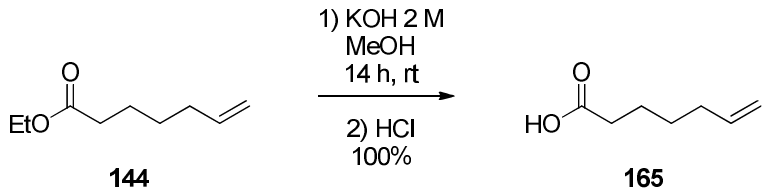

Scheme 2.19: Hydrolysis of ethyl 6-heptenoate **144**.

6-Heptenoic acid **165** (1 eq) was then treated with pivaloyl chloride **166** to generate the mixed anhydride **167** (**Scheme 2.20**). This intermediate was immediately coupled to the Evans auxiliaries 4-(*S*)-4-isopropyl-2-oxazolidinone **168** or 4-(*S*)-4-isopropyl-5,5-diphenyl-2-oxazolidinone **169**. The intermediate was pre-treated in a separate flask with *n*-butyllithium (1 eq), and the coupling of **168** and **169** gave the respective acylated products **170** and **171** in high yields (86% and 91% respectively).[63] In some preparations, pivaloyl chloride **166**, which was in an excess (1.3 eq), reacted with the oxazolidinone to form the *N*-pivaloyloxazolidinone side-product, but this was maintained at low level (<5%).

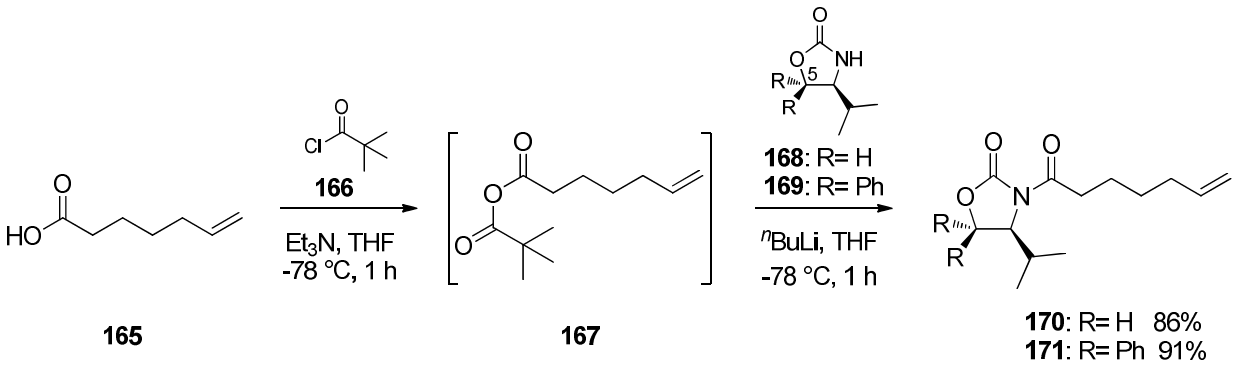

Scheme 2.20: Strategy to the chiral acylated auxiliary.

The two oxazolidinones **168** and **169** were separately investigated in asymmetric fluorination reactions. The fluorination is directed by the configuration of the isopropyl chain and the phenyl substituents at position 5 of **169** should increase its ability to crystallise, an important factor in improving the ultimate enantiopurity.

Asymmetric fluorination of **170** using lithium bis(trimethylsilylamide) (1.1 eq) and NFSI (1.3 eq) was carried out at -78 ^{o}C.[59] This gave **172** with an 80% conversion (GCMS) but the apparatus had not been calibrated specifically before the analysis and the final result showed a loss in the conversion as only 20% of **172** were recovered after purification (**Scheme 2.21**).

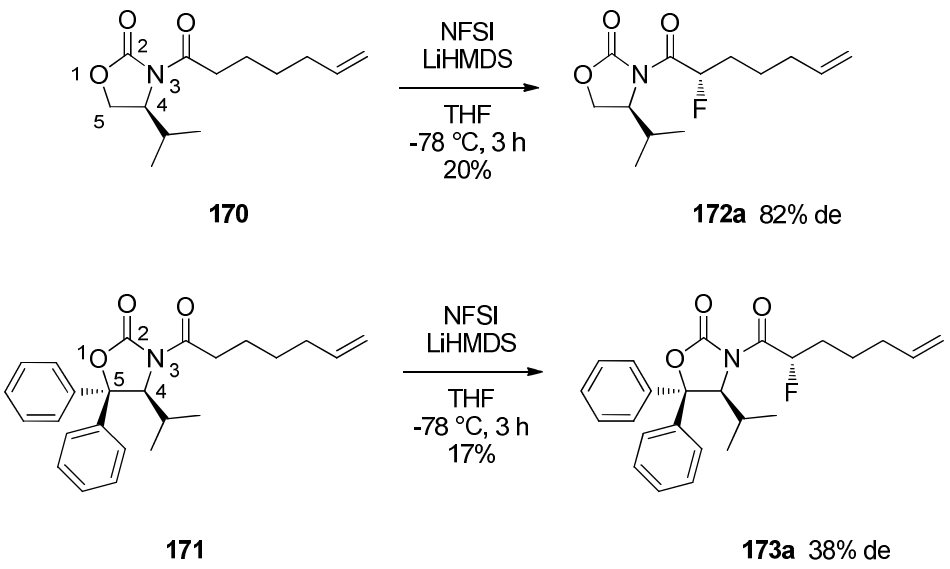

Scheme 2.21: Asymmetric fluorination of *N*-acyloxazolidinones.

Direct ^{19}F NMR analysis of the product of **170** indicated a conversion into the two fluorinated diastereoisomers **172a** and **172b** with an 82% diastereomeric excess. The major product was assumed to be the (*S,S*)-**172a** stereoisomer. With **171**, where the C-5 substituents were phenyl groups, the diastereoisomer **173a** was obtained but only with 38% de (see **Figure 2.18**). These

results clearly suggest that the phenyl groups hinder the diastereoselective discrimination by NFSI.

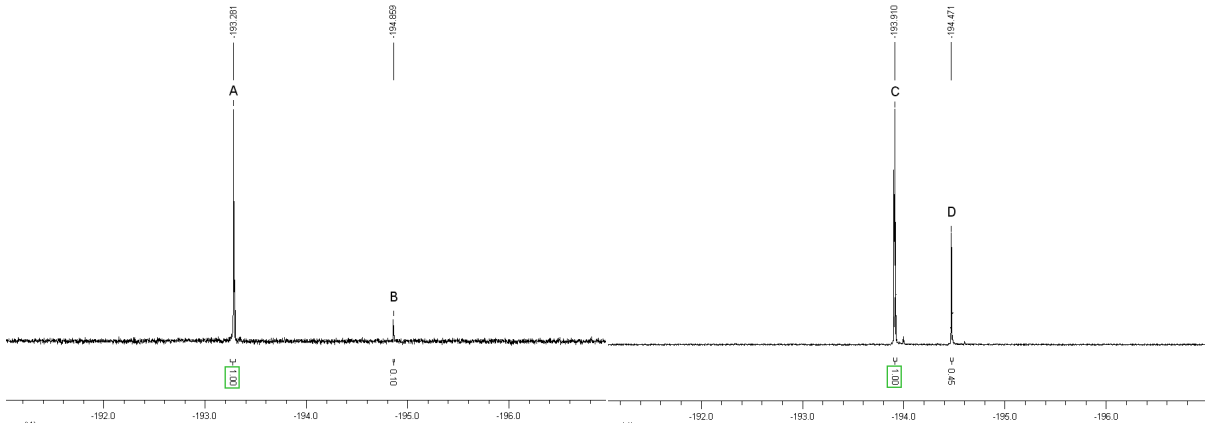

Figure 2.18: ^{19}F NMR (282 MHz) spectra showing the diastereomeric ratios for the products of the asymmetric fluorination reactions (A: (*S,S*)-**172a**, B: (*S,R*)-**172b**, C: (*S,S*)-**173a**, D: (*S,R*)-**173b**).

The previously optimised conditions for the cross-metathesis reaction for use with 3-methyl-1-butene were explored for **172** (**172a**:**172b** 9:1) and **173** (**173a**:**173b** 7:3) (see **Scheme 2.22**). A solution of **172** in DCM was treated with 3-methyl-1-butene (20 eq) and Grubbs II catalyst **142** (10 mol%) for 20 h at 40 °C. This gave (*S,S,E*)-**174a** as the major product and with a 54% yield.

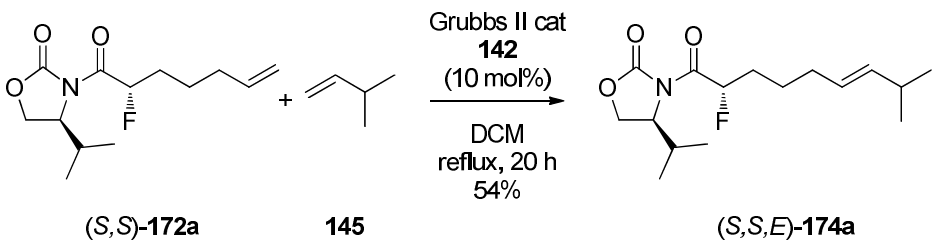

Scheme 2.22: Cross-metathesis reaction on *N*-fluoroacyl oxazolidinone **185**.

^{19}F NMR of the crude mixture (**Figure 2.19**) indicated that the double-bond stereochemistry was formed in a 87:13 ratio in favour of (*E*)-**174a**. It was also noted that (*S*,*R*)-**172b** present in the initial mixture was quantitatively converted to one product that we assumed to be the corresponding *E*-product of the cross-metathesis reaction (*S*,*R*,*E*)-**174c**.

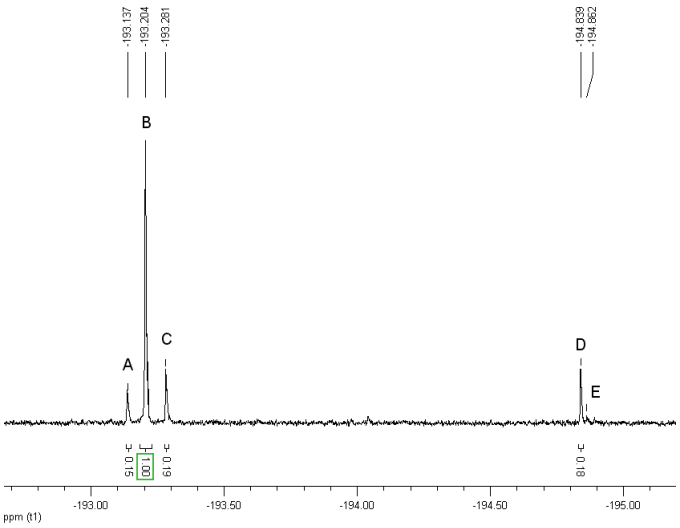

Figure 2.19: ^{19}F NMR (282 MHz) showing the conversion in *E*-and *Z*- alkenes **174** (A: (*S,S,Z*)-**174b**, B: (*S,S,E*)-**174a**, C: (*S,S*)-**172a**, D: (*S,R,E*)-**174c**, E: (*S,R*)-**172b**).

The diastereoselectivity of the fluorination process first described by Davis[59] has been confirmed in these reactions (82% for **172a**). The diastereomeric ratio has been increased after the CM by purification on silica gel where the two diastereoisomers were successfully separated and the (*S,S,E*)-**174a** isomer was recovered in an enantiopure form.

2.6.1.2- Wittig strategy[41]

The Wittig strategy was developed to obtain more material of **174a** and **174c** to explore the syntheses of fluorocapsaicin **97a** and **97b** further. Treatment of triphenylphosphine **175** (1 eq) with 1-iodo-2-methylpropane **176** (1 eq) in refluxing toluene provided the desired phosphonium iodide **177** in good yield (> 80%) (**Scheme 2.23**). This phosphonium salt **177** (1.1 eq) was subsequently treated with *n*-butyllithium (1 eq) to give a solution of ylide **178** that was used directly in a Wittig condensation with aldehyde **180**.

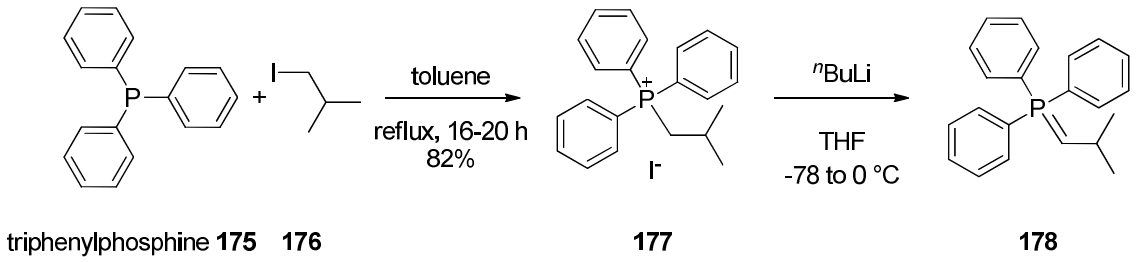

Scheme 2.23: Synthesis of the Wittig reagent.

The required aldehyde **180** was prepared by oxidation of ethyl 6-hydroxyhexanoate **179** (1 eq) with pyridinium chlorochromate (PCC) (**Scheme 2.24).**

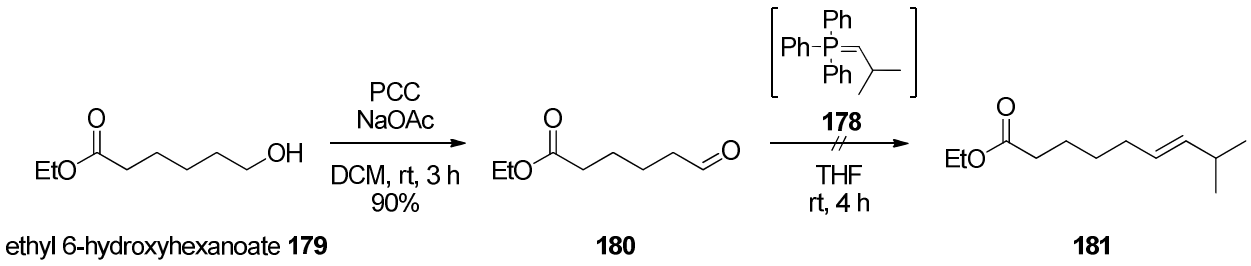

Scheme 2.24: Wittig condensation strategy to generate ester **181**.

However, treatment of ylide **178** (1 eq) with aldehyde **180** (1.3 eq) did not result in the desired olefin **181**, and only starting material was recovered.

In order to establish if the ylide was of good integrity, a reaction with hexanal **182** was carried out under the same conditions, and this proceeded smoothly (82%) as illustrated in **Scheme 2.25**. This observation suggested that the Wittig with aldehyde **180** was in some way compromised by the ester function.

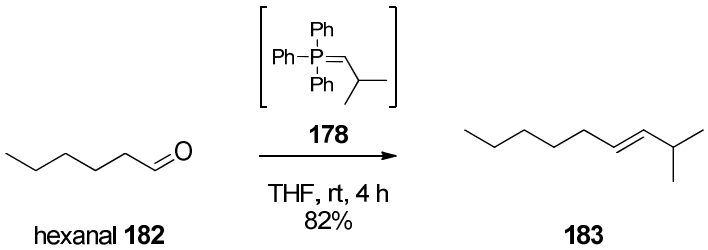

Scheme 2.25: Assay of Wittig condensation.

2.6.1.3- Inverse Wittig route

The Wittig method described by Kaga in 1989, based on an inverse reaction appears well suited to the large scale synthesis of capsaicin.[44] An eight step sequence could then afford the desired fluoro-analogues of capsaicin. Recrystallisation of the intermediates was anticipated to offer a method to improve the enantiomeric purity. After isomerisation of carboxylic acid (*Z*)-**187**, and coupling to the 4-(*S*)-4-isopropyl-2-oxazolidinone **168**, α-fluorination of **189** would then give the *N*-fluoroacyl oxazolidinone **174a**. Hydrolytic cleavage and coupling to vanillylamine **118** would then afford the desired fluorocapsaicin **97a**.

Accordingly, 6-bromohexanoic acid **184** was treated with triphenylphosphine to generate salt **185** in an almost quantitative reaction (97%). The reaction was judged completed when the mixture went glassy. The use of toluene as a solvent gave **185** in a decreased yield (86%) and therefore for future preparations the reaction was conducted without solvent (**Scheme 2.26**).

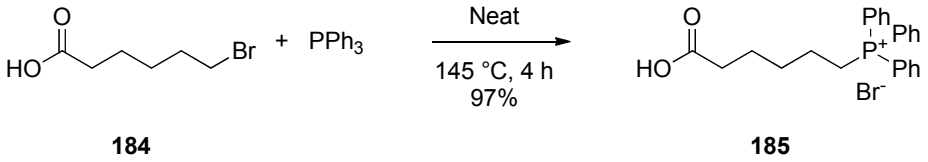

Scheme 2.26: Preparation of phosphonium salt **185**.

The phosphonium salt **185** was then treated with ^{t}BuOK (2 eq) to obtain the corresponding ylide (not isolated) which was reacted directly with isobutylaldehyde **186**. This gave a mixture of (*Z*)- and (*E*)-**187** isomers with a *Z/E* ratio of 90:10 as determined by ^{1}H NMR. This was similar to the ratio (92:8) reported in the literature (**Scheme 2.27**).[44]

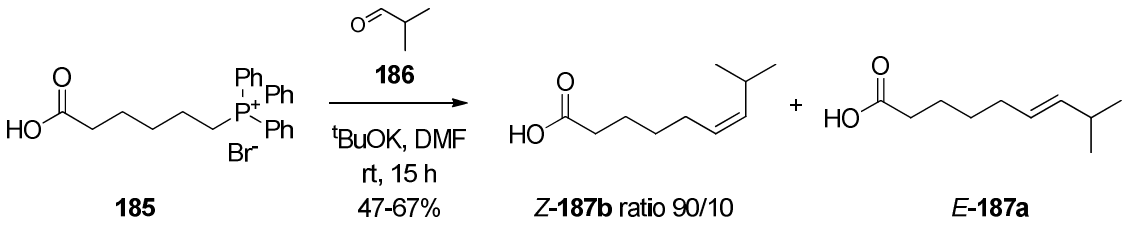

Scheme 2.27: The retro-Wittig condensation to 8-methylnon 6-enoic acid **187**.

This isomer mixture of **187** was treated with 2 M sodium nitrate/6 M nitric acid to promote an isomerisation to the *E*-isomer. This reaction gave an inverse *E/Z* ratio of 86:14, also similar to the 89:11 ratio reported in the literature (**Scheme 2.28**).[44]

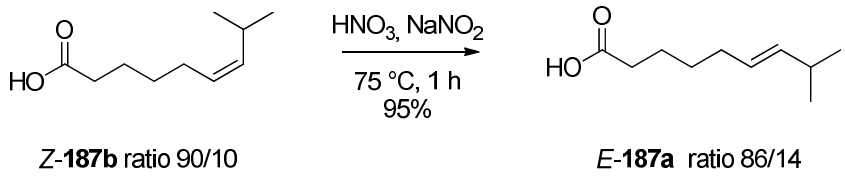

Scheme 2.28: Isomerisation of (*Z*)- to (*E*)-8-methylnon 6-enoic acid **187**.

The coexistence of the *Z* and *E* isomers is illustrated on **Figure 2.20**.

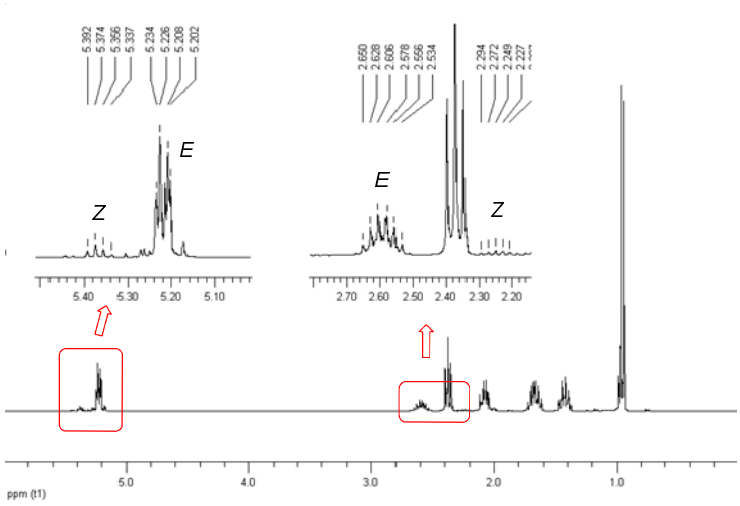

Figure 2.20: ^{1}H NMR (300 MHz) spectrum of *E*-**187** (*E*:*Z* 86:14), expanding the alkene and ^{i}Pr CH signals.

Coupling to the chiral auxiliary was achieved as described previously to give the *N*-acylated oxazolidinone **189** (**Scheme 2.29**). The *E/Z* ratio of 86:14 was kept all over the synthesis.

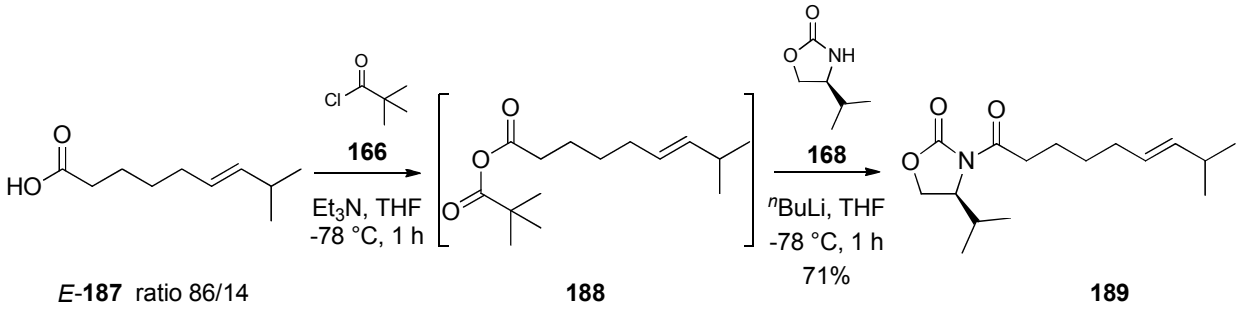

Scheme 2.29: Synthesis of the chiral acylated auxiliary **189**.

This product **189** was fluorinated using LiHMDS/NFSI to give **174a**, according to the established method described above. The conversion of **189** to **174a** was good, consistent with previous reactions (84% de, 83% conversion but only 20% isolated yield) (**Scheme 2.30**).

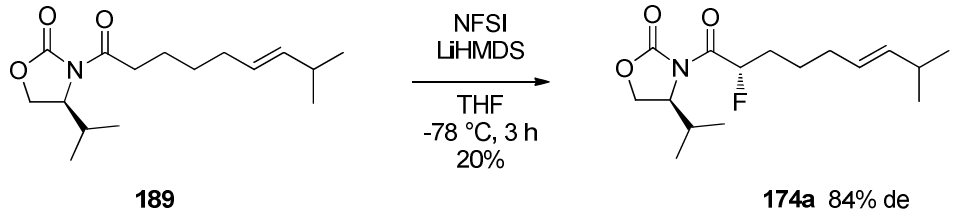

Scheme 2.30: Synthesis of (*S,S,E)*-**174a**.

2.6.1.4- Removal of the Evans auxiliary

Removal of the Evans auxiliary is a challenge, particularly as racemisation needs to be avoided. Several methods (**Scheme 2.31**) have been reported including lithium borohydride to obtain the reduced alcohol **191**,[64] or with lithium hydroperoxide to release the carboxylic acid **192**.[65] Direct formation of a Weinreb amide **193** provides an aldehyde **194** or a ketone **195** after treatment with DIBAL or a Grignard reagent respectively.[66] Finally, DIBAL affords the aldehyde directly from the oxazolidino-imide, but it can also competitively reduce the auxiliary and consequently decreases conversion to the aldehyde.[67]

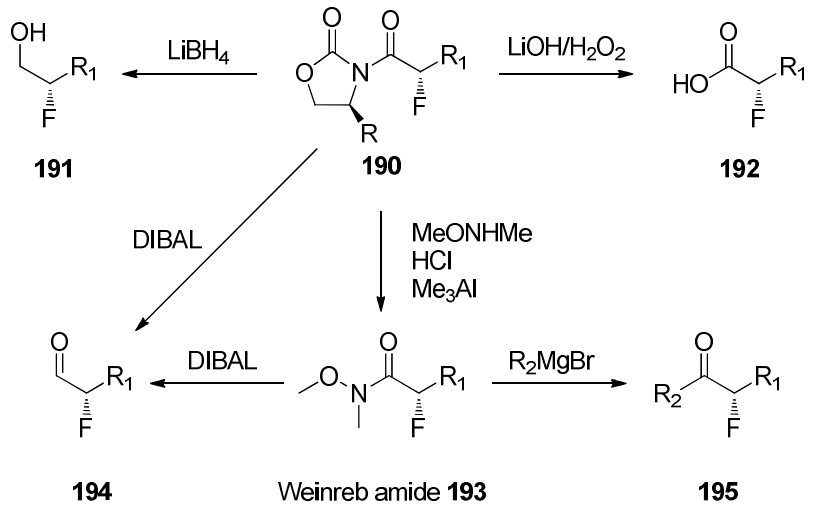

Scheme 2.31: Alternative approaches for Evans auxiliary removal.

Two methods were explored for cleavage of the α-fluoroacyl moiety from the Evans auxiliary. Firstly, the Weinreb amide route was attempted and secondly, hydrolysis was explored with lithium hydroxyperoxide. This latter method was already described by Evans but it was noted that some racemisation of the α-fluorine stereogenic center could occur.[65] Initial studies toward this reaction were explored on *(R)*-3-phenylbutyric acid **196** as a model compound

(**Scheme 2.32**). The synthesis of products **198** and **199** were realised under the same conditions as described previously and in a straightforward manner.

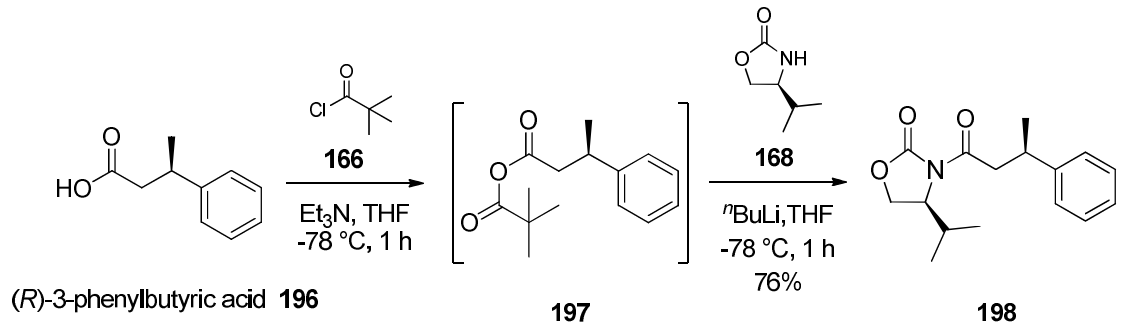

Scheme 2.32: Synthesis of *N*-acyloxazolidinone model **198**.

The fluorinated products were obtained with approximately 70% conversion. Two signals in ^{19}F NMR, at -198.2 ppm and -196.4 ppm, in a ratio of 63:37 were observed in the crude mixture. The major product was purified and isolated to give the *(S,S,S)*-**199** in a 97/3 ratio (51% yield) (**Scheme 2.34**).

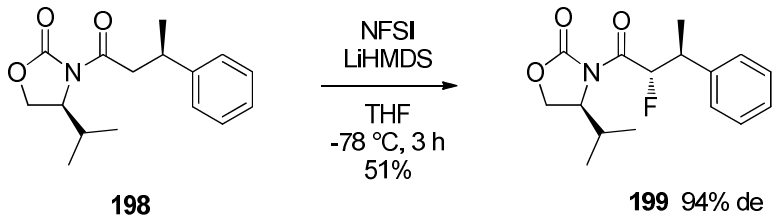

Scheme 2.33: Fluorination of model compound.

The Weinreb amide **201** (96% de) was obtained after treatment of **199** with *N,O*-dimethyl-hydroxylamine hydrochloride **200** (**Scheme 2.34**).[58] Cleavage of **201** with DIBAL was

attempted twice under the same conditions, but these reactions were unsuccessful and only the starting material was recovered.[68]

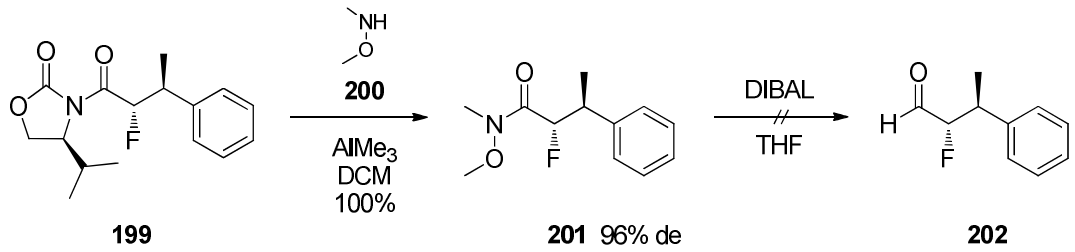

Scheme 2.34: Deacylation *via* reduction of the Weinreb amide intermediate.

Therefore, in a further attempt to perform the acyl cleavage, **199** was treated with an aqueous solution of H_2O_2 (35%) and lithium hydroxide (**Scheme 2.35**). To avoid racemisation of the stereogenic centre carrying the fluorine under the literature conditions,[69] only half an equivalent of hydrogen peroxide was used to provide the α-fluorinated carboxylic acid **203** in good yield (92%), and under these conditions, no racemisation was observed by ^{19}F NMR compared to **199**.

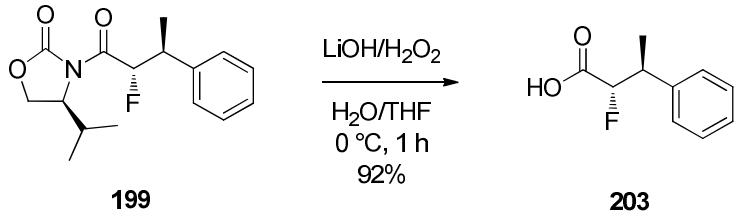

Scheme 2.35: Exploration of deacylation with peroxides.

With this model study completed, *N*-acyl oxazolidinone **174a** was treated similarly (**Scheme 2.36**) with lithium hydroperoxide, affording carboxylic acid **204** was obtained yield (95%).

Two peaks were observed in the fluorine NMR of the product at -192.6 ppm and -192.7 ppm, in a 1:9 ratio, corresponding respectively to (*S,Z*)-**204** and (*S,E*)-**204**. At this stage, it was not possible to determine whether any racemisation had occurred on this product and therefore amide formation with *(S)*-1-phenylethylamine **205a** was carried out as a double check to create a set of diastereoisomers from the product.

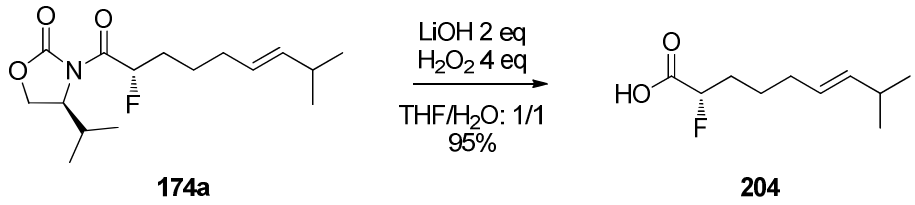

Scheme 2.36: Hydrolysis of **174a**.

The reaction with *(S)*-1-phenylethylamine **205** gave amide (*S,S,E*)-**206a**. As a control, a diastereomeric mixture **206** with the racemic amide was also prepared.

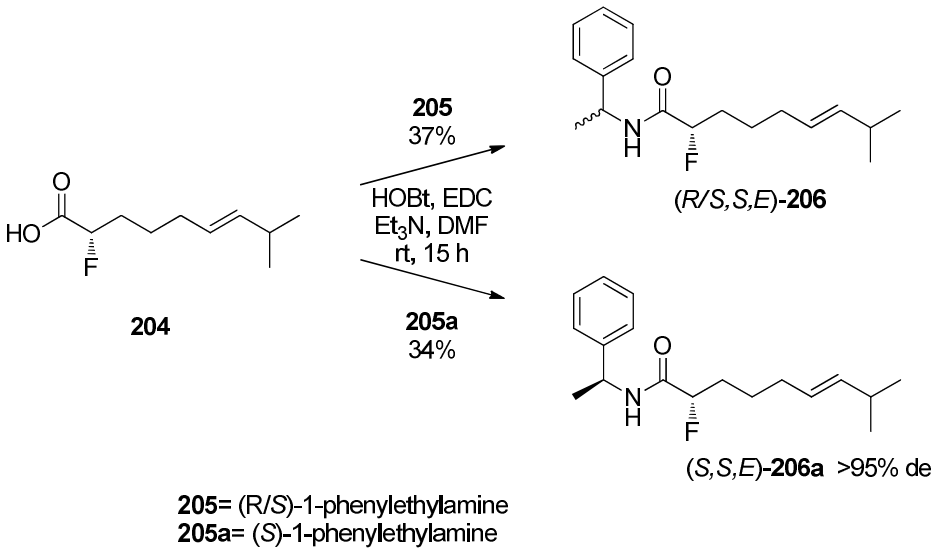

Scheme 2.37: Study on fluorine racemisation.

^{19}F NMR of the synthesised amides shows two signals corresponding to (*S,S,E*)- and (*S,S,Z*)-**206** with a 92/8 ratio (**Figure 2.21** right).

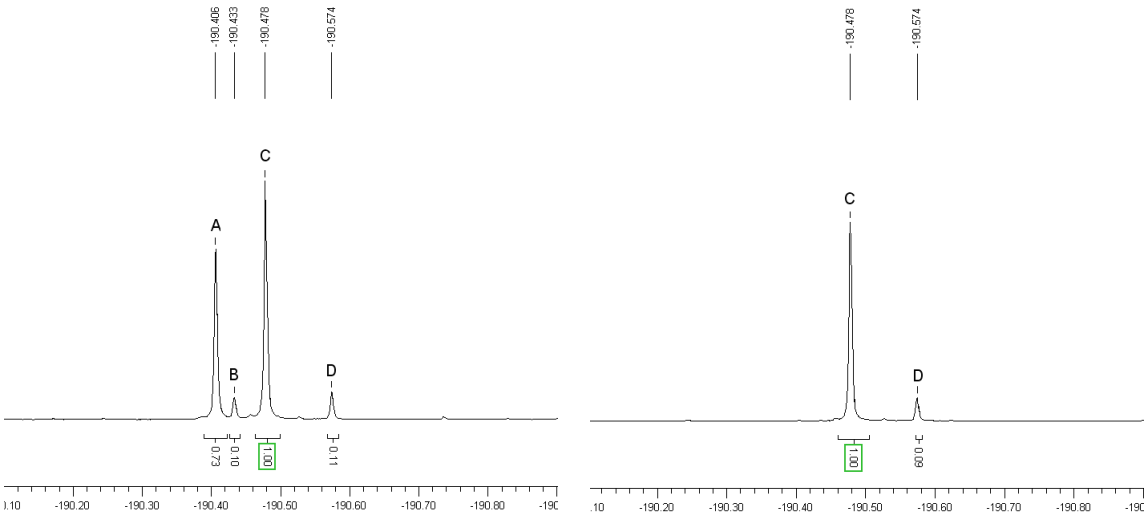

Racemic control *Asymmetric analysis*

Figure 2.21: ^{19}F NMR of **206** (A: (*R,S,E*)-**206c**, B: (*R,S,Z*)-**206d**, C: (*S,S,E*)-**206a**, D: (*S,S,Z*)-**206b**).

For the racemic amide, four signals were observed, indicating now two different sets of signals (**Figure 2.21** left). The minor signals corresponded to the *Z* double-bond (9/1 ratio in favour of the *E*). Accordingly it was concluded that no racemisation occurred during deprotection.

2.6.1.5- Amide coupling to generate α-fluorocapsaicins

The synthesis of oxime **207** was initially attempted by treatment of vanillin (1 eq) with hydroxylammonium chloride (1.1 eq) in refluxing methanol using pyridine or triethylamine as

a base, however, these reactions failed.[41] In the event, the reaction was achieved in water at 80 °C, using sodium acetate (1 eq) as a base, and this gave oxime **121** in good yield (78%) (**Scheme 2.38**).[70]

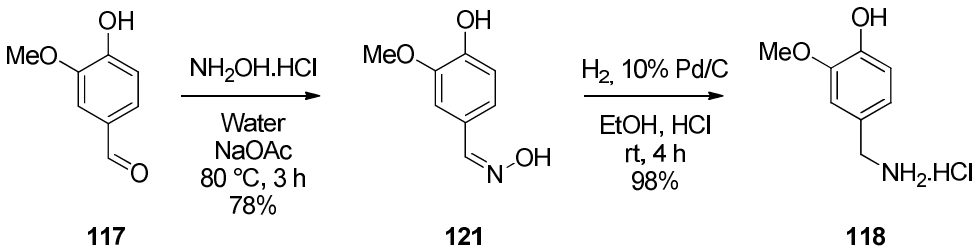

Scheme 2.38: Synthesis of the vanillylamine moiety.

Vanillylamine **118** was then prepared by direct hydrogenation of oxime **121** using 10% palladium on charcoal. The reaction was carried out in ethanol, under acidic conditions using concentrated hydrochloric acid. To avoid over-reduction of the aromatics, hydrogen was used at atmospheric pressure. This reaction gave vanillylamine hydrochloride **118** in high yield (98%) (see **Scheme 2.38**).

In order to complete the synthesis of (*S*)-**97a**, the α-fluorinated carboxylic acid **204** was activated with HOBt (1.05 eq) and EDC (1.05 eq) before coupling to the vanillylamine **118**. This gave the fluorocapsaicin in a modest yield (32%) (**Scheme 2.39**).

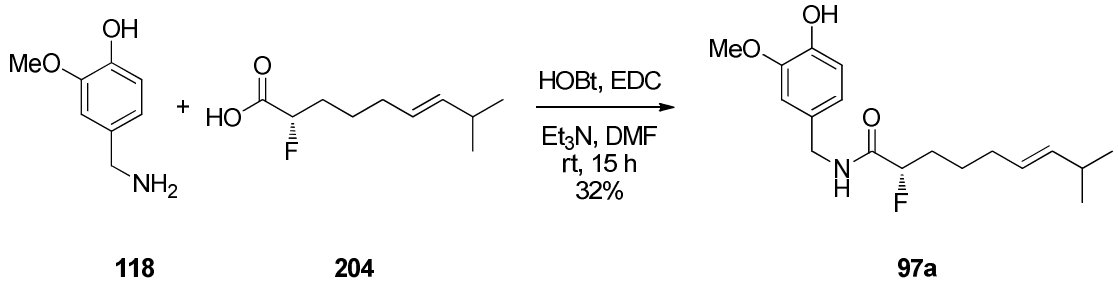

Scheme 2.39: (*S*)-2-Fluorocapsaicin amide coupling.

2.6.1.6- Route to dehydrocapsaicin

The synthesis of the 2-fluorinated dehydrocapsaicin was also explored to evaluate the influence of the saturated chain when assayed with TRPV1, even though this structural variation only causes a small loss of activity on the natural DHC. Direct hydrogenation of oxazolidinone **174a** was first attempted. A total synthesis of α-fluorodehydrocapsaicin was then explored from the saturated carboxylic acid **208**.

Accordingly **174a** was treated under the same conditions as previously described by Ganett[41] for the synthesis of dehydrocapsaicin, using 10% palladium on charcoal. The reaction was carried out in ethanol, under acidic conditions (conc. HCl), and hydrogen gas was introduced at atmospheric pressure (**Scheme 2.40**).

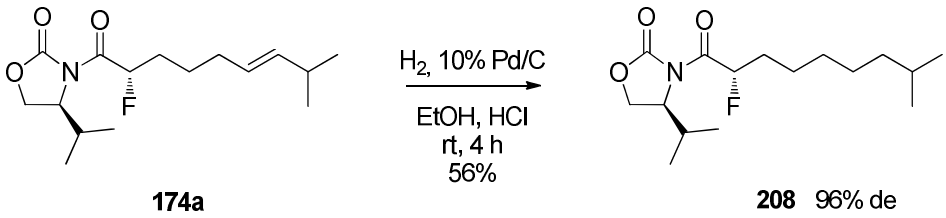

Scheme 2.40: Direct hydrogenation of **174a**.

Product **208** was obtained, in a modest yield and it proved difficult to improve the conversion. However, the removal of the double-bond allowed us to determine with a high degree of accuracy the diastereomeric excess of **208** and ^{19}F NMR analysis revealed that **208** was obtained with 96% ee. This result is to be compared with **199** and **203** and shows that the stereo integrity of the fluorine is maintained along the synthesis.

In an alternative approach to obtain **208**, the carboxylic acid **187b** (as a 90/10 mixture of *Z*/*E* isomers) was first treated with 10% palladium on charcoal. The reaction was carried out

in ethanol, under acidic conditions (conc. HCl) and hydrogen was introduced at atmospheric pressure to provide the saturated carboxylic acid **209** (**Scheme 2.41**).

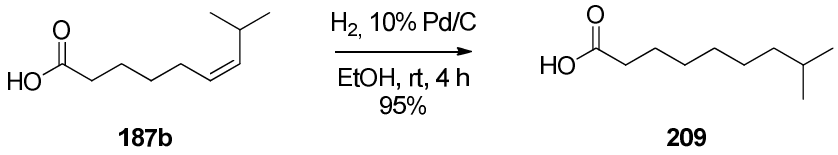

187b **209**

Scheme 2.41: Hydrogenation of (*Z*)-8-methylnonenoic acid **209**.

The saturated acid **209** was used directly for coupling to the oxazolidinone **168** in a straightforward manner (**Scheme 2.42**).

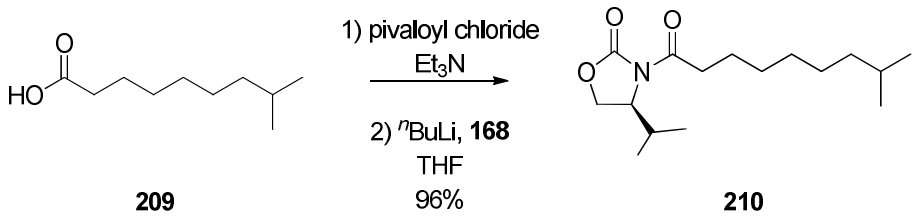

209 **210**

Scheme 2.42: Synthesis of the *N*-acylated oxazolidinone **210**.

The resultant *N*-acylated oxazolidinone **210** was then fluorinated as described earlier with NFSI (**Scheme 2.43**), before undergoing hydrolysis to give carboxylic acid **211**.

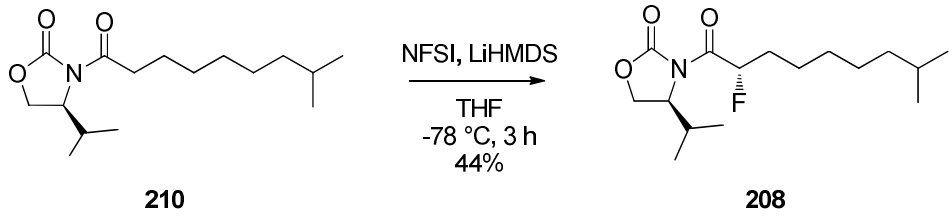

210 **208**

Scheme 2.43: Asymmetric fluorination of *N*-acyl oxazolidinone **210**.

In order to improve the conversion of the fluorination reaction, various fluorinating reagents were assayed for reaction with **210**, and the conditions are summarised in **Table 2.3**.

Entry	Fluorinating reagent	Base	Conditions	^{19}F Peaks, Yield
1	NFSI 1.3 eq	LiHMDS 1.1 eq	*i*	-194.5 ppm 44%
2	NFSI 1.3 eq	LDA 1.1 eq	*i*	-194.5 ppm <5%
3	Selectfluor 1.3 eq	LiHMDS 1.1 eq	*ii*	-173.1, -115.1, -102.6, -99.6, -93.4 ppm
4	Accufluor 1.5 eq	LDA 2 eq	*iii*	-171.5, -187.9 ppm

i: THF,-78 °C, 3 h; *ii*: ACN, 0 °C then rt, 5d; *iii*: ACN, rt, 1d.

Table 2.3: Attempts of fluorination of *N*-acyl oxazolidinone **210**.

Entry 1 shows that the reaction setup in conditions previously used didn't go to completion (44%), but a poorer result was obtained using LDA as a base (entry 2). Other electrophilic fluorinating reagents proved to be less reactive and reactions were carried out at warmer temperatures for up to 5 days but did not give identifiable products (entry 3-4).

Hydrolysis to 2-fluoromethylnonanoic acid **211** was achieved in the same conditions as for 2-fluoromethylnonenoic acid **204 (Scheme 2.44)**.

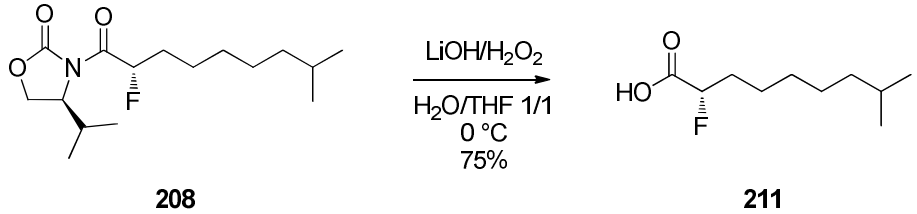

Scheme 2.44: Synthesis of 2-fluoromethylnonanoic acid.

However in this case, product also contained the non-fluorinated acid **209** (<20%). Purification by chromatography proved to be difficult and did not allow separation of the fluorinated from the non-fluorinated product.

2.6.2- The use of imidazolidinones as organocatalyst for asymmetric α-fluorination

When this work started, several organocatalytic methods had just been published separately by Jørgensen,[71] Barbas[72] and MacMillan.[73] Imidazolidinones such as **212** promote enamine catalysis from aldehydes **213**, reacting with a wide variety of electrophiles. For electrophilic fluorination, the enamine intermediate **214a** reacts with electrophilic NFSI to generate an α-fluoroaldehyde **216** (**Scheme 2.45**).[73]

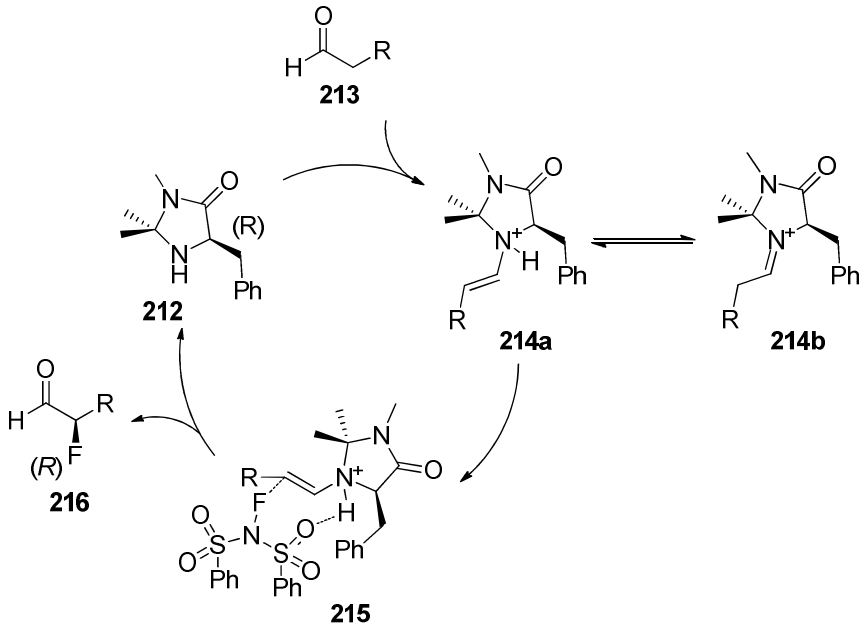

Scheme 2.45: MacMillan catalytic cycle.

Macmillan's method generates an α-fluoroaldehyde **216** which was reduced immediately to facilitate enantiomeric analysis. The enantioselectivity of the reaction is generally high, ranging from 91% to 99% ee.

Alongside the oxazolidinone project, Dr Margit Winkler at St. Andrews, explored the MacMillan asymmetric fluorination method, to access the α-fluoroacid **204** in two steps from the corresponding aldehyde **219**.[74] The synthetic route is shown in **Scheme 2.46**.

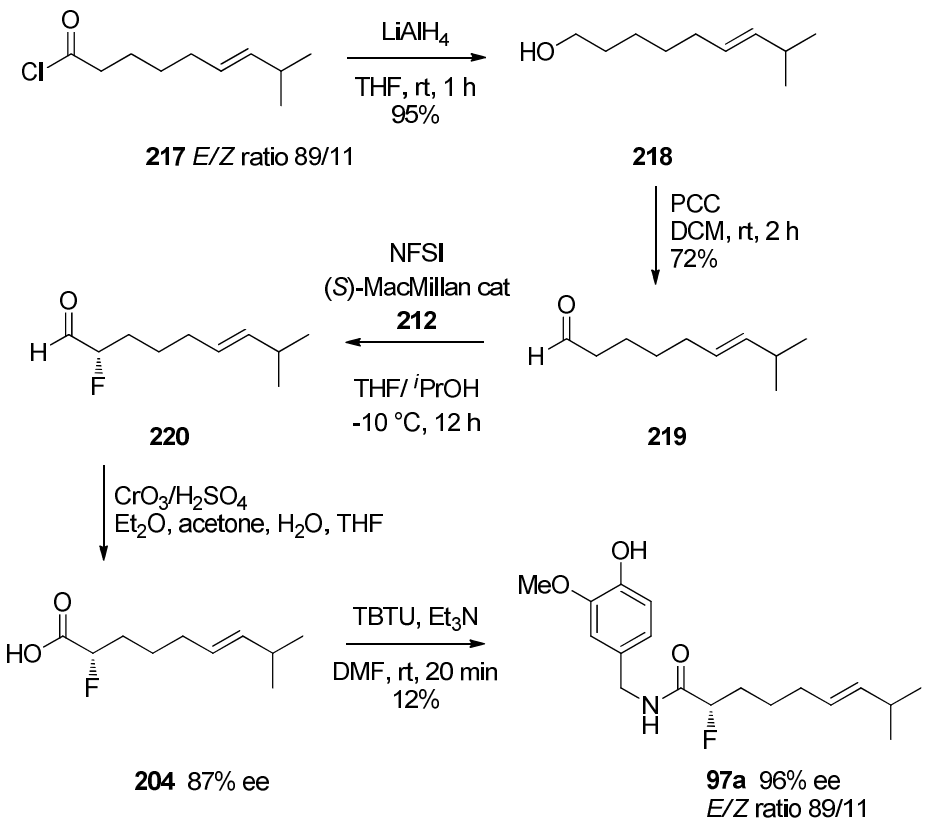

Scheme 2.46: Synthesis of fluorocapsaicin with MacMillan fluorination.[74]

The key reaction involved asymmetric fluorination following the conditions reported by MacMillan.[73] (*R*)- and (*S*)- α-Fluoroaldehydes **220a/b** were thus obtained in high ee (90%). However, imidazolidinone **212** is not very discriminating toward its substrate and thus this

system also generated 15-20% of α,α-difluorinated aldehyde **221** (**Figure 2.24**, **p.107** shows the GC-MS trace).

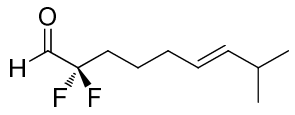

221

Oxidation and then coupling of the resultant carboxylic acid to vanillylamine generated (*R*)- and (*S*)- fluorinated capsaicin **97a/b** (96% and 95% ee after recrystallisation from hexane). The *(E)*-8-methylnon-6-enoyl chloride **217** was provided as "predominantly *E*" by Sigma-Aldrich and GC-MS analysis revealed an *E*/*Z* ratio of 89:11. This ratio was similar to the result of cross-metathesis reaction, and was unfortunately maintained all along the synthesis of **97**.

A suitable crystal was isolated and X-Ray crystallography confirmed the structure and absolute stereochemistry of (*S*)-**97a**. It also revealed the expected *anti* planar orientation of the C–F bond relative to the amide carbonyl (**Figure 2.22**).

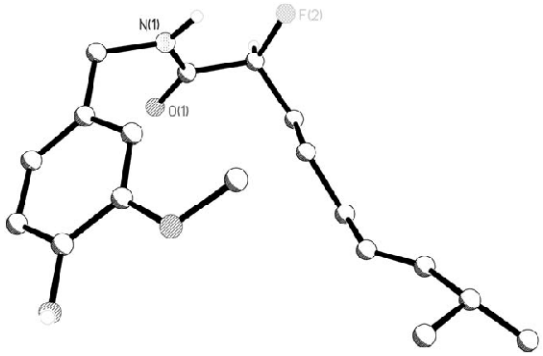

Figure 2.22: X-Ray structure of fluorinated capsaicin (*S*)-**97a**.

2.6.3- Analogues of capsaicin

2.6.3.1- Synthesis of shorter chain capsaicinoids analogues

A recent QSAR study on synthetic capsaicinoids of various chain length[75] highlighted the importance of the acyl moiety for low IC_{50} values against the TRPV1 receptor and correlated it to the lipophilicity of the compound. It appears that the IC_{50} is between 0.188 and 0.728 $mmol.L^{-1}$ when the acyl chain has 4 to 14 carbons. Shorter and longer chains have the IC_{50} values increased, up to 4 $mmol.L^{-1}$. This indicates that the capsaicinoid side-chain should not be shorter than four carbons in length. On the other hand, highly lipophilic capsaicinoids with C14, C18 or C18:1 chains do not activate the TRPV1 receptor in the endoplasmic reticulum but generate instead a small increase in Ca^{2+} influx, suggesting that the agonistic response is not only based on lipophilicity.[76] It emerged from these studies that synthesis of shorter chain capsaicinoids and an evaluation of their biological activity is worthy of investigation.

2.6.3.2- Synthesis of the non-fluorinated short chain analogue

The synthesis of α-fluorinated short chain analogues of capsaicin was carried out to study the effect of the fluorine on the conformation of the molecule and the impact on the binding to the TRPV1 receptor pocket. However, a comparison of (*R*)- and (*S*)- **99a/b** with the non-fluorinated analogue should determine the effect, if any, of the stereogenic fluorine. To this end, a non-fluorinated analogue was also synthesised.

Synthesis of the non-fluorinated analogue proved very straightforward and coupling with HOBt/EDC between **118** and 4-methylvaleric acid **222** provided the desired amide **223** in 43% yield (**Scheme 2.47**).

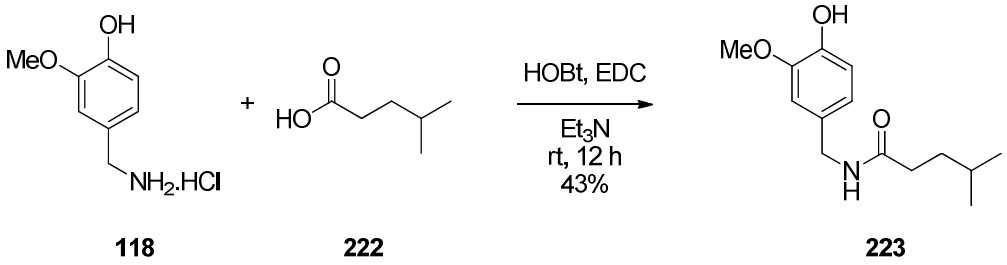

118 **222** **223**

Scheme 2.47: Synthesis of the capsaicin analogue **223**.

2.6.3.3- Deaminative fluorination

A straightforward approach was then taken for the synthesis the shorter chain analogues of capsaicin. A direct method to access appropriate α-fluoroacids involves diazotisation of α-aminoacids, with HF as the mineral acid.[77, 78] The diazonium intermediate is created by treatment of the primary amine with sodium nitrate under acidic conditions (**Scheme 2.48**).

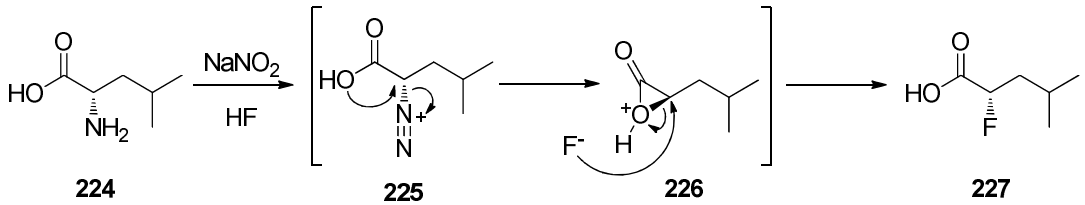

224 **225** **226** **227**

Scheme 2.48: Mechanism of deaminative fluorination on L-leucine.

The instability of the diazonium carboxylic acid **225** leads to cyclisation to an α-lactone **226** with an inversion of configuration. Opening of **226** by fluoride ion then allows the formation of the corresponding α-fluorocarboxylic acid **227**. This mechanism involves a double inversion with predominant overall retention of configuration. Therefore, the predominant stereochemistry of the α-fluoroacid is dictated by the absolute stereochemistry of the starting amino acid.[79]

Accordingly L-leucine **224** was treated with sodium nitrate in a solution of HF/pyridine (70/30) at -78 °C to allow the formation of the diazonium salt. This provided on work-up the α-fluoroacid **227** in modest yield (45%) after distillation (**Scheme 2.49**).

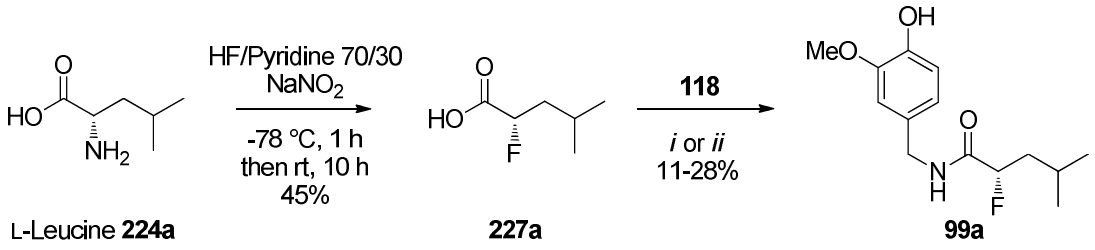

Scheme 2.49: Deaminative fluorination and amide coupling to **99a**.

α-Fluoroacid **227** was then coupled to vanillylamine **118** using a variety of conditions as summarised in **Scheme 2.49**. The HOBt and EDC coupling combination proved poor for capsaicin (32% yield after purification), although it seemed to be even lower in the case of **99** (11-17%). An attempt of coupling *via* an intermediate acylfluoride involved Deoxofluor (1.2 eq) and provided a significantly improved yield to the reaction (24-28%).

In order to establish that there was no racemisation in the coupling step from **227** to **99** (**Scheme 2.50**), chiral analysis of **227** was explored. Thus coupling of (*R*)- and (*S*)- **227a/b** with (*S*)-1-phenylethylamine **205a** under the same coupling conditions (HOBt/EDC) used for the capsaicin analogue, gave a product amide, (*S,S*)-**228a** or (*S,R*)-**228b**, with 96% de and 92% de respectively as outlined on **Scheme 2.50**.

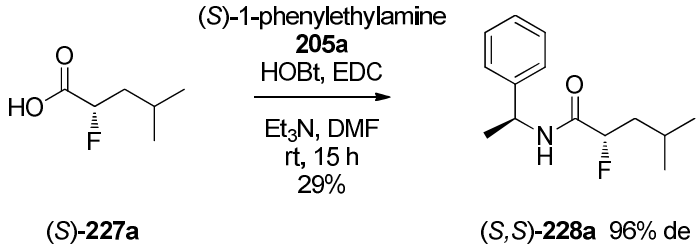

(*S*)-**227a** (*S,S*)-**228a** 96% de

Scheme 2.50: Amide derivatization of (*S*)-2-fluoroacid **227a** to diastereoisomer **228a**.

To assess if the difference in the de values was due to a kinetic resolution between the α-fluoroacid enantiomers, a control experiment was carried out with racemic **227**. The synthesis of racemic 2-fluoroacid (*R/S*)-**227** from DL-leucine was executed, followed by coupling to (*S*)-1-phenylethylamine **205a**. In this case, no kinetic resolution was observed, and both diastereomers of **228** were formed in an equal ratio (**Figure 2.23**). This suggests that the enantiomeric purity varies to some extent with the reaction conditions.

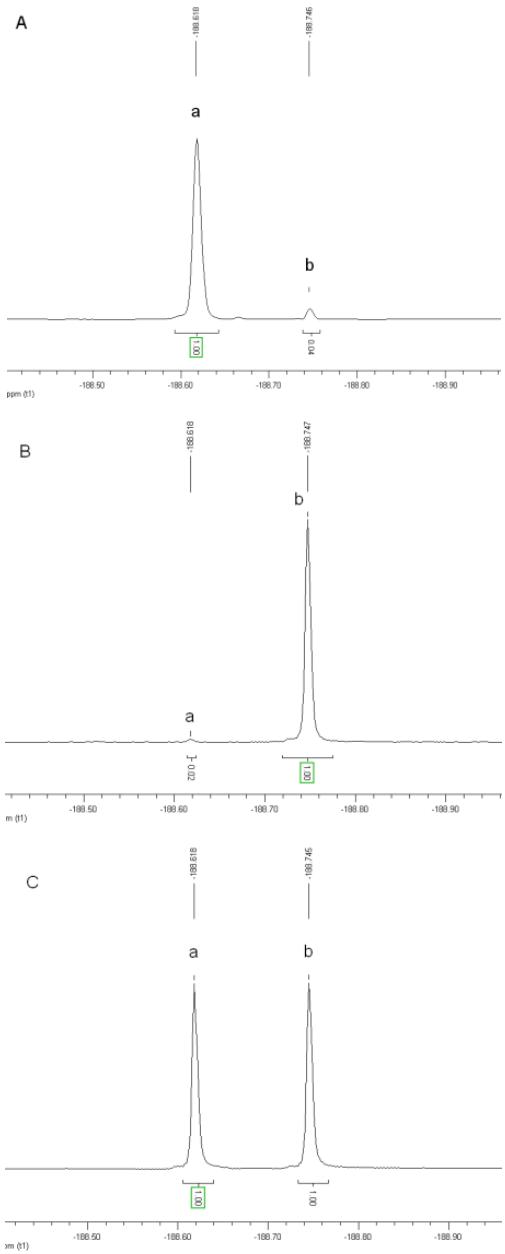

Figure 2.23: ^{19}F NMR showing the absence of kinetic resolution during the amide coupling (A: synthesis of (*S*,*R*)-**228b**, B: synthesis of (*S*,*S*)-**228a**, C: synthesis of (S, *R/S*)-**228**, peak a: (*S*,*R*)-**228b**, peak b: (*S*,*S*)-**228a**).

This method of installing fluorine in an enantioselective enriched manner from an amino acid proved to be efficient (1 step) and thus, it allowed both (*R*)- and (*S*)- fluoro enantiomers of **99** to be obtained. However, the method was less stereoselective for the (*R*)-enantiomer **99b** than the organocatalytic fluorination used for capsaicin (92% de for (*R*)-**99b**, but 96% de for (*S*)-**99a**). Accordingly, the organocatalytic method was explored for comparison.

2.6.3.4- Asymmetric fluorination by organocatalysis

The enantioselective α-fluorination using MacMillan's asymmetric fluorination method was evaluated in section **2.6.2**. Developing this approach, a preliminary study on fluorination of capronaldehyde **229** revealed that this method could be improved when the temperature was decreased to -15 °C and the reaction time monitored carefully by GC-MS (**Scheme 2.51**).

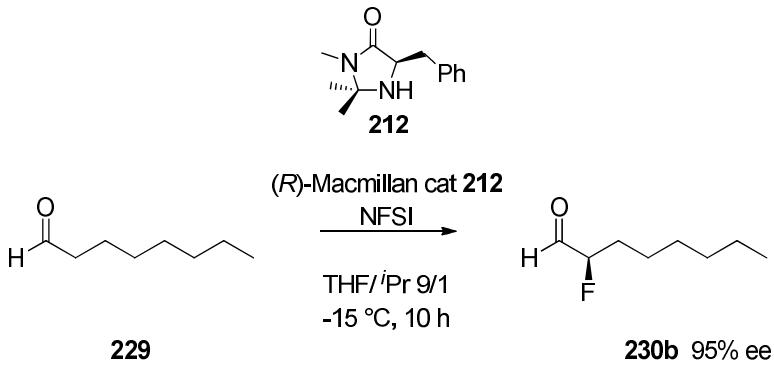

Scheme 2.51: Optimisation of organocatalytic fluorination conditions on capronaldehyde **229**.

Such optimised conditions decreased the 2,2-difluorooctanal side-product **231** to less than 5%, relative to 20% of 2-difluoro-8-methylnon-6-enal **221** initially obtained, during the fluorocapsaicin synthesis (**Figure 2.24**).

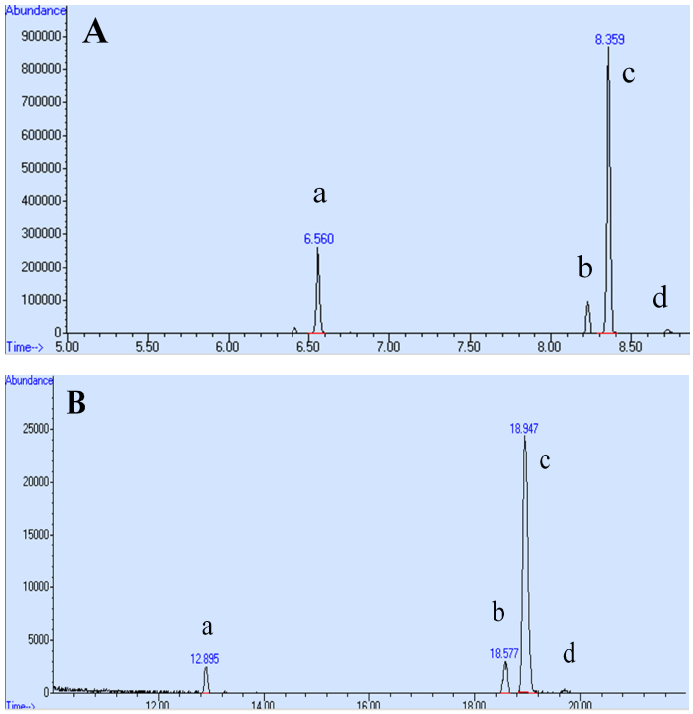

Figure 2.24: Typical MacMillan organocatalysis results monitored on chiral GC-MS (A: 2-fluoro-8-methylnon-6-enal **220**, B: 2-fluorooctanal **230**. peak a: difluorinated aldehyde, peak b: non-fluorinated aldehyde, peak c: (*R*)-fluoroaldehyde, peak d: (*S*)-fluoroaldehyde).

The α-fluorinated aldehyde product **230** was volatile and unstable at ambient temperature. For this reason, it is better analysed after conversion to the more stable alcohol[71, 73] or carboxylic acid,[72] prior to analysis. However, in order to check the ee of the α-fluorinated aldehydes directly at room temperature, an NMR method was applied. Commonly, enantiomeric excesses of aldehydes are assessed by reductive amination.

In this case, 2-fluoro octanaldehyde **230** was derivatized as imine **232** using the commercially available (*S*)-1-methoxy-2-propylamine **231**, by mixing in the NMR tube (**Scheme 2.52**).[80]

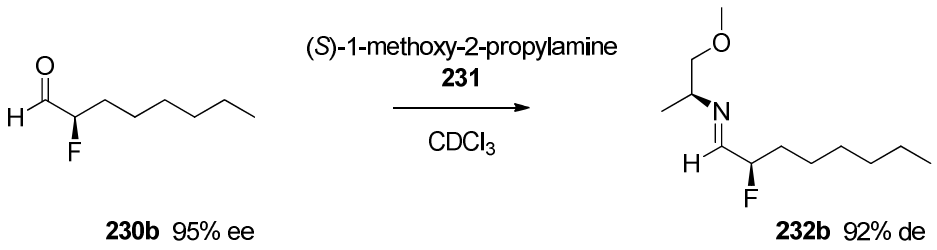

Scheme 2.52: Formation of diastereomeric imines to determinate de by ^{19}F spectroscopy.

The diastereoisomeric imine formation allowed direct evaluation of the ee of the resultant fluoroaldehyde **230** (92% de, relative to 95% ee by chiral GC-MS) by ^{19}F spectroscopy (**Figure 2.25**). In principle both (*E*) and (*Z*) imines can be formed but it is known that the imine configuration is only *E*.[81] This method appeared to be workable on crude mixtures and was a good alternative to chiral GCMS.

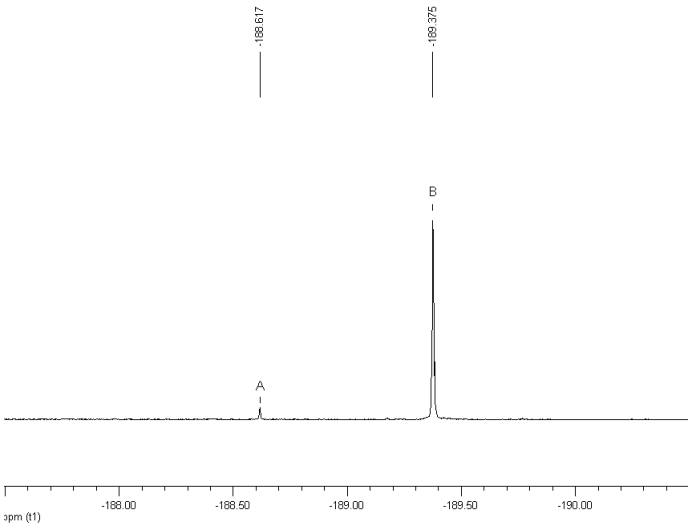

Figure 2.25: ^{19}F NMR of imine **232** showing a high diastereomeric excess (92% de) (A: (*S,E,S*)-**232b**, B: (*S,E,R*)-**232a**).

An attempt towards the preparation of the capsaicin analogue **99** was carried out. The synthesis started with the PCC oxidation of 4-methylpentan-1-ol **233** (see **scheme 2.53**). Fluorination was achieved with either (*R*)- or (*S*)- imidazolidinone catalysts **212**.

The enantiomeric excess of the aldehyde was determined by derivatisation of an aliquot with (*S*)-1-methoxy-2-propylamine **231** and a high de was observed (90% de for (*R*)-**235b**, 88% de for (*S*)-**235a**). α-Fluorinated aldehyde **235b** was oxidised with chromic acid to generate the corresponding α-fluorinated carboxylic acid **227b** without prior purification.

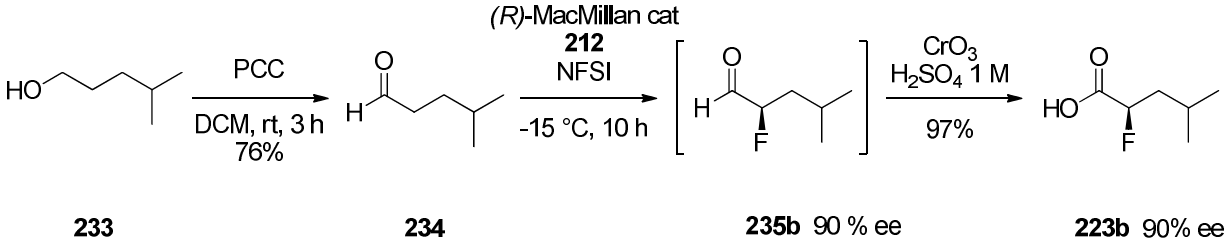

Scheme 2.53: Asymmetric organocatalytic fluorination to (*R*)-2-fluoro-4-methylpentanoic acid **227b**.

Coupling of the acid **227b** to vanillylamine **118**, again with Deoxofluor, allowed recovery of amide **99b** (**Scheme 2.54**). There was no loss of enantiomeric purity during this reaction as suggested by the control coupling in similar conditions of (*S*)-1-methoxy-2-propylamine **231** to **227b**. Indeed, the control reaction gave amide **236b** with 90% de (**Scheme 2.54**).

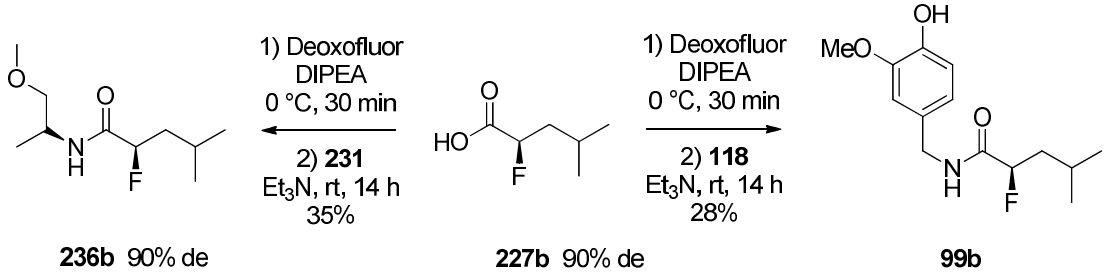

Scheme 2.54: Asymmetric organocatalytic fluorination of short chain fluorocapsaicin analogue **99b**.

2.7- α,α-Difluorinated analogues

2.7.1- Theory study of α,α-difluoroamides

The conformation of α-fluoroamides is well understood and has been described in section **2.6**. However, not much is known about the structure of α,α-difluoroamides, and only a few structures of α,α-difluoroamides are found in the Cambridge Structural Database. Installing a second fluorine atom α to an amide such as in **237** will certainly influence the conformation of the amide but it has not been clearly established in what way. It is not clear whether conformer **237 X** will be favoured from the combination of the C–F/C=O dipole-dipole relaxation to one C–F bond similar to the α-fluoroamides, or whether conformer **237 Y** will be favoured from the average dipole-dipole relaxation from the CF_2 group and the amide (**Figure 2.26**).

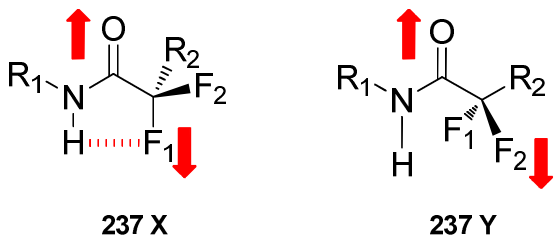

Figure 2.26: Possible conformational preferences of α,α-fluoroamides **237**.

The crystal structure of 2-(2-acetylaminophenyl)-2,2-difluoro-*N*-phenylacetamide **238** suggests the former model **237 X** (**Figure 2.27**, left).[82] However, in the X-ray structure of **239**, the conformation of the simplest difluoroacetamide **239**, none of the C–F bonds are

strictly *anti* planar to the amide. They are *gauche* with torsion angles of around 30° and are interestingly situated on the same side related to the amide plane, suggesting that in this particular case a global repulsion occurs between the amide group NH_2-CO and the difluoro moiety (**Figure 2.27**, right).[83] However this is a solid state structure and solid state interactions will also perturb the conformation.

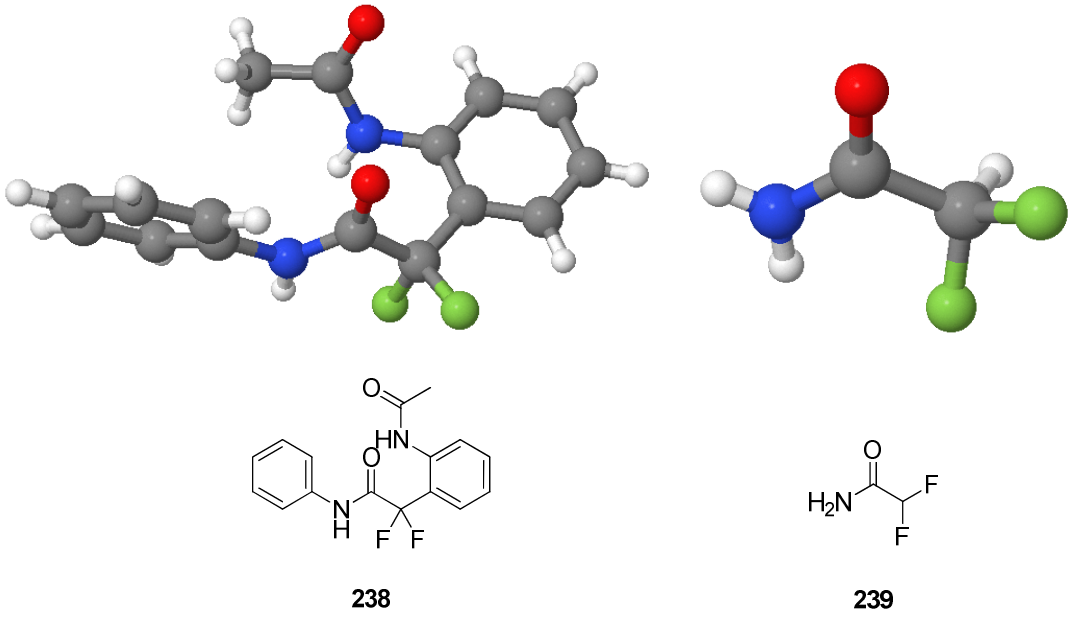

238 **239**

Figure 2.27: Examples of α,α-difluoroamides X-ray crystal structures.[82, 83]

A DFT theory study was therefore carried out examining the rotational energy profile of the model compound *N*-methyl-α,α-difluoroacetamide **240** with B3LYP functional. The changing dipole moment was also calculated during this analysis, as illustrated in **Figure 2.28** (D. Buissonneaud, St. Andrews).

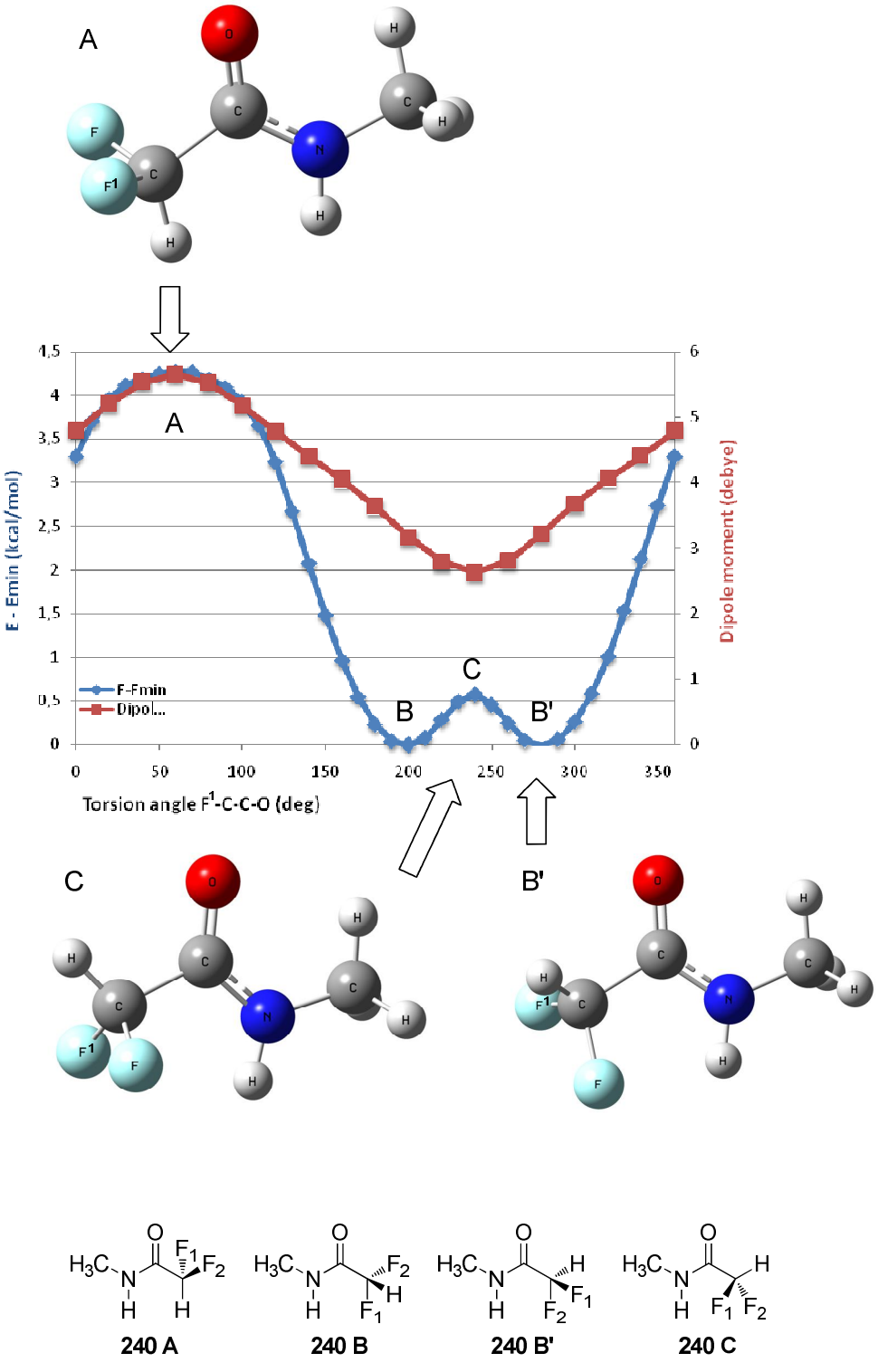

Figure 2.28: DFT theoretical study showing the variation of the dipole moment and the global minimum energy of α,α-difluoroamide **240**.

The dipole moment (red curve) is at a global maximum for a rotation angle of 60°, which coincides with the position of the CF_2 dipole *syn* to the C=O dipole (conformation **A**). The dipole relaxation reaches a global minimum for an angle of 240°, which corresponds to the position of the CF_2 dipole *anti* to the C=O dipole (conformation **C**). However, the two global energy minima (blue curve, conformations **B** and **B'**) coincide with 40° rotations to F–C–C–O angles 200° or 280° (**240 C**). These 40° rotations relax the eclipsing interaction between the C=O and H–CF_2 bonds and thus the global minima **B** and **B'** are a compromise between dipole relaxation and steric relaxation.

2.7.2- Synthesis of 2,2-difluoro-4-methylpentanoic acid 242

2.7.2.1- α,α-Difluorination by organocatalysis

In an effort to prepare the α,α-difluoro aldehyde **241**, the MacMillan asymmetric fluorination was monitored at room temperature to allow the second fluorination to proceed (**Scheme 2.55**). The product mixture of α,α-difluoro aldehyde **241** was directly oxidised using Jones reagent to give the corresponding α,α-difluoro acid **242** (91% yield on two steps).

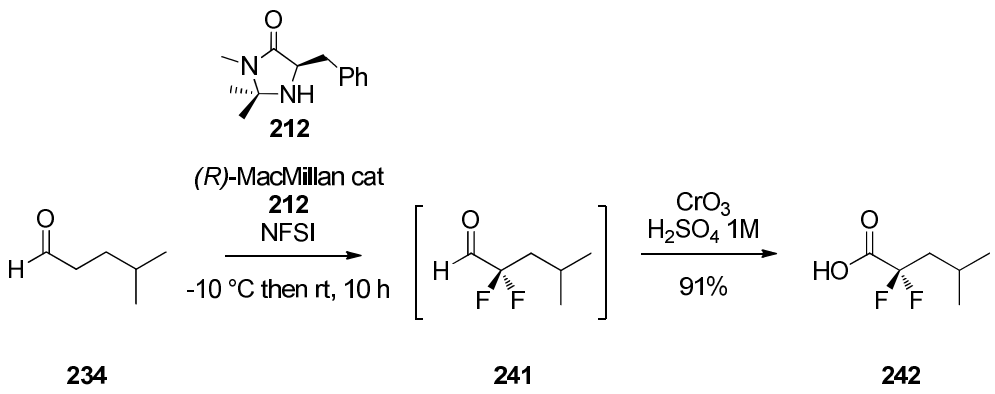

Scheme 2.55: Organocatalytic synthesis of α,α-difluoroamide **242**.

2.7.2.2- α,α-Difluorination of α-ketoesters

The nucleophilic difluorination of an α-ketone was also explored. The first step involved the conversion of the α-ketoacid **243** as α-ketoester **245**. Esterification of **243** with thionyl chloride in methanol lead to a mixture of the desired ester **245** but also the corresponding α-ketal **244** in a 30:70 ratio in favour of the ketal (**Scheme 2.56**). This mixture was then treated with perchloric acid for 3-4 h to give a full conversion into the α-ketoester **245**.[84]

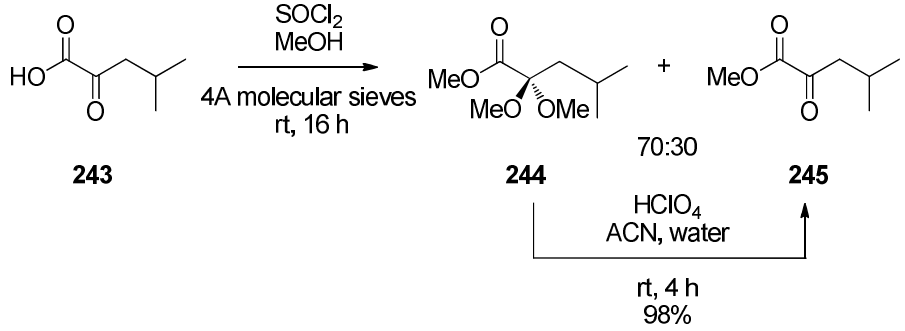

Scheme 2.56: Synthesis of ketoester **245**.

Difluorination was achieved with DAST and provided methyl 2,2-difluoro-4-methylpentanoate **246** with a reasonable conversion. An attempt at this transformation with the new reagent FLUOLEAD (2 eq), either at rt or at reflux of DCM did not give the desired product. The high volatility of **246** depleted the yield to 55% even though solvent removal was cautiously carried out at 0 °C.[85]

2,2-Difluoro-4-methylpentanoic acid **242** was then obtained after hydrolysis of **246** in an ethanolic solution of KOH (10 eq) and acidic work-up (86%) (**Scheme 2.57**).

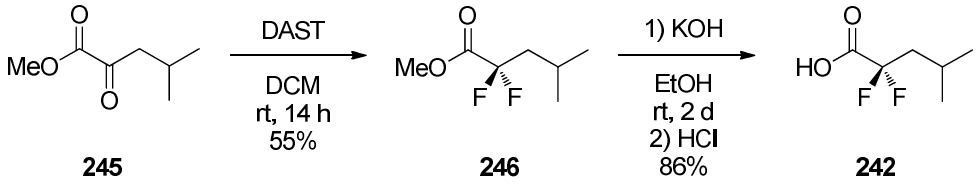

245 **246** **242**

Scheme 2.57: Preparation of α,α-difluorocarboxylic acid **242**.

2.7.3- Amide coupling of α,α-difluoro acid

The carboxylic acid **242** was treated with Deoxofluor in an attempt to couple with vanillylamine **118,** but this was not successful (**Scheme 2.58**). The high electronegativity of the two fluorine atoms clearly deactivates the carboxylic acid group.

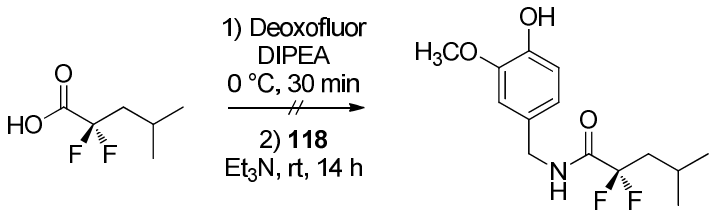

242 **247**

Scheme 2.58: Acyl fluoride mediated amide coupling to **247**.

In the same manner, the uronium salt TBTU **248** when used in excess (1.3 eq), was unable to efficiently activate the α,α-difluoroacid and the difluorinated analogue of capsaicin **247** was obtained in a very modest yield (9%) (**Scheme 2.59**).

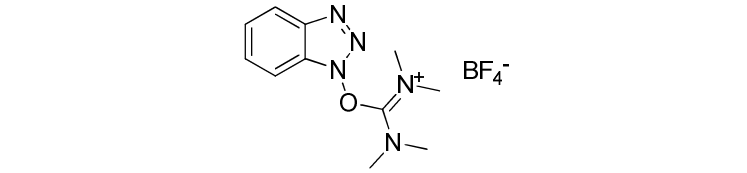

N,*N*,*N*′,*N*′-Tetramethyl-*O*-(benzotriazol-1-yl)uronium tetrafluoroborate
TBTU **248**

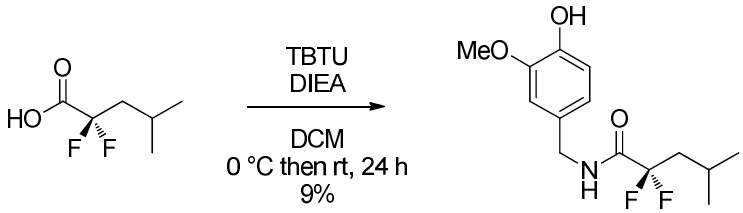

242 **247**

Scheme 2.59: TBTU coupling of α,α-difluoroacids **242**.

An improvement of the coupling was made using the acyl chloride **249**. The one-pot reaction was successful but the yield remained modest (19%) (**Scheme 2.60**).

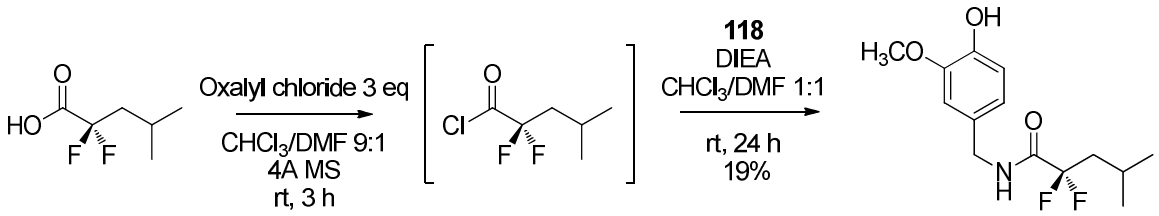

242 **249** **247**

Scheme 2.60: Amide coupling by formation of acyl chloride intermediate **249**.

2.7.4- α,α-Difluorination of α-ketoamides

The amide coupling of the α,α-difluoro-carboxilic acid **242** proved to be very modest. In an attempt to remedy this issue, an alternative pathway was attempted, involving amide coupling of an α-ketoacid prior to the fluorination. Accordingly, 2-oxo-4-methylvaleric acid **243** was activated using isobutylchloroformate and then vanillylamine **118** was added to give the α-ketoamide **250** in a good yield (76%) (**Scheme 2.60**).

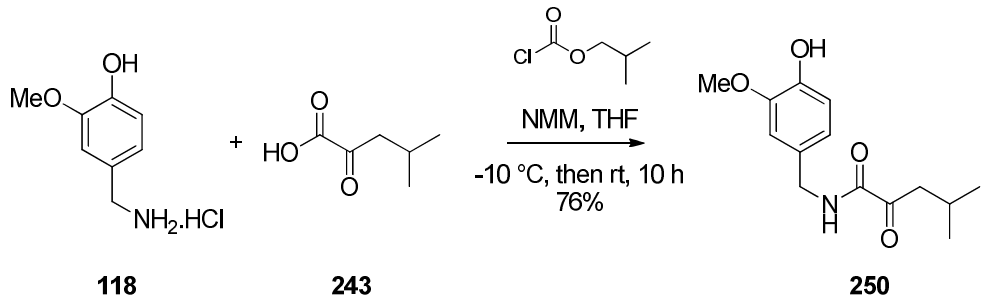

118 **243** **250**

Scheme 2.60: Amide coupling with α-ketoacid **244**.

The fluorination step was achieved by treating the α-keto amide **250** with DAST. The reaction mixture gave a complex mixture, although ^{19}F NMR analysis showed a peak at -104 ppm suggesting the formation of the α,α-difluoramide **247**. Despite considerable effort, the product could not be isolated and the reaction proved unsatisfactory (**Scheme 2.61**).

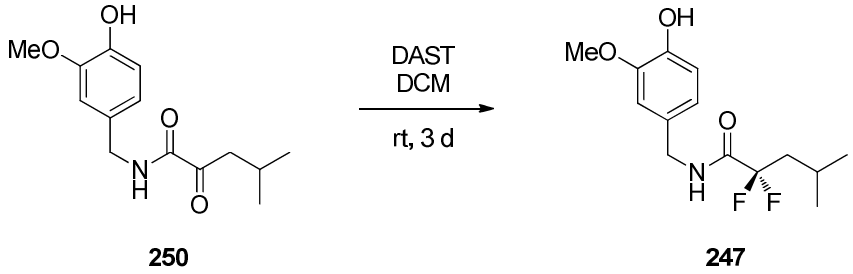

250 **247**

Scheme 2.61: Difluorination of α-keto amides leads to α,α-difluoroamides **247**.

2.8- Biological evaluation

The synthetic analogues (*S*)-**99a** (96% ee), (*R*)-**99b** (92% ee), and **223** described in this chapter were assayed with the TRPV1 receptor derived from rats. This work was carried out by the group of Dr Roderick Scott at Aberdeen University (**Scheme 2.50**). For comparison purposes, the results of the biological assays for (*R*)-**97** (96% ee), (*S*)-**97** (95% ee) are also reported. The biological responses are then compared to that of natural capsaicin **93**.

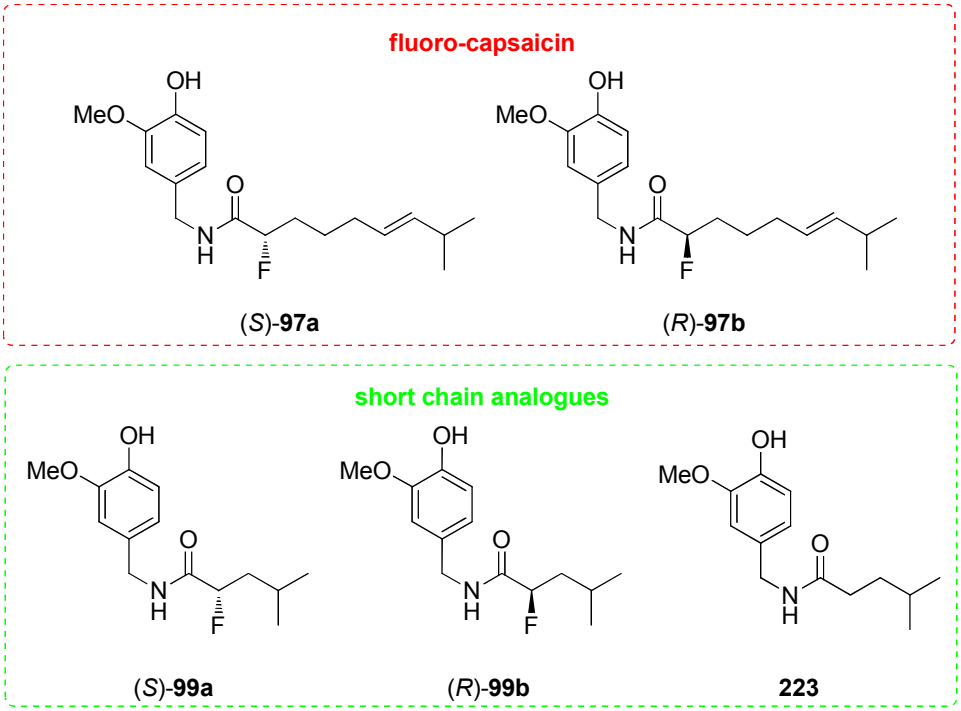

Scheme 2.62: The set of molecules submitted to biological evaluation.

2.8.1- Biological assay

2.8.1.1- Fluorinated enantiomers of capsaicin

Neurones expressing TRPV1 receptors are a subpopulation of dorsal root ganglia (DRG), which are activated by capsaicin as it evokes a transient increase in intracellular Ca^{2+}. In the first study, neurones which showed a 90 % response to a capsaicin application (1 μM) were selected for the fluorocapsaicin assays. (*S*)- and (*R*)-fluorocapsaicin **97** also evoked an increase in intracellular Ca^{2+} in a similar manner to capsaicin. The amplitude of the response was not significantly different at equal concentrations (1 μM) of the enantiomers as illustrated on **Figure 2.29 B** and **D**. The fluorinated capsaicin enantiomers **97a/b** were both agonists and had a similar level of response. There was no obvious enantiomeric discrimination.

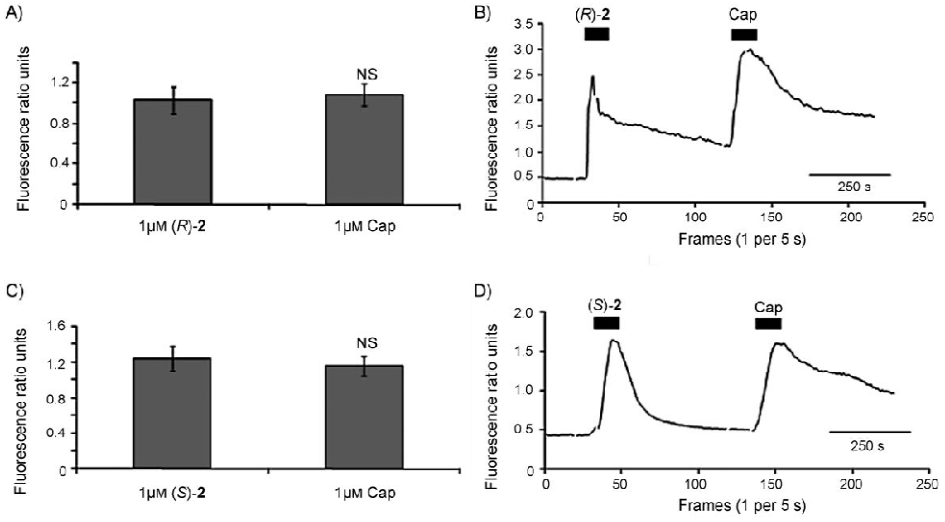

Figure 2.29: Evoked responses in cultured DRG neurones are similar for enantiomers of **97** (top: (*R*)-**97b**, bottom: (*S*)-**97a**).

A second study was used to investigate (*R*)-fluorocapsaicin binding (**Figure 2.30**). Capsazepine **106**, a TRPV1 receptor antagonist, was used (1 mM) to compete with the (*R*)- and (*S*)- enantiomers of **97**.

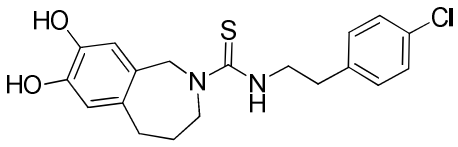

capsazepine **106**

Neurones were pre-treated with capsazepine **106** for 5 min before application of the fluorinated analogues, and this inhibited the response to (*S*)-**97a** and (*R*)-**97b**. After washing, the neurones recovered their sensitivity to capsaicin or its fluorinated analogues indicating capsazepine **106** and fluorocapsaicins **97** are binding at the same site on the receptor.

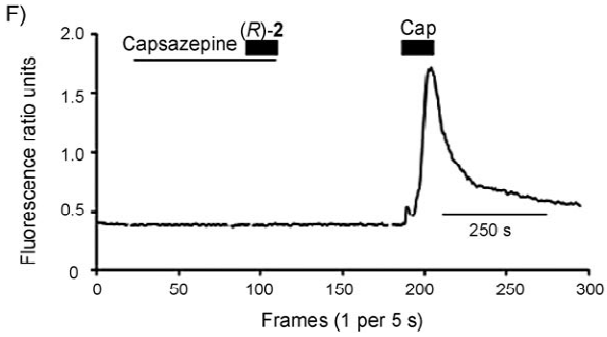

Figure 2.30: Evoked responses by (*R*)-**97b** in cultured DRG neurones indicate an agonistic effect.

Experiments conducted at lower concentrations of the (*R*)-fluoro enantiomer **97b** (330 and 250 nM) showed that responses of the fluorocapsaicins **97** were 20% lower than the maximum response of capsaicin itself. Neurones recovered a full response to both of the

fluoro-enantiomers at 500 nM. In conclusion, (*S*)-**97a** and (*R*)-**97b** displayed equal agonist potency and a similar response to capsaicin. From this result was developed an extended binding model where the side-chain is aligned along the molecular axis of **97** (**Figure 2.31**).

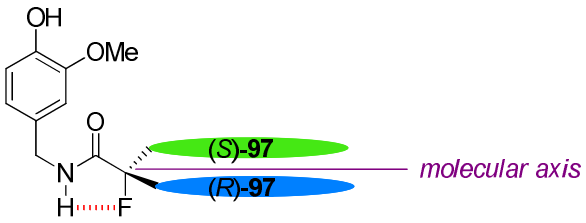

Figure 2.31: Supposed side-chain projection in the two enantiomers of **97**.

2.8.1.2- Short fluorinated analogues of capsaicin

Biological evaluation for the short fluorinated analogue of capsaicin was carried out with slight differences. Both (*R*)- and (*S*)-**99** and also the non-fluorinated control **223** were compared to capsaicin **93**.

The cultured DRG neurons from neonatal rats were exposed to two applications of capsaicin **93** (100 nM, 10 times lower concentration than for α-fluorocapsaicins **97a/b**) with a NaCl media wash between the two applications (**Figure 2.32**).

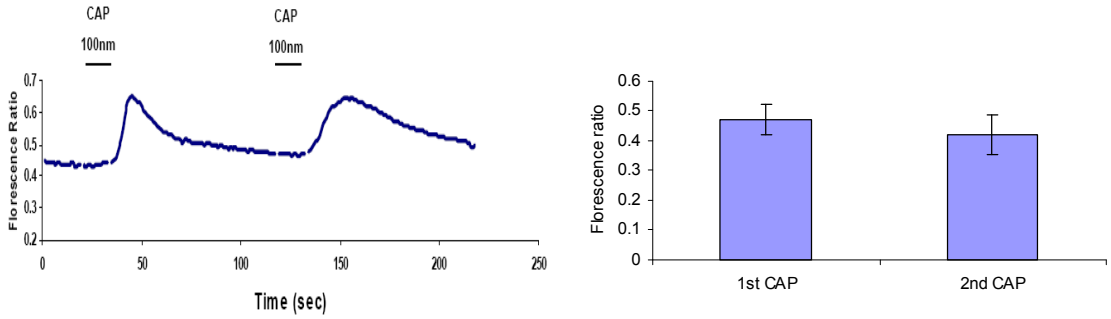

Figure 2.32: Control experiment with capsaicin to select responsive neurones

The results showed there was no significant difference in response between the two applications of capsaicin, and that the neurons fully recovered their response.

The control analogue **223** was applied (100 nM)to neurones evoked by capsaicin (100 nM). This analogue did not evoke any response from the neurones (**Figure 2.33**), whereas when capsaicin **93** is conjointly applied, the response is significantly inhibited. This is consistent with an antagonistic effect of the shorter chain analogue **223**.

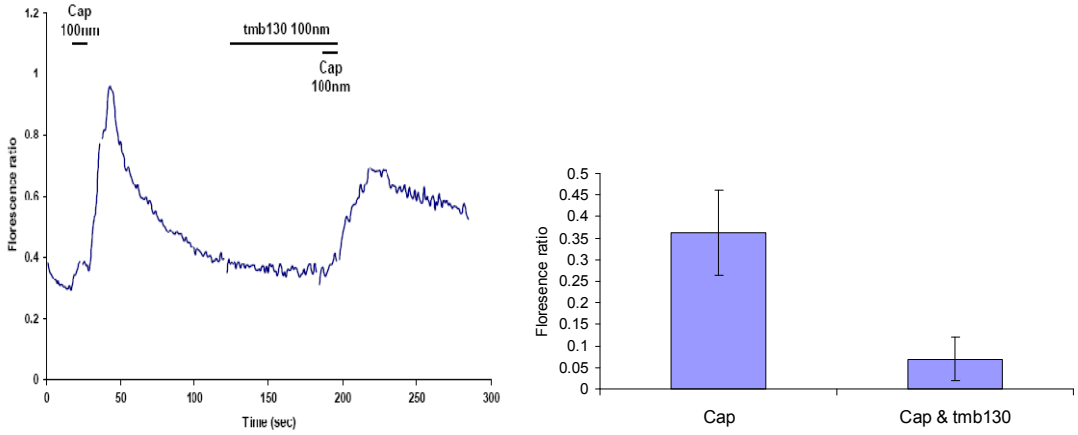

Figure 2.33: Non-fluorinated reference **223** shows partial antagonistic response to capsaicin

The same procedure was applied to the (*R*) enantiomer **99b** (92% e.e.) and the result revealed two responses depending on the sensitivity of the neurones. When neurones were not evoked by capsaicin, **99b** did not show a response by itself, but it could increase the apparent sensitivity of neurones when co-applied with capsaicin. Thus cells that did not respond to the first application of capsaicin subsequently responded when capsaicin was applied in the presence of (*R*)-**99b** (**Figure 2.34**, left). However, in neurons already sensitive to capsaicin, (*R*)-**99b** had no obvious effect on the capsaicin response (**Figure 2.34**, right).

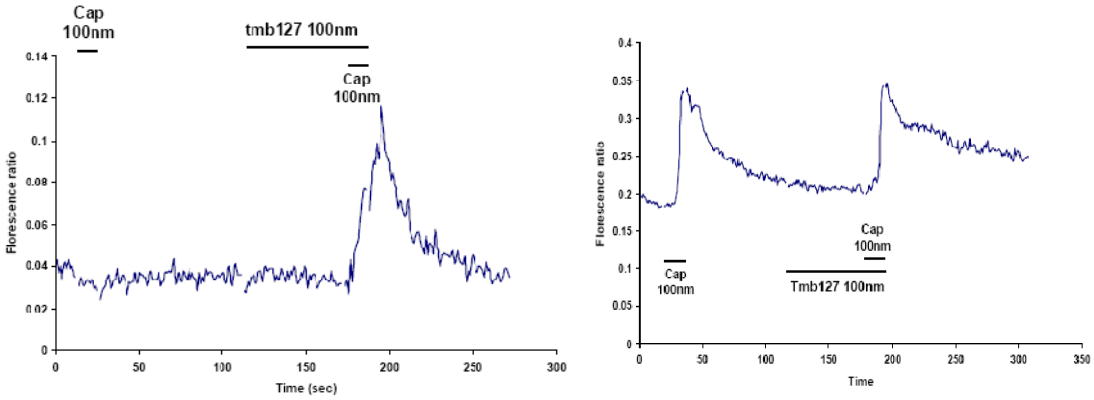

Figure 2.34: The two responses obtained from (*R*)-**99b** showing a full recovery of sensitivity (left) and an absence of effect (right).

The result from the (*S*)-enantiomer proved the most clear of all the analogues. When (*S*)-**99a** (96% e.e.) was applied alone it did not evoke a response in the neurones, and additionally it totally inhibited the response to capsaicin when co-applied. To verify that the neurones did not show any loss of sensitivity, capsaicin was then applied alone and evoked a strong response from the neurones. Thus the (*S*)-enantiomer **99a** clearly acted as a potent antagonist to capsaicin (**Figure 2.34**).

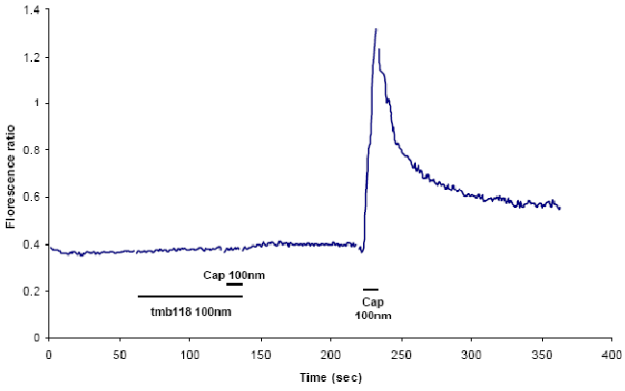

Figure 2.35: A clear antagonistic effect of (*S*)-**99a**.

These assays show that all capsaicin analogues **97a/b**, **99a/b** and **223** were bioactive and this suggests that their vanilloid moieties are binding to the critical residues Tyr 511, Ser 512 and Tyr 550 usually involved in vanilloid binding. The diversity of biological responses was most probably generated by the differences in lipophilic binding.

Short chain analogue **223** show antagonistic properties as expected. Installation of fluorine in (*S*)-**99a** increased the antagonistic potency in a similar manner to capsazepine **106**. It may be due to a specific conformation induced by the C–F bond or less likely a specific interaction of the fluorine with the protein (see **Chapter 1.5.3**), amide carbonyl groups of which provide a fluorophilic environment.

It is interesting that the short chain analogues **99a**, **99b** and **223** are active at ten times lower concentration than capsaicin **93** or its fluorinated analogues **97a** or **97b**. In addition, the compounds **99a** and **99b** performed differentiated biological responses, and these are correlated to their respective stereoisomerism. Finally, the installation of fluorine on the ligand **99a** also increased its potency.

2.9- Conclusion

In conclusion, (*S*)-fluorocapsaicin **97a** and four short-chain analogues of capsaicin were synthesised successfully by different methods. The short-chain difluorinated analogue **247** was also targeted for biological evaluation but proved challenging to prepare.

Biological assays on fluorinated capsaicins **97a/b** proved that they acted as agonists of TRPV1 receptor, in a similar manner and proportions to capsaicin **93**.

Shortening the side-chain in compounds **99a** and **223** reversed the biological response and they now showed antagonist properties on TRPV1 receptor. The short-chain analogues also gained in potency. When the α-fluorocapsaicins **97a/b** lost potency below 500 nM, these compounds still exerted full bioactivity at 100 nM.

Most interestingly, each short-chain analogue displayed a different response and this suggests that the shorter chain is not in an extended form, as observed for **97a/b**. The non-fluorinated compound **223** is a partial antagonist. The (*S*)-fluoro-enantiomer **99a** has its antagonist properties enhanced and is a full antagonist to the TRPV1 receptor. Both of these compounds were reversible antagonists on the TRPV1 receptor, suggesting they truly did locate at the capsaicin binding-site. **99b** does not show proper antagonist or agonist properties, and this particular biological response has never been observed in capsaicinoids. The (*R*)-enantiomer **99b** is of interest in that it can restore sensitivity to capsaicin when the receptor is blocked. The mechanism of this specific action is worthy of further investigation.

There is a current interest in capsaicin antagonists such as capsazepine **106** and (*S*)-**99a** emerges as a drug candidate compound. The TRPV1 receptor is a drug discovery target and antagonists may provide therapies for pain disorders in the near future. Finally it was reported for the first time that the enantioselective introduction of fluorine α- to an amide alters the

bioactivity of a short side-chain capsaicin analogue. The various and specific biological responses to each compound are summarised in **Figure 2.35**.

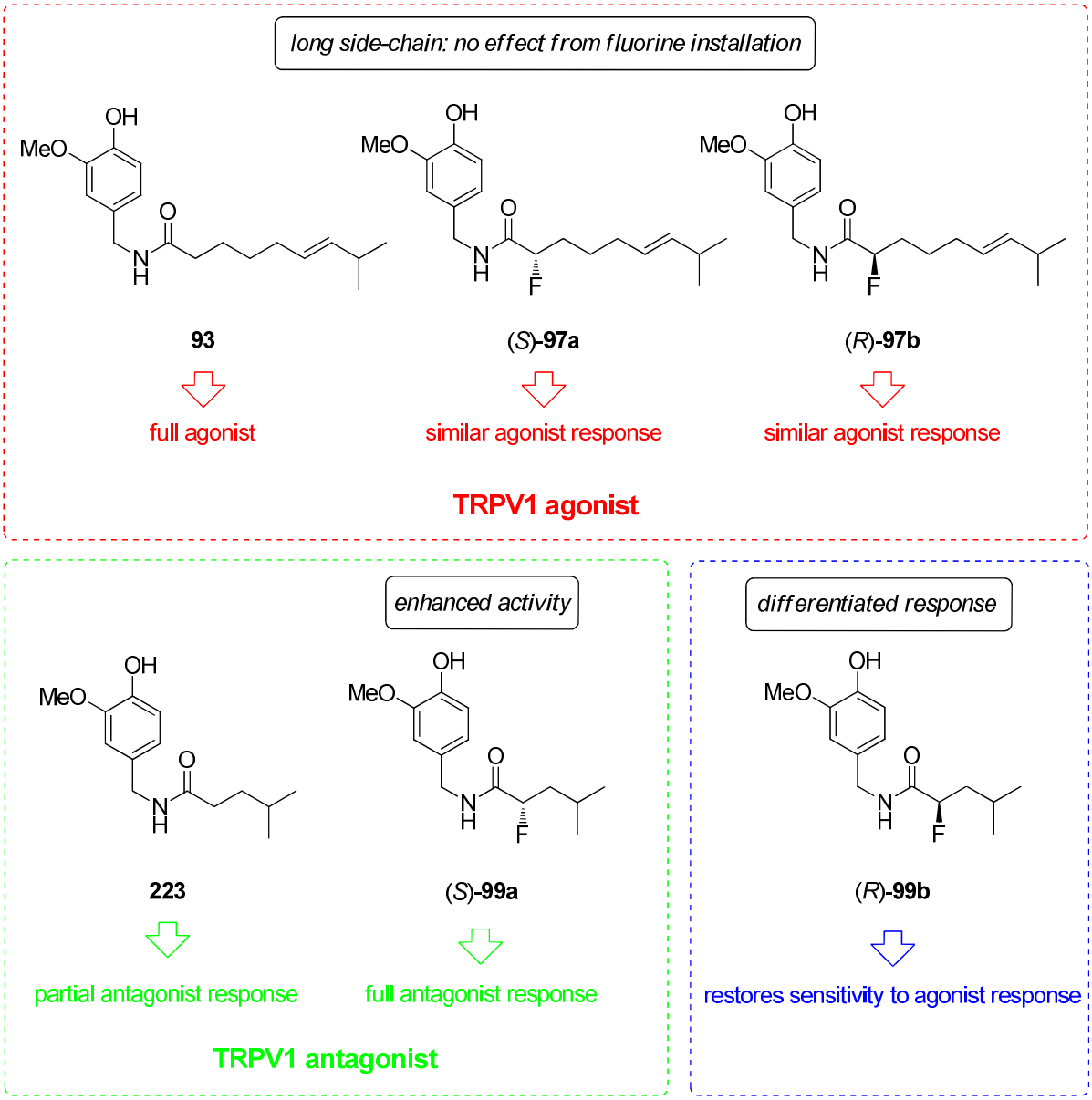

Figure 2.36: Biological effects of enantioselective installation of fluorine on capsaicin analogues.

1. C. Belmonte, F. Cervero and Editors, *Neurobiology of Nociceptors*, 1996.
2. M. J. Caterina, A. Leffler, A. B. Malmberg, W. J. Martin, J. Trafton, K. R. Petersen-Zeitz, M. Koltzenburg, A. I. Basbaum and D. Julius, *Science*, 2000, **288**, 306-313.
3. H.-G. Schaible and F. Richter, *Langenbeck's Arch. Surg.*, 2004, **389**, 237-243.
4. S. J. Conway, *Chem. Soc. Rev.*, 2008, **37**, 1530-1545.
5. J. R. Vane, *Nature*, 1971, **231**, 232-235.
6. C. Sinning, B. Watzer, L. De Petrocellis, V. Di Marzo and P. Imming, *ChemMedChem*, 2008, **3**, 1956-1964.
7. J. W. Banks, A. S. Batsanov, J. A. K. Howard, D. O'Hagan, H. S. Rzepa and S. Martin-Santamaria, *J. Chem. Soc., Perkin Trans. 2*, 1999, **11**, 2409-2411.
8. C. R. S. Briggs, D. O'Hagan, J. A. K. Howard and D. S. Yufit, *J. Fluorine Chem.*, 2003, **119**, 9-13.
9. R. Mathad, B. Jaun, O. Flögel, J. Gardiner, M. Löweneck, J. Codée, P. Seeberger, D. Seebach, M. Edmonds, F. Graichen and A. Abell, *Helv. Chim. Acta*, 2007, **90**, 2251-2273.
10. M. J. Caterina and M. A. Schumacher, *Nature*, 1997, **389**, 816-824.
11. M. Tominaga and T. Tominaga, *Pflüg. Arch. Eur. J. Phys.*, 2005, **451**, 143-150.
12. B. Veronesi and M. Oortgiesen, *Toxicol. Sci.*, 2006, **89**, 1-3.
13. M. S. P. Sansom, I. H. Shrivastava, J. N. Bright, J. Tate, C. E. Capener and P. C. Biggin, *BBA - Biomembranes*, 2002, **1565**, 294-307.
14. S.-E. Jordt and D. Julius, *Cell*, 2002, **108**, 421-430.
15. S. G. Sedgwick and S. J. Smerdon, *Trends Biochem. Sci.*, 1999, **24**, 311-316.
16. T. Rosenbaum, A. Gordon-Shaag, M. Munari and S. E. Gordon, *J. Gen. Physiol.*, 2003, **123**, 53-62.
17. G. Fernández-Ballester and A. Ferrer-Montiel, *J. Membr. Biol.*, 2008, **223**, 161-172.
18. D. E. Clapham, *Nature*, 2003, **426**, 517-524.
19. N. Kedei, T. Szabo, J. D. Lile, J. J. Treanor, Z. Olah, M. J. Iadarola and P. M. Blumberg, *J. Biol. Chem.*, 2001, **276**, 28613-28619.
20. J. Jung, S. W. Hwang, J. Kwak, S.-Y. Lee, C.-J. Kang, W. B. Kim, D. Kim and U. Oh, *J. Neurosci.*, 1999, **19**, 529-538.
21. P. M. Zygmunt, J. Petersson, D. A. Andersson, H.-h. Chuang, M. Sorgard, V. Di Marzo, D. Julius and E. D. Hogestatt, *Nature*, 1999, **400**, 452.
22. C. S. J. Walpole, S. Bevan, G. Bovermann, J. J. Boelsterli, R. Breckenridge, J. W. Davies, G. A. Hughes, I. James and L. Oberer, *J. Med. Chem.*, 1994, **37**, 1942-1954.

23. S.-E. Jordt, M. Tominaga and D. Julius, *Proc. Natl. Acad. Sci. U. S. A.*, 2000, **97**, 8134-8139.
24. M. Z. Chou, T. Mtui, Y.-D. Gao, M. Kohler and R. E. Middleton, *Biochemistry*, 2004, **43**, 2501-2511.
25. E. Phillips, A. Reeve, S. Bevan and P. McIntyre, *J. Biol. Chem.*, 2004, **279**, 17165-17172.
26. N. R. Gavva, L. Klionsky, Y. Qu, L. Shi, R. Tamir, S. Edenson, T. J. Zhang, V. N. Viswanadhan, A. Toth, L. V. Pearce, T. W. Vanderah, F. Porreca, P. M. Blumberg, J. Lile, Y. Sun, K. Wild, J.-C. Louis and J. J. S. Treanor, *J. Biol. Chem.*, 2004, **279**, 20283-20295.
27. J. M. Welch, S. A. Simon and P. H. Reinhart, *Proc. Natl. Acad. Sci. U. S. A.*, 2000, **97**, 13889-13894.
28. S. Ryu, B. Liu and F. Qin, *J. Gen. Physiol.*, 2003, **122**, 45-61.
29. M. Tominaga, M. Wada and M. Masu, *Proc. Natl. Acad. Sci. U. S. A.*, 2001, **98**, 6951-6956.
30. S.-E. Jordt, D. D. McKemy and D. Julius, *Curr. Opin. Neurobiol.*, 2003, **13**, 487-492.
31. M. Numazaki, T. Tominaga, H. Toyooka and M. Tominaga, *J. Biol. Chem.*, 2002, **277**, 13375-13378.
32. A. Szallasi and P. M. Blumberg, *Pharmacol Rev*, 1999, **51**, 159-212.
33. V. Y. Moiseenkova-Bell, L. A. Stanciu, I. I. Serysheva, B. J. Tobe and T. G. Wensel, *Proc. Natl. Acad. Sci.*, 2008, **105**, 7451-7455.
34. S. Kosuge, Y. Inagaki and H. Okumura, *Nippon Nogeik. Kaishi.*, 1961, **35**, 923-927.
35. E. K. Nelson, *J. Am. Chem. Soc.*, 1919, **41**, 2121-2130.
36. E. K. Nelson and L. E. Dawson, *J. Am. Chem. Soc.*, 1923, **45**, 2179-2181.
37. C. S. J. Walpole, R. Wrigglesworth, S. Bevan, E. A. Campbell, A. Dray, I. F. James, K. J. Masdin, M. N. Perkins and J. Winter, *J. Med. Chem.*, 1993, **36**, 2381-2389.
38. M. Mazourek, A. Pujar, Y. Borovsky, I. Paran, L. Mueller and M. M. Jahn, *Plant Physiol.*, 2009, **150**, 1806-1821.
39. E. Spath and S. F. Darling, *Beri. Dtsch. Chem. Gesell.*, 1930, **63B**, 737-743.
40. E. K. Nelson, *J. Am. Chem. Soc.*, 1919, **41**, 1115-1121.
41. P. M. Gannett, D. L. Nagel, P. J. Reilly, T. Lawson, J. Sharpe and B. Toth, *J. Org. Chem.*, 1988, **53**, 1064-1071.
42. L. Crombie, S. H. Dandegaonker and K. B. Simpson, *J. Chem. Soc.*, 1955, 1025-1027.

43. P. J. Kocienski, B. Lythgoe and I. Waterhouse, *J. Chem. Soc., Perkin Trans.1*, 1980, **4**, 1045-1050.
44. H. Kaga, M. Miura and K. Orito, *J. Org. Chem.*, 1989, **54**, 3477-3478.
45. P. E. Sonnet, *J. Org. Chem.*, 1974, **39**, 3793-3794.
46. H. Kaga, K. Goto, T. Takahashi, M. Hino, T. Tokuhashi and K. Orito, *Tetrahedron*, 1996, **52**, 8451-8470.
47. P. Schwab, R. H. Grubbs and J. W. Ziller, *J. Am. Chem. Soc.*, 1996, **118**, 100-110.
48. P. J.-L. Hérisson and Y. Chauvin, *Makromolekul. Chem.*, 1971, **141**, 161-176.
49. D. A. Evans, J. A. Ellman and R. L. Dorow, *Tetrahedron Lett.*, 1987, **28**, 1123-1126.
50. D. A. Evans, J. A. Ellman and R. L. Dorow, *Tetrahedron Lett.*, 1987, **28**, 1123-1126.
51. D. A. Evans and T. C. Britton, *J. Am. Chem. Soc.*, 1987, **109**, 6881-6883.
52. D. A. Evans, M. D. Ennis and D. J. Mathre, *J. Am. Chem. Soc.*, 1982, **104**, 1737-1739.
53. F. A. Davis and W. Han, *Tetrahedron Lett.*, 1992, **33**, 1153-1156.
54. F. A. Davis and W. Han, *Tetrahedron Lett.*, 1992, **33**, 1153-1156.
55. S. Bonazzi, S. Guttinger, I. Zemp, U. Kutay and K. Gademann, *Angew. Chem., Int. Ed.*, 2007, **46**, 8707-8710.
56. R. Sebesta and D. Seebach, *Helv. Chim. Acta*, 2003, **86**, 4061-4072.
57. N. Rabasso, ed., *Chimie organique*, De Boeck Université, 2007.
58. F. A. Davis and P. V. N. Kasu, *Tetrahedron Lett.*, 1998, **39**, 6135-6138.
59. F. A. Davis, H. Qi and G. Sundarababu, *Tetrahedron*, 2000, **56**, 5303-5310.
60. M. A. Siddiqui, V. E. Marquez, J. S. Driscoll and J. J. Barchi, Jr., *Tetrahedron Lett.*, 1994, **35**, 3263-3266.
61. S. L. Less, S. Handa, K. Millburn, P. F. Leadlay, C. J. Dutton and J. Staunton, *Tetrahedron Lett.*, 1996, **37**, 3515-3518.
62. J.-A. Ma and D. Cahard, *Chem. Rev.*, 2004, **104**, 6119-6146.
63. S. Phoenix, E. Bourque and P. Deslongchamps, *Org. Lett.*, 2000, **2**, 4149-4152.
64. D. A. Evans, E. B. Sjogren, J. Bartroli and R. L. Dow, *Tetrahedron Lett.*, 1986, **27**, 4957-4960.
65. D. A. Evans, T. C. Britton and J. A. Ellman, *Tetrahedron Lett.*, 1987, **28**, 6141-6144.
66. D. A. Evans and S. L. Bender, *Tetrahedron Lett.*, 1986, **27**, 799-802.
67. S. D. Bull, S. G. Davies, R. L. Nicholson, H. J. Sanganee and A. D. Smith, *Org. Biomol. Chem.*, 2003, **1**, 2886-2899.
68. G. C. Micalizio, A. N. Pinchuk and W. R. Roush, *J. Org. Chem.*, 2000, **65**, 8730-8736.

69. D. A. Evans, S. J. Miller, M. D. Ennis and P. L. Ornstein, *J. Org. Chem.*, 1992, **57**, 1067-1069.
70. J. P. Ley and H. J. Bertram, *Bioorg. Med. Chem.*, 2001, **9**, 1879-1885.
71. M. Marigo, D. Fielenbach, A. Braunton, A. Kjoersgaard and K. A. Jorgensen, *Angew. Chem., Int. Ed.*, 2005, **44**, 3703-3706.
72. D. D. Steiner, N. Mase and C. F. Barbas III, *Angew. Chem., Int. Ed.*, 2005, **44**, 3706-3710.
73. T. D. Beeson and D. W. C. MacMillan, *J. Am. Chem. Soc.*, 2005, **127**, 8826-8828.
74. M. Winkler, T. Moraux, H. A. Khairy, R. H. Scott, A. M. Z. Slawin and D. O'Hagan, *ChemBioChem*, 2009, **10**, 823-828.
75. G. F. Barbero, J. M. G. Molinillo, R. M. Varela, M. Palma, F. A. Macias and C. G. Barroso, *J. Agric. Food Chem.*, 2010, **58**, 3342-3349.
76. A. Morita, Y. Iwasaki, K. Kobata, T. Iida, T. Higashi, K. Oda, A. Suzuki, M. Narukawa, S. Sasakuma, H. Yokogoshi, S. Yazawa, M. Tominaga and T. Watanabe, *Life Sci.*, 2006, **79**, 2303-2310.
77. G. A. Olah and J. Welch, *Synthesis*, 1974, 652.
78. T. Sierra, J. L. Serrano, M. B. Ros, A. Ezcurra and J. Zubia, *J. Am. Chem. Soc.*, 1992, **114**, 7645-7651.
79. F. Faustini, M. S. De, A. Panzeri, V. Villa and C. A. Gandolfi, *Tetrahedron Lett.*, 1981, **22**, 4533-4536.
80. Y. Chi, T. J. Peelen and S. H. Gellman, *Org. Lett.*, 2005, **7**, 3469-3472.
81. J. Kosmrlj, L. O. Weigel, D. A. Evans, C. W. Downey and J. Wu, *J. Am. Chem. Soc.*, 2003, **125**, 3208-3209.
82. N. Boechat, L. C. Maciel, A. C. Pinto, S. M. S. V. Wardell, J. M. S. Skakle and R. A. Howie, *Acta Crystallogr. C*, 2005, **61**, 270-275.
83. D. O. Hughes and R. W. H. Small, *Acta Crystallogr. B*, 1972, **28**, 2520-2524.
84. J. Zhuang, C. Wang, F. Xie and W. Zhang, *Tetrahedron*, 2009, **65**, 9797-9800.
85. M. F. Parisi, G. Gattuso, A. Notti, F. M. Raymo and R. H. Abeles, *J. Org. Chem.*, 1995, **60**, 5174-5179.

3- Synthesis and organocatalysis from structural motif 2-(aminomethyl)piperidine

3.1- Diamines in medicinal chemistry and catalysis

This chapter describes the development of the chiral diamine 2-(aminomethyl)piperidine **251** (**Figure 3.1**). An enantiopure synthesis is developed and its potential as a synthesis intermediate or as an organocatalyst is explored.

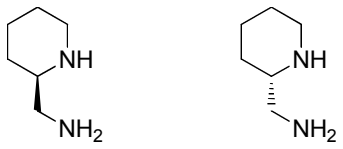

(*R*)-**251** (*S*)-**251**

Figure 3.1: (*R*)- and (*S*)-2-(aminomethyl)piperidine **251**.

Linear diamines have been widely applied in a range of modern industrial fields. For example, hydrazine (H_2N-NH_2) is often used as fuel for satellites and hexamethylenediamine

(C6) **254** is a monomer of nylon-6,6. The 1,2-diamine moiety is a simple structural motif found also in various natural products and bioactive molecules. Putrescine (C4) **252** and cadaverine (C5) **253** are produced in metabolism by decarboxylation of their corresponding amino acids L-ornithine and L-lysine respectively (**Figure 3.2**). Their odour is strong and characteristic of putrefaction processes.

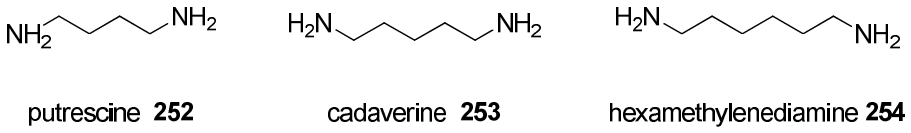

putrescine **252** cadaverine **253** hexamethylenediamine **254**

Figure 3.2: Examples of linear diamines.

Enantiomerically pure 1,2-diamines have found wide currency in catalytic asymmetric synthesis, where they have been explored for diastereoselective and enantioselective syntheses. Examples are described in section **3.1.3**.

3.1.1- The occurrence of vicinal diamines in natural products

The 1,2-diamine motif is often found in heterocyclic moieties. Biotin **255** is an important cofactor in enzymology where it is involved in the biosynthesis of fatty acids (**Figure 3.3**). The structural skeleton contains a vicinal diamine moiety constrained as an imidazolidinone ring system. The penicillin **256** and cephalosporin **257** antibiotics also contain 2,3-diamino carboxylic acid residues. The alkaloid palau'amine **258** contains three 1,2-diamine moieties. This alkaloid was discovered in a sea sponge and its first total synthesis was reported recently.[1]

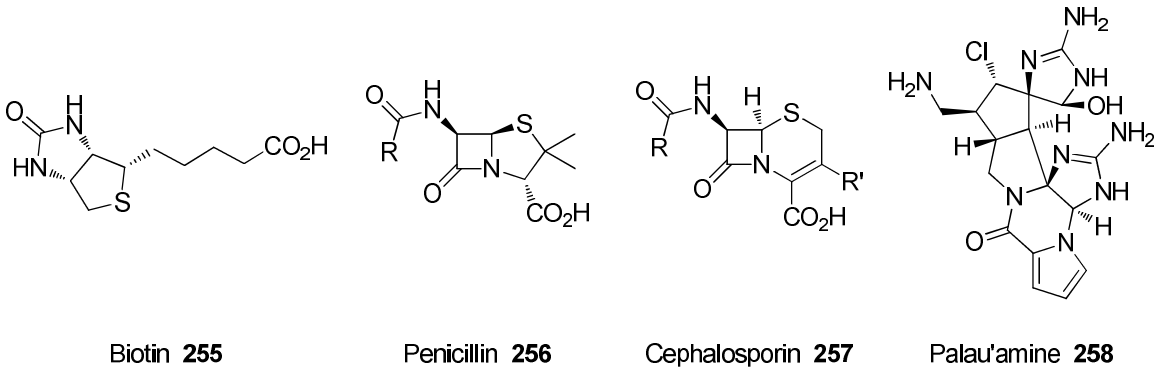

Figure 3.3: The vicinal diamino moiety in natural products.

3.1.2- Applications in medicinal chemistry

The 1,2-diamine unit is also present in a large variety of compounds, many of which possess useful biological activities. Indeed, vicinal diamines are important ligands used to co-ordinate metals or organometallics, such as the antitumor compound oxaliplatine **259** (**Figure 3.4**).

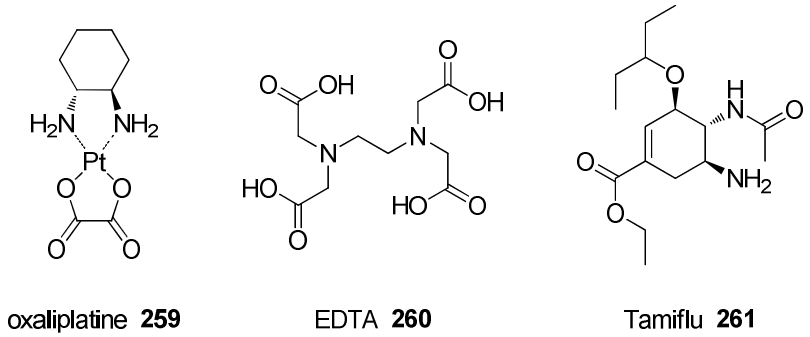

Figure 3.4: The 1,2-diamine moiety in some important drugs.

EDTA **260** was originally used to treat lead poisoning, but many EDTA derivatives are used in nuclear medicine for the chelation of metallic radioactive isotopes.[2] The diamine moiety is also found in the antiviral drug Tamiflu® **261**

3.1.3- Vicinal diamines in synthesis

The availability of enantiomerically pure vicinal diamines has fuelled the development of chiral auxiliaries for asymmetric synthesis. Mangeney *et al.* developed a method to resolve chiral aldehydes using vicinal diamines (**Scheme 3.1**).[3] This involved treatment of racemic aldehydes **262** with an enantiopure diamine **263** to generate diastereoisomeric imidazolines **264**, which could then be separated by chromatography and resolved after hydrolysis.

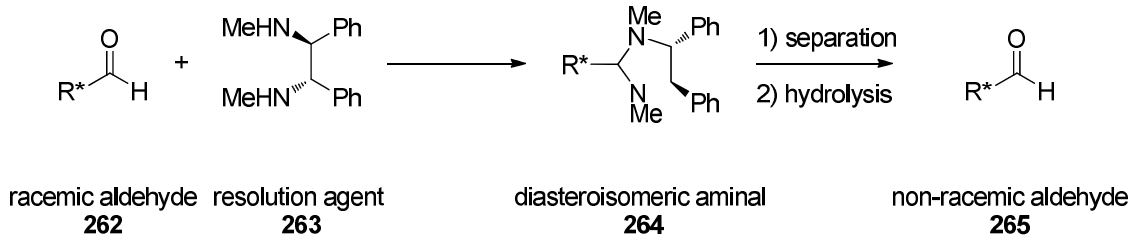

Scheme 3.1: Resolution of racemic mixtures of aldehydes.[3]

The 1,2-diamine moiety is widely represented in the structures of chiral auxiliaries and ligands. Hanessian *et al.* developed a method to obtain α-substituted-α-alkyl phosphonic acids, such as **269,** *via* a chiral bicyclic phosphonamide, developed from (*R,R*)-dimethylcyclohexane-1,2-diamine **266** (**Scheme 3.2**).[4] This synthesis was efficient (71-84%) and highly diastereoselective (68-98% de).

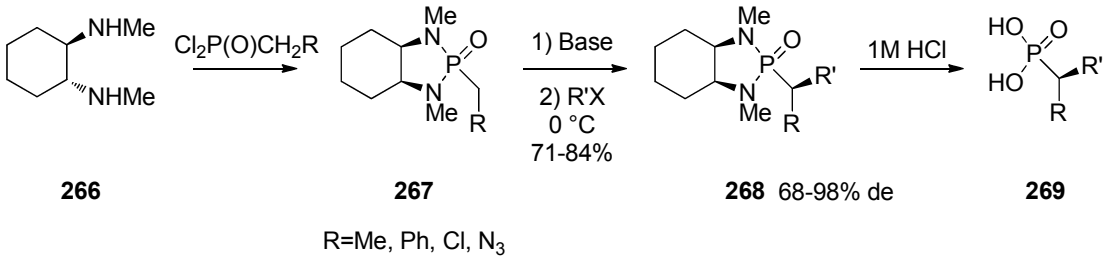

Scheme 3.2: Chiral bicyclic phosphonamide as a chiral auxiliary.[4]

In 1988, Cardillo *et al*. reported the alkylation of 3-acyl-imidazolidin-2-one **270** derived from (*S*)- or (*R*)- ephedrine.[5] This family of imidazolidin-2-ones has been used for asymmetric enolate alkylations (94% de).[6]

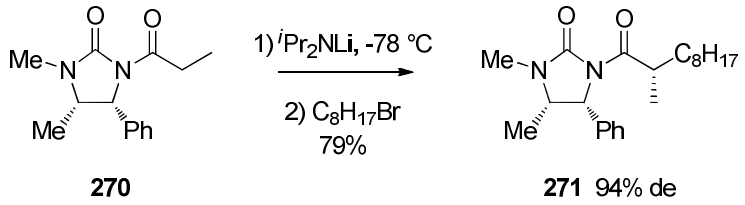

Scheme 3.3: Asymmetric alkylation using oxazolidinone auxiliaries.[5]

Diamine chiral ligands have also been used in asymmetric synthesis. For example, Corey performed the alkylation of aldehydes using dialkylzinc reagents.[7] Nucleophilic addition of diethylzinc to benzaldehyde **272** proved to be highly enantioselective (95% ee) using diamine **273** as the template for Li^+ Lewis acid catalysis (**Scheme 3.4**).

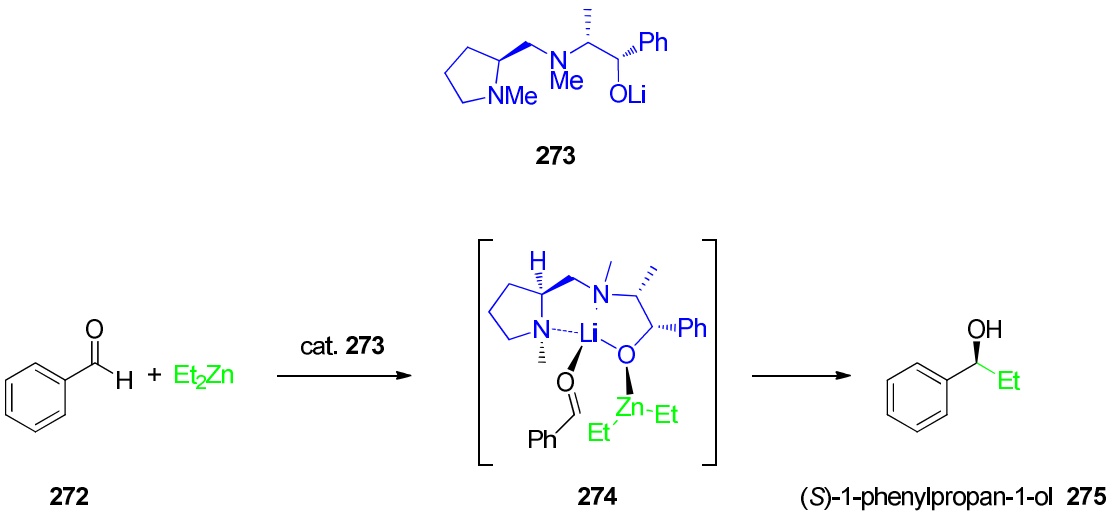

Scheme 3.4: Enantioselective ethylation of benzaldehydes.[7]

Noyori *et al*., used ruthenium complexes to reduce aromatic ketones by asymmetric hydrogen transfer.[8, 9] Using ruthenium complex **276** resulted in 58 to 99% ee, and **277** generated products in the range 66-99% ee as illustrated in **Scheme 3.5**.

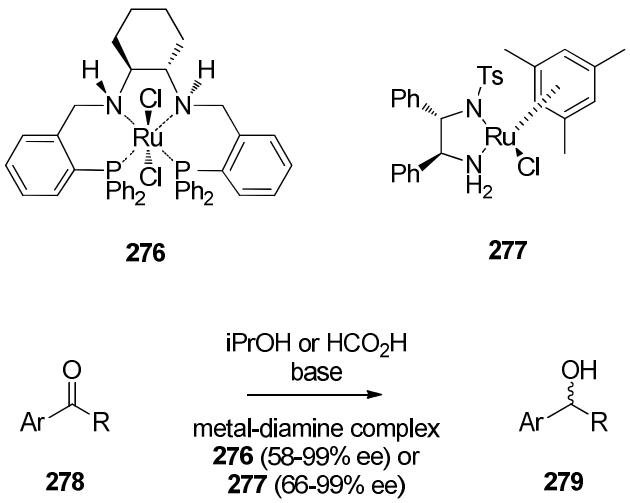

Scheme 3.5: 1,2-Diamino ligands and metal complexes for enantioselective reductions.[8, 9]

3.1.4- Preparation of vicinal diamines

The requirement for specifically substituted vicinal diamines has generated numerous approaches for their preparation. This section will focus on the preparation of heterocycles containing the 1,2-vicinal diamine moiety.

Scheme 3.6 shows how O'brien *et al.* did the one-pot synthesis of diamines (*R*)-**283** or (*R*)-**284** starting from (*R*)-styrene oxide **280**.[10] Pyrrolidine or piperidine reacts with the styrene oxide to generate a tertiary alcohol, which on treatment with mesyl chloride forms the aziridinium rings **281**/**282**. The initial configuration of the epoxide is recovered in **283**/**284** after attack by a primary amine to the more substituted carbon of the aziridinium **281**/**282**.

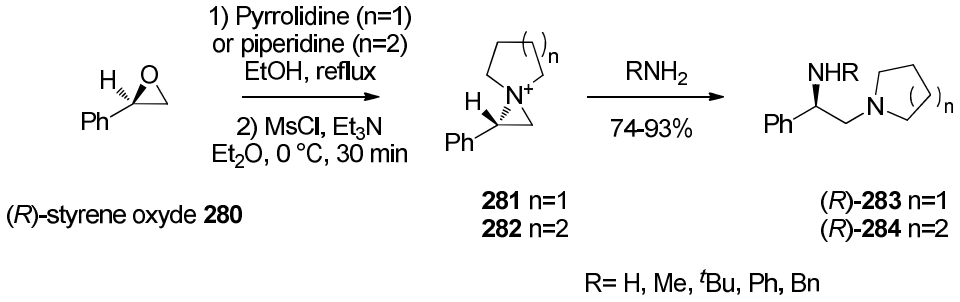

Scheme 3.6: Piperidine and pyrrolidine derivatives.[10]

Taylor *et al.* applied the Ritter reaction to a series of cyclic hydroxyamines, including 3-hydroxy-pyrrolidine **285**.[11] The carbocation formed under acidic conditions provided the expected acetamide **286** in 77% yield (**Scheme 3.7**).

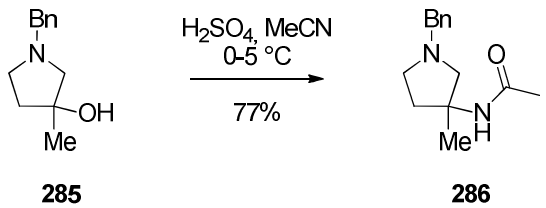

Scheme 3.7: Application of Ritter reaction to cyclic β-hydroxamines synthesis.[11]

When this reaction was attempted on 3-hydroxypiperidine **287**, the acetamide **288** was obtained but only as a minor product (20%). The major product (50%) was the alkene **289** (**Scheme 3.8**). The authors suggested that the formation of the aziridinium **290** would not easily undergo reaction with acetonitrile and the system was prone to elimination.

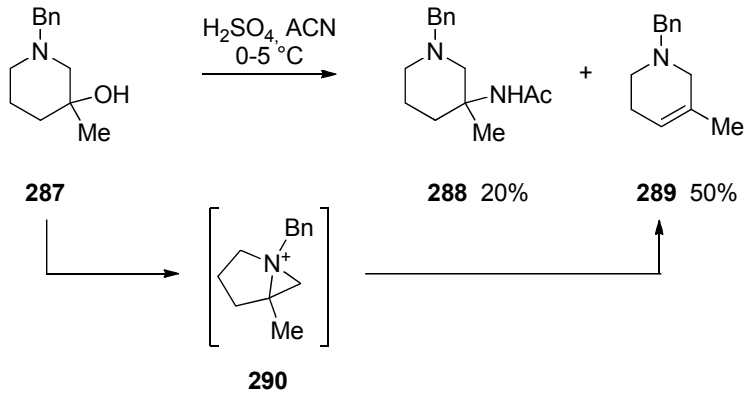

Scheme 3.8: The formation of the aziridinium intermediate favours the elimination reaction.[11]

To avoid such side-reactions, the nitrogen atoms were protected.[12] For example, the intramolecular reductive amination highlighted in **Scheme 3.9** proceeds by the monodeprotection of a carboxybenzyl group prior to cyclisation. This method enables the synthesis of various substituted piperidines, such as **292**.

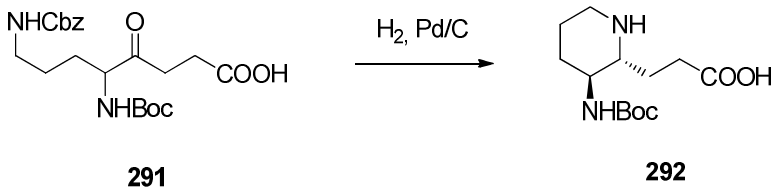

Scheme 3.9: Intramolecular reductive amination.[12]

3.2- Synthesis of enantiopure 2-(aminomethyl)piperidine

3.2.1- Previous syntheses of 2-(aminomethyl)piperidine

A racemic synthesis of 2-(aminomethyl)piperidine **251** was first reported in 1958 by Mortimer in a study aimed at proving the structure of the alkaloid isopelletierene (**Scheme 3.10**).[13] *N*-Acetylated isopelletierene **293** was converted to oxime **294**. A Beckmann rearrangement was then induced under acidic conditions to generate the corresponding diamide **295**. The diamide intermediate was hydrolysed to generate 2-(aminomethyl)-piperidine dihydrochloride **251**.

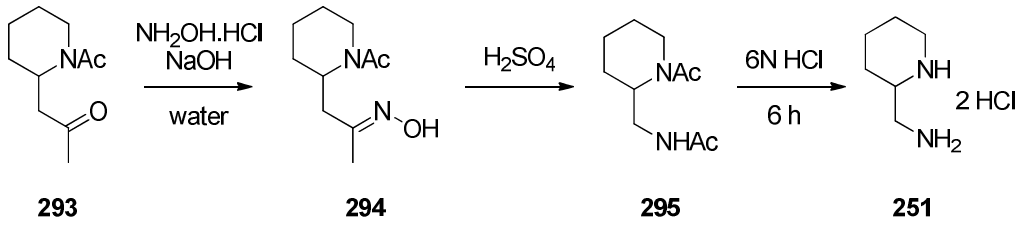

Scheme 3.10: Beckmann rearrangement of isopelletierene.[13]

When isopelletierene oxime **296** was treated with phosphorus pentachloride in phenylethyl ether, it formed 2-methyl-1,3-diazabicyclo[4:3:0]-2-nonene **297** (**Scheme 3.11**).

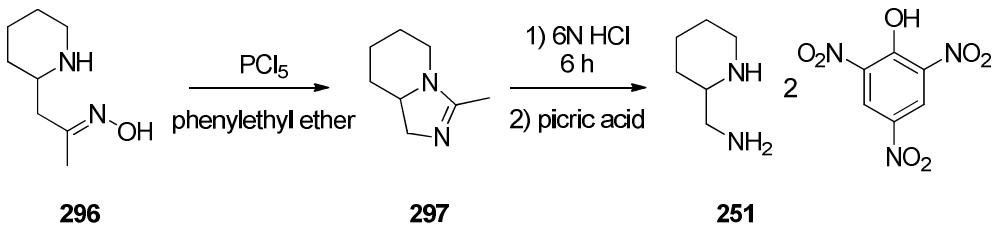

Scheme 3.11: Hydrolysis of amidine **297**.[14]

In this case, the Beckmann rearrangement product was subject to nucleophilic attack by the secondary amine, which led to amidine cyclisation. 2-(Aminomethyl)piperidine **251** was then obtained after hydrolysis of the amidine **297**, and was isolated as its dipicrate salt.[14]

The synthesis of 2-(aminomethyl)piperidine **251** and its substituted derivative 2-(ethylaminomethyl)piperidine **301** have also been described by the hydrolysis of 1,8-diazabicyclo[4:3:0]nonanes **300** (**Scheme 3.12**).[15]

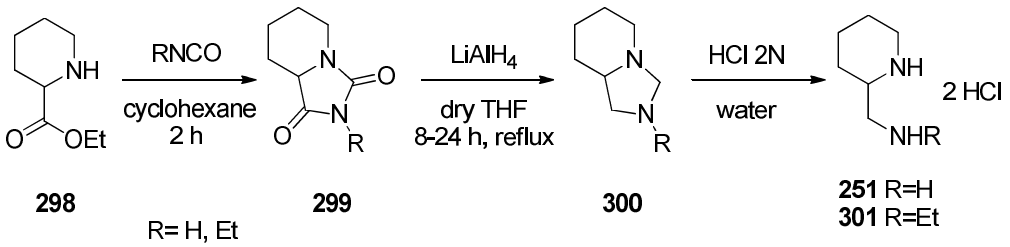

Scheme 3.12: Hydrolysis of 1,8-diazabicyclo[4:3:0]nonanes **300**.[15]

300 was obtained after treatment of ethyl 2-(piperidin-2-yl)acetate **298** with isocyanic acid or isocyanatoethane to give the corresponding hydantoin **299**. Treatment of 5-phenylhydantoins with lithium aluminium hydride is known to result in complete reduction to 4-phenylimidazolidine. Such conditions were used to reduce **299** to 1,8-diazabicyclo[4:3:0]nonanes **300**, which were then hydrolysed with hydrochloric acid to generate **251** or 2-(ethylaminomethyl)piperidine dihydrochloride **301**.

Other reductive methods have been used to provide **251**. 2-(Aminomethyl)pyridine **302** could be hydrogenated using PtO_2 as a catalyst, but best result was given with sodium metal.[16, 17] Wong *et al.* also reported a resolution method of the dihydrochloride salt of 2-(aminomethyl)-piperidine **251** to recover the product as a single stereoisomer. Thus the salt was crystallised with dibenzoyl-(+)-tartaric acid ((+)-DBTA) to give (*S*)-2-(aminomethyl)piperidine **251** (**Scheme 3.13**).

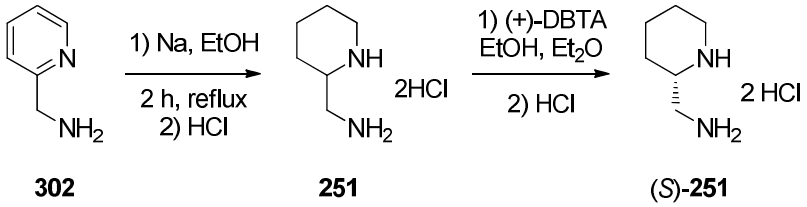

Scheme 3.13: Reduction of 2-(aminomethyl)pyridine with sodium metal and resolution of racemic 2-aminomethylpiperidine **251** with (+)-DBTA.[17]

The first enantiopure synthesis of 2-(aminomethyl)piperidine **251** was reported by Perumattam *et al.* in 1991 and started from (*S*)-pipecolic acid **303** (**Scheme 3.14**).[18]

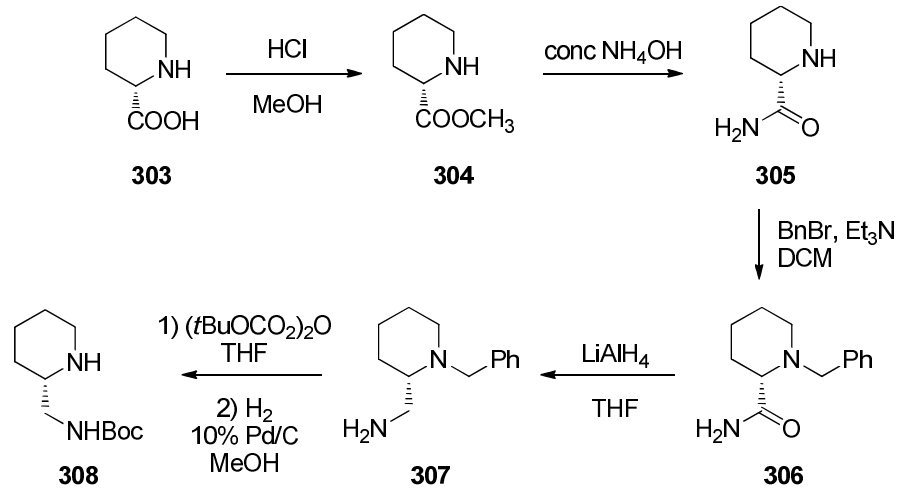

Scheme 3.14: Asymmetric synthesis of Boc-protected 2-(aminomethyl)piperidine **308** from pipecolic acid.[18]

(*S*)-Pipecolic acid **303** was converted to its carboxamide **305** *via* the methyl ester **304**. Reduction of the amide **306** with $LiAlH_4$ was achieved after benzyl protection of the secondary amide. The primary amine of **307** was then Boc protected and the benzyl group removed by hydrogenolysis to give **308**.

Another enantiopure synthesis was described from the (-)-2-cyano-6-phenyloxazolo-piperidine **309** (**Scheme 3.15**).[19] Precursor (-)-**309** was prepared from (*R*)-(-)-phenylglycinol and glutaraldehyde in the presence of KCN. The synthesis started from a reduction of **309** with lithium aluminium hydride which resulted in the diamino alcohol **310**.

2-(Aminomethyl)piperidine (*S*)-**251**was obtained after hydrogenolysis of **310** with palladium on charcoal and the diamine was isolated as its dihydrochloride salt.

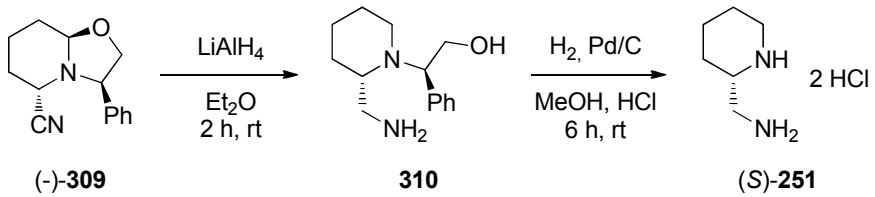

Scheme 3.15: Reduction of an enantiopure cyanopiperidine.[19]

A cyanyl reduction was also reported by Nazabadioko *et al*.[20] In this case, the authors started with 2-cyano-6-phenyloxazolpiperidine (*S*)-**313**. The phenylmethanamine group was incorporated by nucleophilic substitution on the alcohol (*R*)-**311** activated as a triflate, a process that occurred with an inversion of configuration. Cyclisation of intermediate (*S*)-**312** generated the piperidine ring (**Scheme 3.16**).

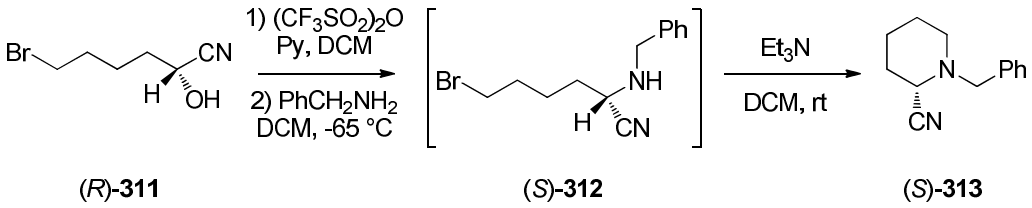

Scheme 3.16: A cyclisation process to obtain an enantiopure cyanopiperidine (*S*)-**313**.[20]

In a similar manner to that for **309**, 2-cyano-6-phenyloxazolpiperidine (*S*)-**313** was then reduced with $LiAlH_4$ to provide the corresponding diamine which was hydrogenated using $Pd(OH)_2$, to give the enantiopure 2-(aminomethyl)piperidine (*S*)-**251** as the dihydrochloride salt.

3.2.2- Aims of project

The importance of chiral diamines as catalysts in asymmetric synthesis renders improved methods for the synthesis of (*R*)- and (*S*)- 2-(aminomethyl)piperidine attractive as these two enantiomers are not commercially available. The approaches described above do not allow reasonable quantities of (*R*)- and (*S*)- **251** to be obtained easily. This research aimed to explore a practical route, as described in **Scheme 3.16,** in order to develop the enantiopure amines as building-blocks for synthesis programmes in medicinal chemistry or for applications in asymmetric catalysis.

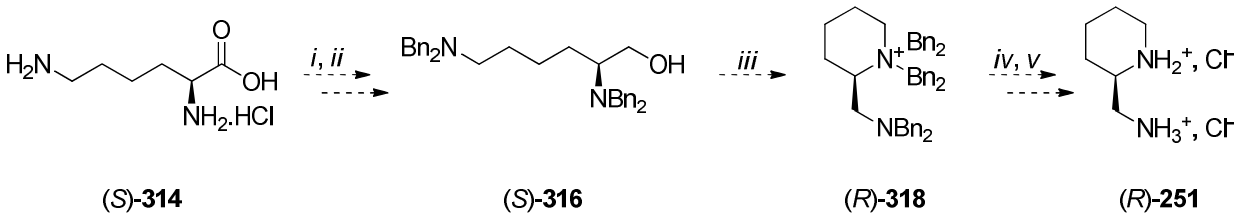

Scheme 3.16: Synthetic approach to (*R*)- **251**.

Figure 3.5 illustrates the structural diversity that was targeted from 2-(aminomethyl)-piperidine in this research.

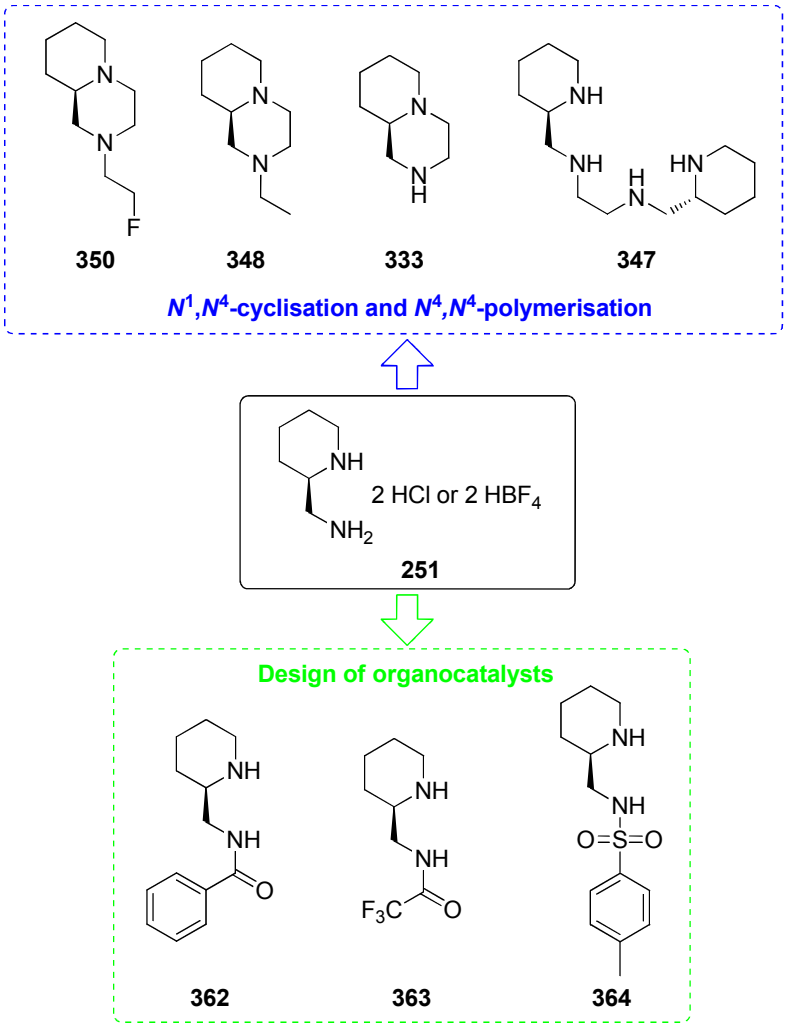

Figure 3.5: New syntheses of 2-(aminomethyl)piperidine derivatives.

3.2.3- Enantioselective synthesis of 2-(aminomethyl)piperidine

3.2.3.1- Development of the cyclisation process

This novel approach starts from the amino acids (*S*)-L- and (*R*)-D- lysine and proved convenient for gram scale synthesis of (*R*)- or (*S*)-2-(aminomethyl)piperidine **251**.

(*S*)-L-Lysine **314** was converted to its pentabenzyl derivative (*S*)-**315** by treatment with benzyl bromide (7 eq) in ethanol, using potassium carbonate as a base (**Scheme 3.17**). The

almost quantitative perbenzylation was followed by reduction of (*S*)-**315** with $LiAlH_4$ in an efficient reaction where the resultant alcohol (*S*)-**316** was obtained in 89% yield.

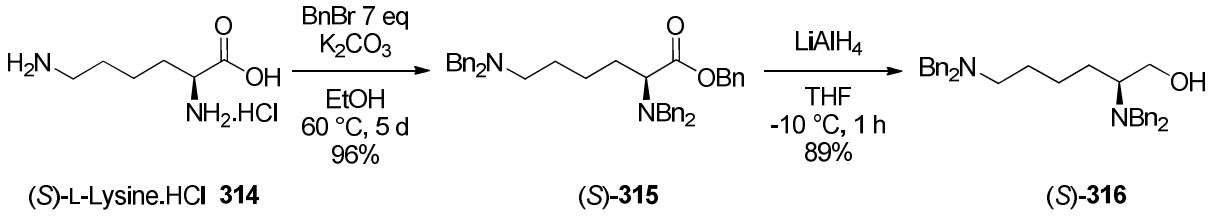

Scheme 3.17: Synthesis of perbenzylated alcohol (*S*)-**316**.

Initial investigations by G. Deniau (St. Andrews, 2006) aimed at obtaining the fluorinated diamine (*R*)-N^1,N^6-tetrabenzyl-2-fluorohexane-1,6-diamine **319** (**Scheme 3.18**). It is known that treatment of *N*,*N*-dibenzyl-α-aminoalcohols with nucleophilic fluorinating reagents produces an *in situ* aziridinium intermediate **317**, which then undergoes ring opening by fluoride ion attack (paths b and c) predominantly forming the more substituted alkyl fluorine (path b) as illustrated in **Scheme 3.18**.[21]

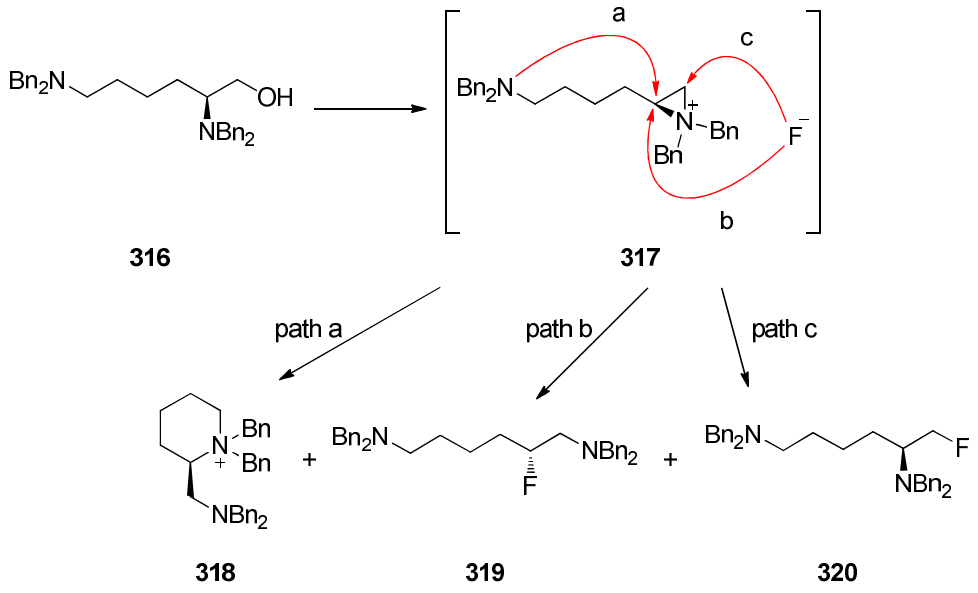

Scheme 3.18: Reaction pathways on treatment of (*S*)-**317** with Deoxofluor.

When this reaction was carried out at -10 °C with Deoxofluor, it gave a mixture of three compounds **318-320** in a ratio of 83:15:2 , in poor yield (11%). It was not anticipated that the peripheral dibenzylamine would compete with the fluoride ion to open the aziridium intermediate (path a), however this proved to be the more efficient process. This then opened up the prospects of a new route to 2-(aminomethyl)piperidine **251**.

The addition of silica gel (SiO_2) to the suspension in solvent was anticipated to favour intramolecular nucleophilic attack of N^6 over the intermolecular attack by fluoride. This was confirmed when an empirical amount of silica (200 mg for 200 mg of perbenzylated alcohol, *i.e.* 8.2 eq) increased the conversion to piperidinium **318** (50%).

In this thesis, an alternative cyclisation was developed with a system involving DAST (1.5 eq) and silica. The use of DAST at room temperature was even more efficient and the conversion improved to above 60%. The conversion reached 80%, with minor traces of **319** and **320**, when four equivalents of silica were added to the mixture.

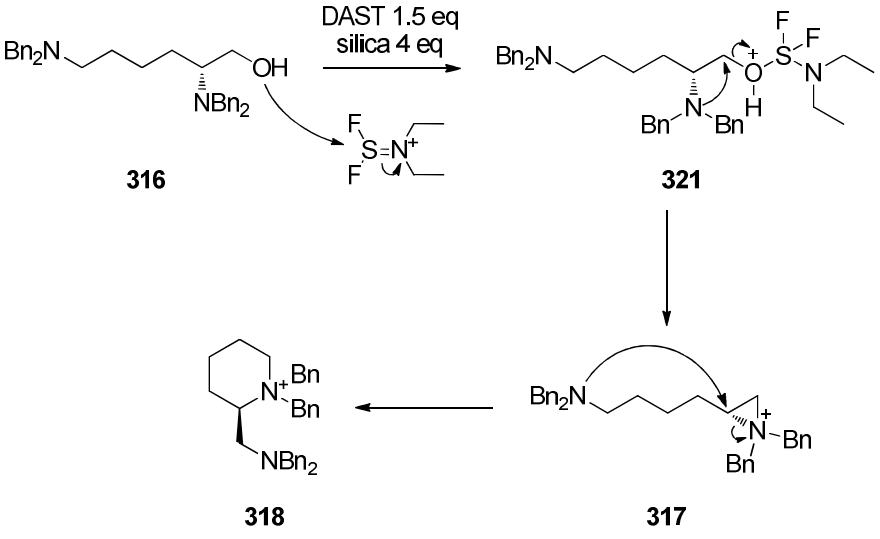

Scheme 3.19: Proposed mechanism of amine cyclisation activated with DAST.

The role of the silica appears to sequester fluoride ions from solution. Consequently, side-reactions are reduced giving a cleaner reaction and more efficient conversion. The diethylaminodifluorosulfinium formed, after elimination of one fluoride, is attacked by the alcohol and the good leaving group formed promotes aziridine cyclisation (**Scheme 3.19**). The aziridinium then undergoes ring opening by N^6 attack.

An improved method for the cyclisation of the *N,N'*-tetrabenzylated alcohol **316** was now considered because DAST cannot reasonably be used on a large scale for both safety and economical reasons. Other reagents were investigated to promote the activation of the amino alcohol **316**. For instance, the use of methanesulfonic anhydride (Ms_2O), methanesulfonyl chloride (MsCl) and trifluoromethanesulfonic anhydride (Tf_2O) had been reported to generate aziridinium rings from *N,N*-dibenzyl-α-aminoalcohols.[22-26] In the following example, mesyl chloride promotes the formation of aziridinium **323** from the dialkylated (*R*)-phenylglycinol **322** (**Scheme 3.20**). Aziridinium **323** is then reacted with methylamine as a nucleophile to generate the 1,2-diamine (*S*)-**324** with 95% ee.

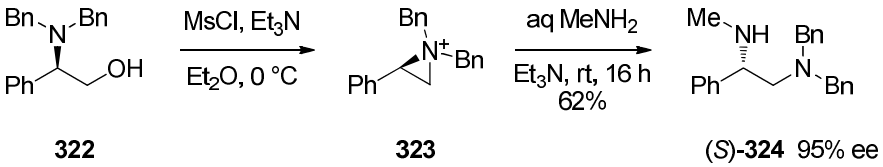

322 **323** (*S*)-**324** 95% ee

Scheme 3.20: Formation of aziridium ion **323** from (*R*)-phenylglycinol using mesyl chloride.[22]

In the same manner, the β-aminoalcohol (*S*)-**325** gave the aziridinium **326** when treated with trifluoromethanesulfonic anhydride. The ring-opening reaction is regioselective as morpholine reacts preferentially on the less substituted carbon of the aziridinium ring to give a mixture of regioisomers (*S*)-**327** and (*R*)-**328** in a 95:5 ratio respectively.

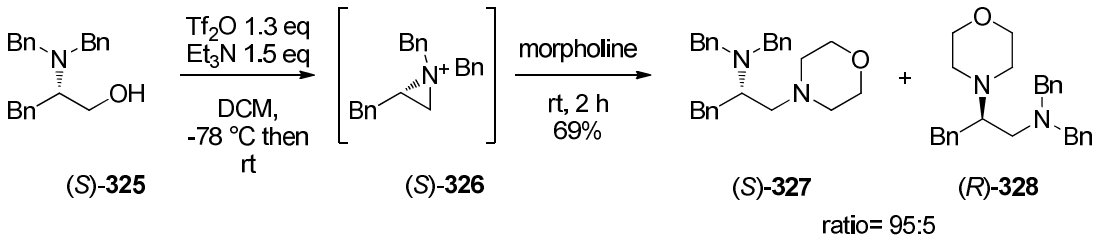

Scheme 3.21: Formation of aziridium ion **326** from (*S*)-2-(dibenzylamino)-3-phenylpropan-1-ol using trifluoromethanesulfonic anhydride.[26]

These reagents were now explored for formation and subsequent cyclisation of aziridinium **317** to generate **318**. A summary of these outcomes is reported in **Table 3.1**.

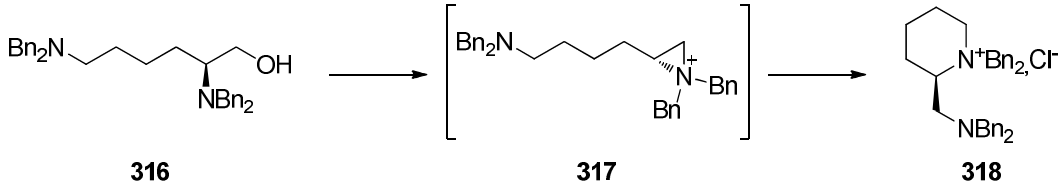

Entry	Reagent	Base	Conditions	Result	
1	Ms_2O	Et_3N 1.5 eq	30 min at 0 °C, then 8 h at rt	No cyclisation	×
2	MsCl	Et_3N 1.5 eq	1 h at 0 °C, then 8 h at rt	Chlorination **329**	×
3	Tf_2O 2 eq	Et_3N 2 eq DMAP cat	2 h at 0 °C, then 36 h at rt	Quantitative conversion **318**	✓
4	$SOCl_2$ 1.2 eq	Pyr 1.2 eq	2 h at 0 °C, then overnight at rt	No cyclisation	×
5	$POCl_3$ 1.5 eq	Et_3N 1.5 eq	1 h at 0 °C, then overnight at rt	No cyclisation	×
6	Tf_2O 2 eq	Et_3N 2 eq DMAP cat	2 h at 0 °C, then overnight at reflux	Traces **318**	×

All reactions carried out in DCM, except entry **4**: THF, and entry **5**: diethyl ether.

Table 3.1: Reagents used to promote the cyclisation of (*R*)-**316** to (*R*)-**318**.

The reactions involving mesyl anhydride, thionyl chloride and phosphorus oxychloride failed to promote any cyclisation (entries 1, 4, 5). The use of mesyl chloride (entry 2) resulted in the regioselective chlorination of **316**, perhaps not surprisingly, as chloride is more nucleophilic than the dibenzylated amine (**Scheme 3.22**).

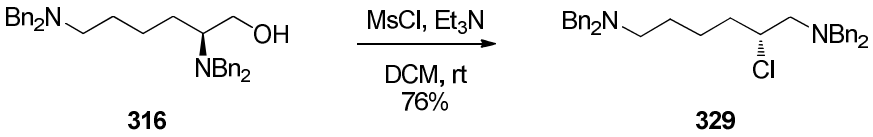

316 **329**

Scheme 3.22: Mesyl chloride promotes the synthesis of alkyl chloride **329**.

Interestingly, the cyclisation of dibenzyl-α-aminoalcohol **330** was reported by Gmeiner *et al*.[27] In this case, the bicyclic product **331** was obtained in an enantiopure form, as a result of the nucleophilic attack from the C^2 carbon of the pyrrole ring on the aziridinium intermediate (**Scheme 3.23**).

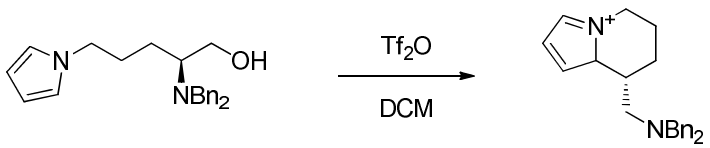

330 **331**

Scheme 3.23: Cyclisation of dibenzyl-α-aminoalcohol is induced by Tf_2O.[27]

Accordingly, treatment of **316** with triflic anhydride (2 eq) resulted in an efficient cyclisation to piperidine **318** after 36 h at room temperature (88% yield).

It appears from these results that DAST/silica and particularly trifluromethanesulfonic anhydride are suitable reagents to promote the cyclisation of (*R*)-**316** to generate the tetrabenzylpiperidinium salt **318** (**Scheme 3.24**).

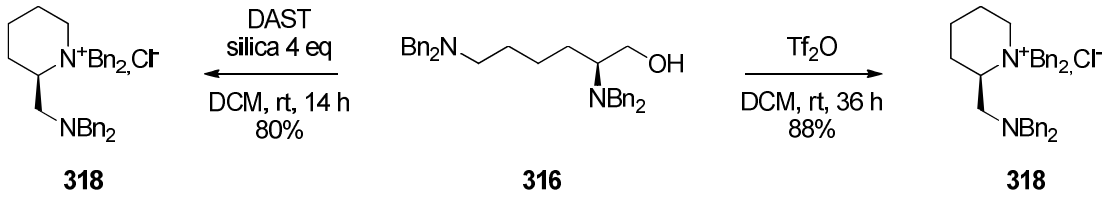

Scheme 3.24: Cyclisation step induced by Tf_2O or DAST/silica.

3.2.3.2- Hydrogenolysis of 318 and preparation of dihydrochloride 251

The next step in the process required debenzylation of **318**. The compound was submitted to hydrogenolysis with 10% Pd/C catalyst in an autoclave (from 5 bars, 2 h to 30 bars, 2 d) but the debenzylation was only partially achieved, resulting in a mixture of mono-, di-, tri- and tetra-benzylated 2-(aminomethyl)piperidines with the required 2-(aminomethyl)piperidine **251** in only 20% conversion (**Scheme 3.25**).

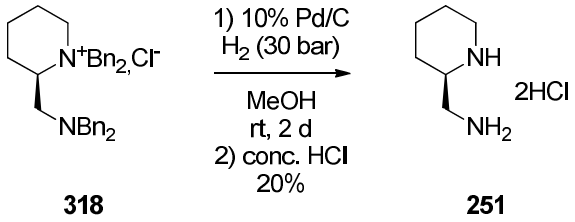

Scheme 3.25: Hydrogenolysis of (*R*)-**318**.

The Pd/C catalyst was not efficient at promoting the reaction and instead, $Pd(OH)_2$ was evaluated. Hydrogenolysis was carried out on a continuous-flow hydrogenation system ("H-cube") which allowed higher pressures and temperature (**Scheme 3.26**). The micro-reactor consisted of a pre-packed cartridge of $Pd(OH)_2$ loaded at 20%. The reagent **318** was diluted to a 0.1 M solution in ethanol at 40 °C and the pressure was varied from 30 to 50 bar, but this did not significantly improve the conversion even after several passages of substrate through the system (<40% conversion).

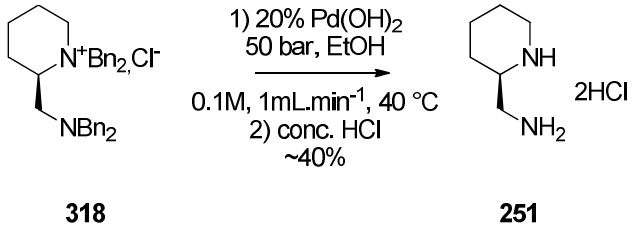

Scheme 3.26: Hydrogenolysis of (*R*)-**318** under high pressure continuous-flow.

Hydrogen transfer was not enhanced at this micro-scale and transfer hydrogenation was then investigated using ammonium formate (5 eq) as a continuous source of hydrogen. The reaction was run at 85 °C at ambient pressure using 20% $Pd(OH)_2$ as a catalyst (**Scheme 3.27**). This proved successful and a quantitative conversion of **318** to **251** was achieved after 24 h. In some reactions, a mixture of 2-(aminomethyl)piperidine and the tetrabenzylated starting-material was observed as determined by ^{13}C-NMR with no trace of the intermediate benzylated products.

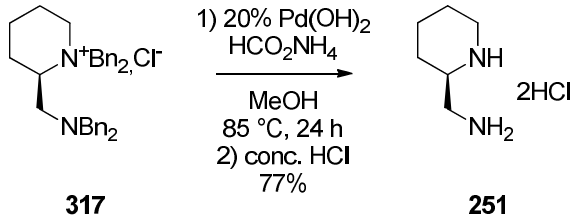

317 **251**

Scheme 3.27: Hydrogenolysis using a continuous source of hydrogen.

This hydrogenolysis was less efficient when the cyclisation was carried out with trifluoromethanesulfonic anhydride, but the reaction proceeded normally after a thorough wash of the starting material with a saturated solution of $NaHCO_3$ (pH 8), presumably to remove the triflate counter-ion (^{19}F NMR showed a peak at -79 ppm). Finally, (*R*)-**251** was converted to its dihydrochloride salt after filtering the catalyst, and the addition of hydrochloric acid. A complete conversion to **251** was always achieved after a second treatment in similar conditions.

The absolute stereochemistry of the diamine **251** was determined by X-Ray structure analysis (**Figure 3.6**). The resultant stereochemistry is consistent with a single inversion of configuration from the original (*S*)-L-Lysine starting material.

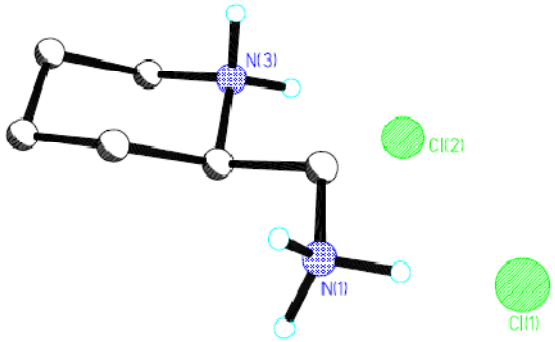

Figure 3.6: X-Ray analysis confirmed the structure and stereochemistry of (*R*)-**251**.

Both the (*R*)- and (*S*)- enantiomers of 2-(aminomethyl)piperidine **251** were prepared on a gram-scale by this method, involving cyclisation with either DAST/silica or trifluoromethanesulfonic anhydride. All steps were optimised on this scale, including the cyclisation and hydrogenolysis.

3.2.3.3- Preparation of 2-(aminomethyl)piperidine tetrafluoroborate salt

The 2-(aminomethyl)piperidine dihydrochloride salt proved to be very poorly soluble in organic solvents. It was thought that a more lipophilic salt could enhance its solubility and thus its utility in further synthesis. Therefore the tetrafluoroborate salt was explored. This latter salt was obtained by treating the dihydrochloride salt with a solution of tetrafluoroboric acid-diethyl ether complex. The conversion was essentially quantitative (98%) (**Scheme 3.28**) and as anticipated the solubility was dramatically increased in solvents such as acetone or acetonitrile.

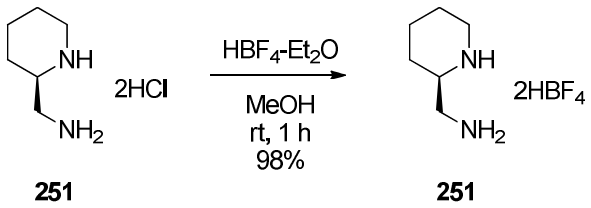

251 **251**

Scheme 3.28: Preparation of 2-(aminomethyl)piperidine ditetrafluoroborate (*R*)-**251**.

3.2.3.4- Enantiopurity and pK_a analysis of dihydrochloride 251

The enantiopurity of dihydrochloride **251** was established in an NMR experiment by titration of racemic and enantiopure samples of (*R*)-**251** with *O*-methylmandelic acid **332** (1 to 5 eq). The mixture of the diastereoisomeric salts from the racemic 2-(aminomethyl)piperidine could be resolved by ^{1}H NMR (400 MHz, MeOD) as illustrated in **Figure 3.7**. The different patterns indicate that only a single enantiomer was formed during the synthesis. The red square highlights the ^{1}H NMR signals on positions 2, 6 and 7.

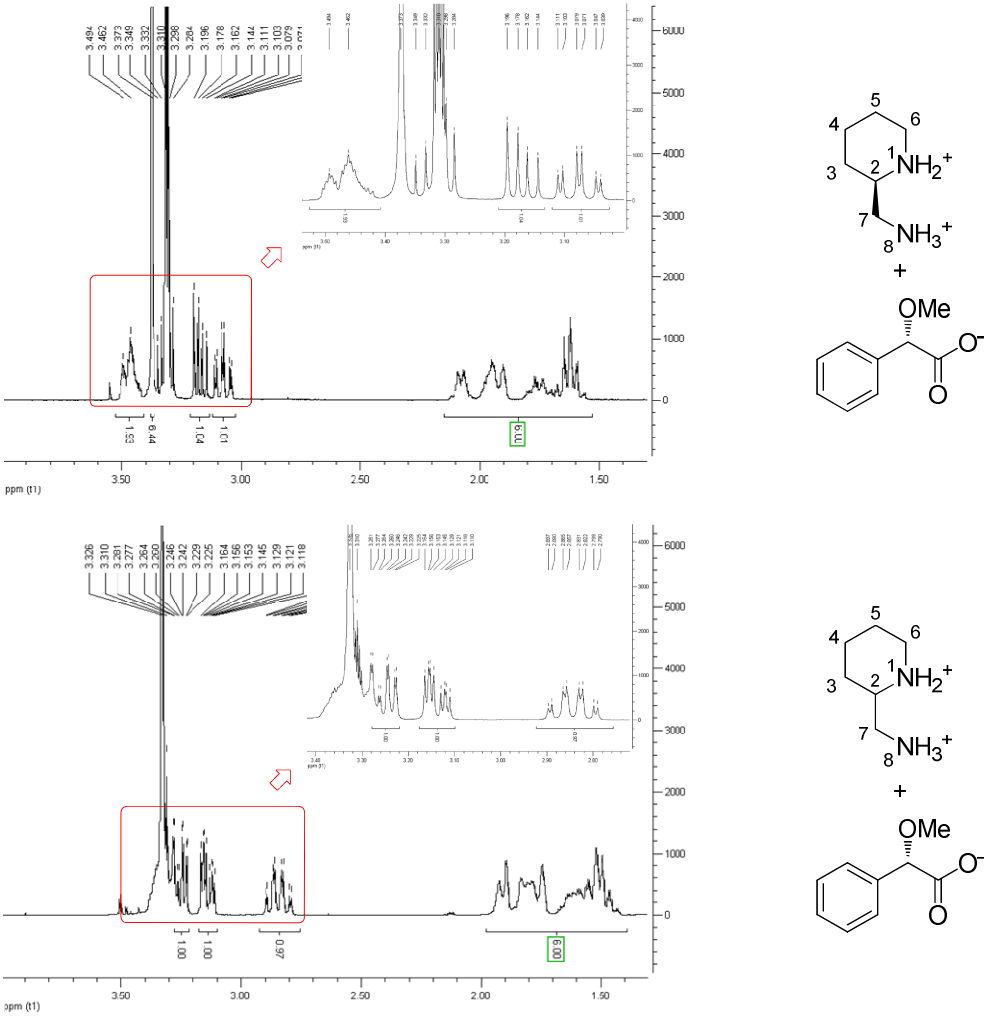

Figure 3.7: ^{1}H NMR spectra of (*S*)-*O*-methylmandelic acid **332** salts of *(R)*-**251** (top) and (*R*/*S*)-**251** (bottom)

The titration of enantiopure diamine dihydrochloride **251** (243 mg, 0.02 M) was determined by a potentiometric method. **Figure 3.8** (blue curve) shows the titration carried out against a 0.05 M NaOH solution. A direct approximation for pK_{a1} and pK_{a2} was read by the geometric method. More accurate values were calculated by the derivative method: $f' = \partial(pH)/\partial(V)$ (red curve) gave the equivalence point and reporting the half equivalence on the graph provided more accurate confirmed values for the pK_a.

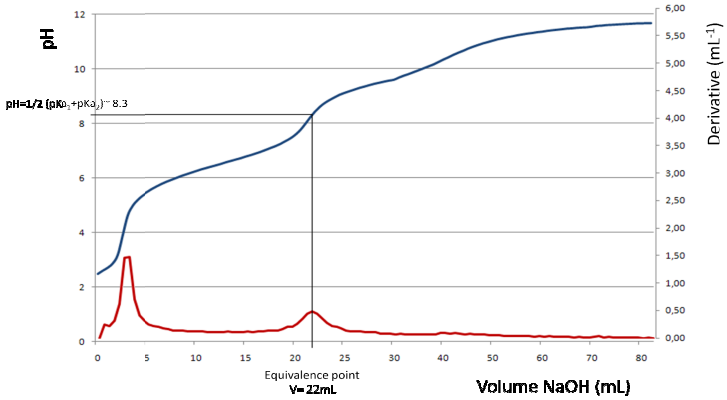

Figure 3.8: Potentiometric titration of **251** diHCl (blue curve) and its derivative (red curve).

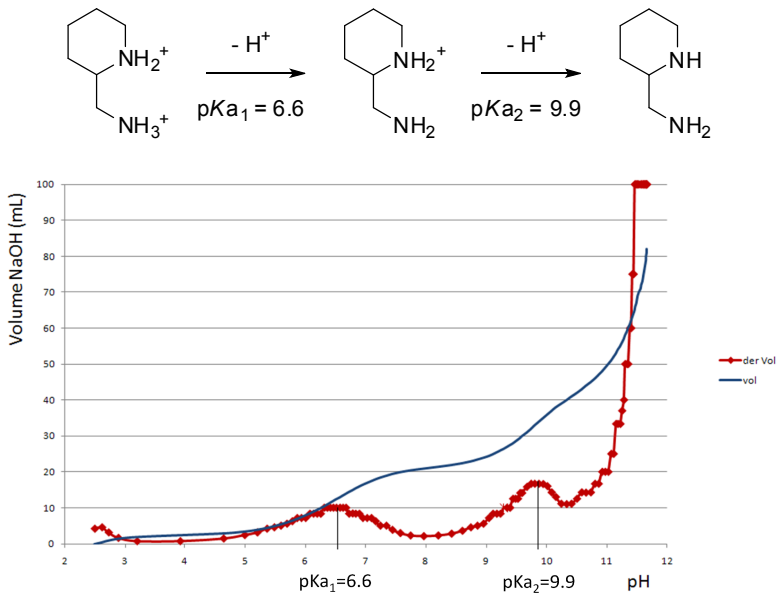

Figure 3.9: Determination of pK_{a1} and pK_{a2} by the derivative method.
(blue curve: Vol (*NaOH*)=f(*pH*); red curve: $f' = \partial(V)/\partial(pH)$)

The derivative $f' = \partial(V)/\partial(pH)$ (**Figure 3.9**) provided direct reading for pK_{a1} = 6.6 and pK_{a2} = 9.9.

The pK_{a2} value is lowered relative to those of piperidine (pK_a = 11.22)[28] and 2-methyl-piperidine (pK_a = 10.99).[29] The two pK_a values are also decreased compared to those of ethylenediamine (pK_{a1} = 7.16 and pK_{a2} = 10.21).[30]

In the literature, 2-aminomethylpiperidine **251** is always reported as a salt. The only reported reaction of **251** salts involved *N,N'*-diprotection as a dicarbamate (**Scheme 3.29**).[20] The authors neutralised the dihydrochloride salt in a KOH solution (1 M) and extracted the free base into DCM before treatment with CbzCl (55%).

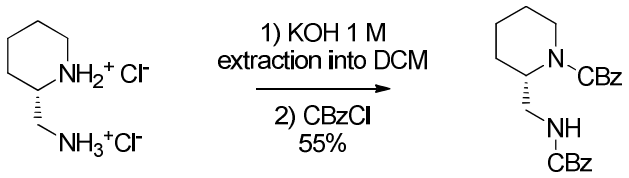

(*S*)-**251** (*S*)-**332**

Scheme 3.29: *N,N'* Dicarbamate protection from **251** dihydrochloride.[20]

In our case, dissolution of the salt in a minimum volume of water and then treatment by NaOH (1 M) to reach pH ≥12, followed by extraction into DCM, gave the expected diamine **251**. The viscous liquid was submitted to distillation (35 °C, 0.1 mBar) but this resulted in degradation products rather than isolation of the free base.

In the following study, the free base was generated *in situ* and the first reactions from (*R*)-2-(aminomethyl)piperidine dihydrochloride or the tetrafluoroborate salt of **251** are described.

3.3- Development of [4,4,0]-1,4-diazobicyclodecane 332 and its derivatives

2-(Aminomethyl)piperidine **251** is a chiral bifunctional amine and its conversion to bicyclic heterocycles was explored. Fused bicycles are readily accessible from 2-(aminomethyl)piperidine, particularly *via* N^1,N^4 cyclisation to piperazines. Piperazines are ubiquitous moieties in drug candidates, either as a core motif or as a substituent. An example is [4,4,0]-1,4-diazobicyclodecane **333**.

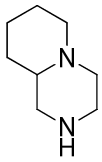

333

Recent drug candidates, as illustrated in **Figure 3.10**, have been designed by structure-activity studies and their respective properties have been tuned by the presence of the [4,4,0]-1,4-diazobicyclodecane **333** motif, most often under its racemic form. For instance, Merck developed histone deacetylase (HDAC) inhibitors from nicotinamide. This class of compounds including **334**, shows an *in vitro* anti-proliferative effect on tumour cells.[31] Merck again synthesised bicyclic piperazine **335** as conformationally constrained piperazine.[32] This derivative was found to be a potent cannabinoid CB1 receptor agonist. Novartis conceived the oestrogen receptor modulator **336** based on a tetraisoquinoline core. This series of compounds is set up as an alternative to hormones in the prevention of breast cancers.[33] The Japanese pharmaceutical company Aska synthesized the selective 5-HT_1 receptor agonists **337** for the treatment of irritable bowel syndrome (IBS).[34]

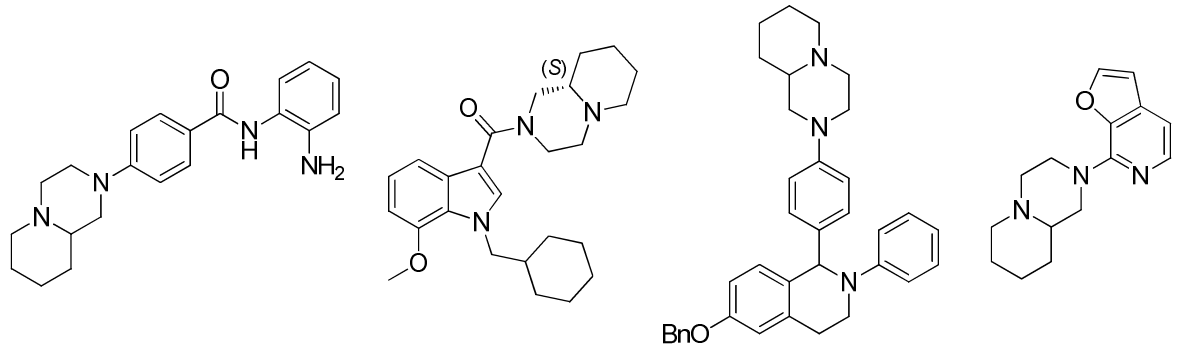

Figure 3.10: Examples of drug candidates containing the [4,4,0]-1,4-diazobicyclodecane motif.

Compound **335** demonstrated higher *in vivo* potent antinociceptive activity than its lead compound **340**. The piperidine ring was tuned to lower the degradative metabolism, however **335** was also found to be metabolised in human liver microsomes. It appeared that the major metabolite **338** resulted from a N^1,N^4-dealkylation as illustrated in **Scheme 3.30**.

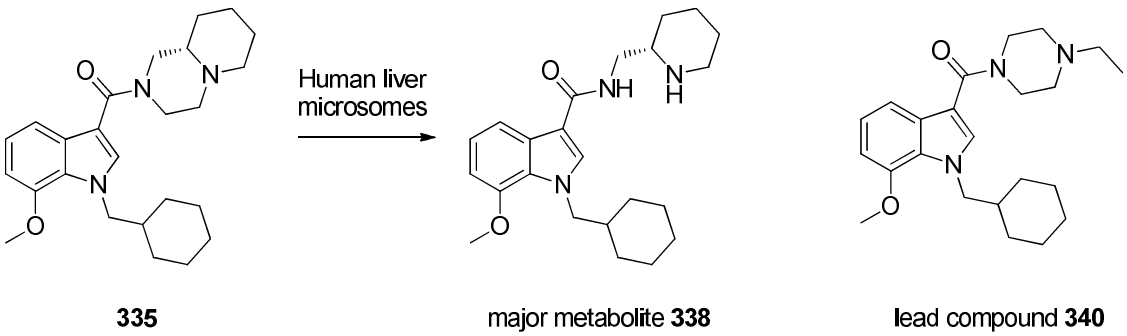

Scheme 3.30: Metabolism of compound **335** in human liver microsomes.[32]

In this research, the synthesis of [4,4,0]-1,4-diazobicyclodecane **333** was achieved in two steps from the diamine **251**. Accordingly, racemic 2-(aminomethyl)piperidine **251** was heated

at reflux with neat diethyl oxalate **341**. Under these conditions, the cyclisation proved to be fast and efficient and 2,3-diketopiperazine **342** was obtained in 92% yield (**Scheme 3.31**). The diketopiperazine **342** was then reduced with a large excess of $LiAlH_4$ (10 eq) in refluxing THF to provide **333** (59%).

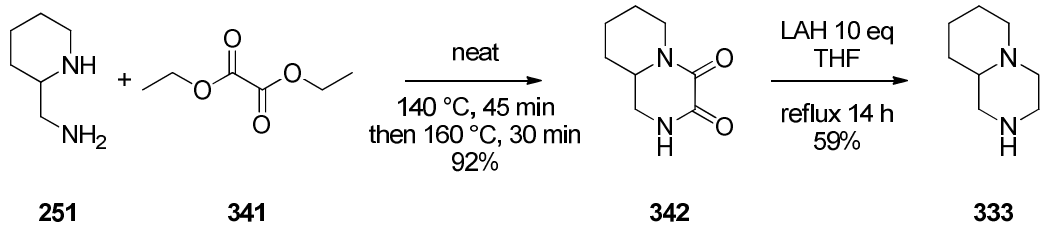

251 **341** **342** **333**

Scheme 3.31: Synthesis of [4,4,0]-1,4-diazobicyclodecane **333**.

The synthesis of diketopiperazine **342** was anticipated to compete with the *bis*-product intermediate **343** but this did not happen (see **Scheme 3.32**). In the event, this could be achieved in an efficient reaction by reacting 2-(aminomethyl)-piperidine **251** with 0.5 eq of diethyl oxalate at low temperature (96%).[35]

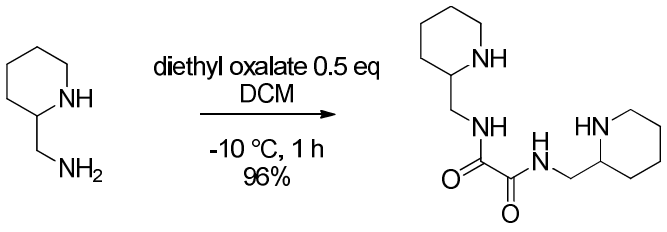

251 **343**

Scheme 3.32: Preparation of intermediate **338**.

The four NH's of **343** make it a potentially interesting tetradentate ligand. For example C-2 symmetric enantiopure tetraamide complexes of Rh or Ir were reported by Alcon to promote

asymmetric hydrogenations.[36] The structural analogue **344** was explored as a ligand for diethyl zinc reactions. This catalytic system could promote enantioselective hydrosilylation of ketones with polymethylhydrosiloxane as reductive agent, as shown in **Scheme 3.33**.[37]

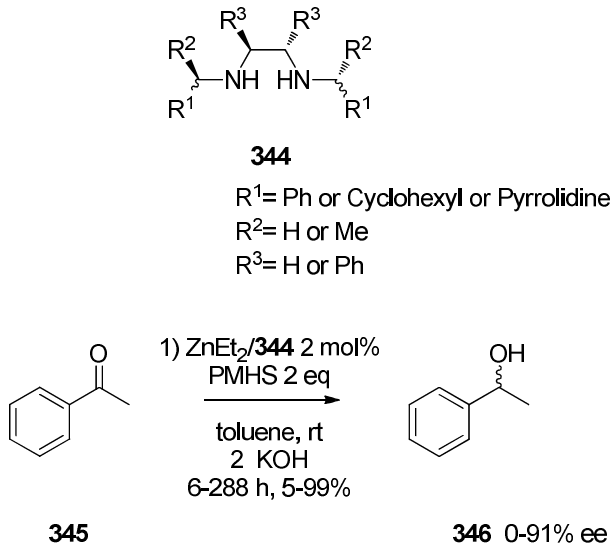

Scheme 3.33: Zinc-catalyzed reduction of acetophenone **340**.[37]

N^1,N^2-*Bis*(piperidin-2-ylmethyl)oxalamide **343** was submitted to a $LiAlH_4$ reduction (**Scheme 3.34**). The diamide **343** had poor solubility in THF and the reduction occurred very slowly (16%). In an effort to improve the solubility a BH_3-THF reaction was set up under constant sonication,[38] however this failed to improve the reaction.

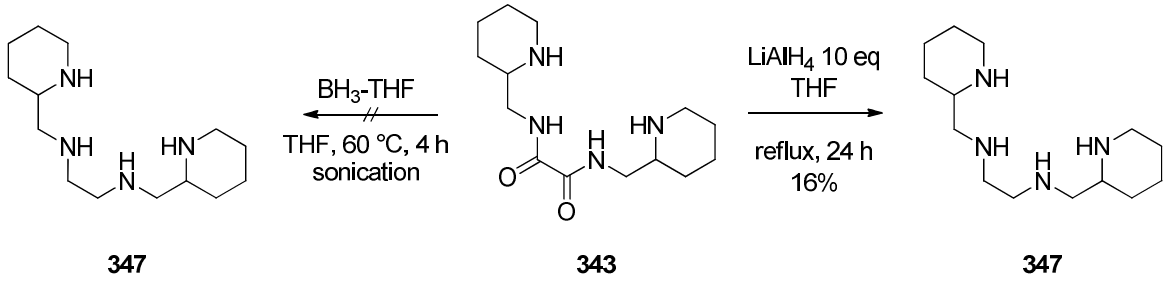

Scheme 3.34: Reduction of **343** to **347**.

Other derivatives could be obtained from [4,4,0]-1,4-diazobicyclodecane **333**, notably *N*-alkylated products, *via* the reduction of intermediate *N*-acyl substituents. *N*-acylation/ reduction of **333** was carried out with appropriate electrophiles in a one-pot reaction.

Thus, the addition of ethyl acetate (1 eq) into the reaction before quenching $LiAlH_4$, resulted in a mixture of **333** and the *N*-ethyl derivative **348** in a 2:1 ratio (**Scheme 3.35**).

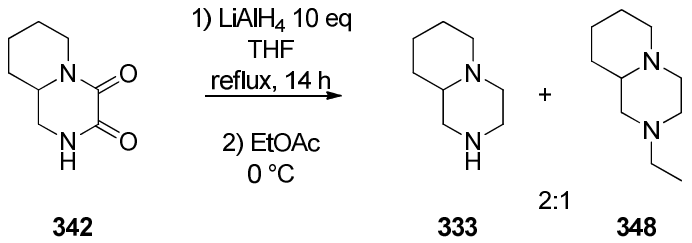

Scheme 3.35: Ethylation of **342** under reductive conditions.

This suggested an *in situ* acylation of the generated secondary amine by ethyl acetate, before its reduction by hydrides. Accordingly, the level of ethyl acetate was varied and at about 10 eq a complete conversion to **348** was achieved (**Table 3.2**).

EtOAc (nb of eq)	1	2	5	10
Ratio **333**/**348**	2:1	3:2	2:3	0:1

Table 3.2: Optimisation of acylation/reduction conditions to generate **348**.

As a consequence of the *N*-ethylation, the lipophilicity of the diamine was enhanced and the product **348** was more readily partitioned than **333** into the organic phase during extraction, leading to an efficient recovery of product (89%).

This *N*-alkylation process has the obvious advantage compared to direct alkylation with alkyl halides, which generally leads to the formation of quaternary ammonium salts. This reaction could be extended to the fluoromethyl derivative **350**. An acylation/reduction was explored with ethyl fluoroacetate, which gave the expected fluoroethyl derivative **350** in good yield (76%).

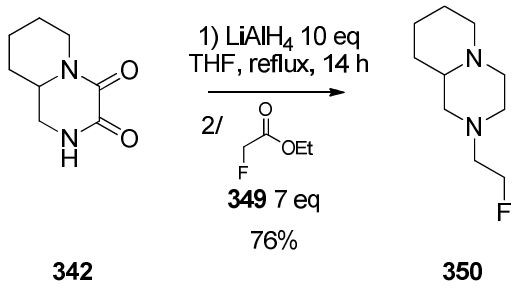

Scheme 3.36: Formation of the fluoroethyl derivative **350**.

For an enantiopure synthesis, on a small scale, it was found that the reactivity of the dihydrochloride salt of **251** was extremely low. The neutralisation process in organic solvents was slow and not effective due to the insolubility of the *di*HCl salt. To improve the contact between the reagents, the reaction was carried out in a sealed tube. Treatment of (*R*)-**251** *di*HCl with KO*t*Bu (2 eq) for 12 h before addition of diethyl oxalate **341** and heating, in a sealed tube, improved the reaction and allowed the recovery of (*R*)-**342** in 21% yield (**Scheme 3.37**)

The reduction to (*R*)-[4,4,0]-1,4-diazobicyclodecane **333** was then achieved as previously described. This gave an enantiopure sample of (*R*)-**333** in 54% yield

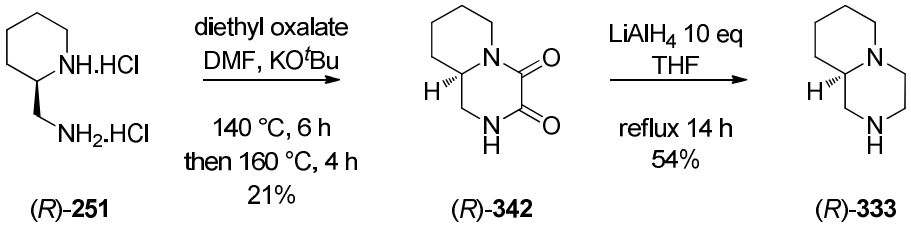

Scheme 3.37: Enantiopure synthesis of (*R*)-[4,4,0]-1,4-diazobicyclodecane (*R*)-**333**.

Diamide (*R*)-**342** crystallised very easily and X-Ray analysis of a suitable crystal confirmed the structure and stereochemistry of (*R*)-**342** (**Figure 3.11**).

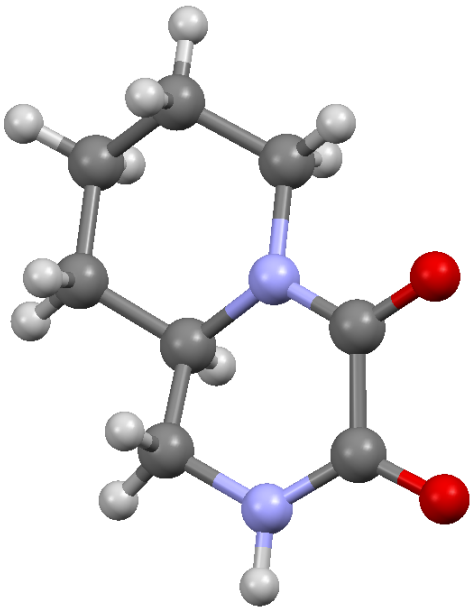

Figure 3.11: X-Ray structure of (*R*)-**342**.

3.4- 2-(Aminomethyl)piperidine as asymmetric organocatalyst

The second part of the 2-(aminomethyl)piperidine research concerned the synthesis of derivatives with potential catalytic properties. In general, secondary amines can induce Lewis base catalytic mechanisms either by forming enamine or iminium intermediates. The role of piperidine **351** as a catalyst was exemplified in a Knoevenagel condensation[39] where piperidine reacts with an aldehyde e.g. **352** to generate an iminium intermediate **353** (**Scheme 3.38**).

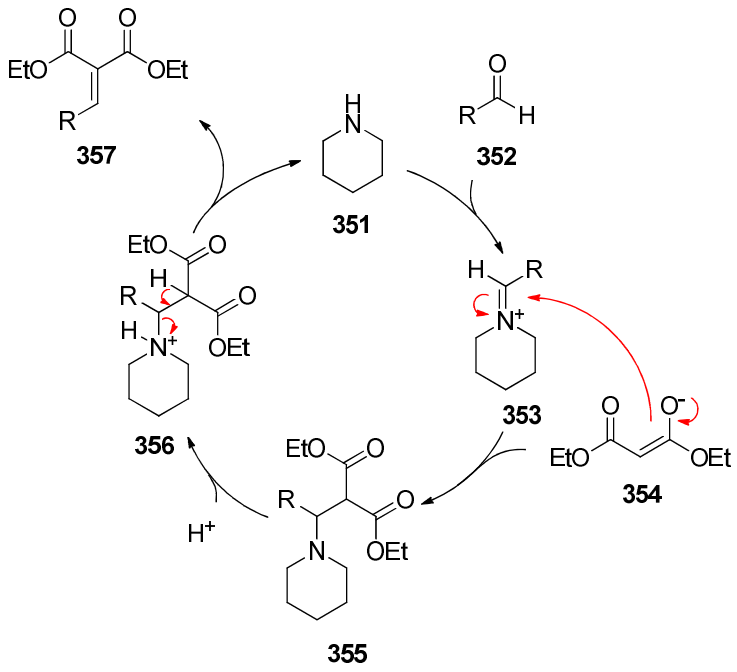

Scheme 3.38: Mechanism of Knoevenagel condensation with piperidine as an organocatalyst.

Asymmetric organocatalysis have typically 5-20 mol% of catalyst. L-Proline has proved to be very effective in this regard as have other enantiopure amines.[40-42]

Attention is also drawn to the development of pyrrolidines notably to expand the scope of catalysts for the model asymmetric Mannich reaction, as illustrated in **Scheme 3.40**.[43-45]

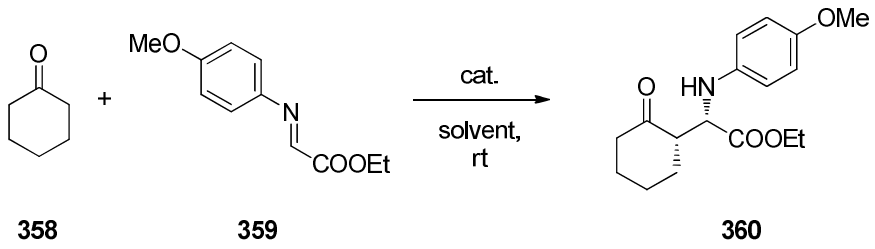

358 **359** **360**

Scheme 3.39: Asymmetric Mannich-like reactions used to assay the catalytic properties of piperidine derivatives.

The basicity of piperidine (pKa$_H$ = 11.1) is very similar to pyrrolidine (pKa$_H$ = 11.3), thus we sought to evaluate **251** as an organocatalyst. In this study, three derivatives of 2-(aminomethyl)piperidine **251** were targeted to tune the electronic properties. It is targeted to obtain organocatalysts able to form strong hydrogen bonds during the transition state and thus lower the activation barrier of the asymmetric Mannich reaction.

3.4.1- *N*-(Piperidin-2-ylmethyl)benzamide

N-Benzoylation of **251** appeared attractive to form an amide as hydrogen bond donor. This was first attempted with benzoyl chloride (**Scheme 3.40**). In an attempt to ensure the chemoselectivity, the amine moieties were initially protected with chlorotrimethylsilane. *N*-Trimethylsilylation occurred with complete conversion of the starting material. The mixture contained around 5% of the mono-protected diamine but no trace of a tri-protected diamine could be detected (95% N^1,N^4-TMS, 5 % N^1- and N^4-TMS). However, in an

attempted one-pot reaction, the *N*-benzoylation failed and after deprotection, only starting material was recovered. Increasing the equivalence of freshly distillated benzoyl chloride (2 eq, rt, 2 h) did not improve the reaction.

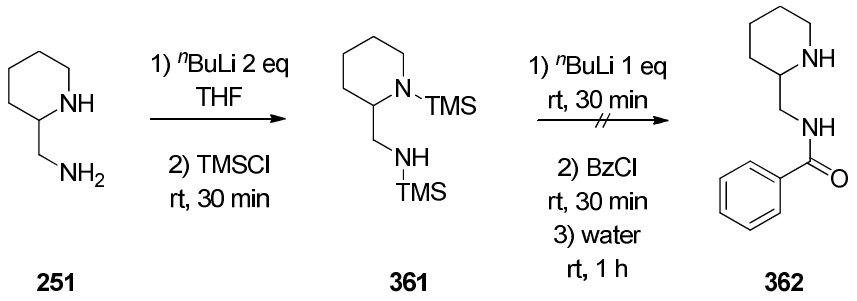

Scheme 3.40: Regioselective *N*-benzoylation of *rac*-**251**.

However, direct acylation was more successful; treatment of **251** with ethyl benzoate (1.7 eq) in various solvents was explored (**Scheme 3.41**). Reaction in ACN/water (6/1) proved to offer the best preparation of **362** (62%). Over reaction to N^1,N^4-dibenzoylation was not observed.

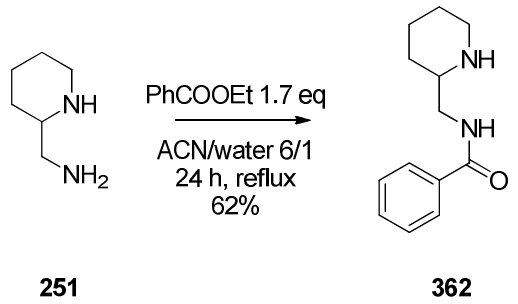

Scheme 3.41: Direct regioselective *N*-benzoylation on *rac*-**251**.

3.4.2- 2,2,2-Trifluoro-*N*-(piperidin-2-ylmethyl)acetamide

In order to increase the potential hydrogen bonding donor ability of the catalyst, a synthesis of trifluoroacetamide **363** was attempted.[46] In this case, the enantiopure (*R*)-2-(aminomethyl)-piperidine dihydrochloride was treated directly with either trifluoroacetic anhydride or ethyl trifluoroacetate. Triethylamine and DIEA were explored as bases to neutralise the salt and the conditions are summarised in **Table 3.4**.

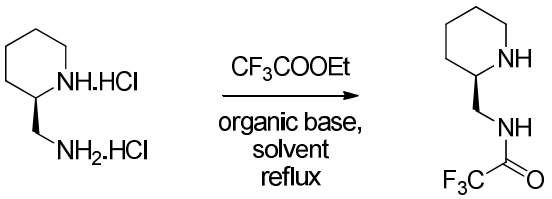

(*R*)-**251** (*R*)-**363**

Entry[i]	Base	Solvent	Result	
1	Et_3N 3 eq	MeOH	39%	✓
2	DIEA 2 eq	MeOH	48%	✓
3	DIEA 3 eq	MeOH	Mixture of N^1-, N^4- and N^1,N^4-trifluoramide	×
4	DIEA 5 eq	MeOH	Mixture of N^1-, N^4- and N^1,N^4-trifluoramide	×
5	DIEA 2 eq	ACN/water 6:1	No reaction	×
6	DIEA 2 eq	THF/DMF 1:1	54%	✓

i: All reactions 8 h, except entry **6**, 14 h

Table 3.4: Exploration of conditions to (*R*)-**363**.

Product (*R*)-**363** was always obtained when 2 or 3 equivalents of base were used, except with ACN/water (6:1) as the solvent. Furthermore, 3-5 equivalents of DIEA provided mixtures of N^1-, N^4- and N^1,N^4-trifluoroamides. DMF assisted the dissolution of (*R*)-**251** dihydrochloride in THF, and the conversion was slightly higher after 14 h at reflux. This emerged as the preferred conditions for reaction of the *di*HCl salt of **251** to provide (*R*)-**363**.

A later development in the programme recognised that the tetrafluoroborate salt of (*R*)-**251** could be solubilised in THF and the nucleophilicity of the amine increased. This modification dramatically improved the synthesis of (*R*)-**363** (88% yield) and this protocol emerged as the method of choice (**Scheme 3.42**).

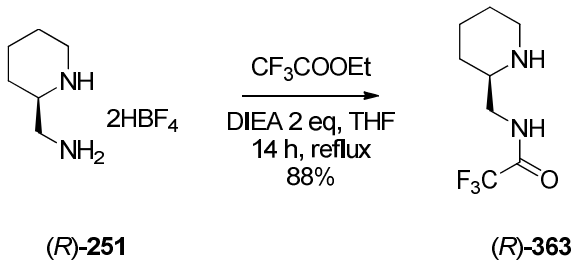

Scheme 3.42: Optimised conditions for the synthesis of (*R*)-**251**.

The trifluoroacetate salt of **363** was a crystalline solid and the structure was confirmed by X-Ray analysis. It was arbitrarily represented as the (*R*)-enantiomer.

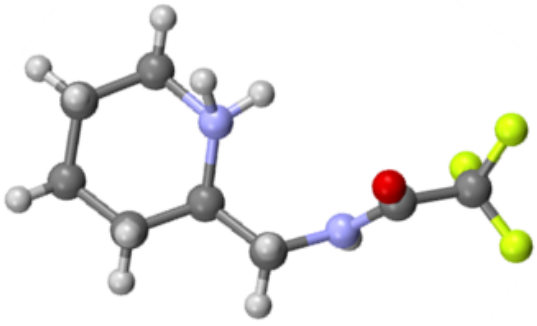

Figure 3.12: X-Ray structure representing protonated (*R*)-**363** (trifluoroacetate salt).

A sample of the hydrochloride salt of (*R*)-**363** (0.01 M) was titrated with an aq NaOH (0,1 M) (**Figure 3.13**). A pK_a = 9.3 was calculated by the derivative method. The inductive effect of the trifluoroacetamide substituent exerts a strong influence on the amine acidity, lowering the pK_a by 0.6 unit relative to the free diamine.[46]

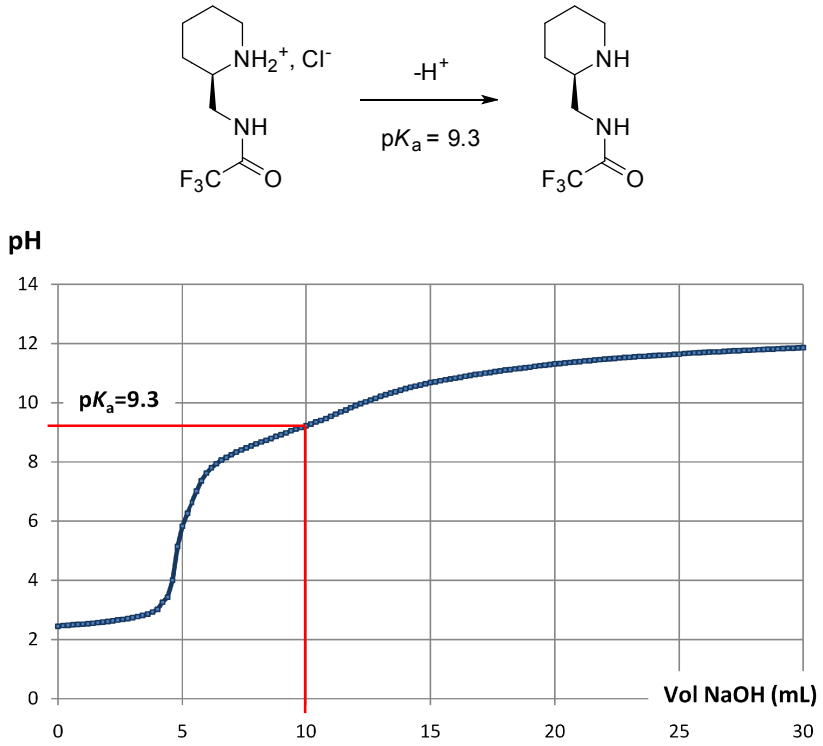

Figure 3.13: Potentiometric titration of (*R*)-**363** hydrochloride salt (pK_a = 9.3)

3.4.3- 4-Methyl-*N*-(piperidin-2-ylmethyl)benzenesulfonamide

A greater polarisation effect induced by the sulfonamide compared to the amide may benefit its catalytic properties. It has been reported that the influence of the remote substituent in the charge delocalization of the amine is less important for sulfonamides.[46] A substituent with a

high steric hindrance could then be evaluated, and for this purpose the benzene sulfonamide **364** was targeted.

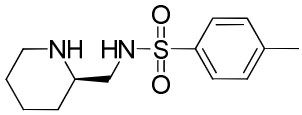

(*R*)-4-methyl-*N*-(piperidin-2-ylmethyl) benzenesulfonamide **364**

Tosylation of the free base required 1 eq of tosyl chloride with potassium carbonate as a base (**Scheme 3.43**). The reaction was carried out at low temperature (0 °C) and proved to be very efficient giving the sulfonamide **364** in a 91% yield.

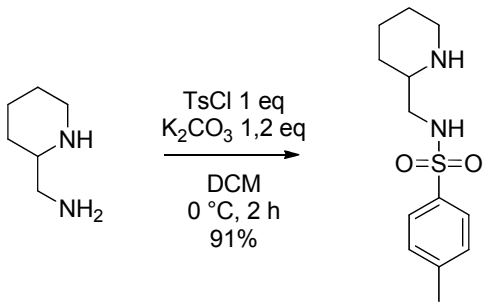

251 **364**

Scheme 3.43: Regioselective tosylation of **251**.

However to prepare an enantiopure sample of **364**, it was important to find a suitable method to address the poor solubility of the dihydrochloride salt. The use of DMF instead of DCM provided the expected hydrochloride salt of **364** however in low yield (28%) (**Scheme 3.44**).

Pre-packed resins have proven to be an efficient method to separate products according to their relative affinity or by ion exchange. The use of basic resins, such as Amberlite IRA 400 and Dowex 1X8, was explored to sequester the hydrochlorides but this was not successful.

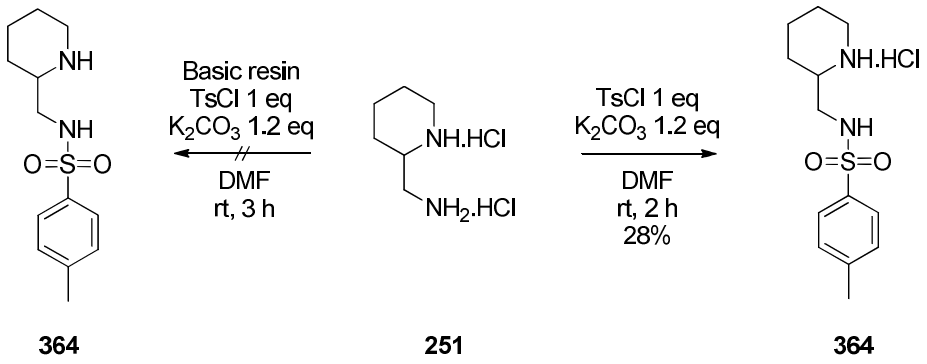

364 **251** **364**

Scheme 3.44: Assays for tosylation of *rac*-**251** dihydrochloride.

The use of silver carbonate as a base was explored and after a 3 h reaction with tosyl chloride, **364** was obtained in a 66% yield (**Scheme 3.45**).

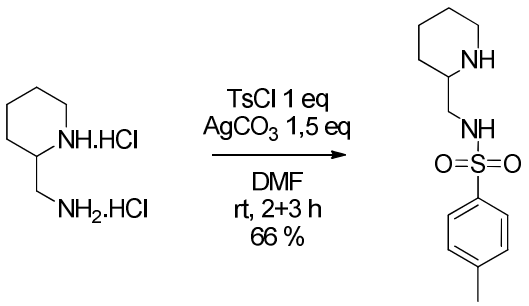

251 **364**

Scheme 3.45: Use of silver carbonate to precipitate hydrochlorides.

However the optically pure base (*R*)-**364** was prepared in a better yield (79%) from its tetrafluoroborate salt (*R*)-**251**. The tetrafluoroborate was successful when first treated with

DIEA (**Scheme 3.46**). Then the conditions developed for the racemic diamine *rac*- **251** could be used. Interestingly, the use of a unique base (DIEA, Et_3N or K_2CO_3, 3 eq) in the reaction did not result in an efficient conversion to allow tosylamide **364**. K_2CO_3 acted to precipitate HBF_4 but the KBF_4 salt generated dissolved slowly, suggesting a constant exchange of BF_4^- with the diamine **251**.

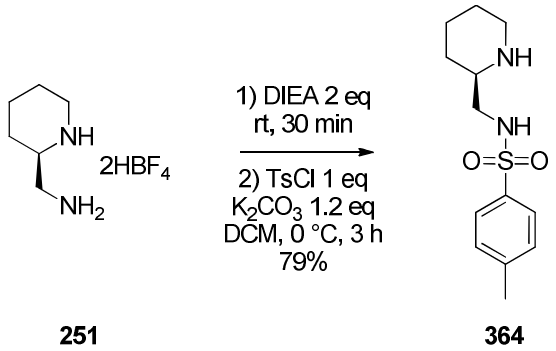

Scheme 3.46: Regioselective tosylation on tetrafluoroborate salt of (*R*)-**251**.

The structure of **360** was confirmed by X-ray structure analysis. Notably the product is the free base without any counter ion. The (*R*)-enantiomer was arbitrarily represented in **Figure 3.14**.

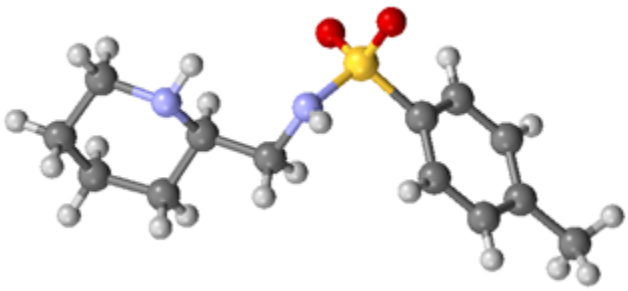

Figure 3.14: X-Ray structure representing (*R*)-**364**.

Tosylamide (*R*)-**364** hydrochloride salt was used for titration to determine its p*K*a. The titration curve of (*R*)-**364** (0.01 M) against an aq NaOH solution (0.1 M) is shown in **Figure 3.15**. The pK_a was calculated by its derivative at pK_a = 9.0. The value is decreased by 0.9 p*K*a unit relative to the amine **251**, and 0.3 units relative to the amide (*R*)-**363**, consistent with the stronger electron withdrawing effect of the sulfonamide relative to the amide.

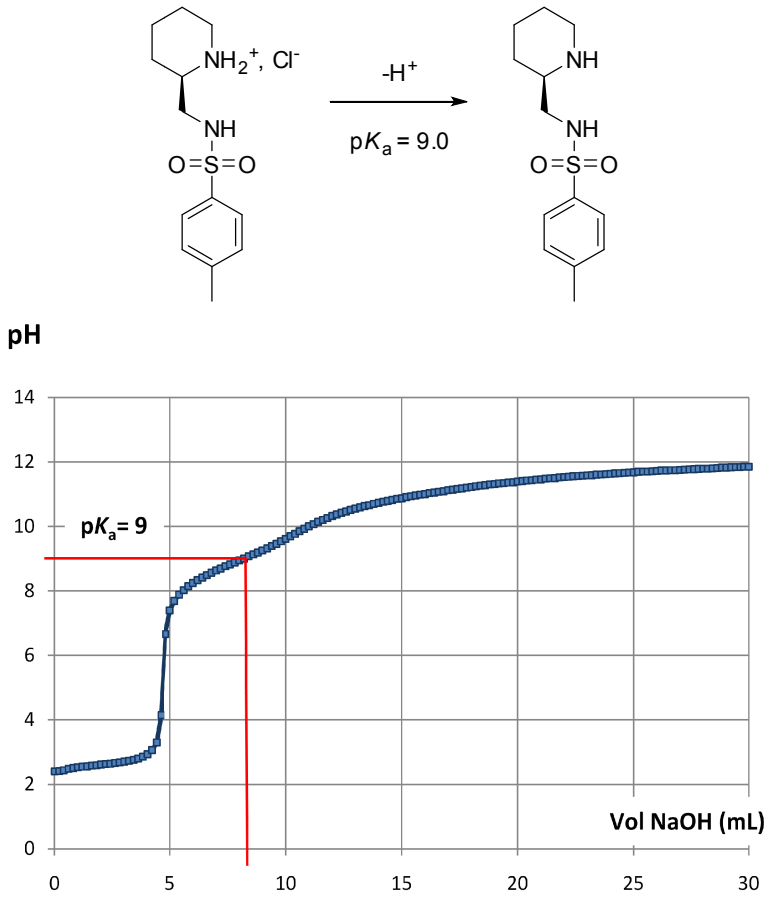

Figure 3.15: Potentiometric titration of (*R*)-**364** hydrochloride salt (pK_a = 9.0).

With regards to the various assays of *N*-derivatization, the tetrafluoroborate salt, once treated with DIEA, presented a similar reactivity to that of the free base. The tetrafluoroborate salt of 2-aminomethylpiperidine emerged as the salt of choice for regioselective reactions on the primary amine. Modified piperidines were prepared as potential organocatalyst. Particular

attention was drawn to tuning the pK_{aH} of the piperidine and to provide good hydrogen bond donor ability (**Figure 3.16**). The trifluoroacetamide moiety carried a reduced pK_{aH} by 0.6 units, and the tosylamide moiety by 0.9 units. The effect of these substituents on the diastereomeric ratio and enantiomeric excess of a model Mannich reaction is described in the following section.

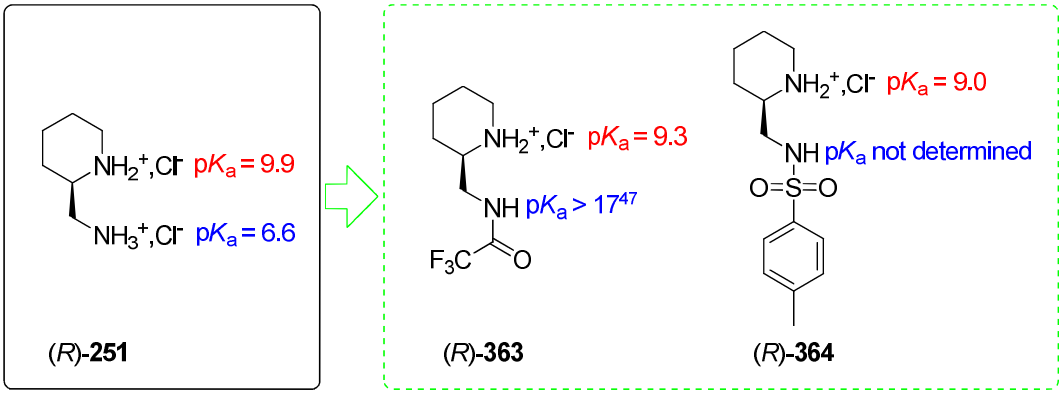

Figure 3.16: Calculated p*K*a of diamine **251**, trifluoroacetamide **363** and tosylamide **364**.[47]

3.5- New catalyst for asymmetric Mannich reactions

One essential parameter for designing new organocatalysts is their pK_a values. A systematic study of proline derivatives highlighted a correlation between the increasing acidities of proline amides and enhancement of enantioselectivity.[46] To examine the scope of the (*R*)-2-(aminomethyl)piperidine derivatives as catalysts, the conditions described by Ley *et al.*[48] for an asymmetric Mannich reaction were used as a frame of reference. The Mannich imine **359** is formed by reaction of *p*-anisidine **365** on ethyl glyoxalate **366,** before dehydration of **367** on molecular sieves. This was achieved in a straightforward manner.

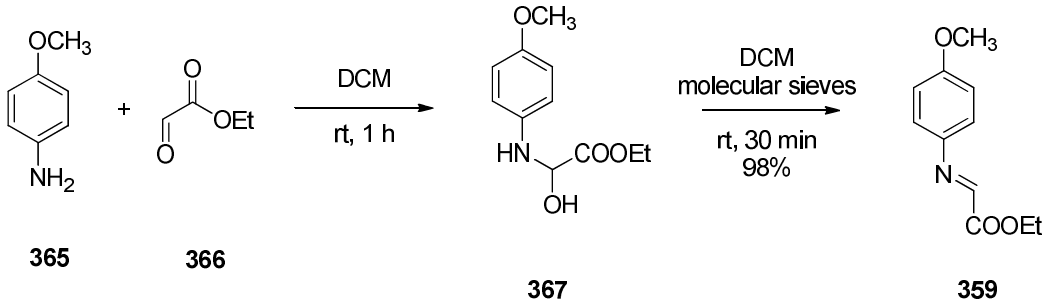

Scheme 3.47: Preparation of the Mannich imine **359**.

3.5.1- Reactions catalysed by proline

As a pre-requisite to this study, a set of reference reactions was carried out to establish the HPLC retention times of the product stereoisomers. A series of reactions catalysed by DL-proline and separately by its enantiomers D- and L- proline (20 mol%, 24 h in ^{i}PrOH) were conducted. Proline has already been shown to be an excellent catalyst for this reaction.[49, 50] The data obtained in this study is shown in **Table 3.5**.

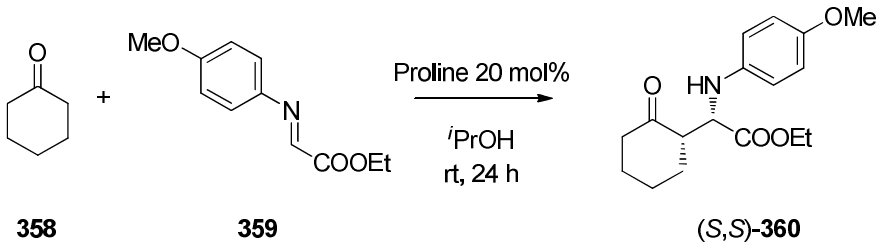

358 **359** (*S*,*S*)-**360**

Entry	Catalyst	Yield	dr *syn*/*anti*[ii]	ee[iii]
1	DL-Proline	97%	93:7	ns[v]
2	L-Proline	91%	94:6	97%
3	D-Proline	96%	94:6	98%[iv]
4	No catalyst	21%	60:40	ns[v]
5	TMP[i]	29%	53:47	ns[v]

i: 2,2,6,6- Tetramethylpiperidine; *ii*: determined by ^{1}H NMR; *iii*: determined by HPLC on the major *syn* diastereomer; *iv*: major *syn* diastereomer was (*R*,*R*)-**360**; *v*: not significant.

Table 3.5: Reference reactions to establish HPLC retention times of product stereoisomers **360**.

The diastereomeric ratio (dr) was determined by ^{1}H NMR, by examination of the NH-C*H*-COOEt signals. ^{1}H NMR for the proline catalysed reactions showed consistent *syn*/*anti* ratios higher than 93:7 (entries 1-3). The retention time of the four enantiomers of **360** was determined by chiral HPLC analysis (column Daicel Chiralpak AS-H, Hexane/^{i}PrOH 9:1, 0.75 mL.min^{-1}) of the DL-proline catalysed reaction at 26.2 min (*anti* 1), 34.0 min (*syn* 1), 38.7 min (*anti* 2) and 47.1 min (*syn* 2) as shown in **Figure 3.17**.

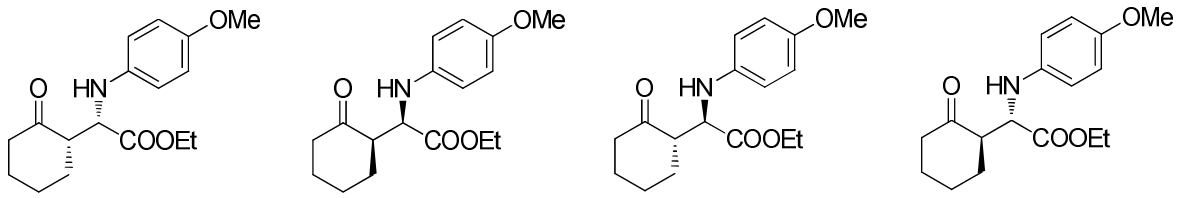

(*S*,*S*)-**360** *Syn1* | (*R*,*R*)-**360** *Syn2* | (*S*,*R*)-**360** *Anti1* | (*R*,*S*)-**360** *Anti2*

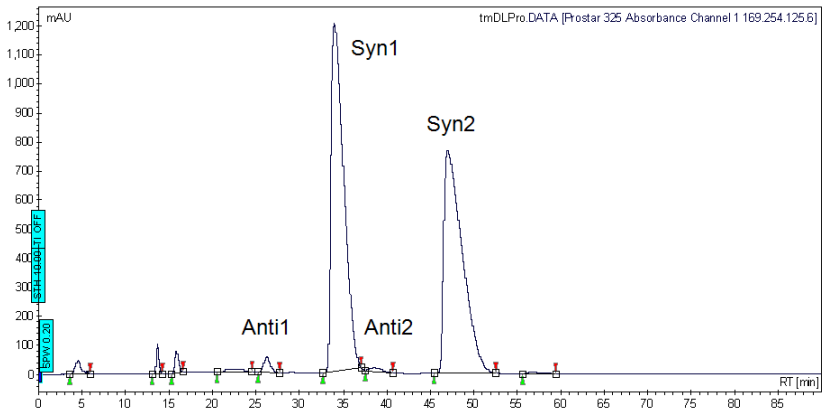

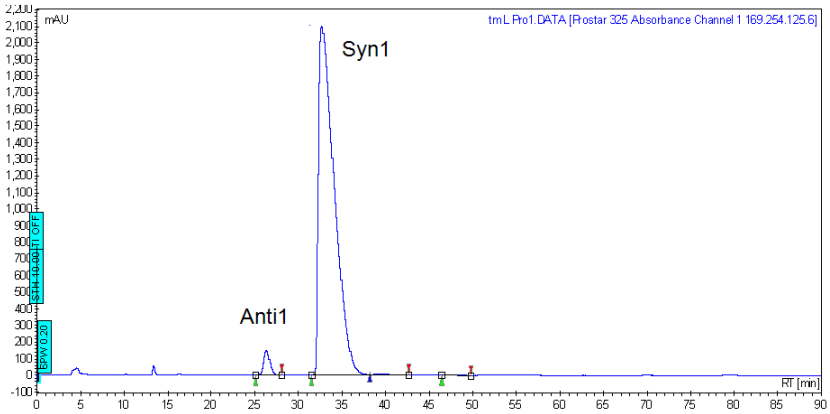

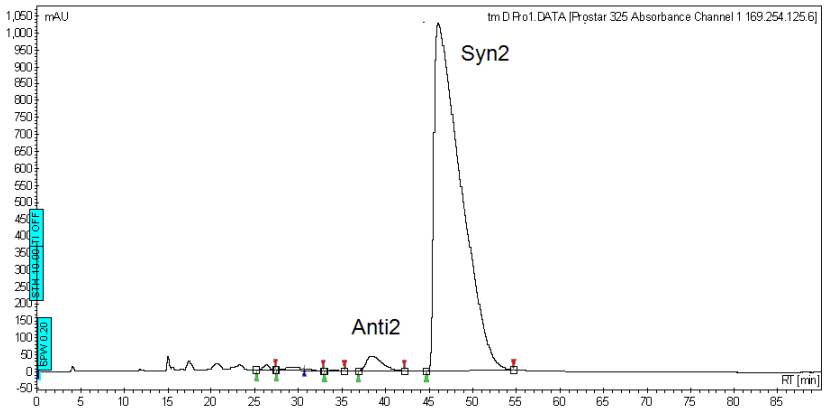

Figure 3.17: HPLC analyses of **355** from control reactions catalysed by Proline (top: DL-Proline, mid: L-Proline, bottom: D-Proline)

In the absence of catalyst (entry 4, **Table 3.5**), the reaction occurred in 21% yield. This highlights the role of the Mannich adduct **360** as an autocatalyst over long reaction times (24 h).[51] DFT calculation have established that the transition state for the *syn* adduct was preferred by 1.8 kcal.mol^{-1}.[52] In our case, a diastereomeric amplification was observed in favour of the *syn* adduct (60:40 dr).

The control reaction with symmetrical 2,2,6,6-tetramethylpiperidine (entry 5) provided the two sets of diastereomers with a low dr, however the reaction proceeded in only a modest yield (29%), suggesting that TMP was not a good catalyst.

With this set of controls in place, (*E*)-*N*-4-methoxybenzyl-α-iminoglyoxalate **359** was reacted with cyclohexanone **358** in the presence of organocatalysts **363** or **364**. The outcomes of these reactions are reported below.

3.5.2- Reaction with trifluoroacetamide organocatalyst 363

Conditions for the reaction catalysed by trifluoroacetamide **363** (20 mol%, 24 h, 0.5 mL of cyclohexanone, 0.5 mL of solvent) were explored. The reaction was carried out in five polar aprotic (DCM, THF, acetone, DMF, DMSO) and one polar protic (^{i}PrOH) solvent (see **Table 3.6**). It was established that the yield is increased with the solvent polarity from 26% in DCM to 44% in DMF. The highest yield observed was however in the neat reaction (61%), which clearly benefited from a concentration effect. In reactions set up in solvents more polar than acetone, there is no trace of the iminoester **359**.

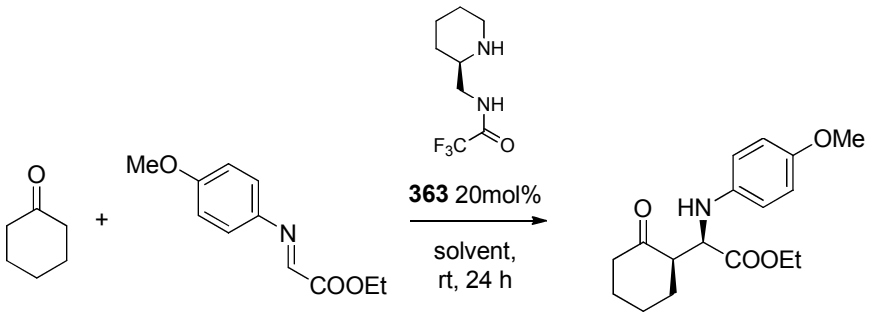

358 **359** (*R*,*R*)-**360**

Entry	Solvent[i]	Yield	dr *syn*/*anti*	ee
1	DCM	26%	66:34	42%
2	^{i}PrOH	45%	69:31	78%
3	THF	29%	63:37	53%
4	Acetone	38%	62:38	54%
5	DMF	44%	61:39	62%
6	DMSO	42%	70:30	78%
7	Water	41%	88:12	86%
8	Neat	61%	67:33	58%

i: Cyclohexanone/solvent 1:1.

Table 3.6: Conditions and outcomes of (*R*)-**363** catalysed reactions.

The *syn*/*anti* ratios remained relatively stable through the reactions at ~65:35, with the exception of *i*PrOH and DMSO, where it was improved (until 70:30 for DMSO). Interestingly, **363** favoured the formation of the (*R*,*R*)-*syn* adduct of **360**. The ee also increased with the polarity of the solvent, again with the exception of ^{i}PrOH (78% ee). In a

solvent like DMSO (78% ee, **Figure 3.18**), the HPLC trace shows enlarged peaks at their bases. It is acknowledged that significant errors are induced in the measure of the ee. The ee of the neat reaction (58%, **Figure 3.19**) is lower. To explore further the importance of a polar protic solvent, a reaction was set up in water. The outcome was improved again with a dr *syn*/*anti* of 88:12 and an ee of 86% (**Figure 3.20**). In water, cyclohexanone is not soluble and a micellar suspension is formed with vigorous stirring. It is known that the concentration of reactants within the micelle or at its aqueous interface can lead to a higher reaction rate.[53] This environment appears to favourably affect the reaction. The presence of water for the autocatalytic Mannich reaction has been noted previously.[54] The authors reported that the ee was dramatically improved (90% ee) but the effect of water was less interesting when the Mannich imine was formed *in situ* (68% ee). The catalyst **363** shows equivalent enantioselectivity but better diastereoselectivity than the autocatalytic Mannich reaction (53:47 *syn*/*anti* ratio).

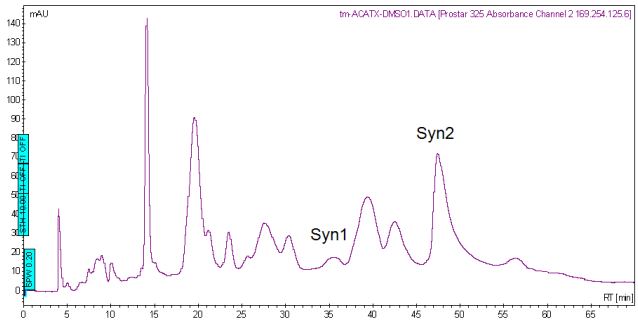

Figure 3.18: HPLC analysis of reaction in DMSO catalysed by **358** (crude mixture, up to 78% ee).

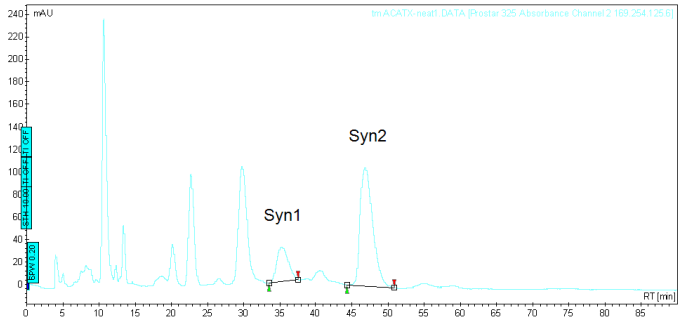

Figure 3.19: HPLC analysis of reaction in neat conditions catalysed by **358** (crude mixture, 58% ee).

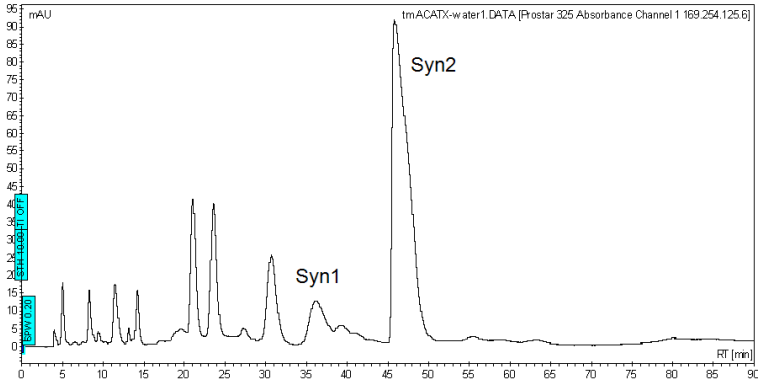

Figure 3.20: HPLC analysis of reaction in water catalysed by **363** (crude mixture, 86% ee).

The influence of catalyst loading was then explored for **363** as summarised in **Table 3.7**.

Entry[i]	**Catalyst 363 (mol%)**	**Time**	**Yield**	**dr *syn*/*anti***	**ee**
1	20	4 d	47%	69:31	45%
2	30	24 h	59%	69:31	73%
3	10	24 h	44%	69:31	63%
4	5	24 h	42%	64:36	31%

i: All reactions carried out in ^{i}PrOH

Table 3.7: Exploration of catalyst **363** loading and time effects on **360** formation.

In ^{i}PrOH, the diastereomeric ratio is constant at 69:31 between 10-30 mol%, however it reduces at 5 mol% (**Figure 3.21**). A reaction run for 4 d at 20 mol% did not improve the outcome (47% yield, 45% ee).

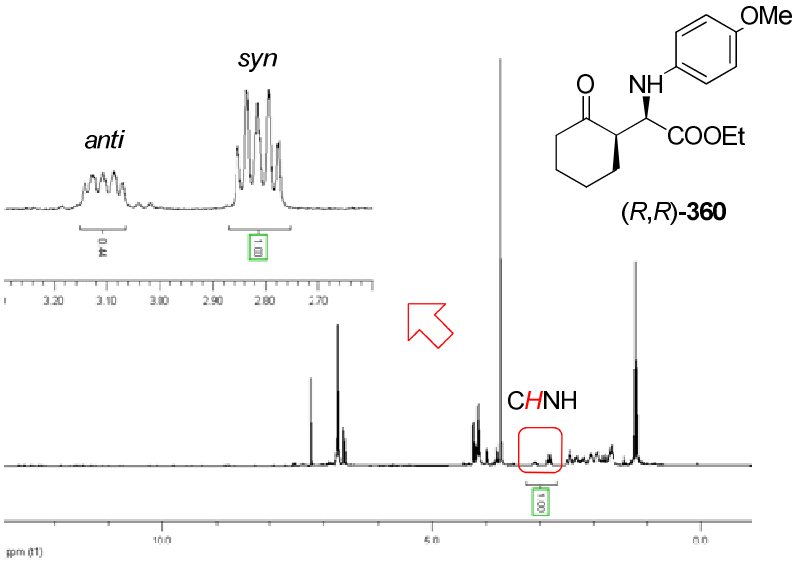

Figure 3.21: ^{1}H NMR of adduct **360** in a **363** catalysed (10 mol%, ^{i}PrOH, 24 h, rt) reaction.

3.5.3- Reactions with organocatalyst 364

The tosylamide **364** was now assayed as a catalyst for the formation of **360**. At a catalyst loading of 20 mol%, the yields were significantly higher and DMSO appeared to be the best solvent. However, the dr was lower for each solvent (67:33 in favour of the *syn* adduct in ^{i}PrOH) when compared to **363** as a catalyst. On the other hand, the ee significantly improved for all the solvents tested (up to 85% ee in DMSO). Interestingly, the favoured enantiomer was inverted with the (*S,S*)-*syn* adduct being favoured over the (*R,R*)-*syn* found for catalyst **363** (**Figure 3.22**).

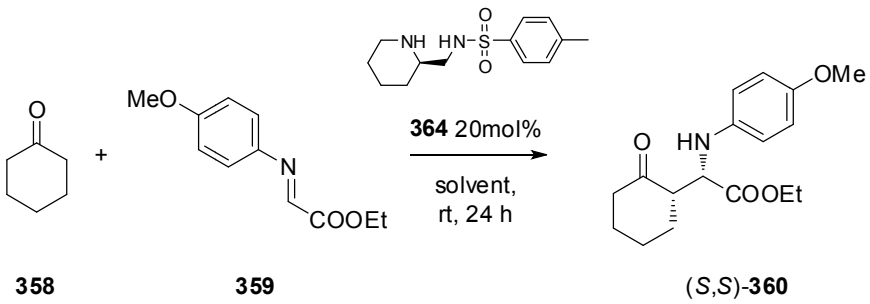

Entry	Solvent	Yield	dr *syn*/*anti*	ee
1	^{i}PrOH	50%	67:33	83%
2	DMSO	53%	nd	85%
3	neat	59%	62:38	83%

Table 3.8: Scope of solvents for catalyst **364**.

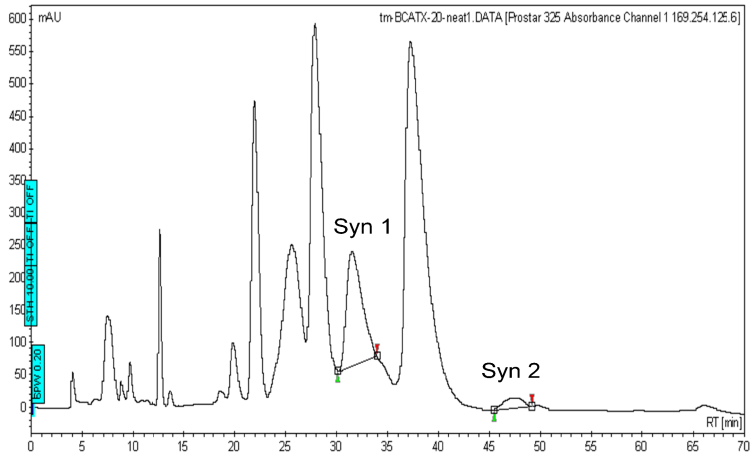

Figure 3.22: HPLC analysis of neat reaction catalysed by **364** (crude mixture, 83% ee).

This study aimed to evaluate the catalytic properties of two piperidine derivatives for a Mannich reaction. Both the trifluoroacetamide **363** and tosylamide **364** proved to be efficient catalysts. Overall the yields were good. The selectivity is high, generating predominantly the

syn adduct of **360**. Overall the ratios were lower than that from the proline catalysed reactions (up to 99:1 dr)[48] but they were comparable to many other chiral catalysts, such as other amino acids.[55]

The ee was significantly increased in the presence of DMSO and ^{i}PrOH (78% ee), but water has the strongest effect on both the dr (88:12) and the ee (86%) for **363**. Water seems to be the most appropriate solvent for these reactions.

3.5.4- Mechanistic insights

The generally accepted mechanism of this Mannich reaction is shown in **Scheme 3.48**, where the ketone will react with tosylamide **364**, resulting in enamine **368** formation. The imine **359** then reacts with the enamine **368** to give the enantiomerically enriched Mannich adduct **360**.

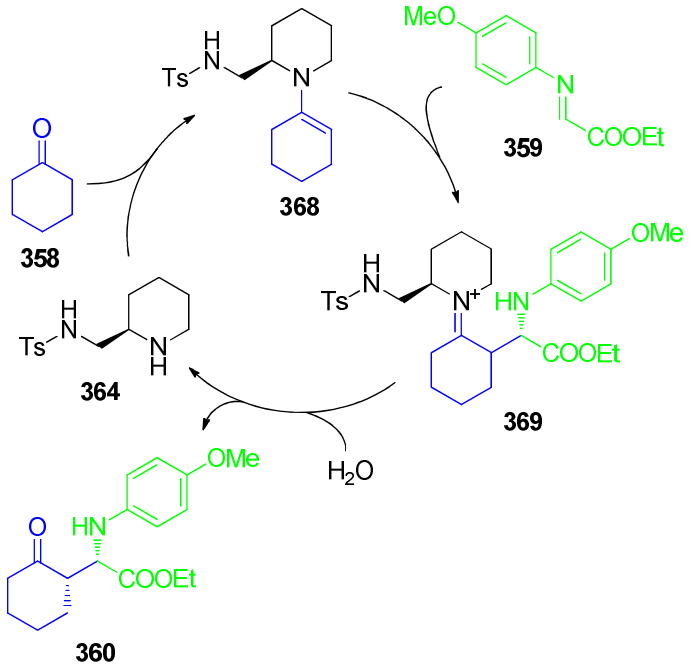

Scheme 3.48: Mechanism for the asymmetric Mannich reaction catalysed by **364**.

Both catalysts favoured formation of the *syn*-adduct. To explain the absolute stereochemistry, two transition states have been proposed based on the literature (**Figure 3.23**).[45, 55-58] When the *Si* face of the chiral enamine is attacked by the *Si* face of the trans-imine, the formation of the (*S*,*S*)-*syn*-adduct is induced, such as for tosylamide **364**. The facial selectivity is induced by steric repulsion between the catalyst and the PMP group. A nine-member ring is formed in the transition state, stabilised by a hydrogen bond between the imine nitrogen and the secondary amine of the catalyst. This ring appears to be more stable with a stronger shorter hydrogen bond between the imine nitrogen and the amide or sulfonamide.

The reversal of the configuration with catalyst **363** involves the formation of a more favourable *Re* face attack by the enamine. This enamine does not suffer from steric repulsion from the trifluoroacetamide group and thus the HC_{α} can generate a strong hydrogen bond with the amide nitrogen. This generates a seven membered ring stabilising the *Re* face.

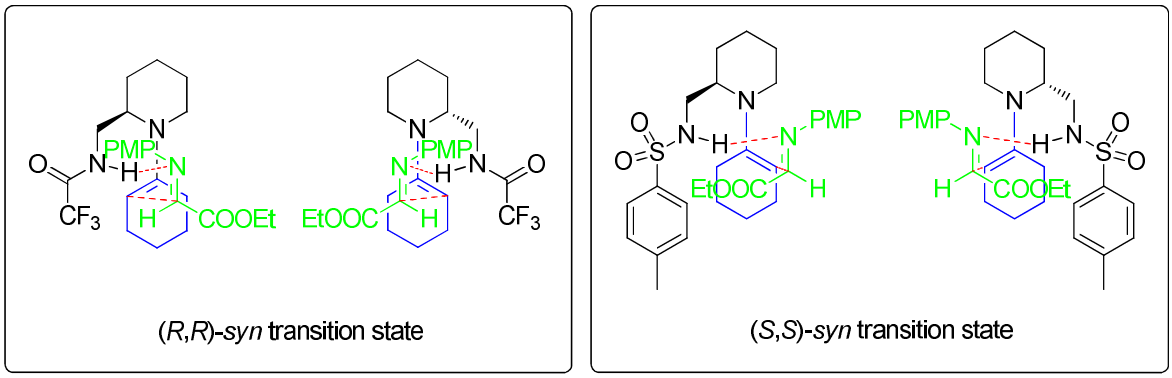

Figure 3.23: Putative transition states for the major *syn*-adduct induced by **363** (left) and **364** (right).

3.6- Conclusion

In the first part of this work, the development of a methodology for the synthesis of the enantiopure diamine 2-(aminomethyl)-piperidine (*R*)-**251**, leading to an efficient gram-scale synthesis, was described (**Figure 3.24**).

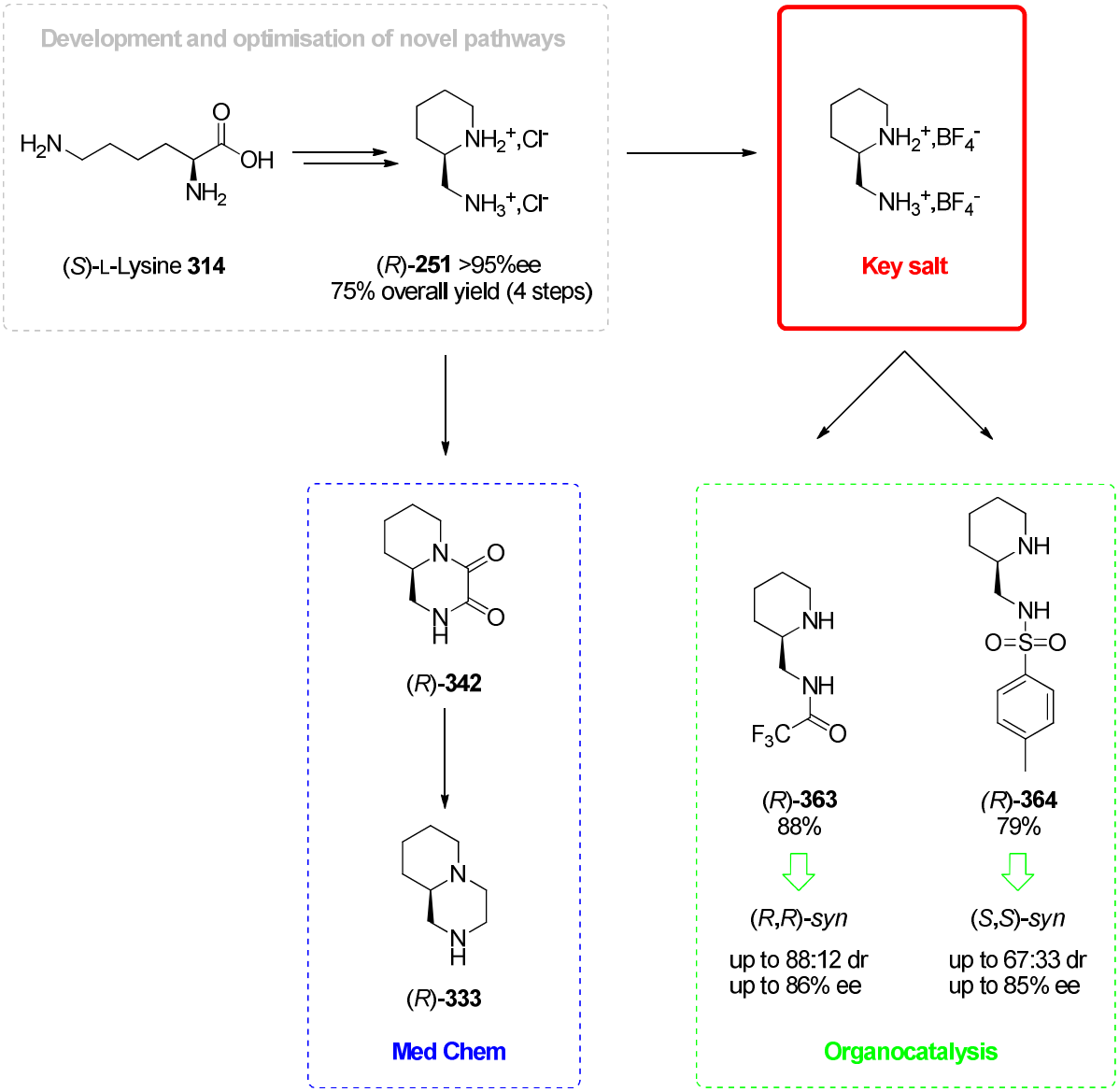

Figure 3.24: 2-(Aminomethyl)piperidine is a versatile structural motif.

As depicted in **Figure 3.24**, a N^1-N^4 cyclization was achieved on (*R*)-**251** *di*HCl and lead to an enantioselective synthesis of (*R*)-**333**.

The use of the tetrafluoroborate salt of (*R*)-**251** significantly improved the regioselective synthesis of the two N^1-derivatives (*R*)-**363** and (*R*)-**364**. In general, the tetrafluoroborate salt of **251** offers excellent reactivity and solubility and constitutes the reagent of choice for all syntheses to 2-(aminomethyl)piperidine derivatives.

When the development of organocatalysts started, it was not obvious that a piperidine derivative would compete with a pyrrolidine in a catalytic process. This study has demonstrated that both (*R*)-**363** and (*R*)-**364** have reasonable catalytic properties, comparable to other chiral entities (up to 86% ee), and with a loading of (*R*)-**363** as low as 5 mol%. Further studies would certainly uncover new highly efficient organocatalysts derived from 2-aminomethylpiperidine tetrafluoroborate (*R*)-**251**. (*R*)-**251** Tetrafluoroborate should also prove useful as an intermediate for the synthesis of other chiral amines.

1. I. B. Seiple, S. Su, I. S. Young, C. A. Lewis, J. Yamaguchi and P. S. Baran, *Angew. Chem. Int. Ed.*, 2010, **49**, 1095-1098.
2. W. Teichmann, *Z. Gesamte Inn. Med.*, 1963, **18**, 597-599.
3. P. Mangeney, A. Alexakis and J. F. Normant, *Tetrahedron Lett.*, 1988, **29**, 2677-2680.
4. S. Hanessian, D. Delorme, S. Beaudoin and Y. Leblanc, *J. Am. Chem. Soc.*, 1984, **106**, 5754-5756.
5. G. Cardillo, A. D'Amico, M. Orena and S. Sandri, *J. Org. Chem.*, 1988, **53**, 2354-2356.
6. S. G. Davies and A. A. Mortlock, *Tetrahedron: Asymmetry*, 1991, **2**, 1001-1004.
7. E. J. Corey and F. J. Hannon, *Tetrahedron Lett.*, 1987, **28**, 5233-5236.
8. J.-X. Gao, T. Ikariya and R. Noyori, *Organometallics*, 1996, **15**, 1087-1089.
9. S. Hashiguchi, A. Fujii, J. Takehara, T. Ikariya and R. Noyori, *J. Am. Chem. Soc.*, 1995, **117**, 7562-7563.
10. P. O'Brien and P. Poumellec, *Tetrahedron Lett.*, 1996, **37**, 5619-5622.
11. G. M. Taylor, S. J. Baker, A. Gedney, D. J. Pearson and G. E. M. Sibley, *Tetrahedron Lett.*, 1996, **37**, 1297-1300.
12. I. Gómez-Monterrey, M. J. Domínguez, R. González-Muñiz, J. R. Harto and M. T. García-López, *Tetrahedron Lett.*, 1991, **32**, 1089-1092.
13. P. I. Mortimer, *Aust. J. Chem.*, 1958, **11**, 82-85.
14. R. L. Augustine, *J. Am. Chem. Soc.*, 1959, **81**, 4664-4667.
15. M. E. Freed and A. R. Day, *J. Org. Chem.*, 1960, **25**, 2108-2113.
16. K. Morikawa, M. Honda, K. Endoh, T. Matsumoto, K. Akamatsu, H. Mitsui and M. Koizumi, *J. Pharm. Sci.*, 1990, **79**, 750-753.
17. H. C. Wong, R. Coogan, F. P. Intini, G. Natile and L. G. Marzilli, *Inorg. Chem.*, 1999, **38**, 777-787.
18. J. Perumattam, B. G. Shearer, W. L. Confer and R. M. Mathew, *Tetrahedron Lett.*, 1991, **32**, 7183-7186.
19. O. Froelich, P. Desos, M. Bonin, J.-C. Quirion, H.-P. Husson and J. Zhu, *J. Org. Chem.*, 1996, **61**, 6700-6705.
20. S. Nazabadioko, R. J. Pérez, R. Brieva and V. Gotor, *Tetrahedron: Asymmetry*, 1998, **9**, 1597-1604.
21. L. Somekh and A. Shanzer, *J. Am. Chem. Soc.*, 1982, **104**, 5836-5837.
22. S. E. de Sousa and P. O'Brien, *Tetrahedron Lett.*, 1997, **38**, 4885-4888.

23. P. Gmeiner, D. Junge and A. Kaertner, *J. Org. Chem.*, 1994, **59**, 6766-6776.
24. P. O'Brien and T. D. Towers, *J. Org. Chem.*, 2001, **67**, 304-307.
25. K. Weber, S. Kuklinski and P. Gmeiner, *Org. Lett.*, 2000, **2**, 647-649.
26. C. McKay, R. J. Wilson and C. M. Rayner, *Chem. Commun.*, 2004, **9**, 1080-1081.
27. T. Lehmann and P. Gmeiner, *Heterocycles*, 2000, **53**, 1371-1378.
28. H. K. Hall, *J. Am. Chem. Soc.*, 1957, **79**, 5441-5444.
29. H. K. Hall, *J. Am. Chem. Soc.*, 1957, **79**, 5439-5441.
30. M. J. Potter, M. K. Gilson and J. A. McCammon, *J. Am. Chem. Soc.*, 1994, **116**, 10298-10299.
31. C. L. Hamblett, J. L. Methot, D. M. Mampreian, D. L. Sloman, M. G. Stanton, A. M. Kral, J. C. Fleming, J. C. Cruz, M. Chenard, N. Ozerova, A. M. Hitz, H. Wang, S. V. Deshmukh, N. Nazef, A. Harsch, B. Hughes, W. K. Dahlberg, A. A. Szewczak, R. E. Middleton, R. T. Mosley, J. P. Secrist and T. A. Miller, *Bioorg. Med. Chem. Lett.*, 2007, **17**, 5300-5309.
32. E. M. Moir, K. Yoshiizumi, J. Cairns, P. Cowley, M. Ferguson, F. Jeremiah, T. Kiyoi, R. Morphy, J. Tierney, G. Wishart, M. York, J. Baker, J. E. Cottney, A. K. Houghton, P. McPhail, A. Osprey, G. Walker and J. M. Adam, *Bioorg. Med. Chem. Lett.*, **20**, 7327-7330.
33. J. Renaud, S. F. Bischoff, T. Buhl, P. Floersheim, B. Fournier, M. Geiser, C. Halleux, J. Kallen, H. Keller and P. Ramage, *J. Med. Chem.*, 2004, **48**, 364-379.
34. A. Asagarasu, T. Matsui, H. Hayashi, S. Tamaoki, Y. Yamauchi and M. Sato, *Chem. Pharm. Bull.*, 2009, **57**, 34-42.
35. K. Winterfeld, H. Lampke and H. Franzke, *Liebigs Ann. Chem.*, 1965, **685**, 181-186.
36. M. J. Alcón, M. Iglesias, F. Sánchez and I. Viani, *J. Organomet. Chem.*, 2000, **601**, 284-292.
37. V. Bette, A. Mortreux, D. Savoia and J.-F. Carpentier, *Tetrahedron*, 2004, **60**, 2837-2842.
38. F. Denat, R. Tripier, F. Boschetti, E. Espinosa and R. Guilard, *ARKIVOC*, 2006, 212-233.
39. E. Knoevenagel, *Ber. Dtsch. Chem. Ges.*, 1898, **31**, 2596-2619.
40. B. List, *J. Am. Chem. Soc.*, 2000, **122**, 9336-9337.
41. B. List, P. Pojarliev, W. T. Biller and H. J. Martin, *J. Am. Chem. Soc.*, 2002, **124**, 827-833.

42. W. Zhuang, S. Saaby and K. A. Jorgensen, *Angew. Chem. Int. Ed.*, 2004, **43**, 476-4478.
43. W. Notz, F. Tanaka, S. Watanabe, N. S. Chowdari, J. M. Turner, R. Thayumanavan and C. F. Barbas, *J. Org. Chem.*, 2003, **68**, 9624-9634.
44. I. Ibrahem and A. Cordova, *Chem. Commun.,* 2006, **16**, 1760-1762.
45. H. Zhang, S. Mitsumori, N. Utsumi, M. Imai, N. Garcia-Delgado, M. Mifsud, K. Albertshofer, P. H.-Y. Cheong, K. N. Houk, F. Tanaka and C. F. Barbas, *J. Am. Chem. Soc.*, 2007, **130**, 875-886.
46. X.-Y. Huang, H.-J. Wang and J. Shi, *J. Phys. Chem. A*, 2009, **114**, 1068-1081.
47. F. G. Bordwell, *Acc. Chem. Res.*, 1988, **21**, 456-463.
48. A. J. A. Cobb, D. M. Shaw, D. A. Longbottom, J. B. Gold and S. V. Ley, *Org. Biomol. Chem.*, 2005, **3**, 84-96.
49. B. List, *J. Am. Chem. Soc.*, 2000, **122**, 9336-9337.
50. W. Notz, K. Sakthivel, T. Bui, G. Zhong and C. F. Barbas III, *Tetrahedron Lett.*, 2001, **42**, 199-201.
51. S. B. Tsogoeva, *Chem. Commun.*, 2010, **46**, 7662-7669.
52. M. Mauksch, S. B. Tsogoeva, I. M. Martynova and S. Wei, *Angew. Chem. Int. Ed.*, 2007, **46**, 393-396.
53. T. Dwars, E. Paetzold and G. Oehme, *Angew. Chem. Int. Ed.*, 2005, **44**, 7174-7199.
54. M. Amedjkouh and M. Brandberg, *Chem. Commun.*, 2008, **26**, 3043-3045.
55. I. Ibrahem, W. Zou, M. Engqvist, Y. Xu and A. Córdova, *Chem. Eur. J.,* 2005, **11**, 7024-7029.
56. S. Sulzer-Mosse, and A. Alexakis, *Chem. Commun.*, 2007, **30**, 3123-3135.
57. A. Fu, H. Li, H. Si, S. Yuan and Y. Duan, *Tetrahedron: Asymmetry*, 2008, **19**, 2285-2292.
58. E. Veverková, J. Strasserová, R. Sebesta and S. Toma, *Tetrahedron: Asymmetry*, 2009, **21**, 58-61.

4- Experimental

4.1- General methods

4.1.1- Reagents, solvents and reaction conditions

All reagents were of synthetic grade and were used without further purification unless otherwise stated. DCM, diethyl ether, hexane, THF were degassed and dried on a solvent purification system MB SPS-800 MBraun by passage through two drying columns; dry methanol was distilled from calcium hydride and dry isopropanol was obtained from Acros.

All moisture sensitive reactions were carried out under a positive pressure of nitrogen in oven-dried glassware (140 °C). Reactions performed at -78 °C to -10 °C were conducted using solid CO_2 in acetone or a cooling bath apparatus Haake EK 90. Organic extracts were dried over anhydrous $MgSO_4$.

4.1.2- Chromatography and mass spectrometry

Thin-layer chromatography (TLC) was performed using Macherey-Nagel Polygram Sil G/UV_{254} plastic backed plates. Developed plates were analysed under UV light (254 nm) or by the use of staining solutions, alkaline potassium permanganate solution, vanillin solution, ethanolic phosphomolybdic acid solution (PMA), 2,4-dinitrophenylhydrazine solution (2,4-DNP), or ninhydrin spray. Column chromatography was performed using silica gel 60 (40-63 μm) from Apollo Scientific Ltd. For GC-MS analyses, columns Supelco MDN-35 (30 m × 250 μm × 0.25 μm) or Supelco Beta-Dex 120 (30 m × 0.25 mm × 0.25 μm) were set on an Agilent 6890 Series GC coupled to an Agilent 5973 Network MSD and 7683 Serie Autosampler. Supplementary chiral analyses were carried out on a Daicel Chiralcel OD-H column (25 cm × 4.6 mm × 5 μm) using a Varian Prostar HPLC equipped with a Model 410 Autosampler. High-resolution mass spectrometry was performed by Mrs. C. Horsburgh on a Waters LCT electrospray or GCT time-of-flight mass spectrometer.

4.1.3- Nuclear magnetic resonance spectroscopy (NMR)

NMR spectra were acquired on either Bruker Avance 300 (^{1}H at 300.06 MHz, ^{13}C at 75.45 MHz, ^{19}F at 282.34 MHz), or Bruker Avance II 400 (^{1}H at 400.14 MHz, ^{13}C at 100.62 MHz and 19F at 376.41 MHz), or Bruker Avance 500 (^{1}H at 499.90 MHz, ^{13}C at 125 MHz, ^{19}F at 470.33 MHz) spectrometers. Chemical shifts δ are reported in parts per million (ppm) and quoted relative to external standard Me_4Si for ^{1}H and ^{13}C and to external standard $CFCl_3$ for ^{19}F. ^{1}H, ^{13}C and ^{19}F spectroscopic data were assigned on a routine basis by a combination of one- and two- dimensional experiments (COSY, HSQC, HMBC, NOESY).

4.1.4- Other analysis

Melting points were measured using a GallenKamp Griffin MPA350.BM2.5 melting point apparatus and are uncorrected. Optical rotations were determined using a Perkin Elmer Model 341 polarimeter, $[\alpha]_D$ values were measured at 589 nm and given in implied units of 10^{-1}deg.cm^2.g^{-1}. pK_a determinations were conducted on a EDT RE 357 Tx pH meter calibrated at pH 4 and pH 7 with standard buffer solutions. Elemental analyses were carried out by Mrs S. Williamson on a CE instrument EA 1110 CHNS analyser. IR spectra were recorded on a Perkin Elmer Spectrum GX FT-IR system as thin film on PTFE disposable card. Single X-ray diffraction analyses were carried out by Prof. A.M.Z Slawin.

4.2- Protocols

***(E)*-8-Methylethylnon-6-enoate 146 and (*E*)-diethyl dodec-6-enedioate 147**

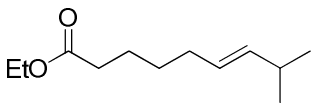

146

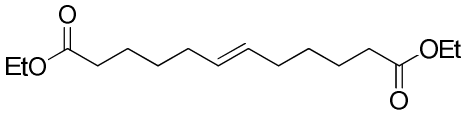

147

*Preparation of **146** and **147**:*

3-Methyl-1-butene (1.5 mL, 12.8 mmol) was added to a solution of ethyl 6-heptenoate (0.12 mL, 0.64 mmol) and Grubbs II catalyst (71 mg, 0.064 mmol) in DCM (6 mL) at 0 °C. The solution was then heated to 40 °C for 20 h. After evaporation of the solvent, the crude product was purified on silica gel, using hexane/acetone (98/2) as eluent to give *(E)*-8-methylethylnon-6-enoate **146** as a clear oil (15 mg, 12%) and (*E*)-diethyl dodec-6-enedioate **147** (28 mg, 22%).

*Data for **146**:*

IR ν_{max} (cm^{-1}): 2921, 2851, 2311, 1730, 1445, 1373. δ_H (300 MHz, $CDCl_3$): 0.95 (6 H, d, *J* 6.8 Hz, 2 × CH_3), 1.24 (3 H, t, *J* 7.1 Hz, CH_3), 1.37 (2 H, t, *J* 7.1 Hz, CH_2), 1.63 (2 H, m, CH_2), 1.98 (2 H, q, *J* 6.5 Hz, CH_2), 2.19 (1 H, dq, *J* 1.2 Hz, *J* 6.7 Hz, CH_2), 2.29 (2 H, t, *J* 7.4 Hz, CH_2), 4.11 (2 H, q, *J* 7.1 Hz, OCH_2), 5.35 (2 H, m, CH=CH). δ_C (75 MHz, $CDCl_3$): 14.3 (CH_3), 22.6 (CH_3), 22.7 (CH_3), 24.5 (CH_2) , 26.9 (CH_2) , 31.0 (CH), 31.6 (2 × CH_2),

60.2 (OCH_2), 125.8 (CH, *Z*, minor isomer), 126.5 (CH, *E*, major isomer), 138.0 (CH, *E*, major isomer), 138.7 (CH, *Z*, minor isomer). ***m/z*** (EI): 198.15 $[M]^+$.

*Data for **147**:*

δ_H (300 MHz, $CDCl_3$): 1.25 (6 H, t, *J* 7.1 Hz, 2 × CH_3), 1.36 (4 H, m, 2 × CH_2), 1.61 (4 H, m, 2 × CH_2), 1.99, (4 H, m, 2 × CH_2), 2.28 (4 H, t, *J* 7.5 Hz, 2 × CH_2), 4.11 (4 H, q, *J* 7.1 Hz, 2 × OCH_2), 5.38 (2 H, m, CH=CH). ***m/z*** (EI): 284.20 $[M]^+$.

Hept-6-enoic acid 165

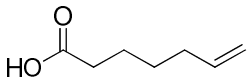

165

A solution of potassium hydroxide (17 mL, 2 M) was added dropwise at 0 °C to a solution of ethyl 6-heptenoate (1.5 mL, 8.55 mmol) in methanol (35 mL). The mixture was stirred for 1 h at 0 °C, then warmed to room temperature and stirred for another 14 h. Methanol was then evaporated under reduced pressure and the residue dissolved in water (50 mL) and acidified to pH = 1 with an aqueous HCl solution (2 M) before extraction into DCM (3 × 50 mL). The combined organic layers were washed with brine (20 mL), dried, filtered and evaporated. The oily product was distilled to give hept-6-enoic acid **165** as a clear oil (1.10 g, 100%).

IR ν_{max} (cm^{-1}): 2921, 2844, 1708, 1022. δ_H (300 MHz, $CDCl_3$): 1.44 (2 H, m, CH_2), 1.65 (2 H, m, CH_2), 2.07 (2 H, m, CH_2), 2.36 (2 H, t, *J* 7.3 Hz, CH_2), 4.98 (2 H, m, CH=C*H*$_2$), 5.79 (1 H, m, C*H*=CH_2). δ_C (75 Hz, $CDCl_3$): 24.1 (CH_2), 28.2 (CH_2), 33.4 (CH_2), 34.6 (CH_2), 114.7 (CH=*C*H_2), 138.0 (*C*H=CH_2). ***m/z*** (EI): 110.07 $[M-H_2O]^+$.

_(S)_-3-Hept-6-enoyl-4-isopropyloxazolidin-2-one 170 and _(S)_-3-hept-6-enoyl-4-isopropyl-5,5-diphenyloxazolidin-2-one 171

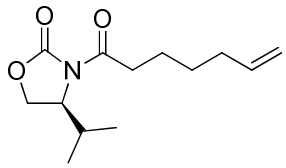

170

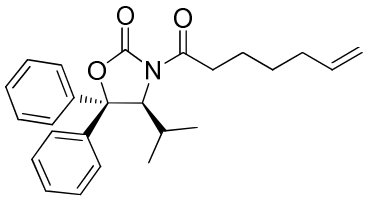

171

*Preparation of **170**:*

Triethylamine (0.91 mL, 6.6 mmol) was added dropwise at 0 °C to a solution of hept-6-enoic acid **165** (807.5 mg, 6.3 mmol) in THF (25.5 mL) and stirred for 15 min at 0 °C before cooling down to -78 °C prior to addition of pivaloyl chloride (0.8 mL, 6.6 mmol). The mixture was stirred for 1 h at -78 °C and then for 15 min at 0 °C. In a separate flask, n-butyllithium (2.5 M, 2.6 mL, 6.3 mmol) was added to a solution of *(S)*-4-isopropyl-2-oxazolidinone (814mg, 6.3 mmol) in THF (20 mL) at -78 °C and the reaction was stirred for 15 min. The resulting solution was added at -78 °C to the white suspension of the mixed anhydride. The mixture was stirred for 30 min, and then an additional hour at 0 °C. The reaction was quenched with saturated ammonium chloride solution (60 mL) and the volatiles were evaporated under vacuum. The aqueous mixture was extracted into DCM (3 × 40 mL)

and the organic layers were washed successively with solutions of 1 M HCl (25 mL) and saturated sodium bicarbonate (25 mL), dried, and concentrated under vacuum. The residue was purified over silica gel (hexane/ethyl acetate 80/20) to afford *(S)*-3-hept-6-enoyl-4-isopropyloxazolidin-2-one **170** as a colourless oil (1.28 g, 86%).

*Preparation of **171**:*

(S)-3-hept-6-enoyl-4-isopropyl-5,5-diphenyloxazolidin-2-one **171** was obtained as a white solid (28 mg, 91%) by the same procedure.

*Data for **170**:*

$[\alpha]_D^{20}$ = +38 (c 1.6, $CHCl_3$). IR ν_{max} (cm^{-1}): 3545, 3382, 3077, 2965, 2876, 1772, 1700, 1385. δ_H (300 MHz , $CDCl_3$): 0.88 (6 H, dd, *J* 7.0 Hz, *J* 13.0 Hz, 2 × CH_3), 1.46 (2 H, m, CH_2), 1.67 (2 H, m, CH_2), 2.08 (2 H, m, CH_2), 2.36 (1 H, m, C*H*$(CH_3)_2$), 2.93 (2 H, m, CH_2), 4.22 (2 H, m, CH and C$H_A$$H_B$), 4.43 (1 H, m, $CH_A$$H_B$), 4.97 (2 H, m, CH=C$H_2$), 5.80 (1 H, m, C*H*=$CH_2$). δ_C (75 Hz, $CDCl_3$): 14.6 (CH_3), 17.9 (CH_3), 23.8 (CH_2), 28.2 (*C*H $(CH_3)_2$), 28.3 (CH_2), 33.4 (CH_2), 35.3 (CH_2), 58.3 (CH), 63.3 (CH_2), 114.6 (CH=*C*H_2), 138.4 (*C*H=CH_2), 173.2 (C=O). ***m/z*** (HRMS) (ES^+): calcd for $C_{13}H_{21}NO_3Na$: 262.1419, found 262.1416 $[M+Na]^+$.

*Data for **171**:*

$[\alpha]_D^{20}$ = -43.6 (c 1.2, $CHCl_3$). **Mp** 87-89 °C. IR ν_{max} (cm^{-1}): 2956, 2363, 1778. δ_H (300 MHz, $CDCl_3$): 0.76 (3 H, d, *J* 6.8 Hz, CH_3), 0.88 (3 H, d, *J* 7.0 Hz, CH_3), 1.32 (3 H, m, CH_2 and C*H*$(CH_3)_2$), 1.55 (2 H, m, CH_2), 1.99 (2 H, m, CH_2), 2.82 (2 H, m, CH_2), 4.94 (2 H, m, CH=CH_2), 5.34 (1 H, m, CH), 5.74 (1 H, m, C*H*=CH_2), 7.33 (8 H, m, Ar H), 7.47 (2 H, m, Ar H). ***m/z*** (HRMS) (ES^+): calcd for $C_{25}H_{29}NO_3Na$: 414.2045, found 414.2037 $[M+Na]^+$.

***(S)*-3-((*(S)*-2-Fluorohept-6-enoyl)-4-isopropyloxazolidin-2-one 172a and (*S*)-3-((*S*)-2-fluorohept-6-enoyl)-4-isopropyl-5,5-diphenyloxazolidin-2-one 173a**

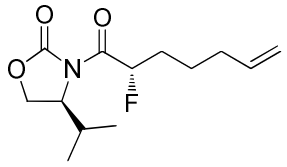

172a

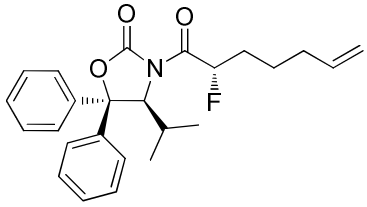

173a

*Preparation of **172a**:*

LiHMDS (1.15 mL, 1 M in hexanes) was added to a solution of **167** (250 mg, 1.05 mmol) in dry THF (5 mL) and stirred for 1 h at -78 °C and then, the reaction was warmed to 0 °C. A solution of NFSI (429 mg, 1.36 mmol) in dry THF (1.7 mL) was added at -78 °C and the mixture stirred for 2 h. Purification over silica gel (neat hexane to hexane/ethyl acetate: 94/6) gave the product as an oil which was precipitated in diethylether to afford the title compound *(S)*-3-((*S)*-2-fluorohept-6-enoyl)-4-isopropyloxazolidin-2-one **172a** as the major component of a mixture of diastereoisomers (82% de), as a white solid (10 mg, 20%).

*Preparation of **173a**:*

The same procedure was applied to obtain the title compound (*S*)-3-((*S*)-2-fluorohept-6-enoyl)-4-isopropyl-5,5-diphenyloxazolidin-2-one **173a** as a mixture of diastereoisomers (38% de) as a white solid (5 mg, 17%).

*Data for **172a**:*

Mp 63-65 °C. IR ν_{max} (cm^{-1}): 2919, 2866, 2336, 1717, 1482, 1388, 1015. δ_H (300 MHz, $CDCl_3$): 0.90 (6 H, dd, *J* 7.0 Hz, *J* 14.1 Hz, 2 × CH_3), 1.64 (2 H, m, CH_2), 1.82 (2 H, dd,

J 7.3 Hz, *J* 14.2 Hz, CH_2), 2.09 (2 H, m, CH_2), 2.48 (1 H, m, C*H*$(CH_3)_2$), 4.34 (3 H, m, CH and CH_2), 4.99 (2 H, m, CH=C*H*$_2$), 5.78 (1 H, ddt, *J* 6.7 Hz, *J* 10.3 Hz, *J* 17.0 Hz, C*H*=CH_2), 5.90 (1 H, ddd, *J* 3.2 Hz, *J* 8.1 Hz, *J* 50.2 Hz, C*H*F). δ_F {^{1}H} (282 MHz, $CDCl_3$): -193.3 (91%, (*S,S*), CHF), -194.9 (9%, (*S,R*), CHF). ***m/z*** (HRMS) (ES^+): calcd for $C_{13}H_{20}NO_3NaF$: 280.1325, found 280.1318 $[M+Na]^+$.

*Data for **173a**:*

Mp 81-83 °C. IR ν_{max} (cm^{-1}): 2920, 2840, 2400, 1743, 1433, 1022. δ_H (300 MHz, $CDCl_3$): 0.68 (3 H, d, *J* 6.6 Hz, CH_3), 0.89 (3 H, d, *J* 6.9 Hz, CH_3), 1.32 (3 H, m, CH_2 and C*H*$(CH_3)_2$), 1.92 (4 H, m, 2 × CH_2), 5.46 (5 H, m, CHF, and CH=CH_2, and CH), 7.40 (10 H, m, Ar H). δ_F {^{1}H} (282 MHz, $CDCl_3$): -193.9 (69%, (*S,S*), CHF), -194.5 (31%, (*S,R*), CHF). ***m/z*** (EI): 409.21 $[M]^+$.

***(S)*-3-*((E)-(S)*-2-Fluoro-8-methylnon 6-enoyl)-isopropyloxazolidin 2-one 174a**

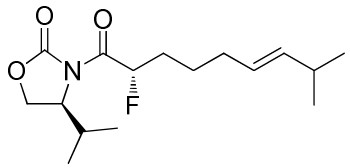

174a

*Preparation by cross-metathesis chain elongation of **172a**:*

3-Methyl-1-butene (0.08 mL, 0.74 mmol) was added at 0 °C to a solution of *(S)*-3-(*(S)*-2-fluorohept-6-enoyl)-4-isopropyloxazolidin-2-one **172a** (9.6 mg, 0.037 mmol) and Grubbs II catalyst (3.1 mg, 0.004 mmol, 0.1 eq) in dry DCM (0.33 mL). The solution was heated to

40 °C for 20 h. After evaporation of the solvent, the crude product was purified by flash chromatography, using hexane/ethyl acetate (98/2) as eluent to provide *(S)*-3-*((E)-(S)*-2-fluoro-8-methylnon 6-enoyl)-isopropyloxazolidin 2-one **174a** as an oil (6 mg, 54%).

*Preparation by fluorination of the N-acyl oxazolidinone **189**:*

LiHMDS (14.9 mL, 1 M in hexanes) was added to a solution of *(S)*-4-isopropyl 3-(*(E)*-8-methylnon-6-enoyl)oxazolidin 2-one **189** (3.80 g, 13.5 mmol) in THF (65 mL) and was stirred for 1 h at -78 °C. The reaction was then warmed up to 0 °C for 20 min. A solution of NFSI (5.50 g, 17.5 mmol) in dry THF (20 mL) was then added at -78 °C and the mixture stirred for 3 h. The reaction was quenched with saturated ammonium chloride solution (200 mL) and the product was extracted into diethyl ether (3 × 200 mL). Purification over silica gel (hexane/DCM 6/4 then 5/5) gave *(S)*-3-*((E)-(S)*-2-fluoro-8-methylnon 6-enoyl)-isopropyloxazolidin 2-one **174a** as an oil (765 mg, 20%).

*Data for **174a**:*

IR $\boldsymbol{\nu_{max}}$ (cm^{-1}): 3269, 2959, 1829, 1745, 1603, 1412, 1084. $\boldsymbol{\delta_H}$ (300 MHz, $CDCl_3$): 0.91 (6 H, dd, *J* 7.0 Hz, *J* 14.1 Hz, 2 × CH_3), 0.95 (6 H, d, *J* 6.7 Hz, 2 × CH_3), 1.59 (2 H, dd, *J* 7.4 Hz, *J* 14.6 Hz, CH_2), 1.81 (2 H, m, CH_2), 2.02 (2 H, m, CH_2), 2.22 (1 H, m, CH), 2.49 (1 H, m, CH), 4.30 (2 H, m, CH_2), 4.42 (1 H, m, CH), 5.34 (2 H, m, CH=CH), 5.91 (1 H, ddd, *J* 3.5 Hz, *J* 7.8 Hz, *J* 50.2 Hz, CHF). $\boldsymbol{\delta_C}$ (75 MHz, $CDCl_3$): 14.3 (CH_3), 17.9 (CH_3), 22.6 (2 × CH_3), 24.8 (CH_2), 27.9 (CH), 31.0 (CH), 32.0 (2 × CH_2), 58.6 (CH), 64.1 (CH_2), 89.1 (d, *J* 178.6 Hz, CHF), 126.0 (*C*H=CH), 138.5 (CH=*C*H), 153.5 (C=O), 169.9 (d, *J* 22.8 Hz, C=O). $\boldsymbol{\delta_F}$ {^{1}H} (282 MHz, $CDCl_3$): -193.2 (*S*, *S*, *E*). ***m/z*** (HRMS) (CI^+): calcd for $C_{16}H_{27}NO_3F$: 300.1975, found 300.1977 $[M+H]^+$.

Isobutyltriphenylphosphonium iodide 177

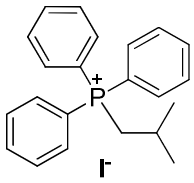

177

1-Iodo-2-methylpropane (0.30 mL, 2.67 mmol) was added to a solution of triphenylphosphine (700 mg, 2.67 mmol) in toluene (0.30 mL). The reaction was then heated under reflux (110-115 °C) for 20 h. After cooling, the precipitate formed was filtered and the filter cake was washed with diethyl ether (3 × 6 mL) and dried under high vacuum to give isobutyltriphenylphosphonium iodide **177** as a white powder (980 mg, 82%).

Mp 201 °C (lit.[1] Mp: 198-201 °C). IR $\boldsymbol{\nu_{max}}$ (cm^{-1}): 3020, 2951, 1584, 1482, 1435, 1191, 1139, 1109. $\boldsymbol{\delta_H}$ (300 MHz, $CDCl_3$): 1.03 (6 H, d, *J* 6.9 Hz, 2 × CH_3), 2.10 (1 H, m, CH), 3.65 (2 H, dd, *J* 12.9 Hz, *J* 6.9 Hz, CH_2), 7.85 (15 H, m, Ar H). $\boldsymbol{\delta_C}$ (75 Hz, $CDC1_3$): 24.5 (CH), 24.9 (2 × CH_3), 31.2 (CH_2), 118.9 (Ar C IV),130.1 (Ar CH), 133.5 (Ar CH), 134.8 (Ar CH). Analytical data identical to literature[1]

Ethyl 6-oxohexanoate 180

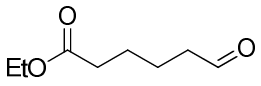

180

Sodium acetate (150 mg, 1.10 mmol) and pyridinium chlorochromate (1.07 g, 4.96 mmol) were added to a solution of ethyl 6-hydroxylhexanoate (0.54 mL, 3.3 mmol) in DCM (10 mL). After stirring at room temperature for 3 h, the mixture was diluted with diethyl ether (100 mL) and filtered through a plug of Florisil®. The filtrate was evaporated under vacuum to obtain the title compound ethyl 6-oxohexanoate **180** as a clear oil (470 mg, 90%).

$\boldsymbol{\delta_H}$ (300 MHz, $CDCl_3$): 1.19 (3 H, t, *J* 7.1 Hz , CH_3), 1.58 (4 H, m, 2 × CH_2), 2.27 (2 H, m, CH_2), 2.42 (2 H, dt, *J* 1.5 Hz, *J* 6.8 Hz, CH_2), 4.06 (2 H, dq, *J* 0.9 Hz, *J* 7.1 Hz, OCH_2), 9.67 (1 H, t, *J* 1.5 Hz, CHO). $\boldsymbol{\delta_C}$ (75 Hz, $CDCl_3$): 14.6 (CH_3), 21.3 (CH_2), 24.2 (CH_2), 33.6 (CH_2), 43.5 (CH_2), 51.7 (OCH_2), 173.6 (COOEt), 201.8 (CHO). ***m/z*** (EI): 158.08 $[M]^+$.

(5-Carboxy-pentyl)-triphenylphosphonium salt 185[2]

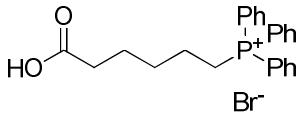

185

A mixture of 6-bromohexanoic acid (25.8 g, 0.13 mmol) and triphenylphosphine (34.7 g, 0.13 mmol) was heated to 145 °C for 4 h. The cooled reaction mixture was triturated in chloroform and precipitated into diethyl ether. The resultant precipitate was filtered, washed with diethyl ether and dried under vacuum to give (5-carboxy-pentyl)-triphenylphosphonium salt **185** as a solid (57.8 g, 97%).

Mp 195-199 °C (lit[2] 200-203 °C). IR $\boldsymbol{\nu_{max}}$ (cm^{-1}): 3392, 3053, 2990, 2597, 2215, 1991, 1723, 1586, 1438, 1337. $\boldsymbol{\delta_H}$ (300 MHz, $CDCl_3$): 1.69 (6 H, m, 3 × CH_2), 2.42 (2 H, t, *J* 6.8 Hz, CH_2), 3.64 (2 H, m, CH_2), 7.75 (15 H, m, Ar H). $\boldsymbol{\delta_C}$ (75 MHz, $CDCl_3$): 21.7 (CH_2), 22.9 (CH_2), 23.9 (CH_2), 29.6 (CH_2), 34.3 (CH_2), 118.1 (d, *J* 86.2 Hz, 3 × Ar C IV), 130.5 (d, *J* 12.5 Hz, 6 × Ar CH), 133.6 (d, *J* 10 Hz, 6 × Ar CH), 135.1 (d, *J* 2.7 Hz, 3 × Ar CH), 175.7 (COOH).

***(Z)*-8-methylnon 6-enoic acid 187b**

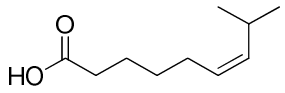

187b

A mixture of (5-carboxy-pentyl)-triphenylphosphonium salt **185** (20.0 g, 43.7 mmol) and iso-butylaldehyde (4.8 mL, 52.5 mmol) in DMF (90 mL) was added to a suspension of potassium *tert*-butylate (10.0 g, 89.6 mmol) in DMF (110 mL) and the reaction stirred at 0 °C for 15 min. After vigorous stirring for 15 h at rt, the resulting slurry was poured into ice-water (13 mL) and the precipitated triphenylphosphine oxide was removed by filtration. The filtrate was washed with toluene (2 × 30 mL) and acidified with HCl (2 M) and then, the aqueous layer was extracted into diethyl ether (4 × 20 mL), washed with brine (4 × 15 mL), and dried over magnesium sulfate. The product was distilled at 110 °C (10-13 mbar) to obtain *(Z)*-8-methylnon 6-enoic acid **187b** (3.51 g, 47%, *Z/E* ratio: 9/1) as a colourless oil.

IR $\boldsymbol{\nu_{max}}$ (cm^{-1}): 2957 (br), 2670, 1709 (br), 1464, 1164. $\boldsymbol{\delta_H}$ (300 MHz, $CDCl_3$): 0.93 (6 H, d, *J* 6.7 Hz, 2 × CH_3), 1.40 (2 H, dt, *J* 7.5 Hz, *J* 14.9 Hz, CH_2), 1.65 (2 H, dt, *J* 7.3 Hz, *J* 15.7 Hz, CH_2), 2.06 (2 H, m, CH_2), 2.22 (1 H, m, CH, (*E*) minor isomer), 2.35 (2 H, t, *J* 7.3 Hz, CH_2), 2.57 (1 H, m, CH, (*Z*) major isomer), 5.20 (2 H, m, CH=CH, (*Z*) major isomer), 5.34(2 H, m, CH=CH, (*E*) minor isomer) , 11.99 (1 H, br s, COOH). $\boldsymbol{\delta_C}$ (75 MHz, $CDCl_3$): 23.1 (2 × CH_3), 24.2 (CH_2), 26.4 (CH), 26.9 (CH_2), 26.8 (CH_2), 29.2 (CH_2), 34.0 (CH_2), 126.5 (*C*H=CH), 138.0 (CH=*C*H), 180.5 (COOH). ***m/z*** (EI): 170.13 $[M]^+$.

***(E)*-8-Methylnon 6-enoic acid 187a**

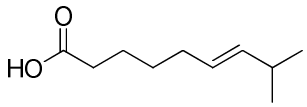

187a

Solutions of sodium nitrate (1.5 mL, 2 M) and nitric acid (1.0 mL, 6 M) were added to *(Z)*-8-methylnon 6-enoic acid **21** (3.51 g, 20.6 mmol). The mixture was stirred vigorously and heated to 75 °C for 1 h. The cooled reaction mixture was diluted into diethyl ether (20 mL), washed successively with water (20 mL) and saturated brine (3 × 12 mL), dried over magnesium sulfate, and evaporated under vacuum to provide *(E)*-8-methylnon 6-enoic acid **187a** as a colourless oil (3.3 g, 95%, *E/Z* ratio: 86/14).

δ_H (300 MHz, $CDCl_3$): 0.95 (6 H, d, *J* 6.7 Hz, 2 × CH_3), 1.39 (2 H, dt, *J* 7.8 Hz, *J* 15.1 Hz, CH_2), 1.63 (2 H, dt, *J* 7.1 Hz, *J* 14.9 Hz, CH_2), 1.99 (2 H, dd, *J* 6.7 Hz, *J* 13.0 Hz, CH_2), 2.22 (1 H, m, CH, (*E*) major isomer), 2.35 (2 H, t, *J* 7.4 Hz, CH_2), 2.57 (1 H, m, CH, (*Z*) minor isomer), 5.20 (2 H, m, CH=CH, (*Z*) minor isomer), 5.34 (2 H, m, CH=CH, (*E*) major isomer), 11.72 (1 H, br s, COOH). **δ_C** (75 Hz, $CDCl_3$): 22.6 (2 × CH_3), 24.1 (CH_2), 29.0 (CH_2), 31.0 (CH), 32.1 (CH_2), 34.0 (CH_2), 126.3 (*C*H=CH), 138.1 (CH=*C*H), 180.6 (COOH). ***m/z*** (EI): 170.13 $[M]^+$.

***(S)*-4-*Iso*propyl 3-((*E*)-8-methylnon-6-enoyl)oxazolidin 2-one 189**

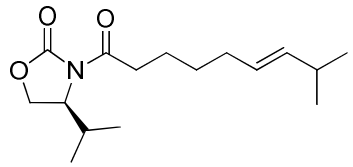

189

Triethylamine (2.9 mL, 20.6 mmol) was added dropwise at 0 °C to a solution of **187a** (3.30 g, 19.6 mmol) in THF (80 mL) and stirred for 15 min at 0 °C before cooling down to -78 °C for addition of pivaloyl chloride (2.5 mL, 20.6 mmol). The mixture was stirred for 1 h at -78 °C and then 15 min at 0 °C. In a separate flask, *n*-butyllithium (7.8 mL ,19.6 mmol, 2.5 M) was added to a solution of *(S)*-4-*iso*propyl-2-oxazolidinone (2.50 g, 19.6 mmol) in THF (60 mL) at -78 °C and the reaction was stirred for 15 min. The resultant solution was added at -78 °C to the white suspension of the mixed anhydride. The mixture was stirred for 30 min, then for 1 additional hour at 0 °C. The reaction mixture was quenched with saturated ammonium chloride solution and the volatiles were evaporated under vacuum. This aqueous mixture was extracted into DCM (3 × 15 mL) and the organic layers were washed successively with solutions of HCl (1 M) and saturated sodium bicarbonate, dried over magnesium sulfate, and concentrated under vacuum. The residue was purified over silica gel (hexane/DCM 7/3 then neat ethyl acetate) to afford *(S)*-4-*iso*propyl 3-(*(E)*-8-methylnon-6-enoyl)oxazolidin 2-one **189** (3.9 g, 71%) as a clear oil.

δ_H (300 MHz, $CDCl_3$): 0.89 (6 H, dd, *J* 7.0 Hz, *J* 12.9 Hz, 2 × CH_3), 0.95 (6 H, d, *J* 6.7 Hz, 2 × CH_3), 1.41 (2 H, dt, *J* 7.7 Hz, *J* 15.3 Hz, CH_2), 1.66 (2 H, m, CH_2), 2.00 (2 H, dd, *J* 6.6 Hz,

J 12.8 Hz, CH_2), 2.21 (1 H, m, CH), 2.37 (1 H, m, CH), 2.91 (2 H, m, CH_2), 4.22 (2 H, m, CH_2), 4.43 (1 H, dt, *J* 3.5 Hz, *J* 7.5 Hz, CH), 5.35 (2 H, m, CH=CH). δ_C (75 MHz, $CDCl_3$): 14.6 (CH_3), 18.0 (CH_3), 22.6 (2 × CH_3), 23.9 (CH_2), 28.3 (CH), 29.0 (CH_2), 31.0 (CH), 32.2 (CH_2), 35.4 (CH_2), 58.3 (CH_2), 63.3 (CH), 126.5 (*C*H=CH), 140.0 (CH=*C*H), 154.0 (C=O), 173.3 (C=O). ν_{max} (cm^{-1}): 2919, 1776, 1700, 1389. ***m/z*** (HRMS) (ES+): calcd for $C_{16}H_{27}NO_3Na$: 304.1889, found 304.1887 $[M+Na]^+$.

(*S*)-4-isopropyl-3-((*R*)-3-phenylbutanoyl)oxazolidin-2-one 198

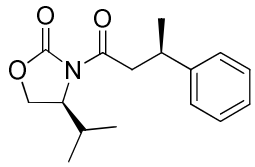

198

Triethylamine (0.47 mL, 3.42 mmol) was added dropwise at 0 °C to a solution of (*R*)-3-phenylbutyric acid (0.50 mL, 3.25 mmol) in THF (13 mL) and stirred for 15 min at 0 °C before cooling down to -78 °C for addition of pivaloyl chloride (0.42 mL, 3.42 mmol). The mixture was stirred for 1 h at -78 °C, then 15 min at 0 °C. In a separate flask, *n*-butyllithium (1.3 mL ,3.26 mmol, 2.5 M) was added to a solution of *(S)*-4-*iso*propyl-2-oxazolidinone (421 mg, 3.26 mmol) in THF (10 mL) at -78 °C and the reaction was stirred for 15 min. The resultant solution was added at -78 °C to the white suspension of the mixed anhydride. The mixture was stirred for 30 min, then for 1 h further at 0 °C. The reaction mixture was quenched with a saturated aqueous solution of ammonium chloride and the volatiles were evaporated under vacuum. This aqueous mixture was extracted into DCM (3 × 10 mL) and

the organic layers were washed successively with solutions of HCl (1 M) and saturated sodium bicarbonate, dried over magnesium sulfate, and concentrated under vacuum. The residue was purified on silica gel (hexane/DCM 1/1 then neat ethyl acetate) to afford (*S*)-4-*iso*propyl-3-((*R*)-3-phenylbutanoyl)oxazolidin-2-one **198** (679 mg, 76%) as a white wax.

$[\alpha]_D^{20}$ = -12 (c 1.1, MeOH). IR ν_{max} **(cm^{-1})**: 2956, 2844, 2333, 1772, 1693, 1493, 1364. δ_H (300 MHz, $CDCl_3$): 0.65 (3 H, d, *J* 6.9 Hz, CH_3), 0.81 (3 H, d, *J* 7.0 Hz, CH_3), 1.32 (3 H, d, *J* 6.9 Hz), 2.16 (1 H, m, CH), 2.99 (1 H, dd, *J* 7.2 Hz, *J* 15.6 Hz, CH_AH_B), 3.38 (1 H, m, CH), 3.51 (1 H, dd, *J* 7.2 Hz, *J* 15.6 Hz, CH_AH_B), 4.13 (1 H, dd, *J* 3.2 Hz, *J* 9.1 Hz, OCH_2), 4.21 (1 H, t, *J* 9.0 Hz, OCH_2), 4.38 (1 H, dt, *J* 3.4 Hz, *J* 8.2 Hz, NCH), 7.19 (5 H, m, Ar H). δ_C (75 MHz, $CDCl_3$): 14.3 (CH_3), 17.8 (CH_3), 21.9 (CH_3), 28.2 ($CH(CH_3)_2$), 36.2 (CH), 43.0 (CH_2), 58.2 (NCH), 63.1 (OCH_2), 126.3 (Ar CH), 126.9 (2 × Ar CH), 128.4 (2 × Ar CH), 145.6 (Ar C IV), 153.9 (O-C=O), 171.9 (N-C=O). ***m/z*** (EI): 275.15 $[M]^+$.

(*S*)-3-((*2S*,*3S*)-2-fluoro-3-phenylbutanoyl)-4-isopropyloxazolidin-2-one 199

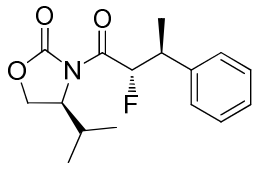

199

LiHMDS (2.42 mL, 1 M in hexanes) was added at -78 °C to a solution of (*S*)-4-*iso*propyl-3-((*R*)-3-phenylbutanoyl)oxazolidin-2-one **198** (612 mg, 2.2 mmol) in THF (10 mL) and was

stirred for 1 h at -78 °C. The reaction mixture was then warmed up to 0 °C for 20 min. A solution of NFSI (902 mg, 2.8 mmol) in THF (4 mL) was added at -78 °C and the mixture stirred for 3 h. The mixture was quenched with a saturated ammonium chloride solution (35 mL) and was extracted into diethylether (3 x 40 mL). The gathered organic layers were dried over magnesium sulfate and concentrated under vacuum to afford an oil which was precipitated in diethylether to give (*S*)-3-((*2S*,*3S*)-2-fluoro-3-phenylbutanoyl)-4-*iso*propyloxazolidin-2-one **199** as a solid (327 mg, 51%).

δ_H (300 MHz, $CDCl_3$): 0.87 (6 H, t, *J* 6.7 Hz, 2 × CH_3), 1.46 (3 H, dd, *J* 0.8 Hz, *J* 7.2 Hz, CH_3), 2.42 (1 H, m, C*H*(CH_3)$_2$), 3.41 (1 H, dm, *J* 26.8 Hz, CHF-C*H*), 4.18 (2 H, m, O-CH_2), 4.25 (1 H, m, N-C*H*), 6.17 (1 H, dd, *J* 4.9 Hz, *J* 48.8 Hz, C*H*F), 7.28 (5 H, m, Ar H). **δ_C** (75 MHz, $CDCl_3$): 14.4 (CH_3), 17.2 (d, *J* 6.2 Hz, CHF-CH-*C*H_3), 17.9 (CH_3), 28.1 (*C*H(CH_3)$_2$), 42.1 (d, *J* 20.7 Hz, CHF-*C*H-CH_3), 58.9 (N*C*H), 64.2 (O-*C*H_2), 91.4 (d, *J* 184 Hz, *C*HF), 127.4 (Ar CH), 128.1 (2 × Ar CH), 128.4 (2 × Ar CH), 139.9 (Ar C), 153.7 (O-*C*=O), 168.3 (N-C=O). **δ_F** {^{1}H} (282 MHz, $CDCl_3$): -196.4 (3 %, (*S*,*R*,*S*)), -198.2 (97 %, (*S*,*S*,*S*)). **δ_F** (282 MHz, $CDCl_3$): -196.4 (dd, *J* 22.7 Hz, *J* 49.1 Hz, (*S*,*R*,*S*)), -198.2 (dd, *J* 26.8 Hz, *J* 48.8 Hz, (*S*,*S*,*S*)). **ν_{max} (cm^{-1})**: 2956, 2844, 1771, 1710, 1485, 1449, 1386. ***m/z*** (HRMS) (ES$^+$): calcd for $C_{16}H_{20}NO_3NaF$: 316.1325, found 316.1326 [M+Na]$^+$.

(*2S*,*3S*)-2-fluoro-*N*-methoxy-*N*-methyl-3-phenylbutanamide 201

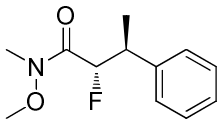

201

A solution of trimethylaluminium (0.28 mL, 2 M, 0.56 mmol,) was added slowly at 0 °C to a suspension of *N,O*-dimethylhydroxylamine hydrochloride (55.2 mg, 0.57 mmol) in DCM (0.8 mL). The reaction mixture was stirred at 0 °C until gas emission ceased (10 min), then the solution was cooled to -10 °C prior addition of (*S*)-3-((*2S*,*3S*)-2-fluoro-3-phenylbutanoyl)-4-*iso*propyloxazolidin-2-one **199** (55 mg, 0.19 mmol). After 1 h, the reaction was warmed up to 0 °C until completion of the reaction (2 h). The mixture was poured with vigorous stirring into an ice-cold mixture of HCl (5 mL, 0.5 M) and DCM (2.5 mL) and extracted into DCM. The combined organic layers were washed with brine, dried over magnesium sulfate, filtered and concentrated under vacuum. The crude product was purified on silica gel (hexane/ethylacetate 7/3) to give (*2S*,*3S*)-2-fluoro-*N*-methoxy-*N*-methyl-3-phenylbutanamide **201** as a colourless oil (43 mg, 100%).

$\boldsymbol{\delta_H}$ (300 MHz, $CDCl_3$): 1.30 (3 H, d, *J* 7.2 Hz, CH_3), 3.18 (3 H, s, CH_3), 3.41 (1 H, m, CH), 3.68 (3 H, s, OCH_3), 5.24 (1 H, dd, *J* 7.6 Hz, *J* 48.9 Hz, CHF), 7.26 (5 H, m, Ar H). $\boldsymbol{\delta_C}$ (75 MHz, $CDCl_3$): 16.6 (d, *J* 7.0 Hz, CH_3), 32.1 (NCH_3), 40.5 (d, *J* 20.6 Hz, CH), 61.6 (OCH_3), 90.7 (d, *J* 179.7 Hz, CHF), 127.1 (Ar CH), 128.0 (2 × Ar CH), 128.4 (2 × Ar CH), 141.1 (Ar C IV). $\boldsymbol{\delta_F}$ (282 MHz, $CDCl_3$): -189. 99 (98%, dd, *J* 18.4 Hz, *J* 48.9 Hz, (*S,S*)), -196.50 (2%). ***m/z*** (EI): 225.12 $[M]^+$.

(2*S*,3*S*)-2-fluoro-3-phenylbutanoic acid 203

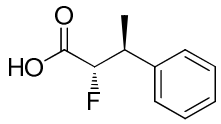

203

Hydrogen peroxide (0.9 mL, 35%) was added at 0 °C to a solution of (*2S*,*3S*)-2-fluoro-*N*-methoxy-*N*-methyl-3-phenylbutanamide **201** (150 mg, 0.51 mmol) dissolved in a mixture of THF and water (1:1, 6 mL). Lithium hydroxide (43 mg, 1.00 mmol) was added, and the reaction was stirred for 1 h at 0 °C. The solvent was evaporated and the aqueous solution (pH= 12) was acidified with HCl (2 M) to pH = 1 and was extracted into DCM (4 × 12 mL). The organic layer was dried over magnesium sulphate and concentrated to give (2*S*,3*S*)-2-fluoro-3-phenylbutanoic acid **203** as a white powder (85 mg, 92%).

Mp: 81 °C. $[\alpha]_D^{20} = +26.4$ (c 1.4, MeOH). IR ν_{max} **(cm^{-1})**: 3031, 2976, 1951, 1735, 1603, 1495, 1383, 1039. δ_H (300 MHz, $CDCl_3$): 1.49 (3 H, d, *J* 7.3 Hz, CH_3), 3.38 (1 H, ddq, *J* 4.1 Hz, *J* 7.3 Hz, *J* 29.8 Hz, CH), 5.06 (1 H, dd, *J* 4.1 Hz, *J* 48.8 Hz, CHF), 7.29 (5 H, Ar H). δ_C (75 MHz, $CDCl_3$): (17.4, d, *J* 4.8 Hz, CH_3), 42.1 (d, *J* 19.7 Hz, CH), 92.1 (d, *J* 190.4 Hz, CHF), 127.82 (Ar CH), 128.1 (2 × Ar CH), 128.5 (2 × Ar CH). δ_F {1H} (282 MHz, $CDCl_3$): -196.78 (CHF). δ_F (282 MHz, $CDCl_3$): -196.78 (dd, *J* 29.7 Hz, *J* 48.3 Hz, CHF). ***m/z*** (HRMS) (ES^-): calcd for $C_{10}H_{10}O_2F$: 181.0665, found 181.0663 $[M-H]^-$.

***(E)-(S)*-2-Fluoro 8-methylnon 6-enoic acid 204**

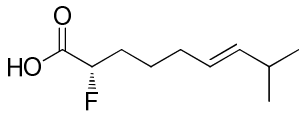

204

Hydrogen peroxide (4.5 mL, 35%) was added at 0 °C to a solution of **174a** (756 mg, 2.55 mmol) dissolved in a mixture of THF and water (1:1, 35 mL). Then, lithium hydroxide (214 mg, 5.10 mmol) was added, and the reaction was stirred for 1 h at 0 °C. THF was evaporated under vacuum and the aqueous solution (pH = 12) was acidified with HCl (2 M) to pH = 1 and was extracted into DCM (4 × 70 mL). The organic layer was dried over magnesium sulfate and concentrated to give *(E)-(S)*-2-fluoro 8-methylnon 6-enoic acid **204** as an oil (456 mg, 95%)

IR $\boldsymbol{\nu_{max}}$ **(cm^{-1})**: 2958, 2644, 1734, 1460, 1362. $\boldsymbol{\delta_H}$ (300 MHz, $CDCl_3$): 0.95 (6 H, d, *J* 6.8 Hz, 2 × CH_3), 1.56 (2 H, dd, *J* 7.3 Hz, *J* 14.9 Hz, CH_2), 1.89 (2 H, m, CH_2), 2.03 (2 H, m, CH_2), 2.23 (1 H, m, C*H*$(CH_3)_2$), 4.94 (1 H, ddd, *J* 4.6 Hz, *J* 7.2 Hz, *J* 49.2 Hz, CHF), 5.29 (1 H, dt, *J* 5.8 Hz, *J* 15.4 Hz, C*H*=CH), 5.40 (1 H, dd, CH=C*H*), 8.47 (1 H, br s, 8.47, COOH). $\boldsymbol{\delta_C}$ (75 MHz, $CDCl_3$): 22.6 (2 × CH_3), 24.2 (CH_2), 31.0 (*C*H$(CH_3)_2$), 31.7 (CH_2), 31.8 (CH_2), 88.4 (d, *J* 184.3 Hz, CHF), 125.7 (CH_2-*C*H=CH), 138.7 (CH=*C*H-CH), 175.1 (d, *J* 24.3 Hz, COOH). $\boldsymbol{\delta_F}$ {1H} (282 MHz, $CDCl_3$): -192.67 (10%, (*S,Z*)) , -192.73 (90%, (*S,E*)). ***m/z*** (EI):188.12 $[M]^+$.

***(E)-(S)*-Fluoro 8-methylnon 6-enoic acid (*(S)*-1-phenylethyl) amide (*S,S,E*)-206 and *(E)-(S)*-Fluoro-8-methylnon 6-enoic acid (*(R/S)*-1-phenylethyl) amide 206**

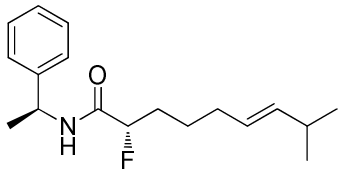

206a

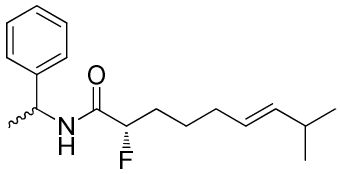

206

*Preparation of **206a**:*

HOBt (38 mg, 0.28 mmol) and EDC (54 mg, 0.28 mmol) were added at 0 °C to a solution of *(E)-(S)*-2-fluoro 8-methylnon 6-enoic acid **204** (50 mg, 0.27 mmol,) in DMF (4 mL). After 15 min stirring, *(S)*-(-)-1-phenylethylamine (32 mg, 2.66 mmol) and triethylamine (37 µL, 0.27 mmol) were added, and the mixture was stirred for 14 h at rt. The mixture was then diluted in brine, and extracted into ethyl acetate. The organic layers were washed successively with a citric acid solution (10%), saturated brine, dried over magnesium sulfate, and concentrated under vacuum to give *(E)-(S)*-fluoro 8-methylnon 6-enoic acid (*(S)*-1-phenylethyl) amide **206a** as a white solid (27 mg, 34%).

*Preparation of **206**:*

(E)-(S)-Fluoro-8-methylnon 6-enoic acid (*(R/S)*-1-phenylethyl) amide **206** was obtained by reacting *(R/S)*-(+/-)-1-phenylethylamine (32 mg, 2.66 mmol) on **204** according the same procedure. **206** was obtained as a solid (29 mg, 37%).

*Data for **206a**:*

Mp 71 °C. δ_H (300 MHz, $CDCl_3$): 0.96 (6 H, d, *J* 6.7 Hz, 2 × CH_3), 1.53 (3 H, d, *J* 6.9 Hz, CH_3), 1.54 (2 H, m, CH_2), 1.84 (2 H, m, CH_2), 2.03 (2 H, m, CH_2), 2.23 (1 H, m, C*H*$(CH_3)_2$),

4.87 (1 H, ddd, *J* 3.7 Hz, *J* 7.6 Hz, *J* 49.9 Hz, CHF), 5.17 (1 H, m, NC*H*), 5.32 (1 H, dt, *J* 5.6 Hz, *J* 15.3 Hz, C*H*=CH), 5.41 (1 H, dd, *J* 5.8 Hz, *J* 15.4 Hz, CH=C*H*), 6.54 (1 H, br s, NH), 7.33 (5 H, m, Ar H). δ_C (75 MHz, $CDCl_3$): 21.8 (CH_3), 22.6 (2 × CH3), 24.3 (CH_2), 31.0 (*C*H(CH_3)$_2$), 32.0 (2 × CH_2), 48.4 (NH*C*H), 92.1 (d, *J* 185.3 Hz, CHF), 126.0 (*C*H=CH), 126.2 (2 × Ar CH), 127.6 (Ar CH), 128.8 (2 × Ar CH), 138.5 (CH=*C*H). δ_F {1H} (282 MHz, $CDCl_3$): -190.48 (91%, (*S,S,E*)), -190.57 (9%, (*S,S,Z*)). δ_F (282 MHz, $CDCl_3$): -190.48 (dddd, *J* 4.7 Hz, *J* 26.3 Hz, *J* 30.0 Hz, *J* 54.9 Hz, (*S,S,E*)). ***m/z*** (HRMS) (CI^+): calcd for $C_{18}H_{27}NOF$: 292.2077, found 292.2076 $[M+H]^+$.

*Data for **206**:*

δ_F {1H} (282 MHz, $CDCl_3$): -190.44 (37%, (*R,S,E*)), -190.47 (6%, (*R,S,Z*)), -190.51 (51%, (*S,S,E*)), -190.60 (6%, (*S,S,Z*)). ***m/z*** (EI): 291.20 $[M]^+$.

4-Hydroxy 3-methoxybenzaldehyde oxime 207

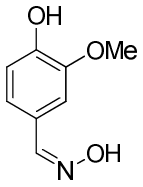

207

A solution of hydroxylammonium hydrochloride (99.4 mg, 1.43 mmol) and sodium acetate (176.9 mg, 1.30 mmol) in water (0.4 mL) was added to a solution of vanillin (200 mg, 1.30 mmol) in water (0.7 mL). The reaction was stirred at 50 °C for 5 min and then the mixture was heated at 80 °C for 2-3 h. After cooling, the product was extracted into DCM

(3 × 10 mL) and the organic layers were washed with a saturated bine solution, dried over magnesium sulfate and evaporated under vacuum, to obtain 4-hydroxy 3-methoxy-benzaldehyde oxime **207** as a white solid (170 mg, 78%).

Mp 125 °C (lit. Mp 118-120 °C). IR ν_{max} **(cm^{-1})**: 3448, 3283, 2996, 1641, 1596, 1520, 1455, 1428. δ_H (300 MHz, $(CD_3)_2CO$)): 2.95 (1 H, br s, NOH), 3.85 (3 H, s, OCH_3), 6.83 (1 H, d, *J* 8.1 Hz, Ar H), 7.02 (1 H, dd, *J* 1.9 Hz, *J* 8.1 Hz, Ar H), 7.24 (1 H, d, *J* 1.8 Hz, Ar H), 8.00 (1 H, s, CH=N), 8.36 (1 H, br s, Ar OH). δ_C (75 MHz, (CD_3OD)): 56.3 (Ar OCH_3), 109.8 (Ar CH), 116.2 (Ar CH), 122.5 (Ar CH), 150.5 (*C*H=N).). ***m/z*** (HRMS) (TOF CI^+): found 168.0664, calcd for $C_8H_{10}NO_3$: 168.0661 $[M+H]^+$.

4-Hydroxy-3-methoxybenzylamine hydrochloride 118

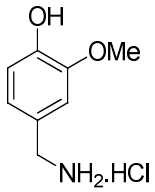

118

A solution of 4-hydroxy 3-methoxybenzaldehyde oxime **207** (1.00 g, 5.98 mmol) in ethanol (110 mL) and concentrated HCl (4.5 mL, 37%) was treated with hydrogen gas at atmospheric pressure in presence of Pd/C 10% (220 mg) for 4 h. The mixture was then filtered through a plug of Celite and the filtrate was concentrated to dryness to provide 4-hydroxy 3-methoxy-benzylamine hydrochloride **118** as a yellow fluffy solid (1.11 g, 98%).

Mp 225 °C (lit. 221-223 °C). IR ν_{max} **(cm^{-1})**: 3311, 3096, 2873, 2679, 2357, 1601, 1527, 1508, 1464, 1452, 1383, 1365, 1281. δ_H (300 MHz, $(CD_3)_2SO$): 3.77 (3 H, s, OCH_3), 3.89 (2 H, dt, *J* 2.5 Hz, *J* 5.6 Hz, CH_2), 6.78 (1 H, d, *J* 8.0 Hz, Ar H), 6.84 (1 H, dd, *J* 2.0 Hz, *J* 8.1 Hz, Ar H), 7.10 (1 H, d, *J* 1.9 Hz, Ar H), 8.15 (3 H, br s, NH_3), 9.18 (1 H, br s, Ar OH). δ_C (75 MHz, (CD_3OD)): 44.4 (NCH_2), 56.5 (OCH_3), 113.6 (Ar CH), 116.7 (Ar CH), 123.2 (Ar CH).). ***m/z*** (ES^+): 152.96 $[M\text{-}HCl\text{-}H]^+$, ($ES^-$): 188.99 $[M\text{-}H]^-$.

(*S*)-α-Fluorocapsaicin (*S*)-97a

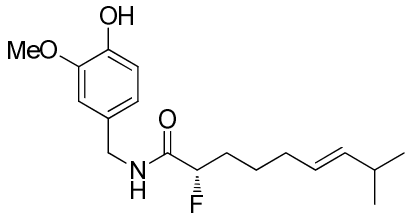

97a

HOBt (37.7 mg, 0.28 mmol) and EDC (53.5 mg, 0.28 mmol) were added at 0 °C to a solution of *(E)-(S)*-2-fluoro 8-methylnon 6-enoic acid **204** (50 mg, 0.27 mmol) in DMF. After 15 min stirring at 0 °C, vanillylamine **118** (50.4 mg, 2.66 mmol) and triethylamine (37 µL, 0.27 mmol) were added, and the mixture was stirred overnight at 20 °C. The mixture was then diluted with brine, and extracted into ethylacetate. The organic layer was washed successively with a citric acid solution (10%), saturated brine, dried over magnesium sulfate, concentrated under vacuum to afford (*S*)-α-fluorocapsaicin **97a** as a white solid (28 mg, 32%).

Mp: 78-79 °C. $[\alpha]_D^{20}$ = -20.6 (c 0.9, MeOH). IR ν_{max} **(cm^{-1})**: 2911, 1654. δ_H (300 MHz, $CDCl_3$): 0.94 (6 H, d, *J* 6.7 Hz, 2 × CH_3), 1.50 (2 H, m, CH_2), 1.82 (2 H, m, CH_2), 2.01 (2 H, dd, *J* 7.4 Hz, *J* 13.3 Hz, CH_2), 2.22 (1 H, dd, *J* 6.7 Hz, *J* 13.4 Hz, CH), 3.87 (3 H, s, OCH_3), 4.39 (1 H, dd, *J* 2.8 Hz, *J* 5.7 Hz, CH_2NH), 4.92 (1 H, ddd, *J* 3.7 Hz, *J* 7.5 Hz, *J* 49.8 Hz, CHF), 5.29 (1 H, dt, *J* 5.7 Hz, *J* 15.3 Hz, C*H*=CH), 5.38 (1 H, dd, *J* 5.9 Hz; *J* 15.4 Hz, CH=C*H*), 5.73 (1 H, br s, Ar OH), 6.60 (1 H, br s, NH), 6.77 (2 H, m, 2 x Ar H), 6.86 (1 H, d, *J* 7.9 Hz, Ar H). δ_C (75 MHz, $CDCl_3$): 22.6 (2 × CH_3), 24.3 (CH_2), 30.9 (C*H*(CH_3)$_2$), 32.0 (2 × CH_2), 42.9 (N-CH_2), 55.9 (OCH_3), 92.0 (d, *J* 185.4 Hz, CHF), 110.5 (Ar CH), 114.4 (Ar CH), 120.8 (Ar CH), 125.9 (*C*H=CH), 129.5 (Ar C IV), 138.5 (CH=*C*H), 145.2 (Ar OH), 146.7 (Ar OMe), 170.0 (C=O). δ_F {^{1}H} (282 MHz, $CDCl_3$): -190.73 (90%, (*S,E*)), -190.76 (10%, (*S,Z*)). δ_F (282 MHz, $CDCl_3$): -190.73 (dddd, *J* 4.5 Hz, *J* 26.3 Hz, *J* 30.3 Hz, *J* 55.2 Hz, (*S,E*)).). ***m/z*** (HRMS) (ES$^+$): found 346.1793, calcd for $C_{18}H_{26}NO_3FNa$: 346.1794 [M+Na]$^+$.

***(S)*-3-(*(S)*-Fluoro 8-methylnonanoyl)-4-isopropyloxazolidin 2-one (*S*)-208**

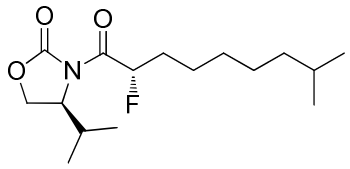

208

Preparation by hydrogenation of the double-bond:

A solution of *(S)*-3-*((E)-(S)*-2-fluoro-8-methylnon 6-enoyl)-isopropyloxazolidin 2-one **174a** (123 mg, 0.41 mmol) and 10% Pd/C (100 mg) in ethanol (20 mL) was treated with hydrogen

gas at atmospheric pressure for 4 h. The catalyst was then removed by filtration through a plug of Celite and the solvent was evaporated under reduced pressure to obtain unpure *(S)*-3-(*(S)*-fluoro 8-methylnonanoyl)-4-isopropyloxazolidin 2-one **208** as an oil (69 mg, 56%).

Preparation by fluorination of the N-acyl oxazolidinone:

LiHMDS (3.2 mL, 1 M in hexanes) was added to a solution of *(S)*-4-*iso*propyl 3-(*(E)*-8-methylnon-6-enoyl)oxazolidin 2-one **189** (700 mg, 2.47 mmol) in THF (12 mL) and stirred for 1 h at -78 °C. A solution of NFSI (860 mg, 2.7 mmol) in THF (4 mL) was then added and the mixture was stirred for 3 h. The mixture was quenched with a saturated solution of ammonium chloride (30 mL) and extracted into diethylether (3 × 40 mL), and concentrated under vacuum to provide *(S)*-3-(*(S)*-fluoro 8-methylnonanoyl)-4-isopropyloxazolidin 2-one **208** (984 mg, 130%) as a not pure waxy product. This product was used further on without any purification.

δ_H (300 MHz, CD_3OD): 0.88 (6 H, dd, *J* 1.5 Hz, *J* 5.6 Hz, 2 × CH_3), 0.93 (6 H, dd, *J* 1.5 Hz, *J* 7.1 Hz, 2 × CH_3), 1.18 (2 H, m, CH_2), 1.32 (6 H, m, 3 × CH_2), 1.53 (2 H, m, CH_2), 1.77 (1 H, m, $CH_2CH(CH_3)_2$), 2.43 (1 H, m, $CHCH(CH_3)_2$), 4.41 (1 H, m, NCH), 4.42 (2 H, m, OCH_2), 5.89 (1 H, ddd, *J* 2.8 Hz, *J* 8.6 Hz, *J* 50.4 Hz, CHF). **δ_C** (75 MHz, $CDCl_3$): 14.8 (CH_3), 18.0 (CH_3), 23.1 (2 × CH_3), 28.3 (CH_2), 29.6 (CH), 30.4 (CH), 30.8 (2 × CH_2), 60.2 (NCH), 65.3 (OCH_2), 90.5 (d, *J* 177.1 Hz, CHF). **δ_F** $\{^1H\}$ (282 MHz, CD_3OD): -194.28 (2%, (*S,R*)), -194.49 (98%, (*S,S*)). **δ_F** (282 MHz, CD_3OD) -194.46 (ddd, *J* 21.2 Hz, *J* 34.4 Hz, *J* 55.6 Hz). ***m/z*** (HRMS) (CI^+): found 302.2134, calcd for $C_{16}H_{29}NO_3F$: 302.2131 $[M+H]^+$.

8-Methylnonanoic acid 209

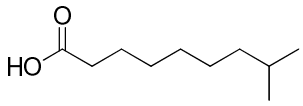

209

A solution of *(Z)*-8-methylnon 6-enoic acid **187b** (800 mg, 0.47 mmol) and 10% Pd/C (1.15 g) in ethanol (120 mL) was treated with hydrogen gas at atmospheric pressure for 4 h. The catalyst was removed by filtration through a plug of Celite and the solvent was evaporated under vacuum. The crude product was distilled to provide 8-methylnonanoic acid **209** as colourless oil (769 mg, 95%).

δ_H (300 MHz, $CDCl_3$): 0.85 (6 H, d, *J* 6.6 Hz, 2 × CH_3), 1.15 (2 H, m, CH_2), 1.28 (6 H, m, 3 × CH_2), 1.50 (1 H, m, CH), 1.63 (2 H, m, CH_2), 2.34 (2 H, t, *J* 7.4 Hz, CH_2), 11.37 (1 H, br s, COOH). δ_C (75 Hz, $CDCl_3$): 22.6 (2 × CH_3), 24.7 (CH_2), 27.2 (CH_2), 27.9 (CH), 29.1 (CH_2), 29.5 (CH), 34.1 (CH_2), 38.9 (CH_2), 180.6 (COOH). ***m/z*** (EI): 172.15.

***(S)*-4-Isopropyl 3-(8-methylnonanoyl) oxazolidin 2-one (*S*)-210**

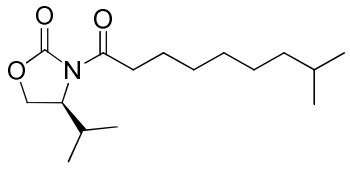

210

Triethylamine (0.65 mL, 4.68 mmol) was added dropwise at 0 °C to a solution of 8-methylnonanoic acid **209** (769 mg, 4.46 mmol) in THF (18 mL). This reaction was stirred for 15 min at 0 °C and then cooled to -78 °C prior addition of pivaloyl chloride (0.40 mL, 3.29 mmol). The mixture was then stirred for 1 h at -78 °C and then 15 min at 0 °C. In a separate flask, *n*-butyllithium (1.8 mL, 2.5 M, 4.46 mmol) was added to a solution of *(S)*-4-*iso*propyl-2-oxazolidinone (577 mg, 4.46 mmol) in THF (10 mL) at -78 °C and the reaction was stirred for 15 min. The resultant solution was added at -78 °C to the white suspension of the mixed anhydride. The mixture was stirred for 30 min, and then 1 h further at 0 °C. The reaction was quenched with ammonium chloride and the volatiles were evaporated under vacuum. This aqueous mixture was extracted into DCM and the organic layers were washed successively with solutions of HCl (1 M) and saturated sodium bicarbonate, dried over magnesium sulfate, concentrated under vacuum to afford *(S)*-4-isopropyl 3-(8-methyl-nonanoyl) oxazolidin 2-one **210** (1.21 g, 96%) as a waxy product. The compound was used further without any purification.

IR $\boldsymbol{\nu_{max}}$ **(cm^{-1})**: 3542, 3377, 2932, 2871, 1780, 1704, 1466, 1387, 1301. $\boldsymbol{\delta_H}$ (300 MHz, $CDCl_3$): 0.83 (6 H, d, *J* 6.6 Hz, 2 × CH_3), 0.88 (6 H, dd, *J* 7.0 Hz, *J* 12.9 Hz, 2 × CH_3), 1.14 (2 H, m, CH_2), 1.28 (6 H, m, 3 × CH_2), 1.49 (1 H, m, $CH_2CH(CH_3)_2$), 1.63 (2 H, m, CH_2), 2.35 (2 H, m, CH_2), 2.79 (1 H, m, $CHCH(CH_3)_2$), 2.89 (2 H, m, CH_2), 4.25 (1 H, m, NC*H*), 4.31 (2 H, m, OCH_2). $\boldsymbol{\delta_C}$ (75 MHz, $CDCl_3$): 14.6 (CH_3), 17.9 (CH_3), 22.6 (2 × CH_3), 24.4 (CH_2), 27.2 (CH_2), 27.2 (CH), 27.9 (CH), 29.1 (CH_2), 29.6 (CH_2), 35.5 (CH_2), 38.9 (CH_2), 58.3 (CH), 63.2 (CH_2), 154.0 (*C*OO), 173.4 (N*C*=O). ***m/z*** (HRMS) (ES^+): found 306.2048, calcd for $C_{16}H_{29}NO_3Na$: 306.2045 $[M+Na]^+$.

***(S)*-2-Fluoro 8-methylnonanoic acid (*S*)-211**

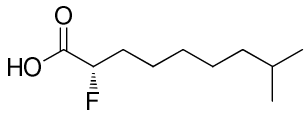

211

Hydrogen peroxide (0.47 mL, 35 %) was added at 0 °C to a solution of *(S)*-3-(*(S)*-fluoro 8-methylnonanoyl)-4-isopropyloxazolidin 2-one **208** (400 mg, 1.33 mmol) dissolved in a mixture of THF and water (1:1, 35 mL). Lithium hydroxide (112 mg, 2.66 mmol) was then added, and the reaction was stirred for 1 h at 0 °C. The solvent was evaporated and the aqueous solution (pH = 12) was extracted into DCM (3 × 30 mL) for recovery of the chiral auxiliary. The aqueous solution was acidified with HCl (2 M) until pH = 1 and was extracted into DCM (4 × 50 mL). The organic layer was dried over magnesium sulfate and concentrated to give *(S)*-2-fluoro 8-methylnonanoic acid **211** (190 mg, 75 %) as a colourless oil.

$[\alpha]_D^{20}$ = -7.6 (c 1.2, MeOH). IR ν_{max} **(cm^{-1})**: 3255, 2958, 2920, 2849, 1737, 1446, 1281. δ_H (300 MHz, $CDCl_3$): 0.86 (6 H, d, *J* 6.6 Hz, 2 × CH_3), 1.17 (2 H, m, CH_2), 1.31 (6 H, m, 3 × CH_2), 1.51 (2 H, m, CH_2), 1.94 (1 H, m, $CH(CH_3)_2$), 4.97 (1 H, ddd, *J* 4.9 Hz, *J* 6.9 Hz, *J* 49.2 Hz, CHF). δ_C (75 MHz, $CDCl_3$): 22.6 (2 × CH3), 24.4 (CH_2), 27.0 (CH_2), 27.9 (CH), 29.3 (CH_2), 32.2 (d, *J* 20.8 Hz, CH_2), 38.8 (CH_2), 88.5 (d, *J* 184.3 Hz, CHF), 174.9 (d, *J* 24.1 Hz, COOH). δ_F {^{1}H} (282 MHz, $CDCl_3$): -189.2 (1%), -192.5 (98%, (*S*)), -192.7 (1%). δ_F (282 MHz, $CDCl_3$): -192.5 (dt, *J* 25.7 Hz, *J* 50.6 Hz). ***m/z*** (HRMS) (ES^-): found 189.1294, calcd for $C_{10}H_{18}O_2F$: 189.1279 $[M-H]^-$.

***N*-(4-hydroxy-3-methoxybenzyl)-4-methylpentanamide 223**

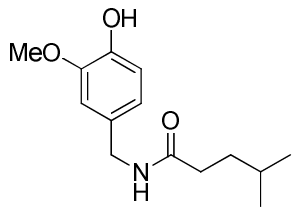

223

HOBt (245 mg, 1.81 mmol) and EDC (347 mg, 1.81 mmol) were added at 0 °C to a solution of 4-methyl valeric acid (0.22 mL, 1.72 mmol) in DMF (4 mL). After 30 min at rt, vanillylamine hydrochloride **118** (343 mg, 1.81 mmol) and Et_3N (0.25 mL, 1.81 mmol) were added, and the mixture was stirred overnight at rt. The mixture was then diluted with brine, and extracted into ethyl acetate. The organic layer was washed successively with a citric acid solution (10%), saturated brine, dried over magnesium sulfate, and concentrated under vacuum. Purification on silica gel (hexane/ethylacetate 1/1) provided *N*-(4-hydroxy-3-methoxybenzyl)-4-methylpentanamide **213** as a white solid (186 mg, 43% yield).

Mp 63-64 °C. δ_H (300 MHz, $CDCl_3$): 0.90 (6 H, d, *J* 6.3 Hz, 2 × CH_3), 1.55 (3 H, m, CH and CH_2), 2.20 (2 H, m, CH_2), 3.88 (3 H, s, OCH_3), 4.35 (2 H, d, *J* 5.6 Hz, NCH_2), 5.68 (1 H, br s, Ar OH), 6.62 (1 H, br s, NH), 6.77 (2 H, dt, *J* 1.9 Hz, *J* 10.1 Hz, 2 Ar H), 6.86 (2 H, d, *J* 8.0 Hz, Ar-H). δ_C (75 MHz, $CDCl_3$): 22.2 (2 × CH_3), 27.5 (CH), 32.8 (CH_2), 34.8 (CH_2), 42.8 (NCH_2), 55.9 (OCH_3), 110.6 (Ar CH), 114.4 (Ar CH), 120.9 (Ar CH), 129.5 (Ar C IV), 145.2 (Ar OH), 146.7 (Ar OMe). ***m/z*** (EI): 251.15 $[M]^+$.

(*S*)-2-fluoro-4-methylpentanoic acid (*S*)-227a, (*R*)-2-fluoro-4-methylpentanoic acid (*R*)-227b and (*R,S*)-2-fluoro-4-methylpentanoic acid (*R,S*)-227

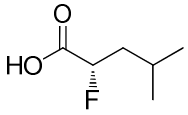

227a

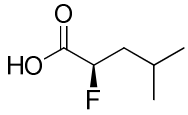

227b

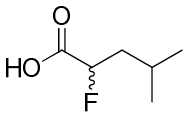

227

*Preparation of **227a** by deaminative fluorination:*

Sodium nitrite (284 mg, 4.10 mmol) was cautiously added to a solution of L-leucine (300 mg, 2.29 mmol) in HF/Py [70:30] (3.45 mL) cooled down at -78 °C. After 2 h at this temperature, the mixture was allowed to warm up to 0 °C and stirred for another 2 h. Then the mixture was stirred for 6 h at rt before quenching with a solution of sodium carbonate (5 %). The solution was extracted with diethyl ether (3 × 10 mL) and the organic layers washed with brine (10 mL), dried over magnesium sulfate and concentrated under vacuum. The product was distilled on kugelrohr (60 °C, 0.1 mBar) to provide (*S*)-2-fluoro-4-methylpentanoic acid **227a** as a clear oil (138 mg, 45%).

*Preparation of **227b** by deaminative fluorination:*

(*R*)-2-fluoro-4-methylpentanoic acid **227b** was obtained as a clear oil (461 mg, 43%) according the procedure described above.

*Preparation of **227** by deaminative fluorination:*

(*R,S*)-2-fluoro-4-methylpentanoic acid **227** was obtained as a clear oil (492 mg, 48%) with the same method.

*Preparation of **227a** by oxidation:*

(*S*)-2-fluoro-4-methylpentanal **235a** (591 mg, 5.00 mmol) was dissolved in a mixture acetone/water (30 mL, 5:1) and treated dropwise with CrO_3 (1 M in 30 % H_2SO_4) for 30 min. After addition of water (50 mL), the aqueous phase was extracted into diethyl ether (3 × 30 mL). The organic layer was dried over magnesium sulfate and concentrated under vacuum to give (*S*)-**227a** as pale yellow oil (656 mg, 98%).

*Preparation of **227b** by oxidation:*

The method described above was used to obtained (*R*)-**227b** as pale yellow oil (499 mg, 97%).

*Data for **227a**:*

IR ν_{max} **(cm^{-1})**: 3489, 2960, 1979, 1734, 1469. δ_H (300 MHz, $CDCl_3$): 0.98 (6 H, d, *J* 6.2 Hz, 2 × CH_3), 1.64 (1 H, m, C*H*(CH_3)$_2$), 1.88 (2 H, m, CH_2), 4.99 (1 H, ddd, *J* 3.3 Hz, *J* 9.2 Hz, *J* 49.6 Hz, CHF), 10.22 (1 H, br s, COOH). δ_C (75 MHz, $CDCl_3$): 21.5 (CH_3), 22.9 (CH_3), 24.4 (CH), 40.8 (d, *J* 20.8 Hz, CH_2), 87.3 (d, *J* 184.2 Hz, CHF), 175.9 (d, *J* 24.2 Hz, COOH). δ_F {^{1}H} (282 MHz, $CDCl_3$): -191.49, CHF). δ_F (282 MHz, $CDCl_3$): -191.49 (ddd, *J* 18.0 Hz, *J* 34.5 Hz, *J* 50.2 Hz, (*S*), CHF). ***m/z*** (HRMS) (ES^-): found 133.0667, calcd for $C_6H_{10}O_2F$: 133.0665 $[M-H]^-$.

*Data for **227b**:*

All spectroscopic data are identical to (*S*)-**227a**

*Data for **227**:*

Analytical data identical to (*R*)**-** and (*S*)-**227**

***(S)*-2-fluoro-*N*-(4-hydroxy-3-methoxybenzyl)-4-methylpentanamide (*S*)-99a and *(R)*-2-fluoro-*N*-(4-hydroxy-3-methoxybenzyl)-4-methylpentanamide (*R*)-99b**

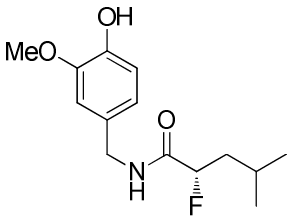

99a

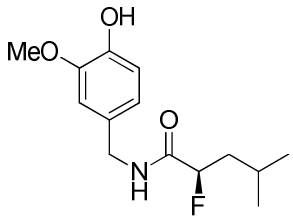

99b

*Preparation of **99a** by acyl fluoride mediated amide-coupling:*

2-Fluorocarboxylic acid (*S*)-**227a** (268 mg, 2.00 mmol) was dissolved in DCM (20 mL) under an N_2 atmosphere, cooled down to 0 °C prior addition of DIEA (523 µL, 3.00 mmol) and Deoxofluor (1.0 mL, 2.40 mmol). After stirring for 30 min, vanillylamine **118** (417 mg, 2.20 mmol) in DCM (5 mL) was added slowly. This mixture was warmed up to rt and stirred for 6-8 h. The mixture was then diluted in DCM (30 mL), and consecutively washed with an aqueous saturated sodium bicarbonate solution (5 mL), water (5 mL) and brine (5 mL). The organic layers were dried over magnesium sulfate, filtered, concentrated under vacuum. Purification on silica gel (hexane/ethyl acetate 1:1) allowed recovering *(S)*-2-fluoro-*N*-(4-hydroxy-3-methoxybenzyl)-4-methylpentanamide (*S*)-**99a** as a clear oil, which recrystallised after trituration in diethyl ether (121 mg, 24%).

*Preparation of **99b** by amide-coupling:*

HOBt (130 mg, 1.02 mmol) and EDC (196 mg, 1.02 mmol) were added at 0 °C to a solution of (*R*)-**227b** (130 mg, 0.97 mmol) in DMF (2 mL). After 30 min at rt, vanillylamine **118** (193 mg, 1.02 mmol) and Et_3N (0.14 mL, 1.02 mmol) were added, the mixture was stirred overnight at rt. The mixture was diluted in brine, and extracted into ethyl acetate. The organic

layer was washed successively with citric acid (10%), brine, dried over magnesium sulfate, and concentrated under vacuum to recover *(R)*-2-fluoro-*N*-(4-hydroxy-3-methoxybenzyl)-4-methylpentanamide (*R*)-**99b** (44 mg, 17% yield).

*Preparation of **99b** by acyl fluoride mediated amide-coupling:*

(R)-2-fluoro-*N*-(4-hydroxy-3-methoxybenzyl)-4-methylpentanamide **99b** (151 mg, 28% yield) was obtained according the procedure described above.

*Preparation of **99a** by amide-coupling:*

(S)-2-fluoro-*N*-(4-hydroxy-3-methoxybenzyl)-4-methylpentanamide **99a** was prepared according the same procedure (28 mg, 11%)

*Data for **99a**:*

Mp 52 °C. $[\alpha]_D^{20}$ = -12.8 (c 1.2, MeOH). IR ν_{max} **(cm^{-1})**: 3325, 3064, 2956, 2495, 1770, 1644, 1446, 1367, 1277. δ_H (300 MHz, $CDCl_3$): 0.97 (6 H, dd, *J* 1.3 Hz, *J* 6.4 Hz, 2 × CH_3), 1.76 (1 H, m, CH), 1.87 (2 H, m, CH_2), 3.88 (3 H, s, OCH_3), 4.39 (2 H, d, *J* 5.8 Hz, NCH_2), 4.96 (1 H, ddd, *J* 2.7 Hz, *J* 9.4 Hz, *J* 50.1 Hz, CHF), 5.67 (1 H, br s, Ar OH), 6.58 (1 H, br s, NH), 6.78 (2 H, m, 2 Ar H), 6.88 (2 H, d, *J* 7.8 Hz, Ar H). δ_C (75 MHz, $CDCl_3$): 21.6 (CH_3), 23.1 (CH_3), 24.6 (CH), 41.2 (d, *J* 19.6 Hz, CH_2), 43.0 (NCH_2), 55.9 (OCH_3), 90.8 (d, *J* 185.2 Hz, CHF), 110.6 (Ar CH), 114.4 (Ar CH), 120.9 (Ar CH), 129.5 (Ar C), 145.2 (Ar OH), 146.7 (Ar OMe). δ_F {^{1}H} (282 MHz, $CDCl_3$): -188.92. δ_F (282 MHz, $CDCl_3$): -188.91 (dddd, *J* 4.7 Hz, *J* 20.7 Hz, *J* 37.3 Hz, *J* 50.3 Hz, CHF). ***m/z*** (HRMS) (CI^+): found 270.1499, calcd for $C_{14}H_{21}NO_3F$: 270.1505 $[M+H]^+$.

*Data for **99b**:* Analytical data are identical to (*S*)-**99a** except: $[\alpha]_D^{20}$ = + 12.8 (c 1.2, MeOH).

(*S*)-2-fluoro-4-methyl-*N*-((*S*)-1-phenylethyl)pentanamide (*S,S*)-228a, (*R*)-2-fluoro-4-methyl-*N*-((S)-1-phenylethyl)pentanamide (*R,S*)-228b and (*R,S*)-2-fluoro-4-methyl-*N*-((S)-1-phenylethyl)pentanamide (*S,R/S*)-228

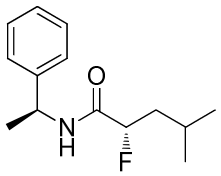

228a

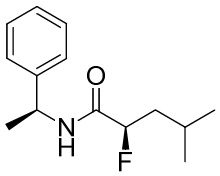

228b

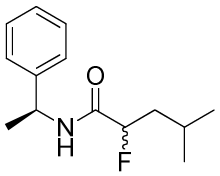

228

*Preparation of **228a**:*

HOBt (318 mg, 2.35mmol) and EDC (451 mg, 2.35 mmol) were added at 0 °C to a solution of 2-fluorocarboxylic acid (*S*)-**227a** (300 mg, 2.24 mmol) in DMF (5 mL). After 30 min at rt, (*S*)-(-)-1-phenylethylamine (0.30 mL, 2.35 mmol) was added, and the mixture was stirred overnight at rt. The mixture was then diluted with brine, and extracted into ethyl acetate. The organic layer was washed successively with a citric acid solution (10 %), brine, dried over magnesium sulfate, and concentrated under vacuum to recover (*S*)-2-fluoro-4-methyl-*N*-((*S*)-1-phenylethyl)pentanamide (*S*)-**228** (155 mg, 29% yield).

*Preparation of **228b**:*

(*R*)-2-fluoro-4-methyl-*N*-((S)-1-phenylethyl)pentanamide **228b** was synthesised according the same procedure (14 mg, 21% yield).

*Preparation of **228**:*

The procedure described above allowed to obtain **(***R,S*)-2-fluoro-4-methyl-*N*-((S)-1-phenylethyl)pentanamide **228** (23 mg, 35% yield).

*Data for **228a**:*

IR ν_{max} **(cm^{-1})**: 2920, 2823, 1789, 1689, 1020. δ_H (300 MHz, $CDCl_3$): 0.91 (6 H, dd, *J* 1.7 Hz, *J* 6.5 Hz), 1.46 (3 H, d, *J* 6.9 Hz, CHC*H*$_3$), 1.69 (1 H, m, C*H*$(CH_3)_2$), 1.81 (2 H, m, CH_2), 4.83 (1 H, ddd, *J* 3.0 Hz, *J* 9.3 Hz, *J* 50.2 Hz, CHF), 5.08 (1 H, m, C*H*CH_3), 6.47 (1 H, br s, NH), 7.26 (5 H, m, Ar H). δ_C (75 MHz, $CDCl_3$): 21.6 (CH_3), 21.7 (CH_3), 23.1 (NHCHC*H*$_3$), 24.6 (d, *J* 1.5 Hz, CH), 41.2 (d, *J* 19.5 Hz, CH_2), 48.3 (NCH), 91.1 (d, *J* 185.1 Hz, CHF), 126.2 (2 × Ar CH), 127.6 (Ar CH), 128.7 (2 × Ar CH). δ_F {^{1}H} (282 MHz, $CDCl_3$): -188.62 (2%, CHF, (*S*,*R*)), -188.75 (98%, CHF, (*S*,*S*)). ***m/z*** (HRMS) (CI^+): found 238.1605, calcd for $C_{14}H_{21}NOF$: 238.1607 $[M+H]^+$.

*Data for **228b**:*

Spectroscopic data are identical to (*S,S*)-**228a**, except: δ_F {^{1}H} (282 MHz, $CDCl_3$): -188.62 (96%, (*S*,*R*), CHF), -188.75 (4%, (*S*,*S*), CHF)

*Data for **228**:*

Spectroscopic data are identical to (*R*)- and (*S*)-**228**, except: δ_F {^{1}H} (282 MHz, $CDCl_3$): -188.62 (50%, (*S*,*R*)), -188.75 (50%, (*S*,*S*)).

(*R*)-2-fluorooctanal 230b and (*S*,*E*)-*N*-((*R*)-2-fluorooctylidene)-1-methoxypropan-2-amine 232b

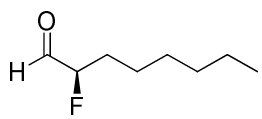

230b

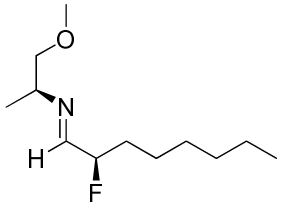

232b

*Preparation of **230b** and **232b**:*

To a solution of NFSI (8 mmol, 2.5g) and (*R*)-5-benzyl-2,2,3-trimethylimidazolin-4-one dichloroacetic salt (0.8 mmol, 277 mg) in a mixture THF/^{i}Propanol (30 mL, 9:1) cooled down to -30 °C, was added octanaldehyde (4 mmol, 400 mg). After 10 hours at -15 °C, the solution was filtered over a pad of silica gel and eluted with diethyl ether. After concentration under vacuum, an aliquot of (*R*)-2-fluorooctanal **230b** was derivatised with (*S*)-1-methoxy-2-propylamine and the ee of (*S*,*E*)-*N*-((*R*)-2-fluorooctylidene)-1-methoxypropan-2-amine **232b** (92 % ee) was determined by ^{19}F spectroscopy.

*Data for **230b**:*

IR $\boldsymbol{\nu_{max}}$ **(cm^{-1})**: 3445, 2932, 1977, 1820, 1742, 1581, 1367.$\boldsymbol{\delta_H}$ (300 MHz, $CDCl_3$): 0.88 (3 H, s, CH_3), 1.25 (8 H, br s, 4 × CH_2), 4.75 (1 H, ddd, *J* 4.9 Hz, *J* 8.2 Hz, *J* 49.4 Hz, CHF), 9.77 (1 H, dd, *J* 0.8 Hz, *J* 6.3 Hz, CHO). $\boldsymbol{\delta_C}$ (75 MHz, $CDCl_3$): 22.5 (CH_2), 24.2 (CH_2), 28.8 (CH_2), 29.7 (CH_2), 31.5 (CH_2), 95.1 (d, *J* 179.0 Hz, CHF), 200.4 (d, *J* 34.6 Hz, CHO). $\boldsymbol{\delta_F}$ {^{1}H} (282 MHz, $CDCl_3$): -200.10. $\boldsymbol{\delta_F}$ (282 MHz, $CDCl_3$): -200.10 (dddd, *J* 6.4 Hz, *J* 23.3 Hz, *J* 27.9 Hz, *J* 49.7 Hz, CHF). ***m/z*** (EI): 146.1 $[M]^+$.

*Data for **232b**:*

$\boldsymbol{\delta_C}$ (75 MHz, $CDCl_3$): 13.7 (CH_3), 18.3 (CH_3), 22.2 (CH_2), 23.9 (d, *J* 4.0 Hz, CH_2), 28.7 (CH_2), 31.3 (CH_2), 32.8 (d, *J* 21.3 Hz, CH_2), 48.9 (d, *J* 8.9 Hz, OCH_2CHN), 64.8 (OCH_3), 75.4 (OCH_2), 92.7 (d, *J* 167.9 Hz, CHF), 162.3 (d, *J* 29.5 Hz, (*E*)-CH=N). $\boldsymbol{\delta_F}$ {^{1}H} (282 MHz, $CDCl_3$): -188.62 (4 %, (*S*,*E*,*S*), CHF), -189.38 (96 %, (*S*,*E*,*R*), CHF). $\boldsymbol{\delta_F}$ (282 MHz, $CDCl_3$): -189.38 (dddd, *J* 8.5 Hz, *J* 20.1 Hz, *J* 28.4 Hz, *J* 48.7 Hz, (*S,E,R*), CHF). ***m/z*** (EI): 217.2 $[M]^+$.

(*R*)-2-fluoro-4-methylpentanal (*R*)-235b, (*S*)-2-fluoro-4-methylpentanal (*S*)-235a, (*S,E*)-*N*-((*R*)-2-fluoro-4-methylpentylidene)-1-methoxypropan-2-amine 235b' and (*S,E*)-*N*-((*S*)-2-fluoro-4-methylpentylidene)-1-methoxypropan-2-amine 235a'

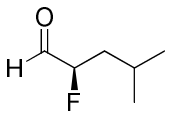

235b

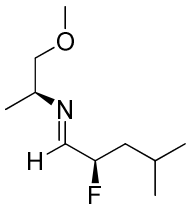

235b'

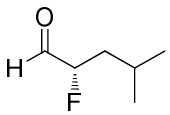

235a

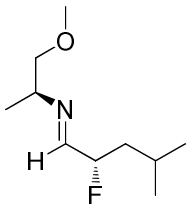

235a'

*Preparation of **235b**:*

To a solution of NFSI (8.00 mmol, 2.50 g) and (*R*)-5-benzyl-2,2,3-trimethylimidazolin-4-one dichloroacetic salt (0.8 mmol, 277 mg) in THF/^{i}Propanol (30 mL, 9:1) cooled down to -30 °C, was added 4-methylpentanal (4.00 mmol, 400 mg). After 10 hours at -15 °C, the solution was filtered over a pad of silica gel and eluted with diethyl ether to give (*R*)-2-fluoro-4-methylpentanal **235b**.

*Preparation of **235a**:*

(*S*)-2-fluoro-4-methylpentanal **235a** was obtained according the same procedure.

*Preparation of **235b'**:*

After concentration under vacuum, an aliquot of the residue was derivatized with (*S*)-1-methoxy-2-propylamine and the ee of (*S,E*)-*N*-((*R*)-2-fluoro-4-methylpentylidene)-1-methoxypropan-2-amine **235b'** (90% ee) was determined by ^{19}F spectroscopy.

*Preparation of **235a'**:*

(*S,E*)-*N*-((*S*)-2-fluoro-4-methylpentylidene)-1-methoxypropan-2-amine **235a'** was obtained according the same procedure as **235b'** (88% ee).

*Data for **235b**:*

δ_F {^{1}H} (282 MHz, $CDCl_3$): -199.48 (CHF)

*Data for **235a**:*

δ_F {^{1}H} (282 MHz, $CDCl_3$): -199.41 (CHF)

*Data for **235b'**:*

δ_F {^{1}H} (282 MHz, $CDCl_3$): -188.90 (5%, (*S*,*S*)), -189.38 (95%, (*S*,*R*)).

δ_F (282 MHz, $CDCl_3$): -189.38 (ddq, *J* 7.7 Hz, *J* 34.6 Hz, *J* 49.6 Hz, CHF).

*Data for **235a'**:*

δ_F {^{1}H} (282 MHz, $CDCl_3$): -188.93 (94%, (*S*,*S*)), -189.39 (6%, (*S*,*R*)).

δ_F (282 MHz, $CDCl_3$): -189.38 (ddq, *J* 7.7 Hz, *J* 34.6 Hz, *J* 49.6 Hz, CHF).

(*R*)-2-fluoro-*N*-((*S*)-1-methoxypropan-2-yl)-4-methylpentanamide (*R*)-236b and (*S*)-2-fluoro-*N*-((*S*)-1-methoxypropan-2-yl)-4-methylpentanamide (S)-236a

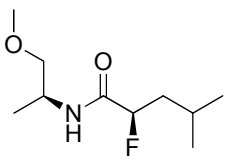

236b

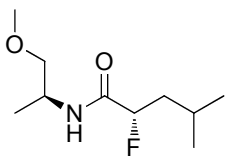

236a

*Preparation of **236b**:*

(*S*)-1-Methoxy-2-propylamine was added to a solution of 2-fluorocarboxilic acid (*R*)- **227b** (40 mg, 0.30 mmol) in DMF (1 mL), Et_3N (92 μL, 0.66 mmol) and TBTU (96 mg, 0.30 mmol). The reaction was stirred at rt for 1 h and then the mixture was quenched with brine (5 mL), and extracted in ethyl acetate (2 × 5 mL). The organic layer was successively washed with HCl (1 M), $NaHCO_3$, brine, dried over magnesium sulfate and concentrated under vacuum. The oily crude of (*R*)-2-fluoro-*N*-((*S*)-1-methoxypropan-2-yl)-4-methyl-pentanamide **236b** was directly analysed by ^{19}F spectroscopy to determine the ee (89% ee) (23 mg, 35%).

*Preparation of **236a**:*

(*S*)-2-fluoro-*N*-((*S*)-1-methoxypropan-2-yl)-4-methylpentanamide **236a** was obtained by the same method (21 mg, 32% yield).

*Data for **236b**:*

δ_F $\{^1H\}$ (282 MHz, $CDCl_3$): -189.34 (6%, (*S*,*S*), CHF), -189.36 (94%, (*S*,*R*), CHF). δ_F (282 MHz, $CDCl_3$): -189.36 (dddd, *J* 4.2 Hz, *J* 22.1 Hz, *J* 35.6 Hz, *J* 50.5 Hz, (*S*,*R*), CHF).

*Data for **236a**:*

Spectroscopic data identical to (*S,R*)-**236a**, except: δ_F $\{^1H\}$ (282 MHz, $CDCl_3$): -189.34 (95%, (*S*,*S*), CHF), -189.36 (5%, (*S*,*R*), CHF). δ_F (282 MHz, $CDCl_3$): -189.34 (dddd, *J* 4.1 Hz, *J* 22.1 Hz, *J* 35.6 Hz, *J* 50.4 Hz, (*S*,*S*), CHF).

2,2-difluoro-4-methylpentanal 241 and (*S*,*E*)-*N*-(2,2-difluoro-4-methylpentylidene)-1-methoxypropan-2-amine 241'

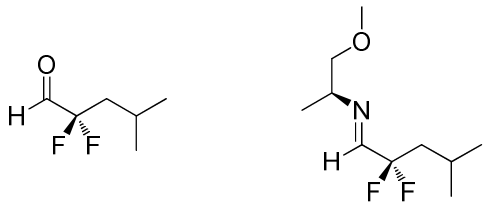

241 **241'**

*Preparation of **241** and **241':***

To a solution of NFSI (4 g, 12.5 mmol) and (*R*)-5-benzyl-2,2,3-trimethylimidazolin-4-one dichloroacetic salt (347 mg, 1 mmol) in THF/^{i}Propanol (38.5 mL, 9:1) cooled down to -10 °C, was added 4-methylpentanal (500 mg, 5 mmol). After 12 hours at rt, the solution was filtered over a pad of silica gel and eluted with diethyl ether. An aliquot of the residue 2,2-difluoro-4-methylpentanal **241** was derivatised with (*S*)-1-methoxy-2-propylamine to give (*S*,*E*)-*N*-(2,2-difluoro-4-methylpentylidene)-1-methoxypropan-2-amine **241'** for analysis.

*Data for **241**:*

δ_F {^{1}H} (282 MHz, $CDCl_3$): -112.52 (d, *J* 249.7 Hz, C*F*FCHO), -116.15 (d, *J* 250.2 Hz, CF*F*CHO). **δ_F** (282 MHz, $CDCl_3$): -112.52 (dddd, *J* 4.7 Hz, *J* 13.1 Hz, *J* 26.6 Hz, *J* 249.7 Hz, C*F*FCHO), -116.15 (dm, *J* 250.2 Hz, CF*F*CHO).

*Data for **241'**:*

δ_F {^{1}H} (282 MHz, $CDCl_3$): -112.29 (dd, *J* 26.1 Hz, *J* 245.8 Hz, C*F*FCHN), -113.81 (dd, *J* 49.2 Hz, *J* 245.6 Hz, CF*F*CHN).

2,2-difluoro-4-methylpentanoic acid 242

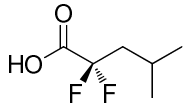

242

*Preparation by oxidation of **241**:*

2,2-Difluoro-4-methylpentanal **241** (680 mg, 5 mmol) was dissolved in acetone/water (40 mL, 5:1) and treated dropwise with CrO_3 (1 M in 30 % H_2SO_4) for 30 min. After addition of water (50 mL), the aqueous phase was extracted into diethyl ether (3 × 35 mL). The organic layer was dried over magnesium sulfate and concentrated under vacuum to give 2,2-difluoro-4-methylpentanoic acid **242** as pale yellow oil (91%, 692 mg).

*Preparation by saponification of **246**:*

To a solution of difluoroester **246** (200 mg, 1.2 mmol) dissolved in EtOH (5 mL) was added at 0 °C KOH (673 mg, 10 eq). The reaction mixture was stirred at rt for 2 days before concentration under vacuum. The residue was diluted in water (5 mL) and acidified with HCl (1 M) to pH= 2. Extraction into ethyl acetate (3 × 10 mL) and concentration of the organic phase under vacuum provided 2,2-difluoro-4-methylpentanoic acid **242** in good yield (86%).

*Data for **242**:*

IR ν_{max} **(cm^{-1})**: 2958, 1979, 1700, 1582, 1449, 1370. δ_H (300 MHz, $CDCl_3$): 0.87 (6 H, dd, *J* 1.2 Hz, *J* 6.2 Hz, 2 × CH_3), 1.57 (1 H, m, CH), 1.69 (2 H, m, CH_2), 9.63 (1 H, d, J 7.2 Hz, COOH). δ_C (75 MHz, $CDCl_3$): 22.5 (CH), 24.3 (2 × CH_3), 40.6 (d, *J* 20.4 Hz, CH_2), 42.1 (t,

J 22.1 Hz, C*H*$_2$ CF$_2$), 118.0 (d, *J* 249.6 Hz, CF$_2$), 165.8 (COOH). δ_F {^{1}H} (282 MHz, $CDCl_3$): -104.87. δ_F (282 MHz, $CDCl_3$): -104.87 (t, *J* 17.2 Hz, CF$_2$). ***m/z*** (HRMS) (ES^-): found 151.0568, calcd for $C_6H_9OF_2$: 151.0571 $[M-H]^-$.

Methyl 2,2-dimethoxy-4-methylpentanoate 244 and methyl 4-methyl-2-oxopentanoate 245

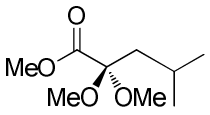

244

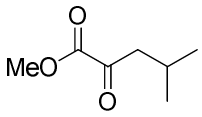

245

*Preparation of **244/245**:*

To an ice-cooled solution of 4-methylvaleric acid (0.95 mL, 7.7 mmol) in MeOH (8 mL), was added 4Å molecular sieves. Thionyl chloride (1.12 mL, 1.5 mmol) was then added dropwise and the mixture was stirred at rt for 16 h. After filtration, the mixture was evaporated under vacuum to give a 2:1 mixture of methyl 2,2-dimethoxy-4-methylpentanoate **244** and methyl 4-methyl-2-oxopentanoate **245** (1.4 g).

*Preparation of **245**:*

The residue was dissolved in acetonitrile (24 mL) and water (2.4 mL). Perchloric acid (1.2 mL) was then added slowly and the reaction mixture was stirred at rt for 4 h. Excess acid was neutralised by a solution of saturated sodium carbonate (5 mL) before evaporation under vacuum of the solvent. The aqueous phase was extracted into ethyl acetate (3 × 10 mL) and

the organic layer washed by brine, dried over magnesium sulfate, and concentrated under vacuum to give **245** as pale yellow oil (98%, 1.1 g)

*Data for **244**:*

δ_H (300 MHz, $CDCl_3$): 0.84 (6 H, d, *J* 6.5 Hz, 2 × CH_3), 1.52 (1 H, m, *J* 6.5 Hz, CH), 1.73 (2 H, d, *J* 6.7 Hz, CH_2), 3.15 (6 H, s, 2 × OCH_3), 3.72 (3 H, s, OCH_3).**δ_C** (75 MHz, $CDCl_3$): 22.4 (CH), 23.2 (2 × CH_3), 41.9 (CH_2), 49.6 (2 × OCH_3), 52.4 (OCH_3), 102.2 (C IV), 170.0 (CO).

*Data for **245**:*

δ_H (300 MHz, $CDCl_3$): 0.96 (6 H, d, *J* 6.7 Hz, 2 × CH_3), 2.19 (1 H, m, *J* 6.8 Hz, CH), 2.71 (2 H, d, *J* 6.8 Hz, CH_2), 3.85 (3 H, s, OCH_3). **δ_C** (75 MHz, $CDCl_3$): 23.7 (2 × CH_3), 24.1 (CH), 47.9 (CH_2), 52.9 (OCH_3), 138.9 (CO), 161.7 (CO).

Methyl 2,2-difluoro-4-methylpentanoate 246

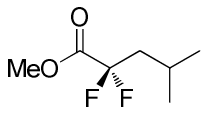

246

To a solution of methyl 4-methyl-2-oxopentanoate **245** (0.8 mmol, 100 mg) in DCM (2 mL) was added dropwise at 0 °C a solution of DAST (0.9 mmol, 0.1 mL). The reaction mixture

was stirred at rt for 14 h before addition of saturated $NaHCO_3$ (5 mL) and extraction into DCM (15 mL). The organic layer was dried over magnesium sulfate and concentrated under vacuum to give methyl 2,2-difluoro-4-methylpentanoate **246** as oil (55%, 63 mg).

*Data for **246**:*

IR ν_{max} **(cm^{-1})**: 2955, 1981, 1917, 1700, 1582, 1447, 1370. δ_H (300 MHz, $CDCl_3$): 1.02 (6 H, d, *J* 6.5 Hz, 2 × CH_3), 1.86 (1 H, m, CH), 1.98 (2 H, t, *J* 17.2 Hz, CH_2), 3.87 (3 H, s, OCH_3). δ_C (75 MHz, $CDCl_3$): 22.9 (CH, t, *J* 3.6 Hz), 23.1 (2 × CH_3), 42.7 (t, *J* 22.1 Hz, CH_2), 53.2 (OCH_3), 118.1 (d, *J* 250 Hz, CF_2), 137.9 (CO). δ_F {^{1}H} (282 MHz, $CDCl_3$): -104.20. δ_F (282 MHz, $CDCl_3$): -104.20 (t, *J* 17.3 Hz, CF_2). ***m/z*** (EI): 166.1 $[M]^+$.

2,2-Difluoro-*N*-(4-hydroxy-3-methoxybenzyl)-4-methylpentanamide 247

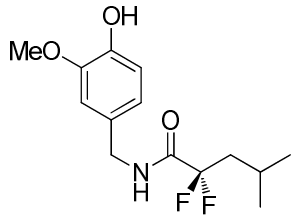

247

*Preparation by coupling of acyl chloride intermediate **249**:*

To a solution of 2,2-difluoro-4-methylpentanoic acid **242** (320 mg, 2.10 mmol) in a mixture of chloroform/DMF 9:1 (15 mL), was added 4 Å MS and then dropwise at 0 °C oxalyl chloride (0.54 mL, 6.3 mmol). The reaction mixture was stirred vigorously for 3 h at rt. An

aliquot of the intermediate acyl chloride **246** was analysed by ^{19}F NMR. A solution of vanillylamine **118** (392 mg, 2.10 mmol), in DMF (12 mL) and previously treated by DIEA (0.72 mL, 4.20 mmol), was then added. The reaction mixture was stirred for another 24 h. The mixture was then diluted in chloroform (50 mL), and washed with a saturated sodium bicarbonate solution (3 × 5 mL). The organic layers were dried over magnesium sulfate, filtered and concentrated under vacuum. Purification over silica gel gave 2,2-difluoro-*N*-(4-hydroxy-3-methoxybenzyl)-4-methylpentanamide **247** as a waxy solid (19%, 114 mg).

*Preparation by fluorination of **250**:*

To a solution of *N*-(4-hydroxy-3-methoxybenzyl)-4-methyl-2-oxopentanamide **250** (20 mg, 7.5×10^{-5} mol) in DCM (1 mL) was added DAST (20 μL, 0.15 mmol), and the reaction was stirred at 40 °C for 3 days. The crude mixture was analysed directly.

IR $\boldsymbol{\nu_{max}}$ **(cm^{-1})**: 2982, 2849, 2479, 2219, 1607, 1454, 1198. $\boldsymbol{\delta_H}$ (300 MHz, $CDCl_3$): 0.87 (6 H, d, *J* 7.4 Hz, 2 × CH_3), 1.50 (1 H, m, CH), 1.61 (2 H, m, CH_2), 3.66 (3 H, s, OCH_3), 4.41 (2 H, NCH_2), 6.87 (2 H, Ar H), 6.90 (1 H, Ar H). $\boldsymbol{\delta_C}$ (75 MHz, $CDCl_3$): 22.7 (2 × CH_3), 24.6 (CH), 43.4 (CH_2), 45.3 (NCH_2), 56.0 (OCH_3), 110.6 (Ar CH), 114.5 (Ar CH), 121.1 (Ar CH). $\boldsymbol{\delta_F}$ $\{^1H\}$ (282 MHz, $CDCl_3$): -104.59.

***N*-(4-hydroxy-3-methoxybenzyl)-4-methyl-2-oxopentanamide 250**

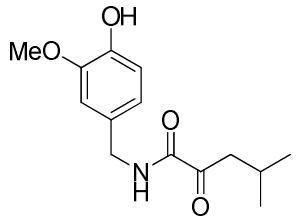

250

To a solution of 2-oxo-4-methylvaleric acid (34.4 mg, 0.26 mmol) in THF (1.5 mL) cooled down to -10 °C, were added dropwise *N*-methyl morpholine (29 µL, 0.26 mmol) and ethyl chloroformate (25.2 µL, 0.26 mmol). After 30 min, was added a solution of vanillylamine hydrochloride **118** (50 mg, 0.26 mmol) previously treated by K_2CO_3 (36.5 mg, 0.26 mmol). The mixture was stirred at rt for further 12 h. Volatiles were evaporated under vacuum and the residue dissolved in EtOAc (10 mL). The organic layer was successively washed with brine, 0.5 M HCl, brine, 5% $NaHCO_3$, brine, dried over magnesium sulfate, concentrated under vacuum. Purification on silica gel (Petroleum ether/EtOAc 7/3) gave *N*-(4-hydroxy-3-methoxybenzyl)-4-methyl-2-oxopentanamide **250** as clear oil (76%, 52.2 mg).

IR ν_{max} **(cm^{-1})**: 2982, 2479, 2219, 1669, 1588, 1452, 1287. δ_H (500 MHz, $CDCl_3$): 0.95 (6 H, d, *J* 6.7 Hz, 2 × CH_3), 2.15 (1 H, m, CH), 2.83 (2 H, d, *J* 6.9 Hz, CH_2), 3.88 (3 H, s, OCH_3), 4.37 (2 H, d, *J* 6.0 Hz, NCH_2), 5.63 (1 H, s, OH), 6.78 (2 H, m, 2 × Ar-H), 6.87 (1 H, d, *J* 8.5 Hz, Ar-H), 7.19 (1 H, br s, NH). δ_C (125 MHz, $CDCl_3$): 22.5 (2 × CH3), 24.3 (CH), 43.4 (CH_2), 45.3 (NCH_2), 55.9 (OCH_3), 110.6 (Ar CH), 114.5 (Ar CH), 121.1 (Ar CH), 128.9 (Ar C), 145.3 (Ar OH), 146.7 (Ar OMe), 160.0 (NH*C*=O), 198.8 (CH_2*C*=O). ***m/z*** (EI): 265.13 $[M]^+$.

***(S)*-benzyl 2,6-*bis*(dibenzylamino)hexanoate** (*S*)-**315**

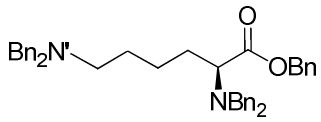

(*S*)-**315**

Anhydrous potassium carbonate (242 g, 1.75 mol) and benzyl bromide (182 mL, 1.53 mol) were added to a solution of (*S*)-L-lysine (40 g, 0.22 mol) in EtOH (400 mL). After stirring at 60 °C for 4 days, the resulting white slurry was filtered over Celite and the solids were washed with ethyl acetate. After evaporation of solvents, the residue was re-dissolved in ethyl acetate and washed with saturated NaCl solution. The organic layer was dried, filtered, concentrate under vacuum. Purification of the residue by distillation (100 °C, 0.01 mBar) gave *(S)*-benzyl 2,6-bis(dibenzylamino)hexanoate **315** as a pale yellow oil (125.5 g, 96%).

$\boldsymbol{[\alpha]_D^{20}}$ = -46.9 (c= 1.6, $CHCl_3$), {lit $[\alpha]_D^{20}$ = -52.5 ° (c 2.8, $CHCl_3$). IR $\boldsymbol{\nu_{max}}$ **(cm^{-1})**: 3032, 2941, 2798, 1731, 1494, 1454, 1365. $\boldsymbol{\delta_H}$ (300 MHz, $CDCl_3$): 1.11-1.72 (6 H, m, CH_2), 2.30 (2 H, t, *J* 6.8 Hz, CH_2N'), 3.30 (1 H, dd, *J* 6.2 Hz, *J* 8.7 Hz, CHN), 3.44 (4 H, d, *J* 3.94 Hz, 2 × PhCH_2N'), 3.46 (2 H, d, *J* 13.8 Hz, 2 × PhC$H_A H_B$N), 3.86 (2 H, d, *J* 13.9 Hz, 2 × PhCH_AH$_B$N), 5.08 (1 H, d, *J* 12.3 Hz, PhC$H_A H_B$O), 5.20 (1 H, d, *J* 12.3 Hz, PhCH_AH$_B$O), 7.15-7.38 (25 H, m, Ar *H*). $\boldsymbol{\delta_C}$ (75 MHz, $CDCl_3$): 23.7 (*C*H$_2$), 26.6 (*C*H$_2$), 29.2 (*C*H$_2$), 53.0 (*C*H$_2$N'), 54.4 (2 × Ph*C*H$_2$N), 58.2 (2 × Ph*C*H$_2$N'), 60.6 (*C*HN), 65.8 (Ph*C*H$_2$O), 126.7 (2 × Ar CH), 126.9 (2 x Ar CH), 128.1 (4 × Ar CH), 128.2 (4 × Ar CH), 128.3 (Ar CH), 128.4 (2 × Ar CH), 128.5 (2 × Ar CH), 128.7 (4 × Ar CH), 128.8 (4 × Ar CH), 136.1 (Ar C),

139.6 (2 × Ar C), 140.0 (2 × Ar C), 172.9 (COO). ***m/z*** (HRMS)(ES^+): found 597.3475, calcd for $C_{41}H_{45}N_2O_2$: 597.3479 $[M+H]^+$.

Spectroscopic data similar to literature [3]

(*S*)-2,6-Bis(dibenzylamino)hexan-1-ol (*S*)-**316**

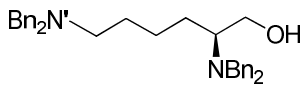

(*S*)-**316**

A solution of *(S)*-benzyl 2,6-bis(dibenzylamino)hexanoate **315** (126 g, 210 mmol) in THF (600 mL) was added dropwise over 45 min at -10 °C to a suspension of $LiAlH_4$ (12 g, 320 mmol) in THF (300 mL). The mixture was stirred for 3 h at this temperature and the excess of hydride was quenched by successive addition of ethyl acetate and aq NaOH (1 M). The mixture was extracted into ethyl acetate, the organic extracts were combined, dried over magnesium sulfate and the solvent removed under reduced pressure. The product was distilled (120 °C, 0.01 mbar) to give (*S*)-2,6-*bis*(dibenzylamino)hexan-1-ol **316** as a clear viscous oil (92.1 g, 89%)

$\boldsymbol{[\alpha]_D^{20}}$ = +49.5 (c 0.8, $CHCl_3$). IR $\boldsymbol{\nu_{max}}$ **(cm^{-1})**: 3443, 3027, 2935, 2799, 2360, 1602, 1365, 1129. $\boldsymbol{\delta_H}$ (300 MHz, $CDCl_3$): 1.01-1.65 (6 H, m, 3 × CH_2), 2.41 (2 H, dt, *J* 3.1 Hz, *J* 7.1 Hz, CH_2N'), 2.76 (1 H, m, C*H*N), 3.16 (1 H, br s, OH), 3.31-3.45 (2 H, m, CH_2OH), 3.32 (2 H, d, *J* 13.3 Hz, 2 × PhC$H_A H_B$N), 3.49 (2 H, d, *J* 13.6 Hz, 2 × PhC$H_A H_B$N'), 3.58 (2 H, d,

J 13.6 Hz, 2 × PhC$H_A$$H_B$N'), 3.76 (2 H, d, *J* 13.3 Hz, 2 × PhC$H_A$$H_B$N), 7.30 (20 H, m, 20 × Ar H). δ_C (75 MHz, $CDCl_3$): 24.6 (CH_2), 24.7 (CH_2), 27.3 (CH_2), 52.8 (CH_2N'), 53.1 (2 × PhCH_2N), 58.4 (2 × PhCH_2N'), 58.9 (*C*HN), 60.8 (CH_2OH), 126.8 (2 × Ar CH), 127.2 (2 × Ar CH), 128.2 (4 × Ar CH), 128.4 (4 × Ar CH), 128.7 (4 × Ar CH), 129.0 (4 × Ar CH), 139.3 (2 × Ar C), 139.9 (2 × Ar C). ***m/z*** HRMS (CI^+): found 493.3221, calcd for $C_{34}H_{41}N_2O$: 493.3219 $[M+H]^+$.

(*R*)-1,1-dibenzyl-2 ((dibenzylamino)methyl)piperidinium chloride (*R*)**-318**

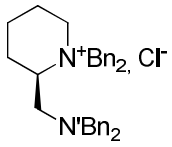

(*R*)**-318**

Preparation through cyclisation induced by DAST

Silica gel (3.46 g, 58 mmol) and then DAST (3.8 mL, 28.8 mmol) were added to a solution of (*S*)-2,6-*bis*(dibenzylamino)hexan-1-ol **316** (9.45 g, 19.2 mmol) in DCM (200 mL) at 0 °C. The mixture was warmed up to rt and stirred for 24 h and the reaction was quenched with brine, before extraction into DCM. The combined organic layers were dried and evaporated to dryness to provide (*R*)-1,1-dibenzyl-2 ((dibenzylamino) methyl)-piperidinium chloride **318** (7.76 g, 80%) as an off white powder.

Preparation through cyclisation induced by trifluoromethanesulfonic anhydride

Et_3N (0.85 mL, 6.09 mmol) and a catalytic amount of DMAP (50 mg, 0.41 mmol) were added to a solution of (*S*)-**316** (1.00 g, 2.03 mmol) in DCM (25 mL). The mixture was cooled to 0 °C and the trifluoromethanesulfonic anhydride (0.68 mL, 4.06 mmol) was added. The reaction was allowed to stir for 2 h at 0^oC, warmed up to rt and stirred at ambient temperature for further 12 h. The reaction was then quenched with a saturated NaCl solution and the products extracted into DCM. The organic layers were then washed with saturated $NaHCO_3$ solution, dried over magnesium sulfate and evaporated to give (*R*)-1,1-dibenzyl-2 ((dibenzylamino) methyl)-piperidinium chloride **318** (920 mg, 88%) as a pale orange powder.

Data for (*R*)-**318***:*

Mp 200 °C. $\boldsymbol{[\alpha]_D^{20}}$ = -73.5 (c 1.1, $CHCl_3$). IR $\boldsymbol{\nu_{max}}$ **(cm^{-1}):** 2348, 2283, 1187, 1128, 929. $\boldsymbol{\delta_H}$ (300 MHz, $CDCl_3$): 1.54-1.93 (6 H, m, 3 × CH_2), 2.16 (1 H, d, *J* 14.8 Hz, N'CH_AH_B), 2.48 (1 H, d, *J* 14.8 Hz, N'CH_AH_B), 2.87 (1 H, dd *J* 9.9 Hz, *J* 13.5 Hz, N^+CH), 3.09 (1 H, t, *J* 10.3 Hz, $N^+CH_ACH_B$), 3.30 (1 H, t, *J* 10.6 Hz, $N^+CH_ACH_B$), 3.47 (2 H, d, *J* 13.5 Hz, 2 × N'CH_AH_B), 3.90 (2 H, d, *J* 13.5 Hz, 2 × N'CH_AH_B), 4.39 (1 H, d, *J* 13.5 Hz, $N^+CH_AH_B$), 4.71 (1 H, d, *J* 12.9 Hz, $N^+CH_AH_B$), 4.97 (1 H, d, *J* 12.9 Hz, $N^+CH_AH_B$), 5.58 (1 H, d, *J* 13.5 Hz, $N^+CH_AH_B$)7.20-7.33 (8 H, m, 8 × Ar H), 7.36-7.54 (8 H, m, 8 × Ar H), 7.64 (2 H, d, *J* 7.4 Hz, 2 × Ar CH), 7.74 (2 H, d, *J* 7.4 Hz, 2 × Ar H). $\boldsymbol{\delta_C}$ (75 MHz, $CDCl_3$): 20.8 (CH_2), 22.1 (CH_2), 25.9 (CH_2), 52.7 (CH_2N'), 57.3 (CH_2N), 58.1 (PhCH_2N), 59.0 (2 × PhCH_2N'), 63.7 (PhCH_2N), 67.0 (CHN), 128.4 (4 × Ar CH), 129.1 (2 × Ar CH), 129.2 (4 × Ar CH), 129.3 (2 × Ar CH), 130.5 (Ar CH), 130.7 (Ar CH), 133.7 (2 × Ar CH), 133.8 (2 × Ar CH), 138.5 (4 × Ar C). ***m/z*** HRMS (ES^+): found 475.3113, calcd for $C_{34}H_{39}N_2$:475.3113 $[M+H]^+$.

(*R*)-2-(Aminomethyl)piperidine *di*hydrochloride (*R*)-**251, (*S*)-(2-(aminomethyl)piperidine *di*hydrochloride** (*S*)-**251 and (*R*)-2-(aminomethyl)piperidine *di*tetrafluoroborate** (*R*)-**251**

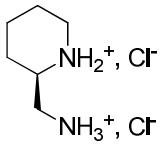

(*R*)-**251** diHCl

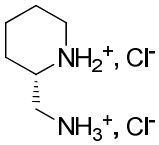

(*S*)-**251** diHCl

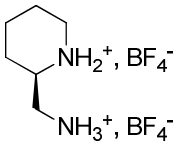

(*R*)-**251** diHBF$_4$

*Preparation of (R)-**251** diHCl:*

Ammonium formate (315 mg, 5 mmol) and 20% $Pd(OH)_2$ (250 mg) were added to a solution of (*R*)-1,1-dibenzyl-2 ((dibenzylamino) methyl)piperidinium chloride **318** (510 mg, 1 mmol) in MeOH (25 mL). The mixture was stirred for 24 h at room temperature. The black suspension was then filtered over a pad of Celite and a solution of HCl in diethyl ether (4 mL, 1 M) was added to the filtrate. Solvents were removed under reduced pressure and the crude product was re-crystallised from methanol/diethyl ether to yield (*R*)-2-(aminomethyl)-piperidine *di*hydrochloride (*R*)-**251** (144 mg, 77%) as a colourless crystalline solid.

*Preparation of (S)-**251** diHCl:*

(*S*)-(2-(aminomethyl)piperidine *di*hydrochloride (*S*)-**251** *di*HCl (140 mg, 75%) was prepared following the same protocol as for (*R*)-**251** *di*HCl.

*Preparation of (R)-**251** diHBF$_4$:*

To (*R*)-2-(aminomethyl)piperidine *di*hydrochloride **251** (1.7 g, 9.09 mmol) dissolved in MeOH (25 mL) was added a solution of tetrafluoroboric acid-diethyl ether complex (2.5 mL, 18.17 mmol) at 0 °C. After 1 hour of stirring at rt, the mixture was evaporated under reduced pressure, the residue was washed with diethyl ether and dried under high vacuum for 12 h.

The *di*tetrafluoroborate salt was recrystallised from acetone/THF to give (*R*)-**251** *di*HBF_4 as long clear needles (2.34 g, 89%).

*Data: for (R)-**251** diHCl:*

Mp 213-215 °C. $[\boldsymbol{\alpha}]_{\boldsymbol{D}}^{\boldsymbol{20}} =$ +2.3 (c 1.4, MeOH). IR $\boldsymbol{\nu_{max}}$ **(cm^{-1})**: 3416, 2955, 2842, 1584, 1514, 1484, 1476, 1440, 1407, 1133, 1022, 1008. $\boldsymbol{\delta_H}$ (300 MHz, CD_3OD): 1.43-1.75 (6 H, m, 3 × CH_2), 2.93 (2 H, t, *J* 15.1 Hz, N^+CH_2), 3.09 (1 H, m, N^+CH), 3.51 (1 H, dd, *J* 6.6 Hz, *J* 11.4 Hz, C*H*$_A$H$_B$N'), 3.70 (1 H, dd, *J* 3.8 Hz, *J* 11.4 Hz, CH$_A$*H*$_B$N'). $\boldsymbol{\delta_C}$ (75 MHz, CD_3OD): 23.4 (CH_2), 28.4 (CH_2), 30.8 (CH_2), 40.5 (CH_2N^+), 54.1 (CHN^+), 63.4 (CH_2N^+). **Elemental analysis (%)**: found C 38.86, H 8.31, N 14.66, calcd for $C_6H_{16}N_2Cl_2$: C, 38.51; H, 8.62; N, 14.97. ***m/z*** HRMS (CI^+): found 115.1236, calcd for $C_6H_{15}N_2$: 115.1234 $[M+H]^+$.

Spectroscopic data similar to literature [4, 5]

*Data for (S)-**251**:*

Analytical data were identical to (*R*)-**251**, except: $[\boldsymbol{\alpha}]_{\boldsymbol{D}}^{\boldsymbol{20}} =$ -2.9 (c 1.4, MeOH).

(lit. $[\boldsymbol{\alpha}]_{\boldsymbol{D}}^{\boldsymbol{25}} =$ -4.7 (c 2.8, MeOH), $[\boldsymbol{\alpha}]_{\boldsymbol{D}}^{\boldsymbol{25}} =$ -5.7 (c 0.42, MeOH),). (lit. **Mp** 240-242 °C)

*Data: for (R)-**251** diHBF$_4$:*

Mp 108-113 °C. $\boldsymbol{\delta_H}$ (300 MHz, CD_3OD): 1.27-1.39 (1 H, m), 1.47-1.73 (3 H, m), 1.94 (1 H, ld, *J* 10.19 Hz), 2.10 (1 H, d, *J* 10.79 Hz), 2.96 (1 H, t, *J* 7.98 Hz), 3;03-3.17 (2 H, m), 3.27 (1 H, dd, *J* 4.9 Hz, *J* 13.4 Hz), 3.39-3.53 (2 H, m). $\boldsymbol{\delta_C}$ (75 MHz, CD_3OD): 22.3 (CH_2), 23.0 (CH_2), 27.3 (CH_2), 42.2 (CH_2N^+), 46.5 (CH_2N^+), 55.3 (CHN^+). $\boldsymbol{\delta_F}$ $\{^1H\}$ (282 MHz, CD_3OD): -154.36, -154.41.

2-(*R*)-[4,4,0]-1,4-diazo-5,6-diketobicyclodecane (*R*)-342

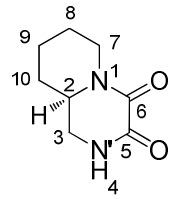

(*R*)-**342**

Diethyl oxalate (98 µL, 668 µmol) was added to a solution of (*R*)-2-(aminomethyl)piperidine dihydrochloride **251** (125 mg, 668 µmol) in DMF (2 mL) previously treated by ^{t}BuOK for 12 h (185 µL, 1.34 mmol). The mixture was heated in a sealed tube at 140 °C for 6 h then 160 °C for another 4 h. All volatiles were then evaporated under reduced pressure and the residue diluted in ethyl acetate (5 mL) and washed with brine (1 mL). The organic layer was dried over magnesium sulfate, and evaporated under vacuum to give 2-(*R*)-[4,4,0]-1,4-diazo-5,6-diketobicyclodecane **342** as a white solid (24 mg, 21%).

Mp 137-139 °C. $[\alpha]_D^{20}$ = +9.5 (c 1.8, MeOH). IR ν_{max} **(cm^{-1})**: 3303, 2929, 1655, 1525, 1434, 1180, 1118. δ_H (300 MHz, $CDCl_3$): 1.45 (2 H, m,CH_2), 1.61-1.95 (4 H, m, 2 × CH_2), 3.35 (1 H, ddd, *J* 1.2 Hz, *J* 9.5 Hz, *J* 12.6 Hz, N'CH_AH$_B$), 3.54 (2 H, dt, *J* 4.2 Hz, *J* 12.9 Hz, NCH_2), 3.61 (1 H, m, N'CH$_A$$H_B$), 4.56 (1 H, dt, *J* 1.8 Hz, *J* 13.6 Hz, NCH), 7.63 (1 H, s, NH). δ_C (75 MHz, $CDCl_3$): 22.5 (CH_2), 24.9 (CH_2), 29.8 (CH_2), 43.3 (N'CH_2), 44.3(NCH_2), 53.8 (NCH), 158.0 (C=O), 158.4 (C=O). ***m/z*** (HRMS) (ES$^+$): found 191.0790, calcd for $C_8H_{12}N_2O_2Na$: 191.0796 [M+Na]$^+$.

2-(*R*)-[4,4,0]-1,4-diazobicyclodecane (*R*)-333

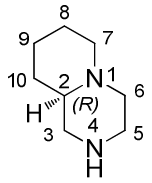

(*R*)-**333**

To a suspension of lithium aluminium hydride (112 mg, 2.96 mmol) in THF (10 mL) was added dropwise at 0 °C a solution of 2-(*R*)-[4,4,0]-1,4-diazo-5,6-diketobicyclodecane **342** (50 mg, 296 μmol) in THF (5 mL). The reaction was heated at reflux for 16 h. The reaction was then quenched by addition of aqueous NaOH (1 M) and water. The solvent was evaporated before extraction of the aqueous layer in ethyl acetate. The organic layer was dried over magnesium sulfate and evaporated under reduced pressure to give 2-(*R*)-[4,4,0]-1,4-diazobicyclodecane **333** as a clear oil (22.3 mg, 54%).

$[\alpha]_D^{20}$ = -7.4 (c 0.5, MeOH). IR ν_{max} **(cm^{-1})**: 3308, 2932, 2854, 1668, 1516, 1455. δ_H (300 MHz, $CDCl_3$): 1.08-1.33 (4 H, m, 2 × CH_2), 1.45 (1 H, m, $C^7H_AH_B$), 1.58 (2 H, m, CH_2), 1.71 (1 H, m, $C^7H_AH_B$), 1.85 (1 H, tt, *J* 2.6 Hz, *J* 10.5 Hz, NCH), 2.02 (1 H, m, $C^6H_ACH_B$), 2.16 (1 H, m, $C^6H_ACH_B$), 2.47 (1 H, dd, *J* 10.4 Hz, *J* 12.1 Hz, N'$C^3H_AH_B$), 2.68 (1 H, dt, *J* 2.3 Hz, *J* 11.5 Hz, $C^5H_ACH_B$), 2.78 (1 H, td, *J* 2.6 Hz, *J* 12.6 Hz, $C^5H_ACH_B$), 2.92 (1 H, dd, *J* 2.4 Hz, *J* 8.9 Hz, N'$C^3H_AH_B$), 3.76 (1 H, br s, NH). δ_C (75 MHz, $CDCl_3$): 24.0 (CH_2), 25.5 (CH_2), 29.6 (CH_2), 45.6 (N'CH_2), 51.6 (NCH_2), 55.6 (NCH_2), 55.9 (N'CH_2), 62.3 (NCH). ***m/z*** (EI): 140.12 $[M]^+$.

2-(*R*)-[4,4,0]-1,4-diazo-4-ethylbicyclodecane 348

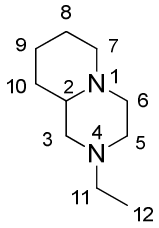

348

To a suspension of lithium aluminium hydride (112 mg, 2.96 mmol) in THF (10 mL) was added dropwise at 0 °Ca solution of 2-(*R*)-[4,4,0]-1,4-diazo-5,6-diketobicyclodecane **342** (50 mg, 296 μmol) in THF (5 mL). The reaction was stirred at reflux for 16 h. The reaction was then quenched by addition of ethyl acetate and water and the aqueous layer was extracted into more ethyl acetate, dried over magnesium sulfate and evaporated under reduced pressure to give 2-(*R*)-[4,4,0]-1,4-diazo-4-ethylbicyclodecane **348** (44 mg, 89%).

δ_H (300 MHz, $CDCl_3$): 0.66 (3 H, t, *J* 7.2 Hz, CH_3), 0.73-0.94 (4 H, m, 2 × CH_2), 1.10 (1 H, d, *J* 10.5 Hz, $C^7H_AH_B$), 1.21 (2 H, m, C^9H_2), 1.33 (1 H, d, *J* 10.5 Hz, $C^7H_AH_B$), 1.38 (1 H, t, *J* 10.7 Hz, NCH), 1.62 (1 H, m, $C^6H_AH_B$), 1.83 (1 H, ddd, *J* 2.6 Hz, *J* 11.4 Hz, *J* 28.8 Hz, $C^6H_AH_B$), 1.98 (2 H, q, *J* 7.1 Hz, $C^{11}H_2$), 2.32 (2 H, d, *J* 11.0 Hz, C^3H_2), 2.42 (2 H, td, *J* 1.5 Hz, *J* 10.5 Hz, C^5H_2). **δ_C** (75 MHz, $CDCl_3$): 11.5 (CH_3), 23.5 (C^9H_2), 25.2 (C^8H_2), 29.5 ($C^{10}H_2$), 51.8 (C^7H_2), 52.3 ($C^{11}H_2$), 54.5 (C^5H_2), 55.1 (C^3H_2), 58.7 (C^6H_2), 60.3 (CH). ***m/z*** (EI): 168.16 $[M]^+$.

2-(2-fluoroethyl)octahydro-1 H-pyrido[1,2-a]pyrazine 350

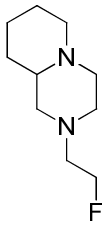

350

To a suspension of lithium aluminium hydride (112 mg, 2.96 mmol) in ice cooled THF (10 mL) was added dropwise at 0 °C a solution of 2-(*R*)-[4,4,0]-1,4-diazo-5,6-diketobicyclo-decane **342** (50 mg, 296 μmol) in THF (5 mL). The reaction was stirred at reflux for 16 h. The reaction was then quenched by addition of ethyl 2-fluoroacetate then ^{i}Pr. The aqueous layer was extracted into more ethyl acetate, dried over magnesium sulfate and evaporated under reduced pressure to give 2-(2-fluoroethyl)octahydro-1 H-pyrido[1,2-a]pyrazine **350** (42 mg, 76%).

δ_H (300 MHz, $CDCl_3$): 1.02-1.24 (4 H, m, C^8H_2 and $C^{10}H_2$), 1.37 (1 H, d, *J* 10.5 Hz, $C^7H_AH_B$), 1.49 (2 H, m, C^9H_2), 1.60 (1 H, d, *J* 10.6 Hz, $C^7H_AH_B$), 2.20 (1 H, m, NCH), 2.53 (2 H, dt, *J* 4.9 Hz, *J* 28 Hz, C^3H_2), 2.60-2.75 (2 H, m, $C^{11}H_2$), 3.49 (1 H, m, $C^6H_AH_B$), 3.65 (2 H, m, $C^6H_AH_B$ and $C^5H_AH_B$), 4.02 (1 H, m, $C^5H_AH_B$), 4.42 (2 H, dt, *J* 5.3 Hz, *J* 47.6 Hz, CH_2F). **δ_C** (75 MHz, $CDCl_3$): 23.5 (C^9H_2), 25.2 (C^8H_2), 29.4 ($C^{10}H_2$), 52.6 (C^7H_2), 54.4 (C^3H_2), 55.1 (C^5H_2), 57.8 (d, *J* 20.5 Hz, $C^{11}H_2$), 60.6 (CH), 63.2 (C^6H2), 81.4 (d, *J* 167.4 CH_2F). **δ_F** {^{1}H} (282 MHz, $CDCl_3$): -218.4 Hz. **δ_F** (282 MHz, $CDCl_3$): -218.4 (tt, *J* 28.3 Hz, *J* 47.7 Hz, CH_2F). ***m/z*** (EI): 186.16 $[M]^+$.

***N*[1],*N*[2]-*bis*(piperidin-2-ylmethyl) 343**

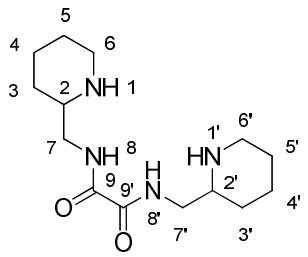

343

To a solution of 2-(aminomethyl)piperidine **251** (1.00 g, 8.76 mmol) in DCM (10 mL) cooled down to -10 °C, was added dropwise diethyl oxalate (598 µL, 4.38 mmol). After 1 hour at this temperature, the white solid was filtered and washed by diethyl ether to give *N*[1],*N*[2]-*bis*(piperidin-2-ylmethyl) **343** (1.20 g, 97%) as an off white powder.

Mp 173-174 °C. **δ_H** (300 MHz, CD_3OD): 1.07-1.21 (1 H, m, $C^3H_AH_B$), 1.41 (2 H, m, C^5H_2), 1.56-1.73 (2 H, m, C^4H_2), 1.81 (1 H, d, *J* 6.9 Hz, $C^3H_AH_B$), 2.59 (1 H, td, *J* 2.8 Hz, *J* 11.8 Hz, $C^6H_AH_B$), 2.70 (1 H, m, $C^6H_AH_B$), 3.02 (1 H, d, *J* 11.3 Hz, CH), 3.23 (2 H, d, *J* 5.3 Hz, C^7H_2). **δ_C** (75 MHz, CD_3OD): 25.3 (CH_2), 26.7 (CH_2), 30.9 (CH_2), 45.9 (CH_2), 47.4 (CH_2), 57.3 (CH), 162.2 (C=O). ***m/z*** (HRMS) (ES^+): found 283.2139, calcd for $C_{14}H_{27}N_4O_2$: 283.2134 $[M+H]^+$.

***N*[1],*N*[2]-*bis*(piperidin-2-ylmethyl)ethane-1,2-diamine 347**

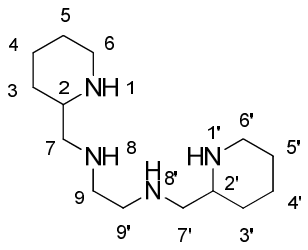

347

To a suspension of lithium alumimium hydride (89 mg, 2.34 mmol) in THF (3 mL), was added dropwise at 0 °C a solution of *N*[1],*N*[2]-*bis*(piperidin-2-ylmethyl) **343** (66.3 mg, 234 µmol) in THF (10 mL). After 24 h at reflux, the reaction was then quenched by addition of aq NAOH (1 M) and water. The solvent was evaporated before extraction of the aqueous layer into ethyl acetate. The organic layer was then dried over magnesium sulfate and evaporated under reduced pressure. Purification over silica gel (DCM/methanol 9/1) did not allow recovering *N*[1],*N*[2]-*bis*(piperidin-2-ylmethyl)ethane-1,2-diamine **347** as a pure product (59.7 mg, ~20% of the crude mixture).

IR ν_{max} **(cm^{-1})**: 3295, 3172, 2923, 2853, 2314, 1654, 1510, 1436, 1199, 1144. δ_C (75 MHz, $CDCl_3$): 24.4 (C^4H_2 and $C^{4'}H_2$), 26.2 (C^5H_2 and $C^{5'}H_2$), 30.6 (C^3H_2 and $C^{3'}H_2$), 46.0 (C^6H_2 and C^6H_2), 52.2 (C^9H_2 and $C^{9'}H_2$), 56.2 (C^7H_2 and $C^{7'}H_2$), 62.9 (C^2H and $C^{2'}H$). ***m/z*** (HRMS) (ES^+): found 255.2546, calcd for $C_{14}H_{31}N_4$: 255.2543 $[M+H]^+$.

(*E*)-*N*-4-methoxybenzyl-α-iminoglyoxalate 359

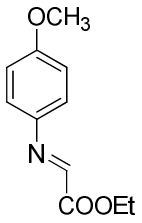

359

To a solution of ethyl glyoxalate (4.07 mL, 50% in toluene, 20.0 mmol) dissolved in DCM (75 mL) was added slowly *p*-anisidin (2.46 g, 20.0 mmol) in DCM (25 mL) and the reaction mixture was stirred at room temperature for 30 min before addition of 4 Å molecular sieves. After stirring one additional hour, the reaction mixture was filtered and the volatiles evaporated under vacuum to give (*E*)-*N*-4-methoxybenzyl-α-iminoglyoxalate **359** as a yellow oil (4.05 g, 98%)

IR ν_{max} **(cm^{-1})**: 3364, 2980, 2936, 2906, 2837, 2048, 1734, 1608, 1590, 1506. δ_H (300 MHz, $CDCl_3$): 1.40 (3 H, t, *J* 7.1 Hz, CH_3), 3.83 (3 H, s, OCH_3), 4.41 (2 H, q, *J* 7.1 Hz, OCH_2), 6.93 (2 H, d, *J* 9.0 Hz, 2 × Ar H), 7.36 (2 H, d, *J* 9.0 Hz, 2 x Ar H), 7.93 (1 H, s, N=CH). δ_C (75 MHz, $CDCl_3$): 14.2 (CH_3), 55.4 (OCH_3), 61.8 (OCH_2), 114.4 (2 × Ar CH), 123.5 (2 × Ar CH), 141.3 (Ar C IV), 147.9 (N=CH), 160.4 (Ar C OMe), 163.5 (C=O).

Spectroscopic data similar to literature[6]

(*S*)-ethyl 2-((4-methoxyphenyl)amino)-2-((*S*)-2-oxocyclohexyl)acetate 360 and (*R*)-ethyl 2-((4-methoxyphenyl)amino)-2-((*R*)-2-oxocyclohexyl)acetate 360

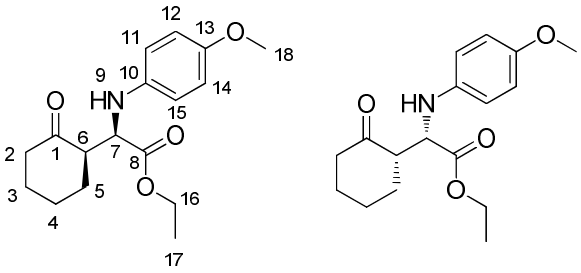

(*R*,*R*)-**360** (*S*,*S*)-**360**

*Typical procedure for reactions catalysed by **363**:*

To the catalyst (*R*)-2,2,2-trifluoro-*N*-(piperidin-2-ylmethyl)acetamide trifluoroacetate **363** (20 mol%, 21 mg) dissolved in ^{i}PrOH (0.5 mL), were added *(E)*-*N*-4-methoxybenzyl-α-iminoglyoxalate **359** (104 mg, 0.5 mmol) and cyclohexanone (0.5 mL, 0.60 mmol). The reaction mixture was stirred 24 h at rt. The reaction mixture was quenched with a saturated ammonium chloride solution (5 mL) and extracted in ethyl acetate (3 × 5 mL). The organic layer was dried over magnesium sulfate, filtered and evaporated under vacuum. The residue was purified on silica gel (ethyl acetate/ petroleum ether 1:1) to give ethyl 2-((4-methoxyphenyl)amino)-2-(2-oxocyclohexyl)acetate **360** as a yellow oil.

Data for syn-adduct:

IR $\boldsymbol{\nu_{max}}$ **(cm^{-1})**: 3367, 2936, 1727, 1710, 1509, 1233, 1034. $\boldsymbol{\delta_H}$ (300 MHz, $CDCl_3$): 1.22 (3 H, t, *J* 7.1 Hz, CH_3), 1.63-1.73 (2 H, m, $C^5H_AH_B$ and $C^4H_AH_B$), 1.80 (1 H, dt, *J* 3.2 Hz, $C^4H_AH_B$), 1.96 (1 H, m, $C^3H_AH_B$), 2.06 (1 H, m, $C^3H_AH_B$), 2.19 (1 H, m, $C^2H_AH_B$), 2.33 (1 H, m, $C^2H_AH_B$), 2.45 (1 H, m, $C^5H_AH_B$), 2.82 (1 H, dt, *J* 4.9 Hz, *J* 10.9 Hz, C^6H), 3.74 (3 H, s,

OCH_3), 4.15 (2 H, q, *J* 7.2 Hz, OCH_2), 4.23 (1 H, d; *J* 5.1 Hz, C^7H), 6.73 (2 H, d, *J* 9.1 Hz, 2 × Ar H), 6.77 (2 H, d, *J* 9.1 Hz, 2 × Ar H). δ_C (75 MHz, $CDCl_3$): 14.1 (CH_3), 24.8 (C^3H_2), 26.8 (C^4H_2), 29.6 (C^5H_2), 41.8 (C^2H2), 53.6 (C^6H), 55.7 (OCH_3), 58.1 (C^7H), 61.1 (OCH_2), 114.7 (2 × Ar CH), 116.2 (2 × Ar CH), 141.0 (Ar C^{10} IV), 153.0 (Ar C^{13}), 173.4 (C^8=O), 211.0 (C^1=O). ***m/z*** (HRMS) (ES^+): found 328.1512, calcd for $C_{17}H_{23}NO_4Na$: 328.1525 $[M+Na]^+$.

Spectroscopic data similar to literature[6]

_N_-(piperidin-2-ylmethyl)benzamide 362

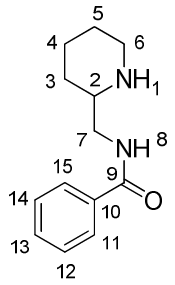

362

To a solution of 2-(aminomethyl)piperidine **251** (200 mg, 1.75 mmol) in a mixture of ACN/water (6/1, 2.8 mL) was added ethyl benzoate (0.45 mL, 3.10 mmol). The reaction mixture was refluxed for 24 h, and after cooling down, volatiles were evaporated under reduced pressure. The residue was dissolved in ethyl acetate (10 mL) and washed by brine (1 mL). The organic layer was then dried over magnesium sulfate and evaporated under reduced pressure to give *N*-(piperidin-2-ylmethyl)benzamide **362** (237 mg, 62%)

Mp: 103-104 °C. **δ_H** (300 MHz, $CDCl_3$): 1.21 (1 H, m, $C^3H_AH_B$), 1.43 (2 H, m, $C^3H_AH_B$ and $C^5H_AH_B$), 1.58-1.68 (1 H, m, $C^5H_AH_B$), 1.75 (1 H, m, $C^4H_AH_B$), 1.83 (1 H, m, $C^4H_AH_B$), 2.62 (2 H, td, *J* 3.1 Hz, *J* 11.9 Hz, $C^6H_AH_B$), 2.78 (1 H, m, $C^6H_AH_B$), 3.05 (1 H, d, *J* 11.9 Hz, CH), 3.35 (2 H, d, *J* 6.2 Hz, C^7H_2), 7.43-7.54 (3 H, m, 3 x Ar H), 7.84 (2 H, dd, *J* 1.5 Hz, *J* 8.4 Hz, 2 x Ar H). **δ_C** (75 MHz, $CDCl_3$): 25.1 (C^4H_2), 26.7 (C^5H_2), 31.1 (C^3H_2), 46.5 (C^7H_2), 47.4 (C^6H_2), 57.5 (CH), 128.4 (2 × Ar CH), 129.6 (2 × Ar CH), 132.7 (Ar $C^{13}H$), 135.7 (Ar C^9 IV). **ν_{max} (cm^{-1})**: 3310, 2913, 2670, 2330, 1639, 1530, 1446, 1192, 1140. ***m/z*** (ES^+): 219.07 (M+H), (HRMS) (ES^+): found 219.1497 (M+H), calc for $C_{13}H_{19}N_2O$: 219.1497.

(*R*)-2,2,2-trifluoro-*N*-(piperidin-2-ylmethyl)acetamide trifluoroacetate (*R*)-363

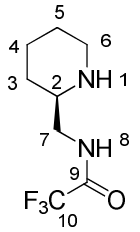

(*R*)-**363**

A suspension of (*R*)-2-(aminomethyl)-piperidine *di*tetrafluoroborate **251** 170 mg, 0.59 mmol) in THF (15 mL) was treated with DIEA (0.2 mL, 1.17 mmol) under sonication (~30 min). Ethyl trifluoroacetate (84 μL, 0.70 mmol) was then added and the reaction mixture was refluxed for 14 h. Volatiles were evaporated under reduced pressure and the residue was dissolved in ethyl acetate (10 mL) and washed with brine (3 × 2 mL). The organic layer was dried over magnesium sulfate, evaporated under reduced pressure to give (*R*)-2,2,2-trifluoro-*N*-(piperidin-2-ylmethyl)acetamide trifluoroacetate **363** as a solid (138 mg, 88%).

$[\alpha]_D^{20}$ = -29.6 (c 1.3, MeOH). IR ν_{max} **(cm^{-1})**: 3327, 3165, 2929, 2720, 1715, 1557, 1422, 1182, 1140.δ_H (300 MHz, CD_3OD): 1.06-1.26 (1 H, m, $C^3H_AH_B$), 1.41 (2 H, m, C^5H_2), 1.57-1.71 (2 H, m, $C^3H_AH_B$ and $C^4H_AH_B$), 1.82 (1 H, d, *J* 6.5 Hz, $C^4H_AH_B$), 2.60 (1 H, td, *J* 2.9 Hz, *J* 11.8 Hz, $C^6H_AH_B$), 2.72 (1 H, m, $C^6H_AH_B$), 3.03 (1 H, d, *J* 10.3 Hz, C^2H), 3.25 (2 H, t, *J* 6.6 Hz, C^7H_2). δ_C (75 MHz, CD_3OD): 25.1 (C^4H_2), 26.6 (C^5H_2), 30.8 (C^3H_2), 46.0 (C^7H_2), 47.3(C^6H_2), 56.9 (C^2H). δ_F (282 MHz, CD_3OD): -77.34 (s, CF_3). **Elemental analysis (%)**: found C 38.99, H 5.58, N 11.0, calcd for $C_8H_{13}N_2OF_3$: C 38.96, H 5.72, N 11.36. ***m/z*** (HRMS) (CI^+): found 211.1062, calcd for $C_8H_{14}N_2OF_3$: 211.1058 $[M+H]^+$.

4-Methyl-*N*-(piperidin-2-ylmethyl)benzenesulfonamide (*R*)-364

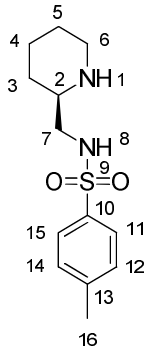

(*R*)-364

DCM (2 mL) and DIEA (0.12 mL, 0.69 mmol) were added to (*R*)-2-(aminomethyl)piperidine *di*tetrafluoroborate **251** (100 mg, 0.35 mmol) and the mixture dissolved by sonication (~30 min). Then this solution was treated with K_2CO_3 (57 mg, 0.41 mmol), *p*-toluenesulfonyl chloride (66 mg, 0.35 mmol) and the mixture stirred for 3 h at 0 °C. The reaction mixture was diluted in DCM (10 mL), washed with brine (3 × 1 mL), dried over magnesium sulfate and

evaporated under reduced pressure. The crude product was purified on silica gel (hexane/ethyl acetate 8:2), to give 4-methyl-*N*-(piperidin-2-ylmethyl)benzenesulfonamide **364** (73 mg, 79%)

Mp: 93-94 °C. IR $\boldsymbol{\nu_{max}}$ **(cm^{-1})**: 3562, 3276, 3062, 2929, 2853, 1598, 1442, 1326, 1150, 1092. $\boldsymbol{\delta_H}$ (300 MHz, $CDCl_3$): 1.05 (1 H, qd, *J* 3.9 Hz, *J* 8.8 Hz, $C^3H_AH_B$), 1.31 (2 H, m, $C^3H_AH_B$ and $C^5H_AH_B$), 1.45-1.61 (2 H, m, $C^5H_AH_B$ and $C^4H_AH_B$), 1.75 (1 H, m, $C^4H_AH_B$), 2.43 (3 H, s, CH_3), 2.57 (2 H, qu d, *J* 2.9 Hz, *J* 11.9 Hz, C^7H_2), 2.73 (1 H, dd, *J* 8.1 Hz, *J* 12.4 Hz, $C^6H_AH_B$), 2.92 (1 H, dd, *J* 3.9 Hz, *J* 12.4 Hz, $C^6H_AH_B$), 3.0 (1 H, dd, *J* 2.5 Hz, *J* 12.1 Hz, C^2H), 7.3 (2 H, d, *J* 8.0 Hz, 2 × Ar H), 7.74 (2 H, d, *J* 8.3 Hz, 2 × Ar H). $\boldsymbol{\delta_C}$ (75 MHz, $CDCl_3$): 21.5 ($C^{16}H_3$), 24.1 (C^4H_2), 26.4 (C^5H_2), 26.1 (C^3H_2), 46.4 (C^6H_2), 48.5 (C^7H_2), 55.5 (CH), 127.1 (2 × Ar CH), 129.7 (2 × Ar CH), 136.8 (Ar C^{10}), 143.3 (Ar C^{13}). ***m/z*** (HRMS) (ES^+): found 269.1325, calcd for $C_{13}H_{21}N_2O_2S$: 269.1324 $[M+H]^+$.

1. P. M. Gannett, D. L. Nagel, P. J. Reilly, T. Lawson, J. Sharpe and B. Toth, *J. Org. Chem.*, 1988, **53**, 1064-1071.
2. H. Kaga, M. Miura and K. Orito, *J. Org. Chem.*, 1989, **54**, 3477-3478.
3. M. G. Banwell, M. J. Coster, M. J. Harvey and J. Moraes, *J. Org. Chem.*, 2003, **68**, 613-616.
4. O. Froelich, P. Desos, M. Bonin, J.-C. Quirion, H.-P. Husson and J. Zhu, *J. Org. Chem.*, 1996, **61**, 6700-6705.
5. S. Nazabadioko, R. J. Pérez, R. Brieva and V. Gotor, *Tetrahedron: Asymmetry*, 1998, **9**, 1597-1604.
6. A. J. A. Cobb, D. M. Shaw, D. A. Longbottom, J. B. Gold and S. V. Ley, *Org. Biomol. Chem.*, 2005, **3**, 84-96.

Appendix 1

Crystallographic data for (*R*)-342

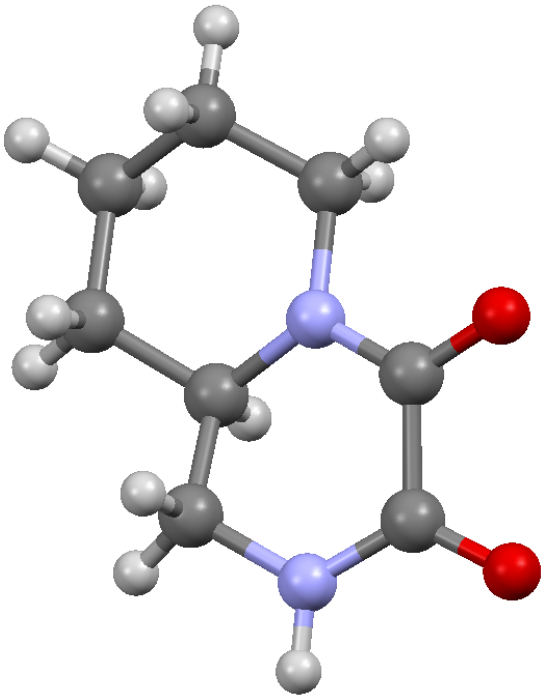

Table 1. Crystal data and structure refinement for (*R*)-**342**.

Identification code	tmdh4	
Empirical formula	C8 H14 N2 O3	
Formula weight	186.21	
Temperature	173(2) K	
Wavelength	1.54178 Å	
Crystal system	Orthorhombic	
Space group	P2(1)2(1)2(1)	
Unit cell dimensions	a = 6.939(3) Å	a= 90°.
	b = 7.847(4) Å	b= 90°.
	c = 16.454(7) Å	g = 90°.
Volume	895.9(7) $Å^3$	
Z	4	
Density (calculated)	1.381 Mg/m^3	
Absorption coefficient	0.887 mm^{-1}	
F(000)	400	
Crystal size	0.3000 x 0.1000 x 0.1000 mm^3	
Theta range for data collection	5.38 to 68.11°.	
Index ranges	-8<=h<=8, -9<=k<=9, -19<=l<=19	
Reflections collected	11795	
Independent reflections	1617 [R(int) = 0.0591]	
Completeness to theta = 67.00°	99.0 %	
Absorption correction	Multiscan	
Max. and min. transmission	1.0000 and 0.8548	
Refinement method	Full-matrix least-squares on F^2	
Data / restraints / parameters	1617 / 3 / 131	
Goodness-of-fit on F^2	1.146	
Final R indices [I>2sigma(I)]	R1 = 0.0304, wR2 = 0.0818	
R indices (all data)	R1 = 0.0325, wR2 = 0.0920	
Absolute structure parameter	-0.1(2)	
Largest diff. peak and hole	0.175 and -0.218 $e.Å^{-3}$	

Crystallographic data for (*R*)-363

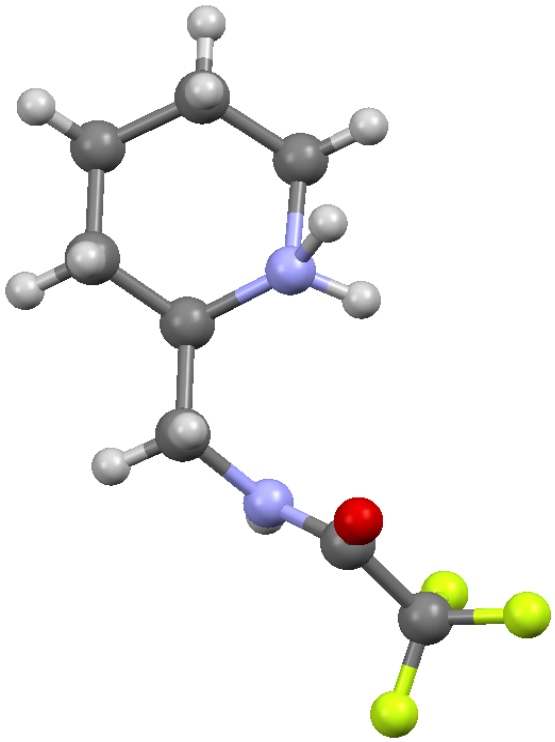

Table 1. Crystal data and structure refinement for (*R*)-**363.**

Identification code	tmdh5	
Empirical formula	C10 H14 F6 N2 O3	
Formula weight	324.23	
Temperature	173(2) K	
Wavelength	1.54178 Å	
Crystal system	Monoclinic	
Space group	P2(1)/c	
Unit cell dimensions	a = 8.834(6) Å	a= 90°.
	b = 14.844(8) Å	b= 90.01(3)°.
	c = 10.865(7) Å	g = 90°.
Volume	1424.7(15) $Å^3$	
Z	4	
Density (calculated)	1.512 Mg/m^3	
Absorption coefficient	1.447 mm^{-1}	
F(000)	664	
Crystal size	0.1000 x 0.1000 x 0.0300 mm^3	
Theta range for data collection	5.01 to 68.05°.	
Index ranges	-10<=h<=10, -17<=k<=17, -13<=l<=13	
Reflections collected	18907	
Independent reflections	2550 [R(int) = 0.1000]	
Completeness to theta = 67.00°	98.4 %	
Absorption correction	Multiscan	
Max. and min. transmission	1.0000 and 0.7001	
Refinement method	Full-matrix least-squares on F^2	
Data / restraints / parameters	2550 / 3 / 204	
Goodness-of-fit on F^2	2.615	
Final R indices [I>2sigma(I)]	R1 = 0.2103, wR2 = 0.5694	
R indices (all data)	R1 = 0.2193, wR2 = 0.5783	
Extinction coefficient	0.15(4)	
Largest diff. peak and hole	0.909 and -0.770 $e.Å^{-3}$	

Crystallographic data for (*R*)-364

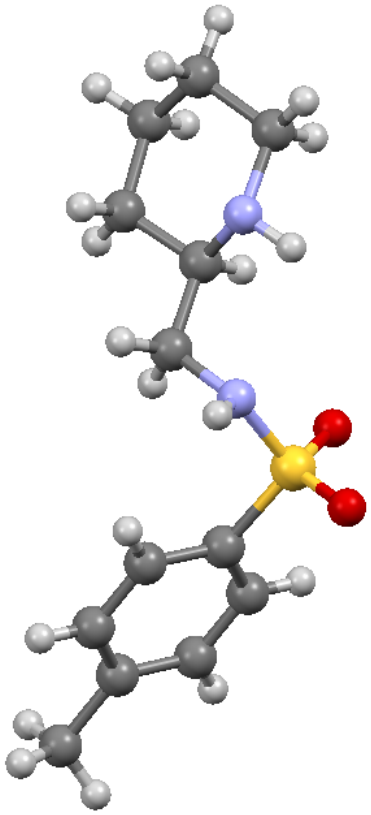

Table 1. Crystal data and structure refinement for (*R*)-**364.**

Identification code	tmdh7	
Empirical formula	C13 H20 N2 O2 S	
Formula weight	268.37	
Temperature	93(2) K	
Wavelength	0.71073 Å	
Crystal system	Triclinic	
Space group	P-1	
Unit cell dimensions	a = 5.756(3) Å	a= 111.717(14)°.
	b = 10.762(6) Å	b= 90.020(5)°.
	c = 12.622(6) Å	g = 105.094(14)°.
Volume	697.3(6) $Å^3$	
Z	2	
Density (calculated)	1.278 Mg/m^3	
Absorption coefficient	0.229 mm^{-1}	
F(000)	288	
Crystal size	0.2700 x 0.0500 x 0.0500 mm^3	
Theta range for data collection	3.23 to 25.35°.	
Index ranges	-5<=h<=6, -12<=k<=12, -12<=l<=15	
Reflections collected	4349	
Independent reflections	2454 [R(int) = 0.0309]	
Completeness to theta = 25.00°	97.2 %	
Absorption correction	Multiscan	
Max. and min. transmission	1.0000 and 0.9509	
Refinement method	Full-matrix least-squares on F^2	
Data / restraints / parameters	2454 / 2 / 174	
Goodness-of-fit on F^2	0.631	
Final R indices [I>2sigma(I)]	R1 = 0.0485, wR2 = 0.1270	
R indices (all data)	R1 = 0.0590, wR2 = 0.1467	
Extinction coefficient	0.036(8)	
Largest diff. peak and hole	0.258 and -0.373 $e.Å^{-3}$	

Appendix 2

List of publications

- G. Deniau, T. Moraux, D. O'Hagan, A. M. Z. Slawin, An efficient synthesis of (*R*)- and (*S*)-2-(aminomethyl)piperidine *di*hydrochloride, *Tetrahedron: Asymmetry*, 2008, **19**, 2330-2333.

- M. Winkler, T. Moraux, H. A. Khairy, R. H. Scott, A. M. Z. Slawin, D. O'Hagan, Synthesis and vanilloid receptor (TRPV1) activity of the enantiomers of α-fluorinated capsaicin, *ChemBioChem,* 2009, **10**, 823-828.

Oral presentation

5th Organic Chemistry Postgraduate Symposium, University of St. Andrews, 2008.

Poster presentation

- 4th Organic Chemistry Postgraduate Symposium, University of St. Andrews, 2007.

- Industry Symposium, University of St. Andrews, 2008.

- 19th Winter Fluorine Conference, Florida, USA, 2009 (ACS Poster Award).

Conferences attended

- 35th Scottish organic division meeting, Strathclyde University, 2005.

- 6th RSC fluorine meeting, University of Manchester, 2006.

- 36th - 36th Scottish organic division meeting, Herriot Watt University, 2006.

- 7th RSC Fluorine meeting, University of Leicester, 2007.

- 37th Scottish organic division meeting, Glasgow University, 2007.

- 8th RSC fluorine meeting, University of Newcastle, 2008.

- 38th Scottish organic division meeting, Aberdeen University, 2008.

- 19th Winter Fluorine Conference, Florida, USA, 2009 (ACS Travel Grant).